



HAL
open science

Preparation of etoposide nanocrystals suspension by co-precipitation for enhanced targeting and sustained release in cancer therapy

Brice Martin

► **To cite this version:**

Brice Martin. Preparation of etoposide nanocrystals suspension by co-precipitation for enhanced targeting and sustained release in cancer therapy. Pharmacology. Université Paris Cité, 2019. English. NNT : 2019UNIP5044 . tel-03626758

HAL Id: tel-03626758

<https://theses.hal.science/tel-03626758v1>

Submitted on 31 Mar 2022

HAL is a multi-disciplinary open access archive for the deposit and dissemination of scientific research documents, whether they are published or not. The documents may come from teaching and research institutions in France or abroad, or from public or private research centers.

L'archive ouverte pluridisciplinaire **HAL**, est destinée au dépôt et à la diffusion de documents scientifiques de niveau recherche, publiés ou non, émanant des établissements d'enseignement et de recherche français ou étrangers, des laboratoires publics ou privés.



Thèse

Pour obtenir le titre de docteur

PREPARATION OF ETOPOSIDE NANOCRYSTALS SUSPENSION BY CO-PRECIPIATION FOR ENHANCED TARGETING AND SUSTAINED RELEASE IN CANCER THERAPY

Présentée et soutenue par Brice Martin

Thèse défendue publiquement le 20 Septembre 2019 devant le jury suivant :

Catherine PASSIRANI	Pr Université d'Angers	Rapporteur
Eric ALLEMANN	Pr Université de Genève	Rapporteur
Chantal PICHON	Pr Université d'Orléans	Examineur
Marie-Christine LALLEMAND	Pr Université de Paris	Examineur
Jean-Louis BEAUDEUX	Pr Université de Paris	Examineur
Nathalie MIGNET	DR HDR CNRS, Université de Paris	Invitée
Yohann CORVIS	DR HDR Université de Paris	Directeur

Unité de Technologies Chimiques et Biologiques pour la Santé

CNRS UMR8258 – INSERM U1267



A ma mère,

Contents

<i>Acknowledgment</i>	4
<i>Abbreviations</i>	10
<i>Abstract</i>	13
<i>I. State of the art</i>	17
Introduction	18
Poorly water-soluble drug	18
Solid forms and their implications on physical, chemical, pharmaceutical and biopharmaceutical properties	20
Nanocrystal particles and their properties	25
Impact of particle size on solubility properties	25
Impact of particle size on dissolution rate properties	26
Physical Stability - Surfactant	28
Chemical Stability	31
Nanocrystals production	32
Precipitation	32
High-pressure homogenizer	32
Ball milling	33
Nanocrystals Drug Delivery Routes	34
Oral Delivery	34
Topical Delivery	36
Ophthalmic Delivery	37
Parenteral delivery	39
Passive and active targeting delivery	41
Nanocrystal overview	45
Drug Nanocrystals on the market	54
Etoposide	55
Production	55
Etoposide-based marketed products	57
Etoposide-based cancer studies	58
Indications	59
<i>II. Aim of the study</i>	73
<i>III. Nanocrystals formulations process</i>	75

Abstract	76
Introduction	77
Material and methods	78
Material	78
Nanocrystal preparation	78
Etoposide nanocrystals particle size, morphology	78
X Ray powder diffraction experiments	79
Dissolution study of etoposide nanocrystals	79
Dynamic Scan Calorimetry	80
Thermal analysis	80
Results and discussion	81
Particle size and morphology	81
X Ray diffraction analysis	89
Dissolution study of etoposide nanocrystals	91
Thermal analysis	93
Thermal microscopy characterization	94
Conclusion and perspectives	95
<i>IV. Etoposide nanocrystals as a new delivery system to treat colon cancer in mice</i>	<i>97</i>
Abstract	98
Introduction	98
Materials and Methods	99
Material	99
Animal	99
In vitro CT26 and 3LL	100
Nanocrystal cellular uptake CT26 and 3LL	100
Plasma and tissues pharmacokinetics of etoposide	101
Antitumoral efficacy	101
Hematological Toxicity	102
Statistical analysis	102
Results and discussion	103
In vitro CT26 and 3LL	103
Nanocrystal cellular uptake on CT26 and 3LL	105
Plasma and tissues pharmacokinetics of etoposide	106
Anticancer Efficacy and Hematological Toxicity	109
Conclusion	113
<i>V. Conclusion and perspectives</i>	<i>114</i>

<i>VI. References</i>	<i>118</i>
<i>Annexes</i>	<i>143</i>

Acknowledgment

I would like to express my gratitude to Doctor Yohann Corvis for supervising, supporting, and helping me throughout the thesis project. Likewise, I would like to thank Doctor Nathalie Mignet for the opportunity that she gave me to integrate her laboratory and perform my thesis. It would have been hopeless for me to achieve this project without their help. I thank the BC Cancer Agency, in particular Marcel Bally and Anita Lam for their friendship and support.

Special thanks to Johanne Seguin, Maxime Annereau, Thomas Fleury, François Lemare, Vincent Boudy for their support regarding the entire in vivo project. René LAI-KUEN for his help in electron microscopy imaging.

In addition, my appreciations go to the Vector and Molecular Imaging and Targeted Therapy team for welcoming me and helping me including Daniel Scherman, Cyrille Richard, Karine Andrieux, Philippe Espeau, Caroline Roques, Pascal Houze, Rabah Gahoual, H  l  ne Dhotel, Hugo Salmon, Geoffroy Goujon, Thomas Lecuyer, Lucie Valero, Morgane Renault-mahieux, Louise Flidel, Shayan Ahmed, Hai-Doan Do, Jianhua Liu, Giovanni Neri.

Also, I would like to thank the Paris University, Paris School of Pharmacy, and the Doctoral School MTCI for giving me the funding that made this project successful.

Manuscript presentation

A review on solid pharmaceuticals and nanocrystal formulations has been published during my PhD and will be part of the introduction.

Brice Martin Couillaud, Philippe Espeau, Nathalie Mignet, Yohann Corvis. *State of the art of pharmaceutical solid forms: from crystal property issues to nanocrystals formulation*. *Chem Med Chem*. 2019. doi.org/10.1002/cmdc.201800612.

The manuscript is presented under the form of two articles. Our objective is to publish these two articles which form the chapters of the PhD, after the extension of the patent which has been filed in august 2018 on the results obtained during this PhD.

Patent

Brice Martin Couillaud, Nathalie Mignet, Yohann Corvis. Patent Application n°EP18306138, *Preparation of nanosuspension comprising nanocrystals of active pharmaceutical ingredients with little or no stabilizing agent*. 2018.

Future publications

Brice Martin Couillaud, Giovanni Neri, Anita Lam, Marcel B. Bally, René Lai-Kuen, Nathalie Mignet, Yohann Corvis. *Investigation of the Formulation Process to Form Etoposide Nanocrystals*. 2019.

Brice Martin Couillaud, Johanne Seguin, Fleury Thomas, Annereau Maxime, René Lai-Kuen, Nathalie Mignet, Yohann Corvis. *Etoposide Nanocrystals as a New Delivery System for Cancer Treatment*. 2019.

Participation to other work of the team conducting to publications throughout the PhD

Hai Doan Do, **Brice Martin Couillaud**, Bich-Thuy Doan, Yohann Corvis, Nathalie Mignet. *Advances on non-invasive physically triggered Nucleic Acid delivery from nanocarriers*. *Adv. Drug Deliv. Rev.* 2018. doi.org/10.1016/j.addr.2018.10.006.

Shayan Ahmed, Yohann Corvis, Rabah Gahoual, Rene Lai-Kuen, **Brice Martin Couillaud**, Johanne Seguin, Khair Alhareth, Nathalie Mignet. *Conception of nanosized hybrid liposome/poloxamer particles to thicken the interior core of liposomes and delay hydrophilic drug delivery*. *Accepted by Int. J. Pharm.* 2019.

Communications

Oral presentation

Brice Martin Couillaud, Giovanni Neri, Johanne Seguin, René Lai-Kuen, Anita Lam, Marcel B. Bally, Nathalie Mignet, Yohann Corvis. *Preparation of Etoposide Nanocrystals Suspension by Co-precipitation for Enhanced Targeting and Sustained Release in Cancer Therapy. Korea. 2018.*

Poster presentation

Brice Martin Couillaud, Giovanni Neri, Johanne Seguin, René Lai-Kuen, Anita Lam, Marcel B. Bally, Nathalie Mignet, Yohann Corvis. *Preparation of Etoposide Nanocrystals Suspension by Co-precipitation for Enhanced Targeting and Sustained Release in Cancer Therapy. Korea. 2018.*

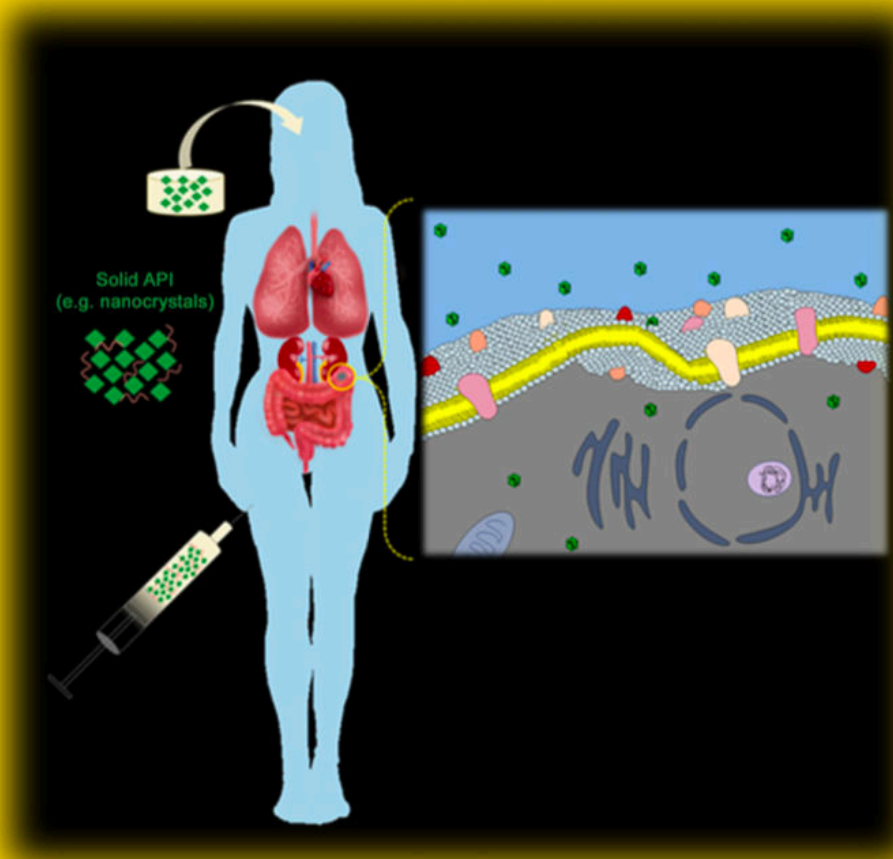
Brice Martin Couillaud, Johanne Seguin, M. Annereau, F. Lemare, Nathalie Mignet, Yohann Corvis. *Nanocrystal formulation to enhance the antitumoral efficacy of Etoposide. CRS Valencia, Spain, July 2019.*

Cover feature

Brice Martin Couillaud, Philippe Espeau, Nathalie Mignet, Yohann Corvis. *State of the art of pharmaceutical solid forms: from crystal property issues to nanocrystals formulation. Chem Med Chem. 2019. doi.org/10.1002/cmdc.201800612.*

CHEM MED CHEM

CHEMISTRY ENABLING DRUG DISCOVERY



1/2019

Cover Feature:

Yohann Corvis et al.

State of the Art of Pharmaceutical Solid Forms:
from Crystal Property Issues to Nanocrystals Formulation

WILEY-VCH

www.chemmedchem.org

A Journal of



Abbreviations

Alb: Albumin
AML: Acute Myeloid Lymphoma
AUC: Area Under Curve
BA: Benzamide
BCS: Biopharmaceuticals Classifications System
CAF: Caffeine
DBSO: Dibenzyl Sulfoxide
DLS: Dynamic Light Scattering
DMSO: Dimethyl Sulfoxide
DPPC: 1,2-Dipalmitoylphosphatidylcholine
DSC: Differential Scanning Calorimetry
DSPC: 1,2-Distearoyl-sn-glycero-3-phosphocholine
IOP: Intraocular Pressure
ETO: Etoposide
EPAS: Evaporative Precipitation into Aqueous Solution
ICN: Itraconazol
iNAM: Isonicotinamide
INH: Isoniazid
i.v.: Intravenous
GIT: Gastrointestinal Track
HCPT: Hydroxycamptothecin
HL: Hodgkins Lymphoma
HPH: High Pressure Homogenizer
HPLC: High Performance Liquid Chromatography
HPMC: Hydroxypropyl Methylcellulose
MCs: Microcrystals
MDR: Multi Drug Resistance
MeOH: Methanol
MRT: Median Residence Time
MTT: Microculture Tetrazolium Test
NAM: Nicotinamide
NCs: Nanocrystals
NSCLC: Non-Small Cell Lung Cancer
PASA: 4 Para-aminosalicylic acid

PEG: Polyethylene Glycol
P-Gp: P-Glycoprotein
PPG: Polypropylene Glycol
PSS: Polystyrene Sulfonate
PTX: Paclitaxel
PU: Precipitation Ultrasonication
PVP: Polyvinylpyrrolidone-K25
PYR: Pyrazinamide
TPH: Theophylline
SA: Schisantherin A
SCLC: Small Cell Lung Cancer
SD: Standard Deviation
SDS: Sodium Dodecyl Sulfate
SEM: Scanning Electron Microscopy
SLS: Sodium Lauryl Sulfate
TEM: Transmission Electron Microscopy
TPGS: Tocopherol Polyethylene Glycol 1000 Succinate
rpm: Revolution per minute
WBC: White Blood Cell
WBM: Wet Ball Milling
w/v: Weight per volume
3PNT: Three-Phase Nanoparticle engineering Technology

Abstract

Abstract

The aims of this current study were to study the formation, the structure, the stability, the *in vitro* and *in vivo* efficiency of etoposide (ETO) nanocrystals (NCs). The NCs were made by coprecipitation, based on the drop-wise addition of a drug solubilized in an organic phase to an aqueous phase in which the drug is insoluble, followed by an evaporation and dispersion in aqueous solvent to form NCs in suspension. For many applications, it is essential to understand nanocrystallization parameters to accurately manage NC properties such as morphology, size, thermal behavior, stability overtime, physical state, dissolution rate and so forth. In this study, the effects of polymer/drug ratio, water/solvent ratio, drug concentration were investigated. The results have been analyzed and compared to select the most suitable NCs formulation for future *in vitro* and *in vivo* studies. The NCs size and morphology were characterized using, transmission and scanning electron microscopy (TEM, SEM). Differential scanning calorimetry (DSC), X ray Diffraction (XDR) and thermal microscopy were used to define the crystallinity of the ETO nanoparticles. *In vitro* drug release profile evidenced that the ETO NCs provided a sustained release kinetics regarding the market product Toposar[®]. The overall results implied that the ETO NCs formulation offer a conceivable therapeutic formulation for further *in vitro* and *in vivo* experiments. Hence, the aims of the next part were to assess the *in vitro* and *in vivo* cytotoxicity of two selected ETO NC formulations in comparison with the conventional marketed product Toposar[®] and the free ETO. The MTT *in vitro* assay was performed on two cell lines (Carcinoma colon CT26 and 3LL Lewis lung cells), the drug uptake was also studied on these cell lines. *In vivo* studies were performed to see whether ETO NC formulations could outperformed standard formulations. The plasma and tissues pharmacokinetics of ETO were done to understand the fate of the drug after administration in mice. Also, the anticancer efficacy was tested after ETO intravenous (i.v.) injection at 10 mg/kg in murine colon carcinoma model. Tumors volume were measured to determine the response to the anticancer treatment, blood samples were withdrawn for hematological analysis. In conclusion, the results obtained imply that the delivery of ETO as a NC suspension is a novel promising technology for the therapy of the cancer.

Résumé

Les objectifs de la présente étude étaient de déterminer la structure, la stabilité, l'efficacité *in vitro* et *in vivo* des nanocristaux (NC) d'étoposide (ETO). Les NCs ont été préparés par coprécipitation, basée sur l'addition goutte à goutte d'un médicament solubilisé en phase organique dans une phase aqueuse où le médicament est insoluble, suivie d'une évaporation et d'une redispersion dans l'eau pour former les NCs en suspension. Pour de nombreuses applications, il est essentiel de comprendre les paramètres de nanocristallisation pour contrôler avec précision les propriétés des NCs, telles que la morphologie, la taille, le comportement thermique, la stabilité, l'état solide ou encore la vitesse de dissolution. Dans cette étude, les effets du rapport massique polymère/médicament, du rapport volumique eau/solvant et de la concentration en médicament ont été étudiés. Les résultats ont été analysés et comparés afin de sélectionner la formulation de NCs la mieux adaptée aux futures études *in vitro* et *in vivo*. La taille et morphologie des NCs ont été caractérisées par microscopie électronique à transmission et balayage (MET, SEM). La calorimétrie à balayage différentiel (DSC), la diffraction des rayons X (XDR) et la thermomicroscopie ont également été utilisées pour définir la cristallinité des nanoparticules d'ETO. Le profil de libération du médicament *in vitro* a montré que les NCs d'ETO offraient une cinétique de libération prolongée vis-à-vis du produit sur le marché appelé Toposar®. Les résultats ont montré que les NCs d'ETO peuvent être utilisés comme nouvelle formulation thérapeutique applicable pour des modèles *in vitro* et *in vivo*. Ainsi, les objectifs de la partie suivante étaient d'évaluer la cytotoxicité *in vitro* et *in vivo* de deux formulations sélectionnées de NCs d'ETO, par rapport au produit conventionnel Toposar® et à l'ETO libre. Le test MTT *in vitro* a été effectué sur deux lignées cellulaires (CT26 : cellules du carcinome du colon et 3LL Lewis : cellule pulmonaires), l'internalisation cellulaire du médicament a également été étudiée. Les études *in vivo* ont été réalisées pour déterminer si les formulations de NCs d'ETO pouvaient être plus performantes que les formulations conventionnelles. La pharmacocinétique dans le plasma et tissus a aussi été réalisée pour comprendre le devenir de l'ETO après administration chez la souris. En outre, l'efficacité anticancéreuse de l'ETO sous différentes formes a été vérifiée après injection par voie intraveineuse à 10 mg/kg sur un modèle murin de carcinome du côlon. Le volume des tumeurs a été mesuré pour déterminer la réponse au traitement anticancéreux, des échantillons de sang ont été prélevés pour analyse hématologique. En conclusion, les résultats obtenus ont montré que la délivrance d'ETO sous forme NC est une nouvelle technologie prometteuse pour la thérapie du cancer.

I. State of the art

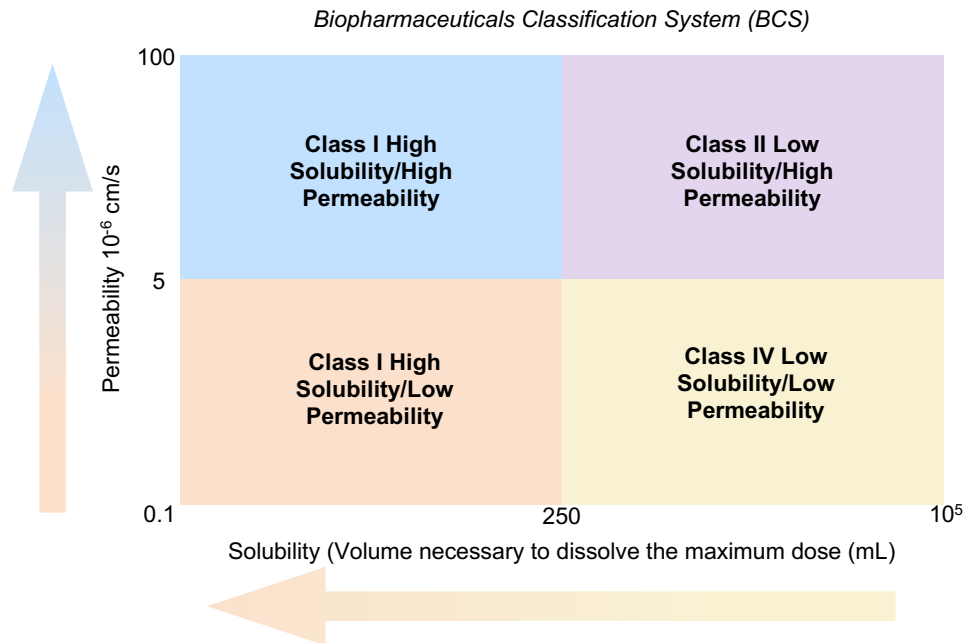
Introduction

Poorly water-soluble drug

More than 80 percent of formulated drugs are in the solid-state due to reasons of stability from the handling and storage of the unprocessed material to the drug development process. In most cases, the pharmaceutical solids present high melting points, *i.e.* low solubility properties. Therefore, drug solubility enhancement is a main challenge in pharmaceutical research and industry in order to ensure the therapeutic efficiency, to reduce the toxicity and to optimize the cost of production. In the solid state, the various structure possibilities of a given active pharmaceutical ingredient (API) can meaningfully influence properties, leading to different chemical, physical and biopharmaceutical properties.¹ Salt formation, co-crystallization techniques, amorphization, polymorphic transition and nanosizing can drastically modify the therapeutic impact of an API. Thereby, the physico-chemical characterization of each possible form allows a better assessment of the pharmaceutical properties. Laboratory and company endeavor seeking for the suitable pharmaceutical forms, also defined as solid form screening,² ensure the quality and effectiveness of the treatment and, in some case, the comfort of patients. The solid form screening will determine the choice of the best pharmaceutical form and the convenient excipients. Finding the suitable solid form allows safer pharmacological and toxicological studies, and therefore saving time, which of course represents a potential benefit to boost the profitability of a drug. The aim of this review is to give a pharmaceutical outlook on different solid forms, namely polymorphs, co-crystals, salts, solvates, amorphous solids, and their eventual combinations with an emphasis on nanocrystals formulation. We will have then a discussion dealing with the advantages and the weaknesses of each solid form in a pharmaceutical point of view.

Solid form screening for pharmaceutical development ended up increasing of poorly drug candidates.³⁻⁵ Currently, around 70% of drugs are classified as poorly soluble.⁶ The solubility of drug changes its dissolution rate which strongly affects its *in vivo* performance, therefore it is crucial to identify drug candidates with the best solubility properties suitable for pharmaceutical applications.

Biopharmaceuticals Classifications System (BCS) established by Amidon and coworkers,⁷ is a tool for decision making in drug development, primarily based on two striking factors: solubility, and permeability (Figure 1). These factors proved themselves to be crucial from drug design to its bioequivalence, notably taking into account the dissolution rate.



BCS classify drugs in 4 classes:

- Class I, referenced as high solubility / high permeability profiles (*e.g.* metoprolol, diltiazem hydrochloride)
- Class II, referenced as low solubility / high permeability profiles (*e.g.* diclofenac sodium, griseofulvin)
- Class III, referenced as high solubility / low permeability profiles (*e.g.* atenolol, lisinopril)
- Class IV, referenced as low solubility / low permeability profiles (*e.g.* etravirine, hydrochlorothiazide)

According to the Food and Drug Administration (FDA) definition of a highly water-soluble drugs, the latter can be dissolved in a quarter of a liter at most whether the aqueous media is acidic, pH of 1 up to 6.8, and considered highly permeable when the absorption in the human body is over 90% compared to the i.v. administered dose, notably.⁸ The expectations from these

four classes as regard to *in vivo* and *in vitro* correlations are described below according to Amidon and coworkers.⁷

BCS class I drugs dissolve and absorb quickly, no rate limiting step is expected for oral absorption. For a drug dissolution rate slower than gastric emptying, *in vitro/in vivo* studies are correlated. BCS class II drugs dissolve slowly and absorb rapidly, thus dissolution is the rate limiting step. Bioavailability is controlled by dosage form and drug dissolution. Consequently, both oral and i.v. administration routes are privileged. BCS class III drugs dissolve quickly and their absorbance is limited, no *in vivo* and *in vitro* correlation is expected with dissolution rate. In this case, both oral and i.v. can be considered. BCS class IV drugs have low dissolution rate and low permeability property implying that *in vitro* and *in vivo* correlation is not expected. This class of API is not preferred for oral administration and i.v. administration is more convenient.⁷ However, in some cases, oral administration route can still be chosen for such BCS class IV API like etravirine by modifying their physicochemical properties.^{9,10} Indeed, a classification of mainly orally administered drugs according to BCS has been made by Lindenberg and coworkers.¹¹ The solid state of a drug can be adapted to optimize its pharmaceutical properties. Selecting the suitable physical form of a drug gives a strategic alternative for optimizing physicochemical properties like chemical and physical stability, solubility, dissolution rate, bioavailability. Those strategies are mainly applied for drugs with low solubility such as BCS class II drugs. In the pharmaceutical research and industry fields, polymorphs, solvates, amorphs, salts or co-crystals are good candidates to increase drug solubility, reducing especially the dosage of the API. Besides, nanocrystals may increase active pharmaceutical ingredient loading in a given formulation with enhanced solubility properties. The present review details the different solid forms encounter in pharmaceutical sciences.

Solid forms and their implications on physical, chemical, pharmaceutical and biopharmaceutical properties

When the external environment cannot provide enough energy to the system, translational movements of the molecules of the system are limited. As a result, particles tend to organize themselves, by forming a lattice in order to minimize the internal energy of the system. The compound is then in the crystalline state, which is the ordered form of the matter, whereas in the amorphous state there is no explicit range order. Various crystalline structures can be used in pharmaceutical sciences to improve drug properties.¹²

Polymorphism, first introduced by McCrone in 1965,¹³ then by Rosenstein and Lamy in 1969,¹⁴ is the ability for a given compound to exist in several crystalline solid states.^{15,16} Therefore, **polymorphs** contain molecules of just one chemical nature in their entity. The term packing polymorphism is used when difference in crystal packing is observed, molecules are in the same molecular arrangement, but are grouped differently.

in three- dimensional space, and conformational polymorphism is used to describe crystal forms that consist of molecules with different conformations packed in several arrangements.¹⁷ In pharmaceutical sciences, most drugs exhibit polymorphism,¹⁸ however the most stable form is recommended to ensure reproducibility of the product formulation and stability throughout its life span.¹⁹ Indeed, the polymorphism may have an influence on powder flow, compactibility, physicochemical stability, and dissolution rate of raw material.²⁰ A well-known example is Ritonavir, an antiretroviral drug used to treat HIV-1 infection. Approved in 1996, it was removed from the market in 1998 because of its polymorphism ability. Indeed crystals of a new polymorph have been discovered in the i.v. bags and exhibited lower solubility as compared to the initially prepared form.²¹ As a matter of fact, lower the stability of a given polymorph, higher its solubility.²² Therefore, in order to enhance drug bioavailability, one can increase its solubility by stabilizing kinetically metastable polymorph of a given API. However, such systems are sensitive to external stimuli such as pH, temperature, radiation, pressure variations.

Solvates are solid crystals with solvent molecules (*e.g.* ethanol, ethyl acetate) included in the lattice structure.²³ It has been demonstrated that an organic compound with high polymorphism abilities has also high propensity to form solvates.²⁴ In the case of one or more water molecules as solvent, solvates are named hydrates, while compounds with no water of crystallization are called anhydrides. Around 33% of API form hydrates, which can be mono- or poly-hydrated according to the number of water molecule embedded in the crystal lattice.²⁵ Hydrates can be sorted into three categories: crystalline hydrates based on their structure (Class I, when the water molecule is interacting only with the main molecule; class II, when channels of water molecules are present through the crystal structure; and class III, when metal ions of the crystal structure are coordinated with water). Interestingly, the hydrate solubility depends on the hydration state of the hydrate. With some drugs such as azithromycin, hydrates are more soluble than the corresponding anhydride, and with other drugs it is the contrary.²⁶ Consequently, it is important to evaluate the ability of a pharmaceutical raw material to form hydrates during its manufacturing or its storage, but also establish its relative stability towards relative humidity.²⁷

Salt crystals are usually formed when drugs bear ionizable groups. Salts have been used to modify the physical and the chemical properties of a drug. Forming a salt improves drug solubility and therefore bioavailability. The nature of the host molecule (anions or cations) can alter salt solubility and overall properties. A study carried out by Jamaludin and coworkers comparing the solubility of different salts of quinine, and recommended the quinine ethyl carbonate salt to heal diseased children as of its neutral taste, compared to quinine hydrochloride and quinine sulphate.²⁸

Co-crystals formulation is a more recent approach to improve drug physicochemical properties. It results in the combination of two or more neutral substances tied together in a unique crystal lattice.^{29,30} Like the former solid forms presented in this paper, co-crystals may improve solubility and bioavailability according to the nature of constituents.³¹ Drozd and coworkers studied the co-crystal structures of anti-tuberculous drug 4 para-aminosalicylic acid (PASA), and observed that PASA solubility increased by two times with PASA-pyrazinamide (PYR), PASA-nicotinamide (NAM), PASA-isonicotinamide (iNAM), PASA-isoniazid (INH), PASA-caffeine (CAF) and PASA-theophylline (TPH) co-crystal forms, in comparison with the intrinsic solubility of the pure form.³² Still, co-crystal form may also decrease pure drug solubility as PASA-TPH lowers the PASA solubility by approximately 2 times.³² This has been also evidenced by, *e.g.* Grossjohann and coworkers with the benzamide (BA):dibenzyl sulfoxide(DBSO) 1:1 cocrystal, embedding the poorly water soluble dibenzyl sulfoxide with the more soluble benzamide. For both components BA and DBSO, the co-crystal solubility was lower compared to the pure components and to an equimolar physical mixture.³³

Polymorphs, solvates, salts or co-crystals (Fig. 2) can be the outcome of a design to enhance drug properties, but under no circumstances, solubility, dissolution rate, and bioavailability can be precisely predicted for drug combination with host molecules, counter-molecules and so forth.

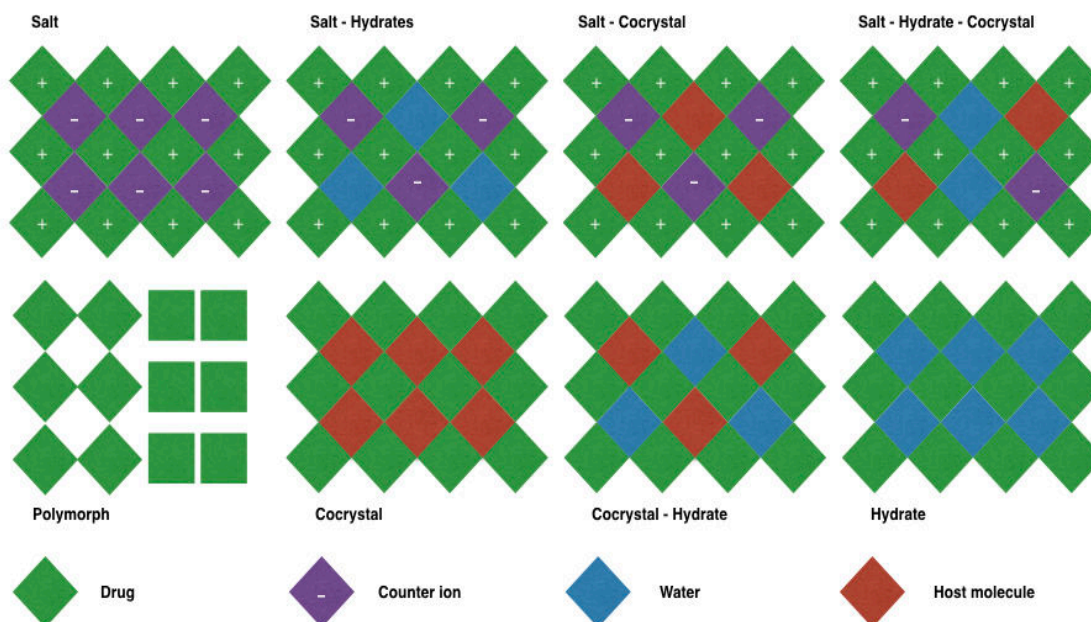


Figure 2 - Various solid-state crystal forms for compounds of pharmaceutical interest.

As mentioned above with some examples, such solid forms can lead to jeopardize drug quality due to their relative stability in presence or not of eventual host molecules. To avoid these issues, drug amorphization approach can be considered as a better means to enhance API bioavailability.

Solid state of **amorphous** drugs is thermodynamically unstable since amorphous compounds display random organization of the molecules within the matter. Due to higher free energy of amorphous forms as compared to crystalline forms, the formers are more metastable, implying better solubility of amorphous pharmaceuticals.³⁴ Indeed, an amorphous form dissolves faster than the crystalline one because of stronger intermolecular forces and better molecule organization in the latter.³⁵ Despite their advantages in solubility and dissolution rate, the amorphous forms have limited use in pharmaceutical field as it is difficult to prevent their crystallization. Vasanthavada and coworkers studied the behavior in amorphous molecular dispersion of trehalose-dextran and trehalose-poly(vinylpyrrolidone) from returning to crystalline state on storage, the two dispersions were exposed to 23, 40 and 50 °C at 75% relative humidity and 23 °C at 69% relative humidity storage conditions, respectively. It was found that trehalose-dextran and trehalose-poly(vinylpyrrolidone) did not crystallize during the 6 months storage.³⁶ The advent of novel techniques to enhance steadiness of amorphous forms improved odds of their use in pharmaceutical formulations. In the two following tables are gathered some examples of marketed products for which the API (Table 1), and the

API/excipient mixture (Table 2) are in the amorphous state.³⁷ Hence, other approaches are required to enhance drug properties for pharmaceutical purposes

Table 1 - Non-exhaustive list of amorphous active pharmaceutical ingredients on market

Trade name	Drug	FDA approval
Accolate [®]	Zafirlukast	1999
Accupril [®]	Quinapril hydrochloride	1991
Ceftin [®]	Cefuroxime Acetyl	1994
Crestor [®]	Rosuvastatin Calcium	2003
Viracept [®]	Nelfinavir Mesylate	1996

Table 2 - Non-exhaustive list of amorphous solid dispersion* on market

Trade name	Drug	FDA approval
Etravirine	Intelence [®]	2008
Fenofibrate	Fenoglide [®]	1993
Griseofulvin	Gris-PEG [®]	1959
Itraconazole	Sporanox [®]	2001
Ivacaftor	Kalydeco [®]	2012
Lopinavir/Ritanovir	Kaletra [®]	2000
Nabilone	Cesamet [®]	1985
Tacrolimus	Prograf [®]	2000
Troglitazone	Rezulin [®]	1999
Verapamil	Isoptin [®]	1982
Verumafenib	Zelboraf [®]	2017

* Solid dispersion stands for API/excipients (mostly polymers) solid mixtures

Nanocrystal particles and their properties

Micronization approach is not efficient enough for drugs that are highly hydrophobic which represents 70% of new drug candidates,⁶ thus further step to lower the particle size to a nanometer size is required. Nanocrystals are an auspicious approach to enhance drug bioavailability by reducing the particle size.³⁸ Nanocrystal technology can thus be considered either as an alternative to other solid states preparation, or as a complementary approach for the solid forms presented in section 3, depending on the choice of the nanocrystal production method.

Impact of particle size on solubility properties

The Kelvin equation (Eq. 1) can be applied to the nanocrystal dissolution pressure taking into consideration its surface tension in solution. Decreasing the nanocrystal size increases the curvature, hence the dissolution pressure P_r . As shown in the equation, the dissolution pressure becomes substantial when the particle size is within the nanometer range.

$$\ln\left(\frac{P_r}{P_\infty}\right) = \left(\frac{4\gamma M}{d_{np}RT\rho}\right) \quad (Eq. 1)$$

where P_r and P_∞ are the nanocrystal and an infinitely large nanocrystal dissolution pressures, respectively, γ the surface tension in N.m^{-1} , M the molecular weight of the nanoparticles in g.mol^{-1} , d_{np} the particle diameter in m, R the gas constant in $\text{J.K}^{-1}.\text{mol}^{-1}$, T the temperature in Kelvin, and ρ the nanocrystal density in g.m^{-3} .

The saturation solubility is also governed by Ostwald–Freundlich equation (Eq. 2) which highlights the difference in solubility between different sizes of particle. It implies in particular, a greater saturation solubility as the radius of the particle becomes smaller.

$$\log\left(\frac{C_s}{C_\alpha}\right) = \frac{4\sigma V}{2.303 \times RT\rho d_{np}} \quad (Eq. 2)$$

where C_s is the saturation solubility, C_a the solubility of large particle, σ the interfacial tension, V the molar volume of the nanocrystal ($\text{m}^3 \cdot \text{mol}^{-1}$), R the gas constant ($\text{J} \cdot \text{K}^{-1} \cdot \text{mol}^{-1}$), T the temperature (K), ρ the particle density ($\text{g} \cdot \text{m}^{-3}$) and d_{np} its diameter (m).

An enhancement in saturation solubility provides a high concentration gradient, fostering permeation and absorption through the gastrointestinal membrane and blood by passive diffusion ³⁹.

Impact of particle size on dissolution rate properties

The dissolution rate can be determined by the Noyes–Whitney and by the Prandtl equations (Eq. 3 and 4, respectively).

$$\frac{dm}{dt} = S \left(\frac{D}{d} \right) (C_s - C_p) \quad (\text{Eq. 3})$$

where dm/dt is the dissolution rate ($\text{kg} \cdot \text{m}^2 \cdot \text{s}^{-1}$), S define the surface area of the particle (m^2), D the coefficient of diffusion ($\text{m} \cdot \text{s}^{-1}$), d the thickness of the hydrodynamic boundary layer (m), C_s the saturation solubility (kg or $\text{mol} \cdot \text{L}^{-1}$), C_p the concentration surrounding the particle (kg or $\text{mol} \cdot \text{L}^{-1}$).

It is noteworthy that the intrinsic dissolution rate is the dissolution rate normalized to the specific surface of the system. Moreover, the size reduction of nanocrystals leads to a decrease of the diffusional distance d , as shown in Figure 3 thus, according to Eq. (3), to a better dissolution of particles.

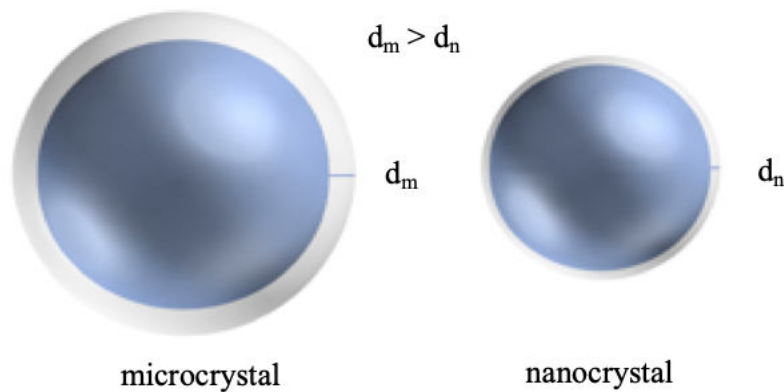


Figure 3 - Comparison of the diffusional distance d for micro and nanocrystal.

The diffusional distance d , related to the hydrodynamic boundary layer h , is correlated to the nanoparticle size owing to Prandtl equation (Eq. 4).⁴⁰

Bisrat and Nyström, used the Prandtl boundary layer equation to clarify the effect of hydrodynamic boundary layer thickness h of flowing particles on their dissolution rate. Their researches have proved that size diminution of solid dispersions in solution under stirring, decreases the particle surface in the flow direction, including a reduction of the flowing liquid velocity near to the nanoparticles.^{40,41}

$$h = c \left(\frac{L}{V} \right)^{1/2} \quad (\text{Eq. 4})$$

where h is the thickness of the hydrodynamic boundary layer, c a constant, L the size of the particle surface in the flow direction, V the speed of the flowing liquid neighboring the particle.

Liversidge and Cundy revealed that nanocrystallization of danazol improves its saturation solubility and the bioavailability properties.⁴² Three formulations, *i.e.* danazol nanocrystals (169 nm) produced by wet milling, danazol-hydroxypropyl- β -cyclodextrin (HPB) complex, and a conventional microcrystals suspension of danazol (10 μ m), were orally administrated at a dose of 3 mg/kg to fasted beagle dogs. The results exhibit 82.3 \pm 10.1% danazol nanocrystals bioavailability, 106 \pm 12.3% danazol nanocrystals-HPB complex and only 5.1 \pm 1.9% for danazol microcrystals, indicating the improvement of nanocrystal uptake compare to the microcrystal suspensions of danazol.⁴² Hecq and coworkers also investigated the dissolution rate of ucb-35440-3 nanocrystals (600nm) produced by HPH and the ucb-35440-3 microcrystals using dialysis bag methods. The results clearly evidenced a dissolution rate improvement for the nanocrystal forms: more than 95% of the drug was solubilized after 1 hour compared to microcrystal forms where only 30% of the drug was dissolved over the same period and complete dissolution was not accomplished for the next 12 hours.⁴³ Same results were obtained with fenofibrate nanocrystals compared to microcrystals.⁴⁴

Physical Stability - Surfactant

Ostwald ripening is the well-known phenomena that occur when nanoparticles are formed, small particles tend to dissolve and diffuse through the gradient concentration to end up accumulating on larger particle size; leading to particle growth overtime and formation of microparticles.⁴⁵ The irreversible particle coalescence is reinforced with the polydispersity (PDI) of the dispersion, unfortunately, it is the case for NCs dispersion in solution where PDIs are often greater than 0.2. Hence, homogeneous NC dispersions are required to reduce the saturation solubility dissimilarity and the concentration gradient of the drug, therefore hampering the crystal growth. Physical NC stability is a crucial feature for *in vivo* application as agglomeration, precipitation can damage the potency of the medicine, change the bioavailability, the drug biodistribution and generate side effects. The NC stabilization has been commonly achieved using surfactant or polymeric stabilizer to repel particles. The nature of stabilizers generally amphiphilic promote the self-assembly around NC surface, as the hydrophobic part of the polymeric chain circle the surface of the hydrophobic nanoparticles and arrange themselves to have the lowest contact area with the aqueous solution. Hydrophobic interactions are stronger forces compared to Van der Waals mainly governed by hydrogen bonds,⁴⁶ hence the surfactant is well-attached to the nanoparticles protecting them from aggregation.

The protection can be steric, electrostatic or both combined. As mentioned, amphiphilic polymers such as Pluronic F-127, F-68 are more used for NC stabilization compared to standard homopolymer. Numerous parameters influence the NC stability, the polymer molecular mass, the hydrophobic/hydrophilic ratio of the chain, the nature of the chain functional groups and the polymer conformation.⁴⁷ Sharma *et al.* examined the size of indomethacin NCs produced by wet milling and high pressure homogenizer (HPH) using two dissimilar surfactants, Polyvinylpyrrolidone-K25 (PVP) and Pluronic F-127, the results indicated a surface modification and a size difference between NC according to the nature of the polymer.⁴⁸ Lee *et al.* evidenced the impact of the hydrophobic/hydrophilic polymer ratio on the NC steadiness by producing a polymer with the same hydrophobic part but diverse hydrophilic groups. The study concluded that the polymer hydrophobicity is a striking parameter to the particle stabilization, and that 15 mol % of hydrophobicity polymer content should be used to have sufficient stabilization, as the adsorption is better on the NC surface.⁴⁹

Ionic polymers give better stability as charges offer stronger repulsive forces between molecule, Karakula *et al.* have tested several cationic chitosan for atorvastatin NC, the better NC preparation, smallest size and stability overtime, was done using the low positively charged chitosan and proved the impact of surfactant charge density.⁵⁰ Another option for enhancing NC stability is to combine ionic and steric polymer, Sun *et al.* made with HPH four itraconazole (ICN) NCs formulations, using either Pluronic F-68 alone or Pluronic F-68 combined with different molecular weight of chitosan. For F-68, the NC size was around 590 nm with a PDI of 0.7 whereas F-68 used in combination with chitosan shown 350 nm NC with 0.4 PDI.

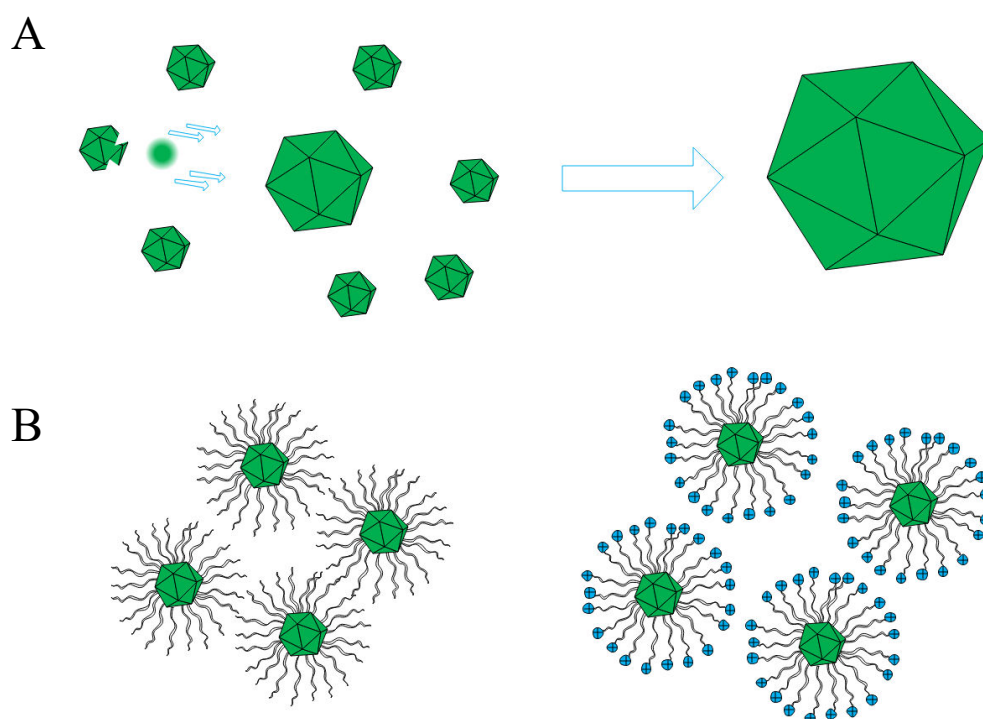


Figure 4 – Representation of Ostwald ripening (A) and steric/ionic stabilization using surfactants (B)

Sun *et al.* explained that chitosan molecular weight affects the polymer stretching behavior in water and the conformation of the other polymer F-68 surrounding NCs, thus providing better surface adsorption and therefore protection.⁵¹ Another overlooked aspect of surfactants is their repercussion on the NC bioavailability *in vivo* via their interactions with the surrounding environment. For most studies, the choice of surfactant to improve the NC physical stability is predominant over its impact on bioavailability of NCs. As an example, Liu *et al.* studied two PTX NC formulations made with polyethylene glycol 1000 succinate (TPGS) and Pluronic F-127. Both formulations exhibited close characteristics in terms of size and morphology, but

PTX NCs with F-127 were less stable at room temperature compared to PTX NCs with TPGS as surfactant. Besides, PTX/ TPGS NCs remained stable at 37 °C for 5 days whereas PTX/F-127 NCs precipitated few hours later after redispersion in solution. For this reason, only PTX/TGPS was selected and used for *in vivo* experiment on ovarian model mice and had better efficiency in contrast with Taxol® injected at 10 mg/kg. Although PTX/F-127 NCs were disregarded for *in vivo* experiments, because of poor stability overtime, they could have possibly outperformed PTX/TGPS NC in terms of efficiency, biodistribution and bioavailability as F-127 interacts differently with the surrounding *in vivo* environment. The PTX NC/F-127 poor stability overtime could have been avoided and used as mice cancer treatment whether the NC were redispersed in solution right before *in vivo* injection.⁵² This strategy has most frequently appeared in NC technology researches leading to overlook new cancer treatments.

Nonetheless, investigations led by Sharma *et al.* understood this aspect and evaluated the oral bioavailability in Wistar rats of PTX NC using polystyrene sulfonate (PSS) and polysorbate 80. It was discovered that both NC formulation were more effective than the pure drug crystals and also that the nature of surfactant changed the *in vivo* oral bioavailability. PTX NCs area under the curve (AUC) was close to 10 fold better as compared to pure PTX both administered at 10 mg/kg.⁵³ Sinico *et al.* also observed skin bioavailability variance with either Pluronic F-68 or polysorbate 80. Resveratrol NCs were tested on pig ear skin model, higher concentration of resveratrol went through deeper skin layers compared to drug crystal dispersion and NCs specifically coated with Pluronic F-68 had the highest skin depth penetration.⁵⁴ The relevance to protect NC with surfactant was also highlighted by Lu *et al.* using PTX bared NCs in contrast with PTX transferrin-coated NCs. Transferrin proved to be the best option for stabilizing NCs among albumin and immunoglobulin G with a stable formulation up to 3 months at 4 °C. The *in vivo* tumor inhibition was carried out using KB nasopharyngeal epidermal carcinoma and SKOV-3 ovarian cancer cells subcutaneously incorporated to female outbred mice. Both bared PTX and transferrin PTX NC were intravenously single-dose injected at 20 mg/kg. Transferrin PTX obtained a tumor inhibition rate of 45.1% and 28.8% for bared PTX NCs 12 day after treatment.⁵⁵ In addition to the physical steadiness provided using surfactants, the physical state of drug NCs preserve them from chemical degradation in the neighboring environment.

Chemical Stability

Since drug NCs are solid nanoparticles dispersed in solution, the likelihood of chemical interactions is rare. The NC surface is exposed to chemical degradation that strongly relies on the nature of molecule functional groups vulnerable to light, pH, temperature, humidity or oxidation and hydrolysis degradation when dispersed in solution.⁵⁶ It has to be kept in mind that the overall rate deterioration of NCs depends on both the solid nature of NCs and the surfactant layer used to physically stabilize the nanoparticle.⁵⁷ For instance, drug omeprazole synthesized as a NC suspension has been made by Möschwitzer *et al.* to evidence the better chemical stability overtime compared to the omeprazole solution form. For the two formulations stored at 4 °C in the dark, after one month, the NC dispersion did not show any signs of chemical degradations.⁵⁸ The same conclusion were obtained by Park *et al.*, where the thermal stability of PTX nanodispersion was enhanced contrary to the conventional Taxol® solution that was sensitive to variations of temperature.⁵⁹ Also, Gao *et al.* reported the photochemical stability by fluorescence of quercetin NC dispersion at 25 °C for 1 months, the effect of the NC was clearly proved compared to the control water quercetin solution. A diminution of 28% of quercetin content and distinct discoloration was seen for the control whereas for NCs, only 19% of drug content diminution with no deterioration were observed.⁶⁰ The impact of the surfactant on NC chemical stability was established by Pu *et al.* who prepared NCs with the lactone form of 10-hydroxycamptothecin using HPH. The NC drug stability was evaluated with the content of the drug measured after 24 h at 4 °C. Precisely, in that study the stability was denoted as the degradation of the drug to the carboxylate form under lighting for various pH conditions. The outcomes showed that the NC lactone form of 10-hydroxycamptothecin was 90% conserved while only 30% remained in the solution form of the drug for the similar conditions.⁶¹ Hence, most of the drugs are upheld in dry form to bypass the chemical degradation in solution and redispersed before use.

Nanocrystals production

The methods presented in section 4 can also be applied to produce NCs, nevertheless most of them are rarely used compared to the precipitation, high pressure homogenizer and milling processes.⁶²⁻⁶⁴ Moreover, each technique of NCs preparation is specific to a given active ingredient.

Precipitation

This process is established on the drop-wise addition under stirring of a drug solubilized in a given solvent to another one in which the drug is unable to be dissolved. The main setback of this method is the irreproducibility, as a lot of parameters must be precisely supervised such as addition speed, temperature, solvent nature, agitation speed to obtain reproducible results. Also, for this technique the drug must have specific physicochemical features that fit the protocol to make it successful.⁶⁵ However, an extended-parameter technique gives diverse combinations and makes it possible to study the impact on the final material in terms of size and morphology. With this bottom up method, the particles obtained are often smaller compared to the top down approach where a drug has to be broken into smaller particles using mechanical energy. Meihua *et al.* synthesized hydroxycamptothecin (HCPT) NCs using precipitation, specifically, HCPT was dissolved in dimethyl sulfoxide (DMSO) and added into a fetal calf serum as antisolvent and surfactant, the resulting particles had a size around 168 nm.⁶⁶ In comparison, Zhao *et al.* also synthesized HCPT NCs but using a top down approach, the HPH, the drug was dispersed in saline solution and broke into smaller particles, the final size were superior to 300 nm whatever the nature of surfactant used.⁶⁷

High-pressure homogenizer

The three most important technologies include, the microfluidizer method (DD-PTM technology), Piston-gap homogenization method in water (Dissocubes[®]) or in water mixture (Nanopure[®]).⁶⁸ The Dissocubes[®] tool, engineered by Müller and Grau at the end of the twentieth century was a breakthrough technology.⁶⁹ It allows applying a high pressure (up to 4,000 bars) to an aqueous solution where the drug is dispersed creating an important shear stress force when the solution goes through a tight gap by means of a homogenizer piston. The range of the gap homogenization covers 5 to 20 μm and has to be chosen according to the viscosity of the solution, and obviously, the process pressure. The diminution of the section from centimeter to

micrometer soars the dynamic pressure and reduces the static pressure under the boiling point of the continuous medium at ambient temperature. Gas bubbles are thus formed under pressure then burst generating a high shear force allowing the decrease of the particle size in solution. The use of water as a dispersant solution may hydrolyze water-sensitive drugs and create abundant foam.⁶⁸ Another way using the piston gap homogenizer is the Nanopure[®] technology. The latter technology consists in homogenization of drug dispersed in a non-aqueous medium at low temperature (close to 0 °C) and even under its freezing point. Besides the applied pressure is low, preventing cavitation phenomena from appearing. The particle size diminution is still acceptable, below 1 µm.^{70,71} Only few studies synthesizing nanocrystals have been reported using piston gap homogenization technologies, generally the Microfluidizer technology is preferred.^{71,72} The Microfluidizer technology uses a high-pressure pump generating forces up to 2000/2500 bar to narrow the particles in suspension by frontal collision in an interaction chamber, then the final solution is recovered in an outlet reservoir. A high number of cycles (50-100) is recommended to have a sufficient particle size reduction; also depending on the structural solidity of the particle. Indeed, the drawback of this method relies on the high heat released that may chemically denature the formulation.⁷³

Ball milling

Commonly, ball milling consists of a cylindrical crushing system that is employed for size reduction of powders in a wet or dry environment.⁷⁴ The rotating crushing cylinder is fulfilled with ceramic or stainless-steel balls falling on powders to produce homogenous solid dispersion with enhanced bioavailability and dissolution rate. For powders, the minimum particle size that can be realized with conventional milling is about 2-3 µm, otherwise, wetting conditions are more suitable to scale down particles size under these values. Tanaka and coworkers were able to achieve a powder formed of 17.1 µm particle size of probucol powder.⁷⁵ Then, using wet-milling with zirconia beads at a rotation speed of 12 m.s⁻¹ combined with dispersing surfactants such as , vitamin E-TPGS, Poloxamer 338, Gelucire[®], the probucol particle sizes decreased to 77–176 nm to form a novel drug delivery system known as nanocrystals. For nanocrystal formulations, milling time longer than the grinding time necessary for microcrystal preparation may decrease the drug crystallinity due to partial or total amorphization. The latter phenomenon has been reported by Dai and coworkers for meloxicam nanocrystals.⁷⁶

Nanocrystals Drug Delivery Routes

Oral Delivery

Oral drug delivery is the handiest route of drug administration as patient compliance, dosage form, sterility, and simplicity of production are promoted. Drug bioavailability is a challenge through oral delivery route that can be governed by three main factors, solubility, dissolution rate and permeability as discussed earlier. Oral route leads to aggressive environments that can degrade drugs in particular in the gastrointestinal track and the liver, thus API should be shielded against unstable milieus. NC technology is among the strategies used to enhance oral bioavailability (*e.g.* cyclodextrin, liposomes, polymers) as their physical properties directly impact drug solubility, dissolution and permeability through the membranes. Previously mentioned, poorly water-soluble and highly permeable drug can be classified as a BCS class II drug. The low oral bioavailability results in a poor concentration of the drug in blood and therefore minimizes the odds of targeting a particular organ. Drug absorption in the gastrointestinal track (GIT), more precisely through the gastrointestinal epithelium layer, is a challenge if the drug is not dissolved. To address this issue, nanocrystal formulation has beneficial effects on the oral drug delivery such as a similar bioequivalence as regard to the fed or fasted state.⁷⁷ Moreover, Chen and coworkers have proved that schisantherin A (SA) nanocrystals formulation (160 nm), orally administered to rats at 4 mg/kg, improved its solubility and pharmacokinetic profile. In that case, concentration of the SA NCs accumulation in the plasma was 6.7 fold higher than the mere SA suspension, after oral administration.⁷⁸ Another study conducted by Hanafy and coworkers ended up to a similar conclusion with fenofibrate nanocrystals formulation confronted with a fenofibrate microsuspension orally administered at 100 mg/kg to the rat. The fenofibrate nanocrystals have shown a two-fold bioavailability enhancement ($C_{\max} = 222.7 \pm 21.9 \mu\text{g/mL}$) as regard to the microcrystals suspension where the C_{\max} was only $96.9 \pm 62.4 \mu\text{g/mL}$.⁷⁹ The efficacy of nanocrystal formulations can be undoubtedly explained by a better saturation solubility and dissolution rate properties. When drugs are delivered as nanocrystal form, a significant drug concentration gradient between the GIT and the systemic circulation does exist, enhancing drug bioavailability inside the blood, Figure 4. This explains, for instance, why the fenofibrate dose has been reduced by 18% in marketed tablets of nanocrystals for the same bioequivalence as compared to micronized fenofibrate.^{68,80}

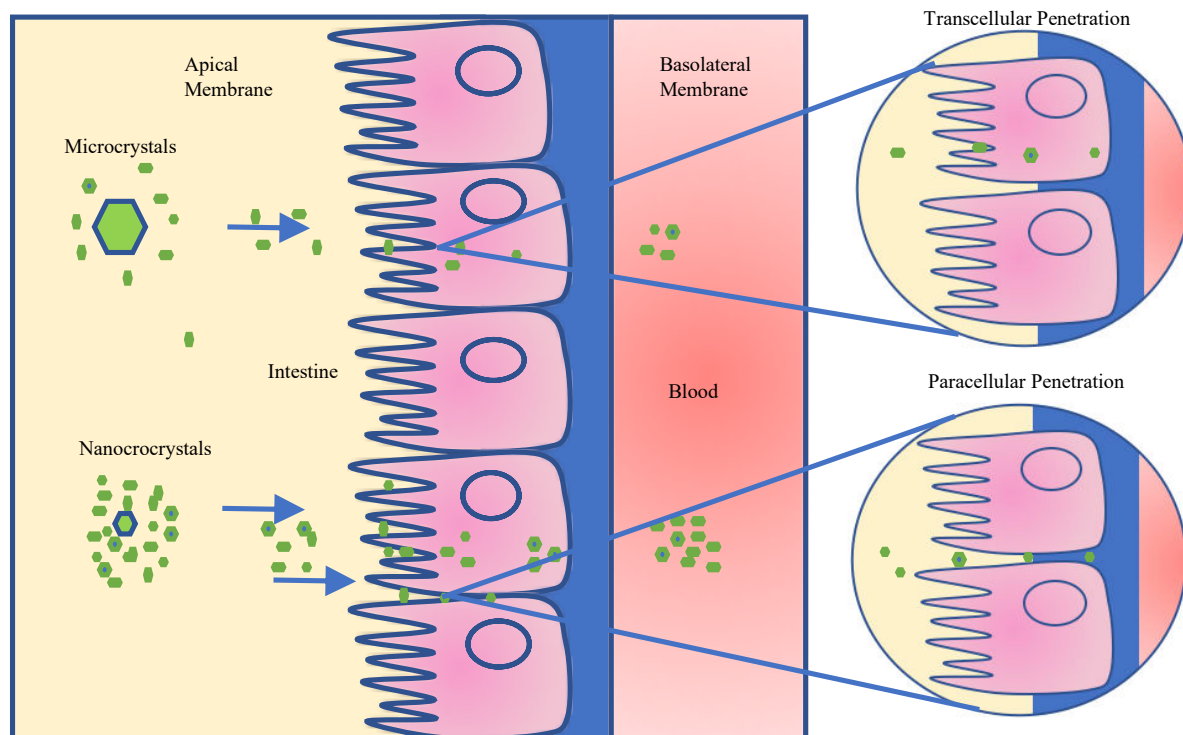


Figure 5 - Nanocrystals induce a high drug concentration gradient in the blood vessel compared to the microcrystal leading a better absorption of the active pharmaceutical ingredient.

In addition to the nanocrystal ability to go across the gastrointestinal epithelium, other researchers attributed the nanocrystal bioavailability enhancement to the inhibition of the P-Glycoprotein (P-Gp) in the apical membrane.^{80,81} More precisely, with the modulation of P-Gp efflux by surfactants added with the nanocrystal formulations. P-Gp efflux across the apical membrane can disturb the rate and amount of drug travelling across the basolateral membrane and passing in the blood circulation. Prakash put in the spotlight some common surfactants that impacts the P-Gp efflux and therefore the drug uptake, surfactants with an optimum hydrophilic-lipophilic balance give better flux pump inhibition than surfactants that are hydrophobic.⁸² For drug nanocrystals, studies are still required to figure out how the uptake pathway is done and what are the striking properties affecting it. Yet, many works have been done on metallic nanoparticles to understand the impact of particle size on their absorption on the intestinal epithelial cells.^{83–85}

Topical Delivery

Topical cancers include approximately 130,000 melanoma skin cancers and 3 million non-melanoma skin cancers worldwide every year. Only, 10% of skin cancers lead to death (world health organization), that is minor in contrast with other fatal cancer such as lung cancer that counts more than 1.70 million deaths each year. However, NC technology still focuses on innovative drug development to overcome skin barrier to heal various topical diseases. Skin is formed with multitude of layers protecting external agents to cross through. Epidermis is the first layer itself made of four coats, the stratum germinativum, spinosum, granulosum and corneum. Dermis is the second protection composed of tight tissues.⁸⁶ There are two ways to bypass skin barriers, the first one, is the trans-epidermal way, the second one, the appendages way (hair follicle, sebaceous gland), represented in Figure 6.⁸⁷

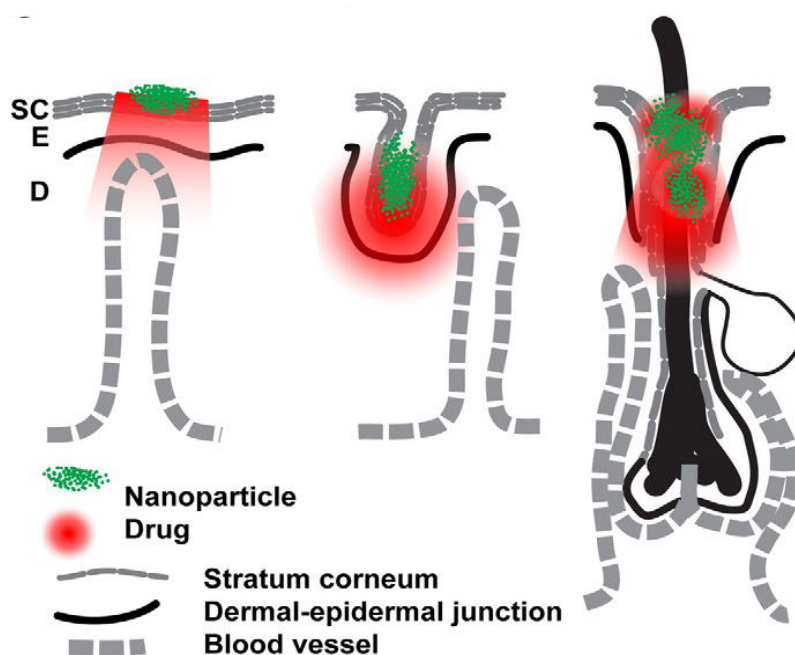


Figure 6 - Drug nanoparticle delivery using transdermal and appendages way. Three main localizations: stratum corneum (SC), epidermis (E) and dermis (D).⁸⁷ Copyright[®] 2019 reused with permission from Elsevier.

Pelikh *et al.* observed the NC size dependence for skin penetration. Hesperetin NCs with diverse size were made using bead milling and HPH. The NCs dermal penetration was determined following a tape stripping procedure, then removed and dosed by HPLC. The upshots clearly supported that reduced sizes increase the passive diffusion through skin of poorly soluble compound and promote penetration into deeper skin layer. For comparison,

hesperetin NCs with the size under 200 nm had 10% of the total applied amount in deeper tissues whereas only 5% of 700 nm-NCs were found. For most formulations, the choice of excipients impacts the drug delivery, it has been found for hesperetin NCs dermal penetration that glycerol, urea, propylene glycol, hydrogel or ethanol, strongly affects the drug permeation as they foster the hydrophilic pathways, hence preventing the delivery of poorly water-soluble ingredient. Only about 10% of the drug penetrated into the skin with glycerol, propylene glycol, compared to 55% drug penetration with suitable excipient.⁸⁸ Also, the skin drug penetration profile depends on the concentration, Vidlárová *et al.* confirmed this feature using curcumin NCs as model produced by milling and HPH. Four formulations were studied (2%, 0.2%, 0.02%, and 0.002% by weight volume) on porcine skin and pictured on confocal microscopy. All formulations showed clear penetration enhancement as regard to the “classic” topical formulation where the drug is dissolved. The main hypothesis brought to the table to explain the outcomes was the NCs high concentration gradient giving a strong driving force to the drug and therefore a deeper skin diffusion.⁸⁹ Even though, NCs technology for topical delivery are rarely developed compared to other nanoparticles, studies have shown that NCs preparation often outperformed conventional formulation used on market and should be further advanced in next years.

Ophthalmic Delivery

The sensitivity and complexity of eye offer a challenge for drug NCs formulation as the eye reduces significantly the drug bioavailability as compared to oral or parenteral route. Usually less than 5% of nanomedicines intraocular bioavailability is expected through ophthalmic delivery.⁹⁰ As some ocular diseases necessitate high drug concentration at the site of interest, it is also fundamental to explore new strategies to meet this need. The nature of eye tissue requires two fundamentals parameters to enhance bioavailability, the drug retention time and the drug permeability.⁹¹ Two features that NC technology can impact. Thus, Ahuja *et al.* studied and compared ICN NC with the ICN marketed product for ocular delivery, a notably higher cumulative permeation of ICN NC (1% w/v) through the goat cornea was evidenced. The NC formulation offer 1.73-fold superior corneal permeability with the conventional marketed formulation, as NCs have particles in the nano-size range fostering the crossing through the cornea.⁹²

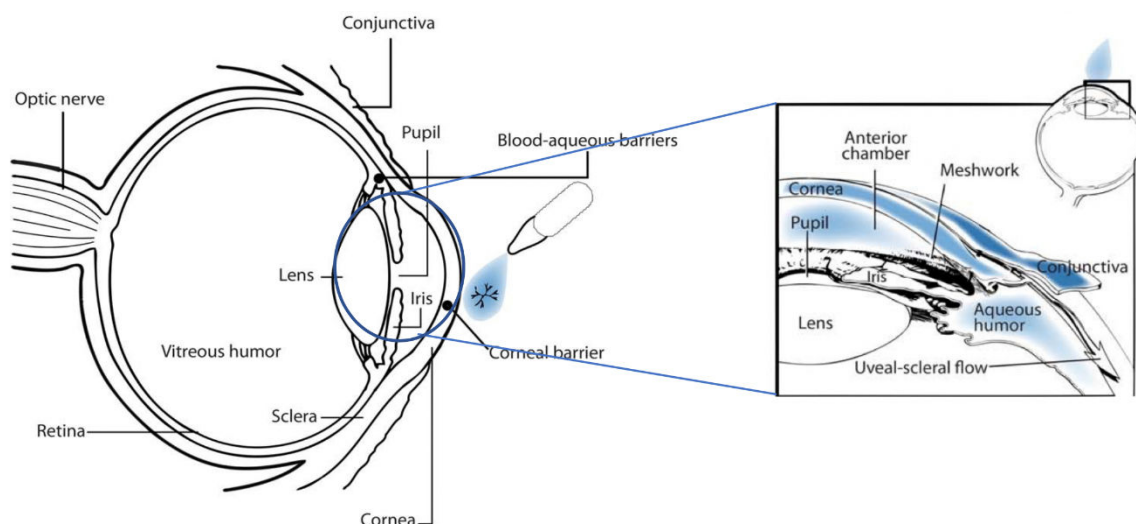


Figure 7 - Structure of Human Eye. Copyright[®] 2014 reused with the permission from Association for research in vision and ophthalmology.

Tuomela *et al.* also formulated a NC-based drug preparation for ocular delivery and compared it in the matter of efficiency, intraocular pressure (IOP) and cytotoxicity on rat ocular hypertensive model with the usual ophthalmic product Azopt[®]. The analysis carried out 3 brinzolamide NC formulations engineered by wet milling using different polymeric surfactant (Pluronic F-127, Pluronic F-68, HPMC), each formulation presented similar toxicity *in vitro* on human corneal epithelia cells with Azopt[®]. NCs formulation killed 70 up to 85% cells viability after 5 min. incubation where Azopt[®] had 69%. The IOP is one of the main parameters to oversee after eyes laser treatment, the mean IOP were evaluated for all NC formulation, 55 to 71% of the IOP was decreased after 60 min. topical administration for brinzolamide NCs. Azopt[®] shown a lower reduction with 49%.⁹³ Pignatello *et al.* investigated another striking parameter that is the drug retention as the pre-corneal drainage on the eye is major problem for ocular drug delivery, considerably reducing drug bioavailability. ICN NCs suspension were added drop by drop on albino rabbits eyes after ocular trauma production. Conventional eyes drop formulation were used as control, NCs were able to prevent the contraction of constrictor muscle of the eye (miotic response) and give sustained release of the drug resulting in greater drug concentration in the aqueous humour, 18 $\mu\text{g}/\text{mL}$, compared to 13 $\mu\text{g}/\text{mL}$ for ICN control.⁹⁴

Parenteral delivery

Intravenous injection is recommended when a drug is not ingested by the digestive tract or when disease treatments require i.v. delivery, as chemotherapy. In oncology, i.v. administration route is preferred when oral forms present unpredictable bioavailability, or side effects, but also in the case of targeted therapies.⁹⁵ Additionally, self-administered chemotherapy drugs efficiency highly depends on patient adherence.⁹⁶ Owing to the nanoscale range, crystal nanoparticles are suitable for parenteral (e.g. intramuscular, transdermal, i.v.), enteral, pulmonary, ocular and transdermal administration routes with faster pharmaceutical effect. Indeed, one of the other advantages of nanocrystal-based drug formulations is that they can be administered whatever the administration route since they are much smaller than the smallest blood vessel diameter of the human being. Regarding the i.v. route, the carrier system will not have to go through the gastrointestinal barrier resulting in higher bioavailability and reduced dosing. Also, i.v. NCs delivery does not require an excess of excipient that may give rise to side-effects for the patient. In the case where drug NCs are dissolved immediately after administration and before hitting the target, thus the nanosuspension will mainly show a solution-like behavior.⁹⁷ Otherwise, whether the nanocrystalline suspension keep its integrity after injection, biodistribution following i.v. injection will be mainly governed by particle shape, size and surface properties.

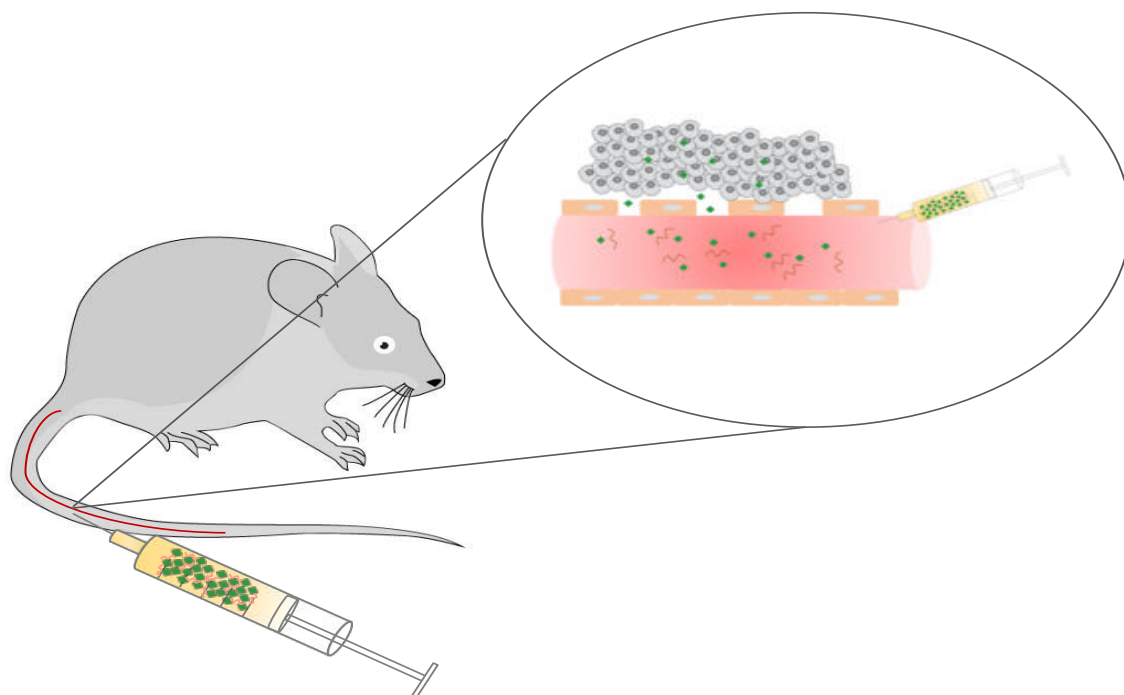


Figure 8 – Stabilized nanocrystals intravenously injected to the mice tail vein and then accumulated to the tumor due to the EPR effect.

Hao *et al.* assessed the *in vitro* anticancer efficiency and *in vitro* biodistribution of 275 nm Amoitone B NCs compared to the free molecule. Experiments were conducted on several cell lines, BGC-823, colon cancer SW620, liver cancer HepG2 cells and lung cancer H460, Amoitone B were added at the concentration of 1-40 $\mu\text{g}/\text{mL}$. After 72 hours, Amoitone B NCs had better cells cytotoxicity than free Amoitone B. IC_{50} were lower with 6.76 ± 0.80 , 6.93 ± 0.76 , 10.03 ± 0.63 , 9.74 ± 0.70 $\mu\text{g}/\text{mL}$ for BGC-823, SW620, HepG2, and H460 respectively, whereas for the free Amoitone B, IC_{50} were 10.38 ± 0.97 , 10.63 ± 1.03 , 13.58 ± 1.12 , 13.90 ± 1.27 $\mu\text{g}/\text{mL}$. The NCs biodistribution after i.v. administration showed higher AUC values in liver and lung were 2.32-fold and 1.50-fold greater than free molecule and a lower concentration in heart and kidneys, thus decreasing side effects.⁹⁸ A desired effect for cancer treatment is the sustained released of drug, reinforcing therapeutic potency and reduced systemic toxicity. Liu *et al.* evidenced a better *in vivo* efficacy against ovarian cancer model with Paclitaxel (PTX) NCs stabilized by TGPS at 10 mg/kg in comparison with Taxol[®] (clinical PTX formulation). Taxol[®] administered at the same concentration was ineffective to hinder tumor growth in contrast with PTX NCs that had significant tumor regression explained by a better cancer cells internalization of the NCs. The aqueous dispersed solid state properties of NC provides a slow release of the API increasing its blood circulation time, and therefore a better targeting.⁵²

Passive and active targeting delivery

Drug targeting refers to a way to enhance the concentration of the drug in the specific site of interest in the human body (tissues and organs). The driving forces to deliver the drug are complex and diverse. For the majority of drugs, their selection is made according to their aptitude to be efficient against a specific disease, the consideration of drug accumulation in the desired area is often overlooked. For most of treatments, the route of administration is chosen to improve the drug accumulation in the targeted tissues and overcome straight natural barriers. However, whatever the administration route used, the drug spreads out in the human body correspondingly with the blood stream flow, therefore medical treatments augment the drug dose to foster the odds of accumulation in the desired region. It implies higher treatment cost, higher systemic toxicity and hence poor quality of life of the patient. Considering these difficulties, there is a strong need to achieve better targeting. Two concepts have to be considered for a better drug targeting, the first one is the features of medicine used including physical state, size, shape, charge surface, therapeutic carrier and so forth. The second one is the features of the therapeutic site of interest, such as specific biological barriers, tumor vascularity and epithelial dilatation surrounding diseases tissues. The modification of the endothelium allows nanoparticles to pass through and reach cancer tissues by diffusion (Fig. 9). This passive targeting effect, otherwise known as the enhanced permeability and retention (EPR) effect, was initially proposed by Maeda *et al.* in 2000.⁹⁹

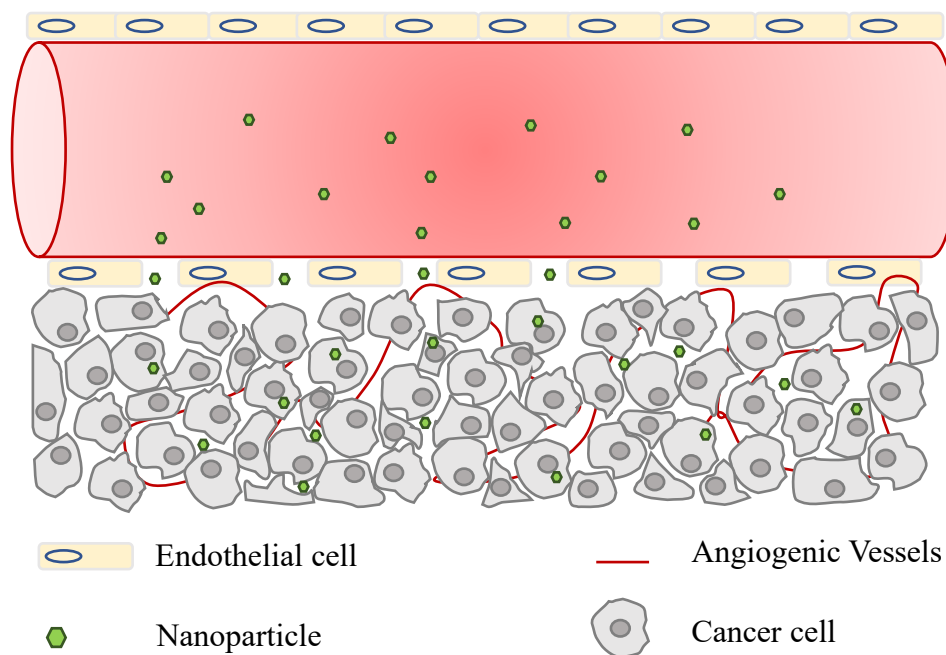


Figure 9 - Illustration of the EPR effect: nanoparticles can shed out into the tumors through the endothelial cells junction.

Studies by Hollis and coworkers, compared the EPR effect on human HT-29 colon cancer xenograft murine model, for both solubilized and NCs formulation of paclitaxel, and found that PTX NCs were as effective as the conventional solubilized formulation with reduced toxic effects.¹⁰⁰ This result confirms that the NC approach is promising for cancer therapies.

However, it has been observed that, once administered intravenously, nanoparticles gather essentially in the tissues of the reticuloendothelial system (liver, spleen). This observation can be explained by a huge specific surface area of nanoparticles on which many plasma proteins, especially opsonins will adhere to the nanoparticles surface. The formation of the protein corona surrounding nanoparticles relies on size, shape, crystallinity, surface instability, hydrophobicity and electronic states.¹⁰¹ Following protein adsorption, nanoparticles are selectively recognized by the macrophages, then internalized and carried to phagosomes and fused with lysosomes.¹⁰² Therefore, a balance between all these parameters is crucial to increase the nanoparticle lifespan in blood circulation to foster the EPR effect. Another way to overcome the recognition by the mononuclear phagocyte system is to dress up the nanoparticle surface to repel these opsonins. Hence, there will be both a selective targeting effect but also, an accumulation effect in the tumor tissues due to the EPR effect.

Today, brand new nanoparticles formulation assimilates the approach of active targeting, which increases the specificity for a precise site. It is primordial to associate with the surface of the nanoparticle molecules such as polymers, acids, proteins, peptides and so forth, which will specifically be identified by receptors present on cancer cells. To understand the impact given by functionalized nanocrystals, Park and coworkers compared the ability of several coated-paclitaxel (PTX) NCs with a conventional Alb-based PTX formulation to treat B16F10 melanoma in mouse. It has been shown that PTX NCs with and without Alb present higher antitumor efficacy compared to Abraxane® at the equivalent dose.¹⁰³ The use of proteins as stabilizers is an encouraging approach as well as their ability to attach on membrane proteins in tumor cells.¹⁰⁴

Likewise, coated-NCs with selective surfactants or polymers, such as sodium dodecyl sulfate, hydroxypropyl methyl cellulose or polyvidone are valuable to improve oral bioavailability, and such surfactants offer steric hindrance, avoiding NCs aggregation and growth.^{105,106} In another study, NCs surface of docetaxel (DTX) has been modified with PEG-modified (pLNS-DTX) and folic acid (tLNS-DTX). Wang and coworkers demonstrated that the cytotoxicity of tLNS-DTX against B16 cells (folate receptor positive) were more efficient than pLNS-DTX, inferring that NCs surface modification is essential to specifically delivery a drug.¹⁰⁷ Tuomela and coworkers investigated the selection of suitable stabilizers, their stabilizing effect, their role in final formulations, difficulties in achieving *in vitro* and *in vivo* delivery. Furthermore, the study presented some NC-API/stabilizer association cases, and also looked into the stabilizer outcomes for higher bioavailability of the drugs.¹⁰⁸

As we previously discussed, solubility enhancement of poorly water-soluble drugs is a major challenge in the pharmaceutical field, as 70% of drugs exhibit low solubility. Modulation of the solid state of pharmaceutical ingredients as function of intermolecular interactions (*e.g.* co-crystallization, polymorphism), chemical modification (*e.g.* solvatomorphism, salt formation), or physical modification (*e.g.* amorphization, particle size reduction) has afforded many opportunities to enhance the bioavailability of some APIs. For a decade, research into NC preparations for drug delivery has driven significant growth in the pharmaceutical field, as it offers several advantages and value. NCs formulation is one of the recent techniques developed to improve dissolution rate, solubility, and therefore the bioavailability of active ingredients, while increasing drug-loading capacity. Moreover, NCs can be administrated through all routes — pulmonary, ocular, transdermal, enteral and parenteral — and provide better performance in

terms of safety, targeting efficiency, pharmacodynamics, and pharmacokinetics than any other drug formulations. One of the main drawbacks of nanomedicines is their persistence in the human body, fostering the risk of toxicity. The outlook regarding the development of NCs should focus on such undesirable toxicity, which could be avoided by improvements in targeted delivery and clearance from the body. To do so, functionalized nanocarriers may be conceptualized for NCs encapsulation. This would allow prevention of systemic administration of the API by targeting the diseased tissues. Thus, the drug would be released with a faster dissolution profile only after opening of the nanocarrier is triggered. Furthermore, by combining crystallization techniques at the nanoscale level to different solid-state organizations, it may drastically improve the bioavailability of APIs for optimized targeted delivery.

Nanocrystal overview

There are plentiful examples in the literature where precipitation, HPH and ball milling methods were used. Even if nanocrystal definition is not well harmonized in the literature, Table 3 shows an overview of the smallest drug nanocrystal manufactured with these technologies using stabilizers. The choice of stabilizer is essential as it influences nanocrystal size and shape. Once, the nanocrystal growth is stopped, stabilizer is strongly associated to the nanocrystal giving it its solubility in a wide range of solvents. Surfactants must be used for both synthesis of nanocrystals and long-term stability during storage.

Table 3 – Examples of pharmaceutical drug nanocrystals prepared by common wet ball milling (WBM), HPH and spray drying

Drug	Type	Technology	Stabilizer	Particles size (nm)	References
1,3- Dicyclohexylurea	Anti-ischemic	WBM	Polysorbate 80	800	109
Acecoflenac	Anti-inflammatory	Precipitation	PVP-K30/HPMC-E5/Sodium Lauryl Sulfate (SLS)	112 - 930	110
Albendazole	Treatment of parasitic worm	HPH	Poloxamer 188	415	111
ALS - 3	Treatment for Amyotrophic Lateral Sclerosis	WBM/Spraydrying	Poloxamer 188/PVPK30/HPMC	300	112
Amoitone B	Antitumoral	HPH	Mannitol	275 ± 8	98
Amphotericin B	Antibiotic	HPH	None	528	113
Aprepitant (MK-069)	Anti-nausea/Anti-vomiting	WBM	With surfactant	120	114
Aripipazole	Antipsychotic	Precipitation	HPMC-E5/Poloxamer 188	450 - 500	115
Ascorbyl palmitate	Antioxidant/ Vitamin C Derivative	HPH	Sodium Dodecyl Sulfate (SDS)	365	116
			Polysorbate 80	348	
Asulacrine	Antitumoral	HPH	Poloxamer 188	133 ± 20	117
Avanafil	Erectyle Dysfunction	Precipitation	Poloxamer 188/Polysorbate 80	128 - 4868	118
AZ68	Schizophrenia Treatment	WBM	PVD/Disodium Salt	125 ± 30	119
Azithromycin	Antibiotic	HPH	Poloxamer 188/Polysorbate 80/Lecithin	400	120
Baicalin	Anxiolytic	HPH	Polysorbate 80/Poloxamer 188/Poloxamer 407/TPGS	200 - 500	121
Bexarotene	Antineoplastic	Precipitation/HPH	Poloxamer 188/Lecithin	200	122

Breviscapine	Anti-inflammatory	Precipitation/Freeze Drying	Poly(lactic-co-glycolic acid)	239	123	
	Anti-inflammatory	Precipitation	Mannitol	440	124	
			Poloxamer 188	259	125	
			Lecithin/Polysorbate 85/Tyloxapol/Cetyl alcohol	599	126	
Budenoside		HPH	/	75 up to 300	127	
			/	less than 1 μm	128	
Bupravaquone	Antibiotic	HPH	Poloxamer 188/Lecithin	601	129	
		WBM	Poloxamer 338	202 \pm 30	130	
Camptothecin	Antitumoral	Precipitation	/	250	131	
			Polydopamine	80 - 150	132	
Candesartan cilexetil	Anti-ischemic	WBM	Poloxamer 338	128	133	
Celecoxib	Anti-inflammatory	HPH	Polysorbate 80	320	134	
			PVP/SDS	360		
			WBM	Hydropropyl Cellulose/Docusate Sodium	260	135
Cilostazol	Anti-platelet	HPH	HPMC (Methocel E15)	500 up to >1000	136	
			WBM	Hydropropyl Cellulose/Docusate Sodium	220	137
				TPGS	366 \pm 12	
Cinnarizine	Antiallergic/Antihistaminic	WBM	TPGS/HPMC	430 up to <1000	138	

Clofazimine	Antibacterial	HPH	Poloxamer 188/Phospholipon/Sodium Cholic Acid/Mannitol	650	139
			/	420	140
Curcumin	Antitumoral/Antioxidant	WBM	Polysorbate 80	924	141
		Precipitation/HPH	/	199	142
Cyclosporine	Anti-inflammatory/Immunosuppressor	WBM	Leucine	125	143
		WBM	Poloxamer 188	213	144
Danazol	Treat endometriosis	WBM/HPH	Sodium Cholate	962	145
		HPH	Poloxamer 407	300	146
Darunavir	Anti-VIH	WBM	Polyvinyl pyrrolidone- K25	169	42
		WBM/Electrospraying	Polysorbate 80/Poloxamer 188/Poloxamer 407/TPGS	295 - 1327	147
Dexamethanose	Anti-inflammatory	HPH		930	148
		WBM	Poloxamer F188	370	149
Diclofenac	Anti-inflammatory	HPH		< 800	150
		WBM	Poloxamer 188	279 ± 8	151
Docetaxel	Antitumoral	HPH	Lecithon/DSPE-PEG2000	204	152
			Lecithin/DSPE-PEG2000/DSPE2000-FA	221	
Doxorubicin	Anticancer	Precipitation	Poloxamer 407	383	153
		Precipitation	DSPE-PEG200	5	154
Efavirenz	HIV therapy	Precipitation	PVP K30/ Lutrol F-127 F128	161 - 5267	155
Fenofibrate	Lowering triglycerides	HPH	Poloxamer 188/PVP K30	356 and 194	156

			Vitamin E/TPGS	340	79
		Precipitation	Polysorbate 80/Polyethylene glycol/PVP K30/Tragacanth	> 1000	157
			Hydrogel	200 - 400	158
Glibenclamide	Antidiabetic	Precipitation	Poloxamer 188	429	159
Griseofulvin	Antifungal	WBM	Tocopherol polyethylene glycol 1000 succinate	256 ± 1	160
			Polysorbate 80	346 ± 30	
		HPH	Poloxamer 188	301 ± 17	161
Hesperetin	Antitumoral		Plantacare 2000	304 ± 30	
			Inutec SP1	304 ± 40	
		WBM/HPH	Polyethylene glycol 30	200	162
HPPH	Antitumoral	Precipitation	/	100 ± 20	163
		PU	Fetal calf serum	168 ± 3	66
			Lipoid S75/Poloxamer 188	283 ± 5	
Hydrocamptothecin	Antitumoral		Lipoid S75 + Solutol®	316 ± 13	
		HPH			67
			Poloxamer 188	345 ± 17	
			Lipoid S75	365 ± 3	
Hydrocortisone	Anti-inflammatory	WBM	PVP/HMPC/Polysorbate 80	295 ± 32	164
		HPH	Poloxamer 338	539	165

Ibuprofen	Anti-inflammatory	Melt-emulsification	Polysorbate 80	175	166	
Indomethacin	Anti-inflammatory	HPH	Polyvinyl pyrrolidone- K25	80 ± 10	48	
			Poloxamer 407	170 ± 30		
			Poloxamer 188	970 ± 30	167	
			Poloxamer 407	550 ± 20	167	
Itraconazole	Antifongic	HPH	Poloxamer 338	128	133	
			Polysorbate 20	677 ± 53	168	
			Spray Freezing	Polysorbate 80/ Poloxamer 407	200 up to 1000	169
			Precipitation	Poloxamer 407	267	170
Ketoconazole	Antifungal	WBM	Poloxamer 188/PVP K-30/Hydroxypropyl methylcellulose	164	171	
			Hydroxypropylcellulose/TPGS	147	172	
Ketoprofen	Anti-inflammatory	WBM	Sodium Lauryl Sulphate	265	173	
			Polysorbate 80/Poloxamer 188	156	174	
Loviride	Antiviral	WBM	Tocopherol polyethylene glycol 1000 succinate	156 ± 2	160	
Lutein	Prevention of age-related macular degeneration	Precipitation	Sodium Dodecyl Sulfate (SDS)/Soy phosphatidylcholine	377	175	
Mebendazole	Anthelmintics	WBM	Tocopherol polyethylene glycol 1000 succinate	190 ± 2	160	
Mefenamic	Anti-inflammatory	Precipitation	Hydroxypropylcellulose	106	176	
			DOSS	312	177	

Meloxicam	Anti-inflammatory	Precipitation	Polysorbate 80/Poloxamer 188/Poloxamer 407	180	178
Methyltryptophan	Inhibitor of the Tryptophan Catabolic Enzyme	Precipitation	Poloxamer 188/TGPS	150 up to 1400	179
Miconazole	Antifungal	WBM	Poloxamer 188/Poloxamer 407	355	180
Monosodium urate	Immune Regulator	Precipitation	DMEM 10%	26 - 137	181
MTKi-327 WBM	Antitumoral	WBM	Poloxamer 338/Lipoid S75/Glucose	195 ± 6	182
			Chitosan	250 ± 60	107
Naproxen	Anti-inflammatory	WBM	Poloxamer 188	270	183
			TPGS/HPMC	370 ± 60	138
			Poloxamer 188/Sodium cholic acid/Mannitol	650	184
Nimodipine	Anti-inflammatory/Anti-ischemic	HPH	Mannitol/ Maltose	159/503/833	185
Nisoldipine	Calcium Channel Blocker	WBM/Jet Milling	PVP-K30/HPMC-E5/SDS	240 - 1227	186
Olmesartan Medoxomil	Angiotensin II Receptor Antagonist	Precipitation/HPH	TPGS/Polysorbate 80	140	187
Omeprazole	Anti-inflammatory	HPH	Poloxamer 188	500	58
			Polyvinyl pyrrolidone- K25/Lecithin	913	188
Oridonin	Antitumoral	HPH	Poloxamer 188	897 ± 14	189
		HPH/WBM	Poloxamer 188/Lecithin	103 ± 2	190
			Transferrin	303	55
Paclitaxel	Antitumoral	Precipitation	Polysorbate 80	5	191
			Poloxamer 407/DOSS	194	192

			Poloxamer 407	150 up to 200	103
			Cyclodextrin	263	179
			Poloxamer 127	200	193
		3PNET	TPGS	150	52
			Poloxamer 407	122	194
		HPH	DOTAP	160 ± 10	195
		EPAS	TPGS	135	196
			Chitosan	330 ± 90	107
		WBM	Poloxamer 407	279	130
			Poloxamer 188 (nontargeted)	182	197
PIK-75	Antitumoral	HPH	Poloxamer 188-folic acid (targeted)	161	148
Piposulfan	Antineoplastic	WBM	Polysorbate 80	210 ± 38	148
Prednisolone	Anti-inflammatory	HPH	Poloxamer 188	211	198
Pueranin	Antitumoral	HPH	Lecithin/HPMC	481 ± 23	199
PX- 18	Neuroprotector	HPH	Polysorbate 80	40 - 980	200
			Polysorbate 80	203 ± 20	
		HPH	Poloxamer 188	153 ± 40	
Resveratrol	Anti-oxydant		Plantacare 2000	169 ± 20	
			Inutec SP1	216 ± 30	
		WBM	Poloxamer 188	304 ± 3	201
			Polysorbate 80	225 ± 35	
Riccardin	Antitumoral	EPAS	Poloxamer 188/PVPK30/HPMC	184	202
		HPH	Poloxamer 188/PVPK30/HPMC	815	
RMKK98	Anti-inflammatory	HPH	Poloxamer 188/Polysorbate 80/Sodium cholate	913	203

RMKP22	Antitumoral	HPH	Polysorbate 80/Glycerol	502	69
Rutin	Antioxidant/ Anti-inflammatory	HPH	Polysorbate 80/Poloxamer 188	721	204
Silybin	Antitumoral	HPH	Lecithin/Poloxamer 188	127 up to 642	198
Simvastatin	Cholesterol Lowering	HPH	Polyvinyl pyrrolidone- K25	360 ± 30	48
			Poloxamer 407	1140 ± 6	
Spironolactone	Treat fluid retention	HPH	Polysorbate 80/Water	400	205
Tarazepide	Antiplasmodic	HPH	Poloxamer 188/Polysorbate 80	400	206
			HPMC (Methocel E15)	182 ± 7	
Ubc-35440-3	Antiallergenic/ Asthma	HPH	Polyvinyl alcohol	262 ± 54	43
			Acaciae Gum	407 ± 6	
			Poloxamer 407	183 ± 3	
UG558	/	WBM	HPMC (Methocel E15)	190	207
Ziprasidone	Antipsychotic	WBM	Poloxamer 407	200 - 1000	208

Precipitation ultrasonication (PU). Three-phase nanoparticle engineering technology (3PNT). Evaporative precipitation into aqueous solution (EPAS)

Drug Nanocrystals on the market

Drug nanocrystals have been investigated and improved since the 1990s. NCs have various indications in the area of pharmaceutical sciences (*e.g.* anti-emetic, anti-psychotic, immunosuppressive, asthma). Yet, none of these formulations are indicated to treat cancer. Today, 11 nanocrystal formulations can be found on the market: 9 as oral pharmaceutical forms, and 2 as injectables pharmaceutical forms (Table 4).

Table 4 - List of marketed nanocrystals from 2002 to 2014 (9 oral pellets, 2 i.v. suspension)

Trade name	Drug	Indication	Pharmaceutical form	Route	Corporation	FDA
Zanaflex [®]	Tizanidine HCl	Muscle Relaxant	Pellets	Oral	Acorda	2002
Ritalin LA [®]	Methyphenidate HCl	Hyperactivity Disorder	Pellets	Oral	Novartis	2002
Emend [®]	Aprepitant	Anti-emetic	Pellets	Oral	Merck	2003
Invega Sustenna [®]	Paliperidone palmitate	Anti-psychotic	Suspension	IV	Janssen	2009
Megace ES [®]	Megestrol	Anti-anorexic	Suspension	Oral	Par Pharmaceutical Companies	2005
Tricor [®]	Fenofibrate	Hypercholesterolemia	Pellets	Oral	Abbott	2004
Triglide [®]	Fenofibrate	Hypercholesterolemia	Pellets	Oral	Sciele Pharma Inc	2005
Naprelan [®]	Naproxen Sodium	Anti-inflammatory	Pellets	Oral	Wyeth	2006
Rapamune [®]	Rapamycin	Immunosuppressive	Pellets	Oral	Wyeth	2000
Theodur [®]	Theophylline	Asthma	Pellets	Oral	Mitsubishi	2008
Ryanodex [®]	Dantrolene Sodium	Malignant Hyperthermia	Suspension	IV	Eagle Pharmaceutical	2014

Etoposide

Production

Etoposide (ETO), also called VP-16, is known as a semi-synthetic derivative of podophyllotoxin that is recovered from *Podophyllum peltatum* dried roots mainly found in the North of America. ETO was synthesized from podophyllotoxin for the first time in 1966 (Fig. 10).^{209,210}

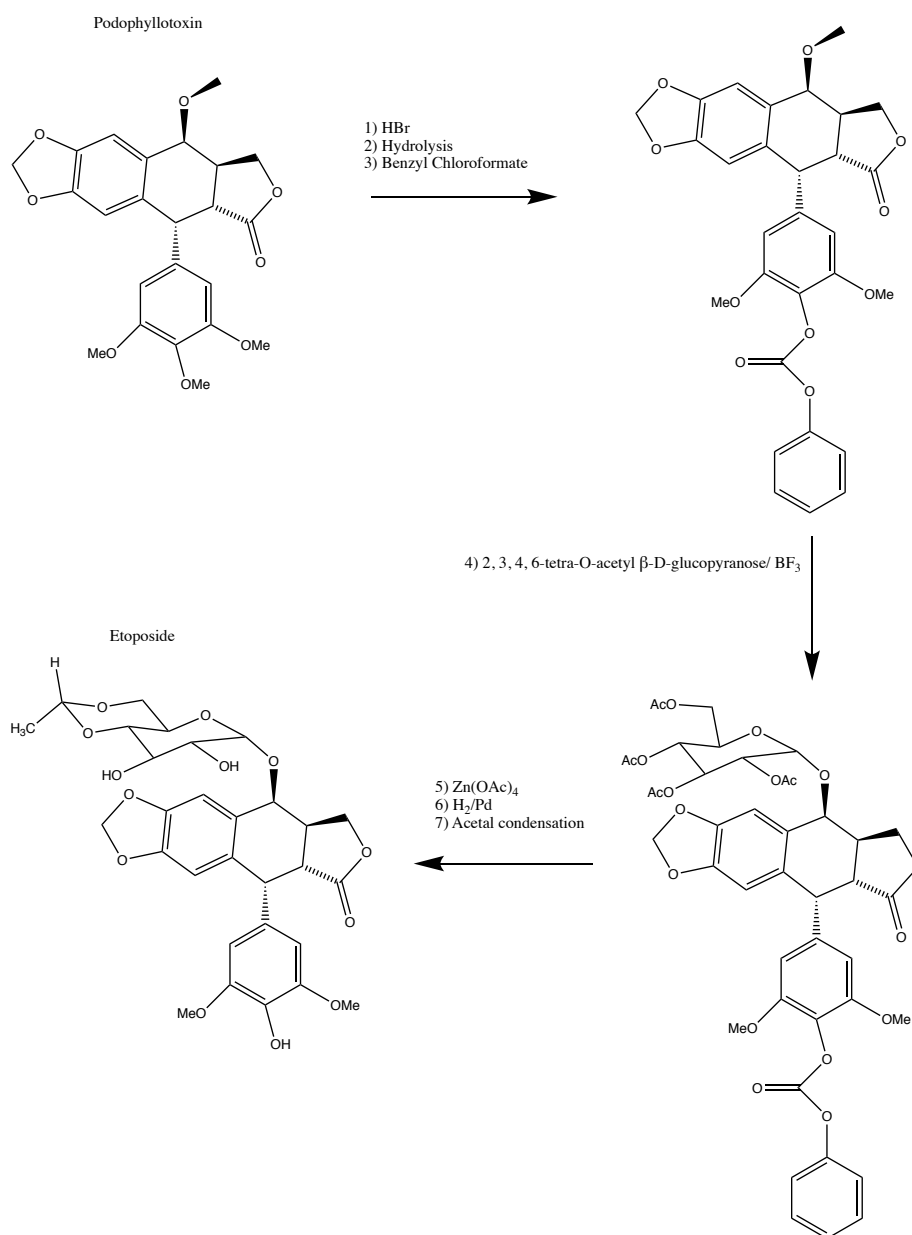


Figure 10 - Synthesis of etoposide from podophyllotoxin.

It has a relative molecular mass of 588.57 g/mol, it is a poorly water-soluble compound in water (< 0.01 mg/mL), slightly soluble in ethanol and highly soluble in methanol, chloroform and dimethyl sulfoxide (> 100 mg/mL). The raw ETO is a white crystalline powder that melts around 235 – 250 °C. ETO inhibits the enzyme topoisomerase II that is crucial to control the DNA conformational arrangement by generating double-strand break in the DNA molecule (Fig. 11).²¹¹ Cells death is induced when sufficient covalent topoisomerase-split DNA complex are formed and stabilized, giving durable DNA strand breaks, swamping cells metabolic activity to apoptosis.²¹²

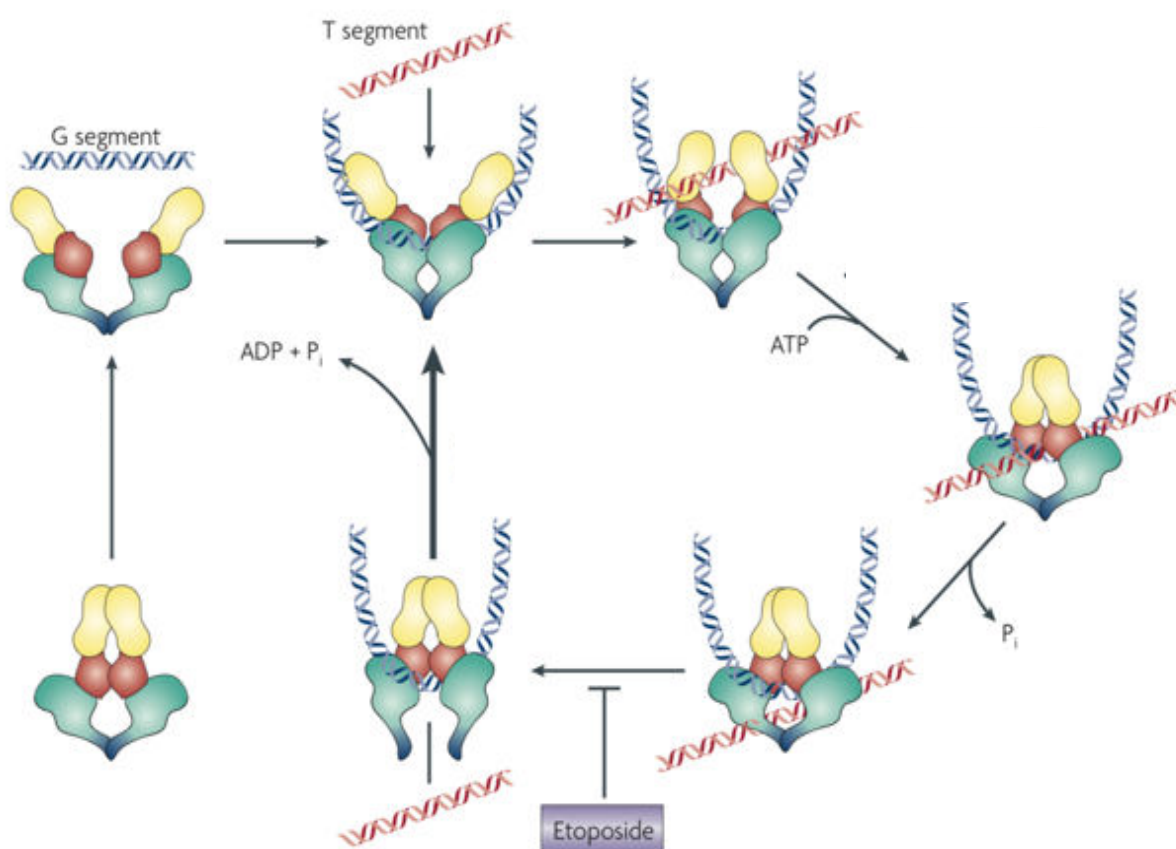









Figure 11 - Topoisomerase II mechanism of action. Topoisomerase II binds a DNA duplex (G segment), followed by the linking of adenosine triphosphate (ATP) to the two N-terminal extremity. This conformational modification conducts to the separation of both strands of the G segment and also to the hookup of the T segment. The T segment drives to the G segment break and then leaves the enzyme. The process restarts after the hydrolysis of ATP in adenosine diphosphate (ADP) that resets the topoisomerase II with the G segment still linked. Etoposide is lately obstructing the catalytic cycle after DNA is cut but ahead of DNA re-ligation. Picture used from reference²¹² with copyright permission. Copyright® 2019 Reused with permission from Springer.

Etoposide-based marketed products

Seven marketed products of ETO can be found on the market, 7 injectable solutions and 1 parenteral as capsules (Table 5). For all solutions, the medicine is contained in a 25 mL vial, each milliliter contains 20 mg ETO, 2 mg citric acid anhydrous, 650 mg polyethylene glycol 300, 80 mg polysorbate 80 and 33% absolute ethanol. Recommendations preconized to dilute the solution at 0.2 to 0.4 mg/ml to avoid precipitation up to 24 hours at 15 – 25 °C. Excipients provide stability overtime and long lifespan in the blood stream but also increasing undesired effects. Oral capsule (Mylan) are composed of gelatin colored with pink with glycerin, iron oxide, anidrisorb and titanium oxide. Each capsule contains 50 mg dose of ETO followed with anhydrous citric acid, polyethylene glycol and water.

Table 5 – Seven injectable etoposide-based marketed products provided by West Ward, Accord Healthcare, Watson Labs Inc, Mylan, Teva, Fresenius). One parenteral Etoposide marketed products provided by Mylan

Trade name	Pharmaceutical form	Laboratory	Logo
Etoposide	Injectable	West-Ward	
		Accord Healthcare	
		Watson Labs Inc	
		Blue Point Laboratories	
	Injectable / Capsule	Mylan	
Toposar [®] (or Vepesid [®])	Injectable	Teva	
Fytosid [®]	Injectable	Fresenius Kabi	

Etoposide-based cancer studies

ETO has been evaluated as a single or synergic anticancer agent in a various type of cancer since the early 1990s, as its high cancer cells cytotoxicity, human mild toxicity and low-cost production that make this drug a good fit for a wide chemotherapy treatment. Loehrer *et al.* assessed the efficiency of ETO as a first line treatment for refractory germinal neoplasm patient (testicular area).²¹³ Three patients denoted as group I, were prescribed with a single dose of ETO at 100 mg/m² for 30 minutes daily for 3 up to 5 days (according to the patient hematologic acceptance) every 3 weeks. Twenty-two patients denoted as group II, received ETO at 20 mg/m² over 30 minutes for 5 days every 3 weeks, then followed by i.v. injection of Adriamycin at 40 – 50 mg/m² every 3 weeks, then i.v. injection of Bleomycin 30 mg/m² weekly for 12 weeks. For group I all subjects had a partial response to the treatment. For group II, 9 patients had a complete response (42.9%), 9 other patients a partial response (42.9%), and the last 4 a partial response sufficiently effective to perform a surgical ablation of the tumor. As a matter of fact, the latter patients were completely healed after the surgical procedure; therefore 13 cases were cancer-free thanks to the therapeutic treatment. Despite promising results, conventional chemotherapies display high blood and healthy organ toxicity leading to collateral harms for patients. This research proved the ETO ability to heal testicular neoplasm and highlight the synergic effect of anticancer drug. As discussed, ETO is often used in second line treatments where patient have undergone and failed a previous treatment. The department of medicine from Texas Tech University carried out a phase II study with ETO on metastatic breast cancer patients, firstly treated with cyclophosphamide, methotrexate, fluorouracil and doxorubicin but a progression of the breast cancer was identified for all patients. For the 30 cases, after ETO therapy comprised of oral ETO at a dose of 50 mg/m² per day given for 21 days in a row. One complete and 4 partial responses were observed (19% objective response), 6 with no progression of cancer and 15 without response and toxicity appeared for 24% of subjects characterized with thrombocytopenia and neutropenia. Administered ETO orally is an acceptable, effective and undoubtedly a mere chemotherapy procedure that may enhance patients with metastatic breast cancer.²¹⁴ Oral administration of ETO has been also verified versus non-small cell lung cancer (NSCLC) and compared with standard i.v. administration (cyclophosphamide, doxorubicin, vincristine or ETO, vincristine) by Dr Thatcher. N *et al.* From September 1992 to August 1995, 171 patients received 50 mg orally of ETO twice per day for 10 days every 3 weeks repeated 4 cycles; 66 patients were administered intravenously for 1 to 3 days, ETO 120 mg/m² over 30 min. and vincristine 1.3 mg/m², 102 received a single i.v.

injection of cyclophosphamide 750 mg/m², doxorubicin 40 mg/m², and vincristine 1.3 mg/m². For oral ETO, 41% had a cancer regression, 4% no change, 10% had a cancer progression and 45% died. In parallel, for standard procedure, 6% presented a cancer regression, 9% no change, 13% a cancer progression and 33% died.²¹⁵ Suggestions following this research recommend not to use ETO orally as a single agent for SCLC and that i.v. ETO in combination with anticancer agent should be preferred.

Likewise, certain studies unusually tried out ETO with different cancer such as thyroid cancer to assess the response of patients. Leaf *et al.* evaluated the toxicity and activity of ETO against inoperable carcinoma thyroid cancer on ten 65 years old patients.²¹⁶ All patients had inoperable medullar, anaplastic, sarcoma or squamous carcinoma, also patients with previous radiation chemotherapy were disqualified to not alter the outcome reliability of treatment. ETO was injected at the concentration of 140 mg/m² for 3 days in a row every 3 weeks. The injected dose was modified according to the white blood cells, 50% of the dose whether the WBC were comprised between 2000 and 4000 per mm³, the chemotherapy was stopped whether the WBC were under 2000 mm³. The experiments did not show benefits for patients with thyroid cancer, mainly explained by the lack of drug accumulation into the site of interest, 50% died after 8 – 10 months, 20% died after 1 – 2 months, only 30% of patients presented long survivals up to 45 months. This minor positive effect on patients was attributed more to the environmental history of the cancer than clear-cut consequences of the chemotherapy.

Indications

ETO is largely used as a cytotoxic agent against testicular, lymphomas, ovarian, small cell lung, colon and breast cancer. Strongly efficient in cases of lung cancer,²¹⁷ it is rarely used as a single anticancer agent and is often combined with Cisplatin, Bleomycin, Adriamycin or Doxorubicin.²¹⁸ It is the only drug that is used to treat refractory cisplatin cancer patients.²¹⁹ Regarding other cancer such as kidney, pancreatic or gastric cancer, ETO is less commonly used for these cancers but can still be employed in patients that were unsuccessfully treated with the adapted first line treatment. The accomplishment of the ETO cancer treatment is timetable dependent and prolonged ETO exposures of 2 up to 5 days being more efficient than a single administration.²²⁰ In the hospital, ETO is often administered as a one-hour administration intravenously. Its maximum dosage is about 500 mg/m² every 3 weeks. Repeated administration over 3 to 5 days increases antitumor activity significantly and the commonly dose is then 60 to 120 mg/m² per day. Severe protocols use the dose of 200 mg/m²

per day up to the 400 mg/m² dose per day in transplantation conditioning. ETO can also be used orally, its bioavailability being close to 50%.²²⁰ It is prescribed intermittently, 80 to 300 mg/m² per day for 3 to 5 days, or continuously at 50 to 100 mg/m² per day for 21 days in a 4-week cycle.²²⁰ For most of anticancer agents and in this case ETO, drug administration schedule is fundamental as it bounds with the topoisomerase II that is overexpress during mitosis while cells are dividing.²²¹ Thus, long-lasting scheduling is preferable as it augments the probability of ETO to interact with cancer cells during crucial steps of the cell cycle. If the ETO is eliminated, the topoisomerase II-ETO bound is reversed leading to fast DNA reparation and cells surviving. Hence, chronic administration of ETO reinforces the lifespan of these links, prolonging the DNA strand breaks leading to apoptosis. Clark *et al.* compared in 1994 the superiority of two ETO long term treatments, 5 and 8 days, with 24 hours infusion in patients diagnosed with small cells lung cancer. Ninety-four patients were randomized and received ETO for 24 hours with one dose at 500 mg/m², for 5 days, 2 hours infusion of 100 mg/m² and for 8 days, 75 minutes infusion at 62.5 mg/m². The overall patient response was only 10% for the 24 hours protocol, whereas for both ETO prolonged treatments, 81% and 87% patient response were obtained for 5 and 8 days treatment respectively.^{222,223} Clinical studies have emphasized the influence of long-lasting administration schedule for enhancing and delimiting the therapeutic index of ETO. However, optimal treatment of the drug is still up to date to reduce side effect and ameliorate patient responses.

Nowadays, 103 active clinical trials can be found for ETO adapted and based on previous results obtained from the 1990 to 2019. Twenty-two clinicals trials phase I, 65 clinical trials phase II, 24 clinical trials phase III, most of them use ETO as a synergic drug and have the objective to evaluate the progression of ill patients regarding the overall survival or cancer recurrence. Table 6 gathers ETO clinical trials over all phases.

All of them collect information about dosage, survival, wellbeing, secondary effects, efficiency and long-term risks against typical ETO-prescribed cancer (*e.g.* lymphoma, SCLC, Hodgkin's, testicular, breast or glioblastoma). Conventionally, brand-new regimens have to be experienced on all phases before coming in hospitalization procedure. Conclusive outcome of these trials would absolutely quicken the application of cutting edges technologies regularly, while unfavorable outcomes allow to exclude poor strategy. As for a lot of study, it is unlikely that any of these try out will result in a novel therapy to treat cancer. Hence, the development of advanced nanomedicines is still needed to have a breakthrough concerning cancer treatment.

Table 6 - Summary tables and detailed descriptions of Etoposide clinical trials for a large variety of cancer

n°	Clinical trials	Goals	Cancer type	Phase
1	Ixazom Mitoxantrone Hydrochloride, Etoposide, and Intermediate-Dose Cytarabine in Relapsed or Refractory Acute Myeloid Leukemia	Studies the side effects and best dose of ixazomib when given in combination with mitoxantrone hydrochloride, etoposide, and intermediate-dose cytarabine in treating patients with acute myeloid leukemia (AML) that is unresponsive to initial induction chemotherapy or recurs following an initial complete remission.	Recurrent Adult Acute Myeloid Leukemia Refractory AML	I
2	Carmustine, Etoposide, Cyclophosphamide, and Stem Cell Transplant in Treating Patients With HIV-Associated Lymphoma	Study the side effects of giving high-dose carmustine, etoposide, and cyclophosphamide together with a stem cell transplant and to see how well it works in treating patients with HIV-associated lymphoma.	Lymphoma	I
3	Pomalidomide After Combination Chemotherapy in Treating Patients With Newly Diagnosed Acute Myeloid Leukemia or High-Risk Myelodysplastic Syndrome	Studies the side effects and best dose of pomalidomide after combination chemotherapy in treating patients with newly diagnosed AML or high-risk myelodysplastic syndrome.	AML Leukemia Myelodysplastic Syndrome Myeloproliferative Neoplasm	I
4	Everolimus MICE-regimen in Treating Older Patients With Newly Diagnosed Acute Myeloid Leukemia	Study the side effects and best dose of everolimus when given together with mitoxantrone hydrochloride, cytarabine, etoposide, and idarubicin in treating older patients with newly diagnosed acute myeloid leukemia (AML).	AML	I
5	Radiation Therapy, Chemotherapy, and Soy Isoflavones in Treating Patients With Stage IIIA-IIIB Non-Small Cell Lung Cancer	Study the side effects of soy isoflavones when given together with radiation therapy and chemotherapy in treating patients with stage IIIA-IIIB non-small cell lung cancer. Radiation therapy uses high energy X rays to kill tumor cells.	Adenocarcinoma of the Lung Adenosquamous Cell Lung Cancer Bronchoalveolar Cell Lung Cancer SCLC, NSCLC	I
6	Brentuximab Vedotin + Re-induction Chemotherapy for AML	Study is a Phase I clinical trial. Phase I trials test the safety of an investigational drug or combination of drugs. These trials also try to define the appropriate dose of the investigational drug to use for further studies. Investigational means that the combination of drugs is still being studied and that research doctors are trying to find out more about it. As part of this research study, patients will be administered brentuximab vedotin in combination with a conventional re-induction chemotherapy, which consists of the chemotherapy drugs mitoxantrone, etoposide, and cytarabine.	AML	I

7	Study of Pembrolizumab (MK-3475) Monotherapy in Advanced Solid Tumors and Pembrolizumab Combination Therapy in Advanced Non-small Cell Lung Cancer/ Extensive-disease Small Cell Lung Cancer	Successive participant cohorts with advanced solid tumors will receive pembrolizumab to assess the safety and tolerability of monotherapy. Participants with advanced NSCLC will receive pembrolizumab in combination with either cisplatin/pemetrexed or carboplatin/pemetrexed; with either carboplatin/paclitaxel or carboplatin/paclitaxel; or with ipilimumab by non-random assignment to assess the safety and tolerability of the combination therapy. Participants with untreated extensive-disease SCLC will receive pembrolizumab in combination with either cisplatin/etoposide, carboplatin/etoposide, or cisplatin/etoposide with prophylactic use of granulocyte colony-stimulating factor by non-random assignment to assess the safety and tolerability of the combination therapy.	SCLC NSCLC	I
8	Gene Therapy-Treated Stem Cells in Treating Patients Undergoing Stem Cell Transplant for Intermediate-Grade or High-Grade AIDS-Related Lymphoma	Study the biological therapy in treating patients with acquired immune deficiency syndrome-related lymphoma undergoing stem cell transplant.	Lymphoma	I
9	CD19-specific T Cell Infusion in Patients With B-Lineage Lymphoid Malignancies	Study if an investigational type of gene transfer can be given reliably and safely in patients with advanced B-cell lymphoma. B cells are a type of white blood cell that fights infection and disease. Lymphoma is a type of cancer that affects the immune system, including B cells.	Lymphoma B-cell Lymphoma	I
10	Safety Study of AG-120 or AG-221 in Combination With Induction and Consolidation Therapy in Patients With Newly Diagnosed Acute Myeloid Leukemia With an IDH1 and/or IDH2 Mutation	Evaluate the safety of AG-120 and AG-221 when given in combination with standard acute myeloid leukemia induction and consolidation therapy. The study plans to evaluate 1 dose level of AG-120 in subjects with an IDH1 mutation and 1 dose level (and 2 dose schedules) of AG-221 in subjects with an IDH2 mutation. AG-120 or AG-221 will be administered with 2 types of acute myeloid leukemia induction therapies (cytarabine with either daunorubicin or idarubicin) and 2 types of AML consolidation therapies (mitoxantrone with etoposide or cytarabine)	AML	I
11	Gene Therapy and Combination Chemotherapy in Treating Patients With AIDS-Related Non-Hodgkin Lymphoma	Study gene therapy following combination chemotherapy (Prednisone, Rituximab, Etoposide, Doxorubicin Hydrochloride, Vincristine Sulfate Cyclophosphamide) treating patients with acquired immune deficiency syndrome-related non-Hodgkin lymphoma (HL).	Lymphoma	I
12	High Dose Therapy and Autologous Stem Cell Transplantation Followed by Infusion of Chimeric Antigen Receptor Modified T-Cells Directed Against CD19+ B-Cells for Relapsed and Refractory Aggressive B Cell Non-HL	Study the safety of delivering the patients' own immune cells, called T cells, after the high-dose chemotherapy (carmustine, etoposide, cytarabine, melphalan) and autologous stem cell transplantation.	Non-HL	I
13	Systemic Chemotherapy and Intra-Arterial Melphalan Chemotherapy in Children With Intra-Ocular Retinoblastoma	Study the safety of the treatment combination of alternating standard chemotherapy (carboplatin, etoposide, vincristine) and another (melphalan) chemotherapy at different interval schedules. Researchers want to find out what effects, good and/or bad, the treatment combination has on the patients and their retinoblastoma.	Advanced Intra-Ocular Retinoblastoma	I
14	Clinical Study of Vorinostat in Combination With Etoposide in Pediatric Patients < 21 Years at Diagnosis With Refractory Solid Tumors	The purpose of this study is to find out how safe and effective treatment with a new combination of drugs, vorinostat and etoposide	Refractory Sarcoma	I-II

15	Bendamustine in Combination With Ofatumumab, Carboplatin and Etoposide for Refractory or Relapsed Aggressive B-Cell Lymphomas	Identify dose-limiting toxicities, maximum-tolerated dose, patients with life-prolonging therapy for a chemoimmunotherapy combination of bendamustine, ofatumumab, carboplatin, and etoposide with refractory patients.	Non-HL	I-II
16	Trilaciclib (G1T28), a CDK 4/6 Inhibitor, in Combination With Etoposide and Carboplatin in Extensive Stage Small Cell Lung Cancer	Study the potential clinical benefit of trilaciclib (G1T28) in preserving the bone marrow and the immune system and enhancing chemotherapy antitumor efficacy when administered prior to carboplatin and etoposide in first line treatment.	SCLC	I-II
17	Dose Escalation and Double-blind Study of Veliparib in Combination With Carboplatin and Etoposide in Treatment-naive Extensive Stage Disease Small Cell Lung Cancer	Assess the efficacy of veliparib in combination with carboplatin and etoposide in patients.	SCLC	I-II
18	Bendamustine Hydrochloride, Rituximab, Etoposide, and Carboplatin in Treating Patients With Relapsed or Refractory Diffuse Large B-cell Lymphoma or HL	Study the side effects and best dose of bendamustine hydrochloride when given together with carboplatin, etoposide, and rituximab in treating patients with diffuse large B cell lymphoma or HL that has come back after a period of improvement or has not responded to previous treatment.	Non-HL	I-II
19	Cisplatin and Etoposide With or Without Veliparib in Treating Patients With Extensive Stage Small Cell Lung Cancer or Metastatic Large Cell Neuroendocrine Non-small Cell Lung Cancer	Studies the side effects and best dose of veliparib when given together with or without cisplatin and etoposide and to see how well they work in treating patients with extensive stage small cell lung cancer or large cell neuroendocrine non-small cell lung cancer that has spread to other parts of the body.	Small/Large Cell Lung Carcinoma Neuroendocrine Carcinoma Stage IV NCLC	I-II
20	Dasatinib, Ifosfamide, Carboplatin, and Etoposide in Treating Young Patients With Metastatic or Recurrent Malignant Solid Tumors	Study the side effects and best dose of dasatinib when given together with ifosfamide, carboplatin, and etoposide and to see how well they work in treating young patients with metastatic or recurrent malignant solid tumors.	Brain and Central Nervous System Tumors Childhood Germ Cell Tumor Extragonadal Germ Cell Tumor Kidney, Liver, Ovarian Cancer Lymphoma Neuroblastoma Sarcoma Testicular Germ Cell Tumor	I-II
21	Intensity-Modulated Radiation Therapy, Etoposide, and Cyclophosphamide Followed By Donor Stem Cell Transplant in Treating Patients With Relapsed or Refractory Acute Lymphoblastic Leukemia or Acute Myeloid Leukemia	Study the side effects and best dose of intensity-modulated radiation therapy when given together with etoposide and cyclophosphamide followed by donor stem cell transplant and to see how well they work in treating patients with relapsed or refractory acute lymphoblastic leukemia or acute myeloid leukemia.	Leukemia	I-II
22	Busulfan, Etoposide, and Intensity-Modulated Radiation Therapy Followed By Donor Stem Cell Transplant in Treating Patients With Advanced Myeloid Cancer	Study the side effects and best dose of intensity-modulated radiation therapy when given together with busulfan and etoposide followed by a donor stem cell transplant and to see how well it works in treating patients with advanced myeloid cancer.	Adult and Childhood AML Blastic Phase Chronic Myelogenous Leukemia Childhood Chronic Myelogenous Leukemia Myelodysplastic Syndromes Previously Treated Myelodysplastic Syndromes	I-II

23	Cisplatin or Carboplatin, and Etoposide With or Without Sunitinib Malate in Treating Patients With Extensive-Stage Small Cell Lung Cancer	Study the side effects and best dose of sunitinib malate and to see how well it works when given together with cisplatin or carboplatin and etoposide in treating patients with extensive-stage SCLC.	Extensive Stage SCLC Carcinoma Recurrent SCLC Carcinoma	I-II
24	Open-Label, Dose Escalation, Safety and Tolerability Study of INCB050465 and Itacitinib in Subjects With Previously Treated B-Cell Malignancies	Open-label, dose-escalation study in subjects with previously treated B-cell malignancies to find maximum tolerated dose or pharmacologic active dose of a PI3K δ inhibitor, INCB050465, as monotherapy and in combination with: itacitinib (INCB039110), a JAK1 inhibitor; rituximab; and rituximab, ifosfamide, carboplatin, and etoposide	B-Cell Malignancies	I-II
25	Study of Crenolanib Combined With Chemotherapy in FLT3-mutated Acute Myeloid Leukemia Patients	Evaluate the dose-limiting toxicity and efficiency of crenolanib with standard chemotherapy.	AML	I-II
26	Yttrium-90-labeled Daclizumab With Chemotherapy and Stem Cell Transplant for HL	Study whether yttrium-90 daclizumab, high-dose chemotherapy, and stem cell transplants can treat HL that has not responded to earlier treatments.	HL	I-II
27	Brentuximab Vedotin in Refractory/Relapsed Hodgkin Lymphoma Treated by Etoposide, Carboplatine, Ifosfamide	Study the dose escalation design to explore the safety and assess the recommended phase 2 dose of brentuximab vedotin in Hodgkin lymphoma patients treated with etoposide, carboplatine, ifosfamide regimen	Hodgkin Disease	I-II
28	Combined SGN-35 (BrentuximabVedotin) Therapy With Cyclophosphamide, Procarbazine, Prednisone, Etoposide and Mitoxantrone for Older Patients With Untreated Hodgkin Lymphoma	Study is to identify the maximum tolerated dose of brentuximab vedotin in combination with EPDM and to assess the toxicity of the combination of brentuximad vedotin.	HL	I-II
29	Lenalidomide Maintenance Therapy After High Dose BEAM With or Without Rituximab	Study the side effects and best dose of lenalidomide when given after combination chemotherapy with or without rituximab and stem cell transplant and to see how well it works in treating patients with persistent or recurrent non-HL that is resistant to chemotherapy. Drugs used in chemotherapy, such as carmustine, etoposide, cytarabine, and melphalan.	Cells Lymphoma	I-II
30	Combination Chemotherapy and Lenalidomide in Treating Patients With Newly Diagnosed Stage II-IV Peripheral T-cell Non-HL	Study the side effects and best dose of lenalidomide when given together with combination chemotherapy and to see how well they work in treating patients with newly diagnosed stage II-IV peripheral T-cell non-HL. Drugs used in chemotherapy, such as cyclophosphamide, doxorubicin hydrochloride, vincristine sulfate, and etoposide.	Cells Lymphoma	I-II
31	Radiolabeled Monoclonal Antibody and Combination Chemotherapy Before Stem Cell Transplant in Treating Patients With High-Risk Lymphoid Malignancies	Study the side effects and the best dose of radiolabeled monoclonal antibody when given together with combination chemotherapy (carmustine, cytarabine, etoposide, melphalan) before stem cell transplant and to see how well it works in treating patients with high-risk lymphoid malignancies.	Lymphoma	I-II
32	Vorinostat and Combination Chemotherapy With Rituximab in Treating Patients With HIV-Related Diffuse Large B-Cell Non-HL or Other Aggressive B-Cell Lymphomas	Study the side effects and the best dose of vorinostat when given together with combination chemotherapy (cyclophosphamide, doxorubicin, hydrochloride, etoposide, prednisone, rituximab, vincristine sulfateand) with rituximab to see how well it works compared to combination chemotherapy alone in treating patients with human immunodeficiency virus-related diffuse large B-cell non-HL or other aggressive B-cell lymphomas	Lymphoma	I-II

33	Study to Determine Safety, Pharmacokinetics and Efficacy of GMI-1271 in Combination With Chemotherapy in Acute Myeloid Leukemia	Evaluate GMI-1271, a specific E-selectin antagonist, in acute myeloid leukemia in combination with standard agents (mitoxantrone etoposide, cytarabine, idarubicin) to treat this disease.	AML	I-II
34	Clinical Trial to Determine Dose, Security and Efficacy of Lenalidomide and Rituximab - Etoposide, SoluMedrol - Methylprednisolone, High-dose Ara-Cytarabine, Platinol - Cisplatin) in Patients With Diffuse Large B-cell Lymphoma	Evaluate the safety and the maximum-tolerated dose of the combination -rituximab, etoposide, solumedrol - methylprednisolone, High-dose ara-cytarabine, platinol - cisplatin with as salvage therapy for patients with relapsed or refractory diffuse large B-cell lymphoma.	Diffuse Large B-cell Lymphoma	I-II
35	Radiolabeled Monoclonal Antibody and Combination Chemotherapy Before Stem Cell Transplant in Treating Patients With High-Risk Lymphoid Malignancies	Study the side effects and the best dose of radiolabeled monoclonal antibody when given together with combination chemotherapy (carmustine, cytarabine, etoposide) before stem cell transplant and to see how well it works in treating patients with high-risk lymphoid malignancies.	Lymphoma	I-II
36	Carboplatin, Etoposide, and Atezolizumab With or Without Trilaciclib (G1T28), a CDK 4/6 Inhibitor, in Extensive Stage Small Cell Lung Cancer	Investigate the benefit of trilaciclib (G1T28) in preserving the bone marrow and the immune system, and enhancing antitumor efficacy when administered with carboplatin, etoposide, and atezolizumab therapy in first line treatment for patients.	SCLC	II
37	Paclitaxel, Ifosfamide and Cisplatin (TIP) Versus Bleomycin, Etoposide and Cisplatin (BEP) for Patients With Previously Untreated Intermediate- and Poor-risk Germ Cell Tumors	Study the safety and effectiveness of two different drug combinations in patients who have intermediate- and poor-risk germ cell tumors.	Germ Cell Tumors	II
38	Phase II Study of Erlotinib With Concurrent Radiotherapy in Unresectable NSCLC With Activating Mutation of epidermal growth factor receptor in Exon 19 or 21	Erlotinib with concurrent radiotherapy has superior efficacy and comparable safety profile in unresectable stage III non-small cell lung cancer patients with activating mutation of epidermal growth factor receptor in exon 19 or 21 versus etoposide plus cis-platin with concurrent radiotherapy.	NSCLC	II
39	Trial of BMS-986012 in Combination With Platinum and Etoposide	Study the administration of BMS-986012 in Combination with Platinum and etoposide as first-line therapy in extensive SCLC.	SCLC	II
40	Busulfan, Etoposide, and Total-Body Irradiation in Treating Patients Undergoing Donor Stem Cell or Bone Marrow Transplant for Advanced Hematologic Cancer	Study the side effects and best way to give busulfan together with etoposide and total-body irradiation and to see how well they work in treating patients who are undergoing a donor stem cell or bone marrow transplant for advanced hematologic cancer.	Leukemia Myelodysplastic Syndromes	II
41	Busulfan, Etoposide, and Total-Body Irradiation Followed by Autologous Stem Cell Transplant and Aldesleukin in Treating Patients With Acute Myeloid Leukemia in First Remission	Study the side effects and how well giving busulfan and etoposide together with total-body irradiation followed by autologous stem cell transplant and aldesleukin works in treating patients with AML in first remission.	Leukemia	II
42	Combination Chemotherapy, Radiation Therapy, and Bevacizumab in Treating Patients With Newly Diagnosed Stage III Non-small Cell Lung Cancer That Cannot Be Removed by Surgery	Study the combination chemotherapy, radiation therapy, and bevacizumab in treating patients with newly diagnosed stage III non-small cell lung cancer that cannot be removed by surgery.	Adenosquamous Lung Carcinoma Large Cell Lung Carcinoma Lung Adenocarcinoma	II

			Minimally Invasive Lung Adenocarcinoma	
			Squamous Cell Lung Carcinoma	
43	Icotinib With Concurrent Radiotherapy Versus Chemotherapy With Concurrent Radiotherapy in Non-small Cell Lung Cancer	Assess the efficacy and safety of icotinib with concurrent radiotherapy versus etoposide/cisplatin with concurrent radiotherapy in non-small cell lung cancer.	NSCLC	II
44	Dose Intensification Study in Refractory Germ Cell Tumors With Relapse and Bad Prognosis	Estimating the efficacy of an intensification protocol in patients with refractory germ cell tumors with relapse and bad prognosis. Treatment consists in two paclitaxel and ifosfamide intensification cycles followed by three carboplatine and etoposide high dose cycles.	Germ Cell Tumors	II
45	Combination Chemotherapy and Cyclosporine Followed by Focal Therapy for Bilateral Retinoblastoma	Study how well giving combination chemotherapy together with cyclosporine followed by cryotherapy and/or laser therapy works in treating patients with newly diagnosed retinoblastoma in both eyes.	Retinoblastoma	II
46	Venetoclax Plus R-ICE Chemotherapy for Relapsed/Refractory Diffuse Large B-Cell Lymphoma	Establishment of safety of V+RICE in order to identify the recommended phase II dose	Diffuse Large B-cell-lymphoma	II
47	A Study of Bevacizumab in Combination With Chemotherapy for Treatment of Osteosarcoma	Study adopts a novel strategy for first-line treatment of osteosarcoma by combining chemotherapy with anti-angiogenic therapy using bevacizumab Avastin®.	Osteosarcoma Malignant Fibrous Histiocytomavof Bone	II
48	High-dose Chemotherapy for Poor-Prognosis Relapsed Germ-Cell Tumors	Study is to learn if two cycles of high-dose chemotherapy combination can help to control germ-cell tumors.	Testicular Cancer	II
49	Immunotherapy as Second-line in Patient With Small Cell Lung Cancer	Study the chemotherapy combination of etoposide, cisplatin efficiency as a second line treatment in patients.	SCLC	II
50	Autologous Peripheral Stem Cell Transplant in Treating Patients With Non-HL or HL	Study how well autologous peripheral stem cell transplant works in treating patients with non-HL or HL.	Lymphoma	II
51	Adcetris (Brentuximab Vedotin), Combination Chemotherapy, and Radiation Therapy in Treating Younger Patients With Stage IIB, IIIB and IV Hodgkin Lymphoma	Evaluate the safety of brentuximab vedotin, etoposide, prednisone and doxorubicin hydrochloride /cyclophosphamide, brentuximab vedotin, prednisone and dacarbazine, as well as the efficacy after 2 cycles of the same chemotherapy agents in high risk patients with Hodgkin lymphoma	HL	II
52	Zevalin/BEAM/Rituximab vs BEAM/Rituximab With or Without Rituximab in Autologous Stem Cell Transplantation	Study the addition of 90Y zevalin to BEAM chemotherapy (carmustine, etoposide, cytarabine, and melphalan) and rituximab is more effective than the combination of BEAM and rituximab alone in patients with lymphoma who receive a stem cell transplant.	Diffuse Large Cell Lymphoma Lymphoma	II
53	Merkel Positron Emission Tomography Protocol (MP3)	Study designed to evaluate the efficacy of chemo-radiotherapy in achieving loco-regional control in patients with merkel cell carcinoma of the skin. Patients will undergo positron emission tomography scans to assist in staging and planning the patient's treatment as well as assessing response at the conclusion of treatment	Merkel Cell Carcinoma	II

54	Intergroup Trial for Children or Adolescents With Primary Mediastinal Large B-Cell Lymphoma: Dose Adjusted-Etoposide, Doxorubicin, Vincristine, Cyclophosphamide, Rituximab Evaluation	Determine the efficacy of dose adjusted-etoposide, doxorubicin, vincristine, cyclophosphamide, rituximab regimen in children and adolescent with primary mediastinal large B cell lymphoma in terms of event free survival.	Primary Mediastinal Large B Cell Lymphoma	II
55	Chemotherapy With or Without Radiation, Low and Intermediate Risk HL, TXCH-HD-12A (TXCH-HD-12A)	Study how the immune system recovers and how certain T-cells in the blood behave after receiving chemotherapy with or without radiation. The investigators also want to identify if bio-markers relate to the response of Hodgkin Disease to study treatment.	Hodgkin Disease	II
56	Chemotherapy Combination (etoposide) Plus Ofatumumab Followed by G-CSF for Mobilization of Peripheral Blood Stem Cells in Patients With Non-HL	Study the stem cells after ofatumumab and chemotherapy treatment. This study will also evaluate side-effects, number of stem cells collected, and the number of procedures that are needed to collect enough stem cells.	Lymphoma	II
57	EPOCH-R Chemotherapy Plus Bortezomib to Treat Mantle Cell Lymphoma	Study the effectiveness of etoposide, prednisone, vincristine, cyclophosphamide, doxorubicin-rituximab chemotherapy plus bortezomib for treating mantle cell lymphoma, a cancer of white blood cells called lymphocytes.	Mantle Cell Lymphoma	II
58	Tailoring Treatment for B Cell Non-HL Based on Positron-emission tomography Scan Results Mid Treatment	Study whether patients who are likely to fail rituximab, cyclophosphamide, doxorubicin, vincristine, prednisone, as predicted by a mid-treatment Positron-emission tomography scan, can have an improved outcome if switched to a standard salvage regimen rituximab, ifosfamide, carboplatin, etoposide.	Non-HL Diffuse Large B-Cell Non-HL	II
59	Response-Based Therapy Assessed By PET Scan in Treating Patients With Bulky Stage I and Stage II Classical HL	Improving treatment outcomes in patients diagnosed with bulky, early stage HL and to reduce the side effects that are associated with use of radiation used in current treatments. The chemotherapy treatment in this study consists of a combination of four drugs: doxorubicin, bleomycin, vinblastine, and dacarbazine. The plan is to identify a group of patients using early positron-emission tomography scans in order to change to a chemotherapy treatment bleomycin, etoposide, doxorubicin, cyclophosphamide, vincristine, procarbazine and prednisone.	Lymphoma	II
60	Decitabine as Maintenance Therapy After Standard Therapy in Treating Patients With Previously Untreated Acute Myeloid Leukemia	Study the side effects and how well decitabine works when given as maintenance therapy after standard therapy in treating patients with previously untreated acute myeloid leukemia. Drugs used in chemotherapy, such as cytarabine, daunorubicin, etoposide, busulfan, and decitabine.	AML	II
61	Autologous Stem Cell Transplant Followed By Maintenance Therapy in Treating Elderly Patients With Multiple Myeloma	Investigate whether patients greater than or equal to 65 years of age diagnosed with myeloma or another plasma cell malignancy will have better outcomes with transplant followed by maintenance therapy (dexamethasone, cisplatin, doxorubicin, cyclophosphamide, etoposide, bortezomib, thalidomide, melphalan) as primarily measured by progression-free survival, versus non-transplant approaches.	Extramedullary Plasmacytoma Isolated Plasmacytoma of Bone Light Chain Deposition Disease Primary Systemic Amyloidosis Multiple Myeloma	II
62	Chemotherapy With Low-Dose Radiation for Pediatric HL	Estimate the percentage of patients with intermediate risk HL who will survive free of disease for three years after treatment with multi-agent chemotherapy (adriamycin, vinblastine, nitrogen,	HL	II

		mustard, cyclophosphamide, cincristine, bleomycin, etoposide, prednisone) and low-dose, tailored-field radiation therapy.		
63	NHL16: Study For Newly Diagnosed Patients With Acute Lymphoblastic Lymphoma	Study the treatment of acute lymphoblastic leukemia-based therapy, using multi-agent (prednisone, vincristine, daunorubicin, asparaginase, erwinia asparaginase, doxorubicin, cyclophosphamide, cytarabine, thioguanine, clofarabine, methotrexate, mercaptopurine, dexamethasone, hydrocortisone, etoposide) regimens comprising of induction, consolidation, and continuation phases delivered over 24-30 months.	Lymphoblastic Lymphoma	II
64	Rituximab, Yttrium Y 90 Ibritumomab Tiuxetan in Patients W/Relapsed Stage II, III, or IV Follicular non-HL	Study the combination chemotherapy (methylprednisolone, etoposide, cytarabine, cisplatin, rituximab, in-zevalin, y-zevalin) followed by rituximab and yttrium Y 90 ibritumomab tiuxetan to see how well it works in treating patients with relapsed stage II, stage III, or stage IV follicular non-HL	Non-HL	II
65	Chemotherapy With Liposomal Cytarabine central nervous system Prophylaxis for Adult Acute Lymphoblastic Leukemia & Lymphoblastic Lymphoma	Improve the survival for adults with acute lymphoblastic leukemia or acute lymphoblastic lymphoma by reducing systemic and central nervous system relapse with acceptable toxicity using intensive chemotherapy (etoposide) with liposomal cytarabine (Depocyt®) central nervous system prophylaxis.	Acute Lymphoblastic Leukemia Lymphoblastic Lymphoma	II
66	Brentuximab Vedotin (SGN-35) in Transplant Eligible Patients With Relapsed or Refractory HL	Study whether 2 cycles of SGN-35 can be used instead of ifosfamide, carboplatin, and etoposide prior to autologous stem cell transplant for relapsed and refractory HL.	HL	II
67	Tandem High Dose Chemotherapy With 131I-MIBG Treatment in High Risk Neuroblastoma	Evaluate the efficacy and toxicity of tandem high dose chemotherapy (cyclophosphamide, carboplatin, etoposide, thiotepa, melphalan) including high-dose 131I-metaiodobenzylguanidine radiation treatment.	High Risk Neuroblastoma	II
68	Rituximab and Combination Chemotherapy in Treating Patients With Stage II, Stage III, or Stage IV Diffuse Large B-Cell Non-HL	Study how well giving rituximab together with combination chemotherapy works in treating patients with stage II, stage III, or stage IV diffuse large B-cell non-HL.	Lymphoma	II
69	Multidisciplinary Approach for Poor Prognosis Sinonasal Tumors in Inoperable Patients and Operable	Study the integration of multiple modality of treatment modulated by histology, molecular profile and response to induction chemotherapy (cisplatin, docetaxel, 5-fluorouracil, etoposide, adriamycin, ifosfamide, leucovorin)	Unresectable Sinonasal Tumors	II
70	Doxorubicin Hydrochloride Liposome and Rituximab With Combination Chemotherapy in Treating Patients With Newly Diagnosed Burkitt's Lymphoma or Burkitt-Like Lymphoma	Study how well giving doxorubicin hydrochloride liposome and rituximab together with combination chemotherapy (etoposide) works in treating patients with newly diagnosed Burkitt's lymphoma or Burkitt-like lymphoma.	Burkitt-like Lymphoma	II
71	Phase II Trial of Alemtuzumab (Campath) and Dose-Adjusted Etoposide Prednisolone Onvocin Cyclophosphamide Hydroxydaunorubicin-Rituximab in Relapsed or Refractory Diffuse Large B-Cell and HL	To test whether giving campath (alemtuzumab) in combination with continuous infusion etoposide prednisolone onvocin cyclophosphamide hydroxydaunorubicin-rituximab chemotherapy will improve the outcome of lymphoma treatment.	HL Diffuse Large B-Cell Lymphoma	II

72	Three Chemotherapy Regimens as an Adjunct to Antiretroviral Therapy for Treatment of Advanced Acquired Immune Deficiency Syndrome- Kaposi's Sarcoma	This study is being done to compare the safety and efficacy of three combination treatments for Kaposi's sarcoma and advanced acquired immune Deficiency Syndrome.	HIV-1 Infection	II
73	Observation or Radiation Therapy and/or Chemotherapy and Second Surgery in Treating Children Who Have Undergone Surgery for Ependymoma	Determine the effectiveness of specialized radiation therapy either alone or after chemotherapy (carboplatin, cyclophosphamide, etoposide, vincristine sulfate) and second surgery in treating children who have undergone surgery for localized ependymoma.	Brain Tumor Central Nervous System Tumor	II
74	Risk-Adapted Therapy for Young Children With Embryonal Brain Tumors, Choroid Plexus Carcinoma, High Grade Glioma or Ependymoma	Study how well giving combination chemotherapy (cyclophosphamide, paraplatin, etoposide, topotecan, erlotinib) together with radiation therapy works in treating young patients with newly diagnosed central nervous system tumors.	Brain and Central Nervous System Tumors	II
75	ChemoImmunotherapy With Early Central Nervous System Prophylaxis	Test whether early central nervous system prophylaxis given at the beginning of therapy for young high risk diffuse large B-cell lymphoma patients is feasible and could reduce the risk of nervous system relapses.	Primary Disease	II
76	S0816 Fludeoxyglucose F 18-Positron Emission Tomography/Chemotherapy Imaging and Combination Chemotherapy With or Without Additional Chemotherapy and Granulocyte-Colony Stimulating Factor in Treating Patients With Stage III or Stage IV HL	Study fludeoxyglucose F 18-Positron Emission Tomography/Chemotherapy imaging to see how well it works in assessing response to combination chemotherapy (cyclophosphamide, dacarbazine, doxorubicin hydrochloride, etoposide, prednisone, procarbazine hydrochloride, vinblastine sulfate) and allow doctors to plan better additional further treatment in treating patients with stage III or stage IV HL.	Lymphoma Nonneoplastic Condition	II
77	Phase II Study of Dose-Adjusted Etoposide Prednisolone Onvocin Cyclophosphamide Hydroxydaunoubicine-Rituximab in Adults With Untreated Burkitt Lymphoma + Diffuse Large B-Cell Lymphoma	Determine the safety and effectiveness of dose adjusted-etoposide prednisolone onvocin cyclophosphamide hydroxydaunorubicin-rituximab in treating Burkitt lymphoma.	Burkitt Lymphoma Diffuse Large B-cell Lymphoma, c-MYC Positive Plasmablastic Lymphoma	II
78	Combination Chemotherapy With or Without Autologous Stem Cell Transplant in Treating Patients With Central Nervous System B-Cell Lymphoma	Study effects (good and/or bad) treatment with chemotherapy (carmustine, cytarabine, etoposide, thiotepe) and stem cell transplant compared with chemotherapy alone will have on primary central nervous system B-cell lymphoma.	Lymphoma	II
79	Therapeutic Trial for Patients With Ewing Sarcoma Family of Tumor and Desmoplastic Small Round Cell Tumors	Study the treatment (vincristine, doxorubicin, cyclophosphamide, ifosfamide, etoposide, temozolomide, temsirolimus, bevacizumab, sorafenib) for Ewing sarcoma family of tumors and desmoplastic small round cell tumor.	Desmoplastic Small Round Cell Tumor Ewing Sarcoma of Bone or Soft Tissue	II
80	Adult Consortium Trial: Adult Acute Lymphoblastic Leukemia Trial	Study the safety and effectiveness of a multi-drug chemotherapy regimen (doxorubicin, cytarabine, methotrexate, vincristine, cyclophosphamide, methylprednisone, hydrocortisone sodium succinate, dexamethasone, asparaginase, imatinib, etoposide) in adult patients with AML	AML	II
81	Combination Chemotherapy With or Without Donor Stem Cell Transplant in Treating Patients With Acute Lymphoblastic Leukemia	Study the side effects of giving combination chemotherapy (cyclophosphamide, cytarabine, dasatinib, dexamethasone, doxorubicin hydrochloride, etoposide) together with or without donor	Acute Lymphoblastic Leukemia	II

		stem cell transplant and to see how well it works in treating patients with acute lymphoblastic leukemia.		
82	Cycle of Adjuvant bleomycin, etoposide, cisplatin Chemotherapy in High Risk, Stage 1 Non-seminomatous Germ Cell Testis Tumours	Evaluate the efficiency of one cycle of adjuvant bleomycin, etoposide, cisplatin in patients.	Testicular Non-Seminomatous Germ Cell Tumor	III
83	A Study of Carboplatin Plus Etoposide With or Without Atezolizumab in Participants With Untreated Extensive-Stage Small Cell Lung Cancer	Evaluate the safety and efficacy of atezolizumab in combination with carboplatin plus (+) etoposide compared with treatment with placebo + carboplatin + etoposide in chemotherapy-naive patients.	SCLC	III
84	A Study of Pembrolizumab (MK-3475) in Combination With Etoposide/Platinum (Cisplatin or Carboplatin) for Participants With Extensive Stage Small Cell Lung Cancer	Assess the safety and efficacy of pembrolizumab plus standard of care chemotherapy etoposide/platinum in participants with newly diagnosed extensive stage small cell lung cancer who have not previously received systemic therapy for this malignancy.	SCLC	III
85	Combination Chemotherapy in Treating Patients With Non-Metastatic Extracranial Ewing Sarcoma	Study the combination chemotherapy to see how well it works compared to combination chemotherapy with topotecan hydrochloride in treating patients with extracranial Ewing sarcoma that has not spread from the primary site to other places in the body.	Ewing Sarcoma	III
86	Total Therapy Study XVI for Newly Diagnosed Patients With Acute Lymphoblastic Leukemia	Study the clinical benefit, the pharmacokinetics, and the pharmacodynamics of polyethylene glycol-conjugated, asparaginase given in higher dose versus those of asparaginase given in conventional dose during the continuation phase.	Acute Lymphoblastic Leukemia	III
87	Clofarabine Plus Cytarabine Versus Conventional Induction Therapy And A Study Of NK Cell Transplantation In Newly Diagnosed Acute Myeloid Leukemia	Study the feasibility and efficacy of a novel form of therapy haploidentical cell transplantation in patients with standard-risk AML. In addition, we will investigate the efficacy of clofarabine + cytarabine in newly diagnosed patients with AML.	AML	III
88	Antiretroviral Therapy Alone or With Delayed Chemo Versus ART With Immediate Chemo for Limited AIDS-related Kaposi's Sarcoma	Study was done to find out if taking antiretroviral therapy alone (ART) with immediate etoposide is better than taking ART alone or ART with delayed etoposide to treat limited stage Kaposi's Sarcoma.	HIV Kaposi's Sarcoma	III
89	Concurrent Once Daily Versus Twice Daily Radiotherapy for Limited Stage Small Cell Lung Cancer	Study two different schedules of radiation therapy to compare how well they work when given together with cisplatin and etoposide in treating patients with limited stage small cell lung cancer.	Lung Cancer	III
90	UARK 2006-66, Total Therapy 3B: An Extension of UARK 2003-33 Total Therapy	Extend the findings of total therapy III (velcade, thalidomide, dexamethasone, adriamycin, cisplatin, cyclophosphamide, etoposide) based what they have learned from the first two studies (Total Therapy I and II), with new research strategies designed to explore why chromosome abnormalities found in persons with multiple myeloma affect the outcome of drug therapy used in this disease.	Multiple Myeloma	III
91	Rituximab and Combination Chemotherapy in Treating Patients With Diffuse Large B-Cell Non-HL	Study rituximab when given together with two different combination chemotherapy regimens (cyclophosphamide, doxorubicin, vincristine, prednisone, etoposide, filgrastim, pegfilgrastim) to compare how well they work in treating patients with diffuse large B-cell lymphoma.	Large B Cell Lymphoma	III

92	Study of Chemotherapy in Combination With All-trans Retinoic Acid With or Without Gemtuzumab Ozogamicin in Patients With Acute Myeloid Leukemia and Mutant Nucleophosmin-1 Gene Mutation	Evaluation of efficacy based on event-free survival after induction and consolidation chemotherapy (idarubicin, etoposide, cytarabine, pegfilgrastim) plus all-trans retinoic acid with or without gemtuzumab ozogamicin in adult patients with acute myeloid leukemia and mutant nucleophosmin-1.	AML	III
93	Fludeoxyglucose F 18-Positron Emission Tomography/Chemotherapy Imaging in Assessing Response to Chemotherapy in Patients With Newly Diagnosed Stage II, Stage III, or Stage IV HL	Study fludeoxyglucose F 18-positron emission tomography/ chemotherapy T imaging to see how well it works in assessing response to chemotherapy in patients with newly diagnosed stage II, stage III, or stage IV HL.	Lymphoma	III
94	Discovery Stage IND EXEMPT Clinical Study - Etoposide and Single Nucleotide Polymorphisms	Study the relationship between drug target topoisomerase II gene single nucleotide polymorphisms and etoposide in patients	SCLC	III
95	Discovery Stage IND Clinical Study - Etoposide Plus Methotrexate and Single Nucleotide Polymorphisms	Correlate topoisomerase II and CYP450 3A4 gene single nucleotide polymorphisms using etoposide therapeutic effects of treating SCLC. Correlate dihydrofolic-acid and dihydrofolate reductase gene single nucleotide polymorphisms using methotrexate therapeutic effects of treating SCLC. Correlate thymidylate synthetase gene single nucleotide polymorphisms to using methotrexate side effects of treating small cell lung cancer.	SCLC	III
96	Combination Chemotherapy, Polyethylene Glycol-Interferon Alfa-2b, and Surgery in Treating Patients With Osteosarcoma	Study combination chemotherapy followed by surgery and two different combination chemotherapy (cisplatin, doxorubicin, hydrochloride, etoposide, ifosfamide, methotrexate) regimens with or without polyethylene glycol-interferon alfa-2b to compare how well it works in treating patients with osteosarcoma.	Localized and Metastatic Osteosarcoma	III
97	Bortezomib and Sorafenib Tosylate in Treating Patients With Newly Diagnosed Acute Myeloid Leukemia	Study how well bortezomib and sorafenib tosylate work in treating patients with newly diagnosed acute myeloid leukemia. Giving bortezomib and sorafenib tosylate together with combination chemotherapy (asparaginase, bortezomib, cytarabine, daunorubicin hydrochloride, etoposide) may be an effective treatment for acute myeloid leukemia.	AML Myeloid Neoplasm Myeloid Sarcoma	III
98	Therapy for Newly Diagnosed Patients With Acute Lymphoblastic Leukemia	Estimate the overall event-free survival of children at least one year of age at diagnosis who are treated with risk-directed therapy (prednisone, dexamethasone, vincristine, daunorubicin, doxorubicin, asparaginase, Erwinia asparaginase, methotrexate, cyclophosphamide, cytarabine, etoposide, mercaptopurine, imatinib) and to monitor the molecular remission induction rate.	Acute Lymphoblastic Leukemia	III
99	International Collaborative Treatment Protocol For Children And Adolescents With Acute Lymphoblastic Leukemia	Study several different combination chemotherapy regimens to compare how well they work in treating young patients with Acute lymphoblastic leukemia.	Acute Lymphoblastic Leukemia	III
100	CTOP/ITE/MTX (cyclophosphamide, vincristin,pirarubicin and predisone/ ifosfamide, pirarubicin, etoposide/methotrexate) Compared With CHOP	Comparison of synergic treatment as first-line therapy for newly diagnosed young patients with T cell lymphoma.	T Cell Lymphoma	IV

	(cyclophosphamide, vincristin, doxorubicin and predisone) as the First-line Therapy for Newly Diagnosed Young Patients With T Cell Lymphoma			
101	Selecting Patient-Specific Biologically Targeted Therapy for Pediatric Patients With Refractory Or Recurrent Brain Tumors	Study whether a medication (temozolomide, etoposide, sorafenib, everolimus, erlotinib, dasatinib) can be chosen based on rapid testing done on tumor tissue. Information from a feasibility or pilot trial will hopefully help researchers plan larger trials in the future to determine the effect of this therapy	Recurrent Childhood Brain Tumor	Not Applicable
102	Rituxan + (Carmustine, Etoposide, Cytarabine, Melphalan) and Auto Stem Cell Transplant for High Risk Lymphoma or Hodgkin's Disease	Confirm that there is a good control of tumor in patients with lymphoma or Hodgkin's disease treated with rituximab and conventional stem cell transplantation.	HL	Not Applicable
103	Vorinostat Combined With Isotretinoin and Chemotherapy in Treating Younger Patients With Embryonal Tumors of the Central Nervous System	Study the side effects and the best way to give vorinostat with isotretinoin and combination chemotherapy and to see how well they work in treating younger patients with embryonal tumors of the central nervous system. Drugs used in chemotherapy, such as isotretinoin, vincristine sulfate, cisplatin, cyclophosphamide and etoposide.	Medulloblastoma Pineoblastoma	Not Applicable

II. Aim of the study

Aim of the study

NCs technology offers solutions to poorly water-soluble compound to be used as a potent drug delivery system for cancer therapy. For the last 20 years, the number of researches regarding drug NCs has considerably boomed signifying that NCs science is a thriving field in which our laboratory is a part of. In that context, this thesis includes two objectives:

- Engineer and characterize an original nanocrystal-based etoposide formulation.
- Assess its *in vitro* and *in vivo* efficiency against colon carcinoma cells and tumor.

The NC drug selection has been based on literature, few studies were focusing on the nanocrystallization of ETO, hence it was more interesting and challenging to select ETO as drug to engineer NCs for the thesis. Besides, ETO is still one of the most active drugs to treat, testicular, lymphomas, ovarian, small cell lung, colon and breast cancer. It is important to notice that ETO phosphate that is the water-soluble version of ETO is preferred for cancer treatment as it offers long term stability in aqueous solution. On the other hand, it implies that ETO phosphate cannot be selected to form NCs in water as this technology is based on the hydrophobicity of an API.

Firstly, the ETO NC formulation has been characterized to understand the chemical and physical properties of NCs. In a second time, NCs biological potential was pre-evaluated *in vitro* on CT26 and 3LL cells line followed by its anticancer efficacy evaluation *in vivo* on murine CT26 colon carcinoma model.

III. Nanocrystals formulations process

Abstract

The aim of the present chapter is to study the formation, the structure, the stability, the *in vitro* and *in vivo* efficiency of ETO nanocrystals. The NCs suspension was made by co-precipitation that is a bottom up synthesis, based on the drop-wise addition of a drug solubilized in an organic phase to an aqueous phase in which the drug is insoluble, followed by an evaporation and dispersion in aqueous solvent to form NCs in suspension. For many applications, it is essential to understand nanocrystallization parameters to accurately manage NC properties such as morphology, size, thermal behavior, stability overtime, physical state, dissolution rate and so forth. In this study, the effects of polymer/drug ratio, water/solvent ratio, drug concentration and nature of polymer were investigated. The results have been analyzed and compared to select the most suitable ETO NC formulation for future *in vitro* and *in vivo* studies. The NCs size and morphology were further characterized using, transmission and scanning electron microscopy (TEM, SEM). Differential scanning calorimetry (DSC), X ray Diffraction (XDR) and thermal microscopy were used to define the crystallinity of the ETO nanoparticles. In vitro drug release profile evidenced that the ETO NCs provided a sustained release kinetics regarding the market product Toposar[®]. The overall results implied that the ETO NCs formulation offer a conceivable therapeutic formulation for nanomedicine.

Introduction

Recent years drug delivery technologies were driving growth in the area of nanomedicine. There is confidence that nanotechnology applied to medicine will provide important progress in the treatment of disease. Nanomedicine could have a major impact on both scientific innovation regarding productive processes that are used to cure cancer, and also the all organization of economic activity of the medicine. About 70% of drug molecules face problems of poor bioavailability and instability.²²⁴ The prominent reason behind these issues is poor aqueous solubility, as the resulting of low bioavailability.²²⁵ Drug NCs with specifics and controlled properties have drawn attention in drug delivery. Stability, dissolution rate, size and long circulation time are examples of these properties that makes drug NCs a suitable

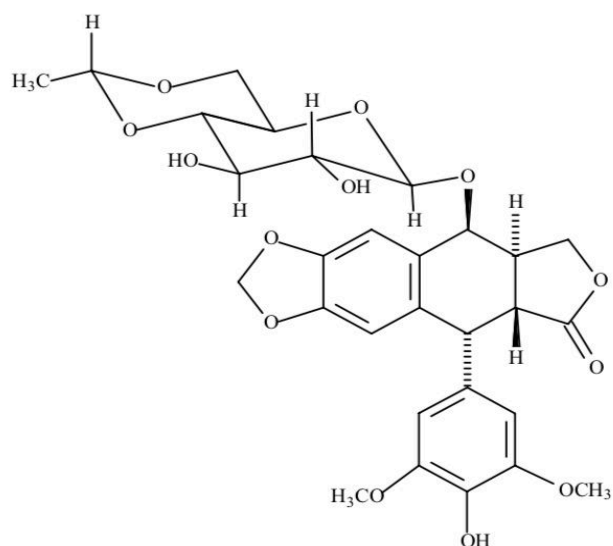


Figure 12 - Etoposide Chemical Formulation
C₂₉H₃₂O₁₃

formulation for efficient cancer treatment. In the last decade, abundance of hydrophobic drugs, such as paclitaxel, camptothecin, docetaxel, itraconazole, amycin and so forth, have been developed into drug NCs form for cancer therapy, as NCs drug reduce the risk of downside effect and toxicity for the patient. NCs can also improve performance as they are in the nanoscale range, are highly potent because of the solid form and could easily be formulated into several dosage forms for

oral, ocular, pulmonary, nasal and injectable administrations, thus broadening their applications for many human diseases. ETO is a powerful anticancer agent used mainly for the treatment of lungs, testicular, breast and gastric cancer, it inhibits the action of the enzyme topoisomerase II crucial for DNA replication, thus inducing cells apoptosis.²²⁰ All anticancer formulations on the market deal with drug precipitation throughout storage or in chemotherapy bags, toxic excipients such as alcohol or acids and high-concentrated stabilizer. Hence, NCs have been suggested as an alternative approach to sidestep these problems while being as efficient as conventional marketed anticancer products.

Material and methods

Material

ETO (> 99% purity, 33419-42-0) was purchased from Santa Cruz Biotechnology (United States of America), Pluronic F-127 was purchased from Sigma Aldrich (St. Louis, Missouri, United States). Toposar[®] was a gift from Hopital Gustave Roussy (Ivry-sur-Seine, France). Methanol and dimethyl sulfoxide were purchased from Fisher Scientific (Waltham, Massachusetts, United States). All products and solvents were used without further purification. Human Serum Albumin (HSA) was purchased from Sigma-Aldrich. Deionized water used for the (by Milli-Q[®], filtered through 0.2 µm membrane) was used for the current study. 0.050 µm Whatman[®] Nuclepore polycarbonate membranes used for filtration were purchased from Thermo Fisher Scientific. Pluronic F-127 and F-68 were purchased from Sigma Aldrich.

Nanocrystal preparation

The ETO NCs were prepared by the method of co-precipitation. Merely, 2.5 mg of ETO was dissolved in 1.5 mL absolute methanol (MeOH) in glass vial and slowly injected under agitation (1200 rpm) in 10 mL of water. The solubilized drug was co-precipitated by evaporating the entire solution using a rotavapor under vacuum for 30 min. The resulting powder was kept under vacuum to remove any traces of MeOH. The powder was hydrated with an aqueous solution containing either F-127 or F-127/albumin, followed by 10 min. sonication using a water-bath sonicator to engineer the NCs solution.

Etoposide nanocrystals particle size, morphology

The NCs size in the formulation was measured using a ZetaSizer Nano-ZS of Malvern Instrument (Westborough, Massachusetts, United States). The F-127-coated NCs size was assessed after the nanocrystallization process. Table 7 shows dynamic light scattering (DLS) measurements of nanoparticle mean diameter in intensity of the ETO NCs synthesized in the study.

The morphological evaluation of NCs has been investigated by a scanning electron microscope (SEM) (Philips XL 30 microscope, Hillsboro, USA). Raw ETO powder and processed NCs powder was placed on a double-sided tape, then coated with a 30 nm layer of gold under vacuum (10^{-6} Pa) for 2 minutes, then observed using SEM at an accelerating voltage of 15 kV under

vacuum. Also, transmission electron microscopy (TEM) was performed to understand the surface morphology and structure of ETO NCs from the dispersion in the aqueous polymeric solution. A drop of the ETO NCs solution was put on a copper grid with Formvar films Cu 200 Mesh[®]. Then, negative staining was performed by adding a drop of uranyl acetate solution (1% w/v). The excess fluid was removed with filter paper. The grids were examined under a transmission electron microscope (JEM-100S, JEOL, Tokyo, Japan) at accelerating voltage of 80 kV.

X Ray powder diffraction experiments

The X-ray diffraction patterns for ETO NCs solutions were obtained using a Bruker APEX DUO diffractometer mounted with a I μ S microsource and APEX II CCD Detector with CuK α radiation. The ETO solution was set in a 0.7 mm capillary and flame sealed before mounting. The results were gathered as three still frames to detect 2θ from 5 to 60 deg. with 300 seconds exposures and analyzed using the Bruker XRD2 Eval and Bruker EVA softwares. The powder X-ray diffraction (PRDX) examinations of ETO NCs powder and raw ETO were made using a Bruker D8-Advance X-ray diffractometer equipped with a LynxEye silicon strip detector. A copper source was used with a nickel filter leaving CuK α radiation. The generator was set at 40 kV and 40 mA. The samples were ground and put in shallow-well sample holders. The results were collected as three frames to detect 2θ from 5 to 60 deg. for 300 seconds exposure and evaluated using the Bruker AXS and EVA softwares.

Dissolution study of etoposide nanocrystals

In vitro release analysis was performed to compare the dissolution rate of ETO NCs/F-127 0.03% and 0.17% w/v with the microcrystals (MCs) from VP-16 powder dispersed in water with 0.03% w/v, and also ETO in Toposar[®] formulation in which ETO is in its solubilized state. *In vitro* release of ETO NCs was assessed by the dialysis bag diffusion technique. The NCs ETO solutions were placed in a cellulose dialysis bag (molecular weight cutoff 12.4 kDa) and sealed at both ends using dialysis tubing closure. The dialysis bag was placed in a compartment containing 40 mL of PBS-buffered saline medium, pH 7.4, which was stirred at 60 rpm and maintained at 37 °C for 6 hours. The receptor compartment was covered to prevent the evaporation of the continuum medium. Aliquots (1 mL) were withdrawn at 10 min, 30 min, 1, 2, 4, 6 hours, and the same volume of fresh HBS was added to the medium in order to maintain

its overall volume at 40 mL after each sampling smear. Then, the samples were analyzed using a Cary 100 Scan UV-visible spectrophotometer (Pittsburgh, USA) set at 283 nm.

Dynamic Scan Calorimetry

The thermal behavior of raw marketed ETO powder, ETO nanostructured powder without F-127, ETO NCs/F-127 0.03% w/v dried solid dispersion and raw F-127 powder were analyzed by differential scanning calorimetry (DSC) technique using a DSC3 from Mettler-Toledo (Greifensee, Switzerland). Each sample with a known mass has been introduced in an aluminum pan that has been sealed afterward. An empty aluminum pan was used as reference. All experiments were performed in the temperature range from 0 to 300 °C at a 5 °C/min scan rate under a 50 mL/min dry air flow in order to homogenize the temperature within the oven.

Thermal analysis

ETO NCs/F-127 0.03% w/v solid dispersions were observed as function of the temperature by means of an LTS 420 Linkam heating cell (Microvision Instruments, Evry, France) placed under a SMZ 168 microscope (Motic, Kowloon, Hong Kong). Temperature range from 23 to 300 °C at 5 °C/min. Cooling of the system was achieved using a T95-HS Linkam device with liquid nitrogen automatically flowed through the cell. The pictures were taken each 5/12 °C (~0.42 °C) with a Moticam 2500, 5.0M pixels, from Motic.

Results and discussion

Particle size and morphology

The methodology used to make the ETO NCs is based on co-precipitation or anti-solvent precipitation process. Basically, the drug is solubilized in an organic solvent and then added to an aqueous solvent containing surfactants or not. The entire solution is completely evaporated to recover a powder containing both drug and stabilizer. Followed by redispersion in a solution where drug is poorly soluble to form a nanodispersion. The striking parameters for the preparation of drug NCs using co-precipitation approach are the solvent/antisolvent volume ratio, the nature of these solvents, the concentration of surfactant and the evaporation rate. The physical properties of drug NC are directly correlated to these factors. Firstly, API/surfactant ratio has been specially studied to find the most suitable ETO NC formulation. Based on the literature, MeOH was used to solubilize the ETO, F-127 was used as surfactant and water as antisolvent solution. More precisely, ETO was dissolved in absolute MeOH in glass vial and slowly injected under agitation (1200 rpm) in water containing the F-127, different API/surfactant (P1) ratios were used. The solubilized drug was co-precipitated by evaporating the entire solution using a rotavapor under vacuum for 0.5 hour. The resulting powder was kept under vacuum to remove any traces of MeOH. Then followed by 10 min. of hydration using water containing poloxamer (P2).

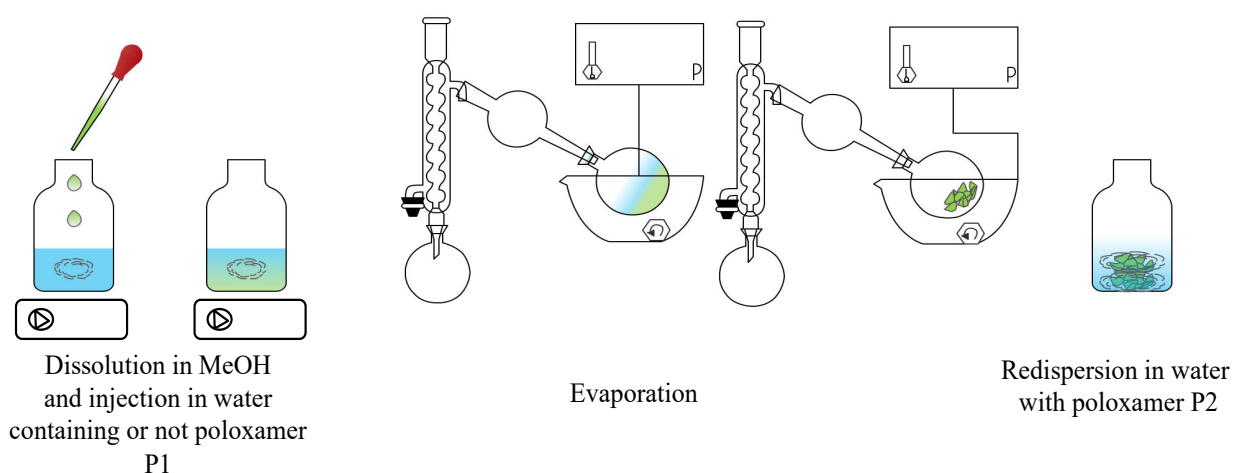


Figure 13 – Scheme of ETO NCs preparation using the co-precipitation process.

As mentioned, the co-precipitation is based on the addition of solubilized drug from organic phase into aqueous solution under agitation, therefore, nucleation and nanocrystals formation appear, strongly depending on organic phase nature and its solubility in the aqueous phase. Indeed, the appearance of nuclei occurs when the organic phase is mixed into the aqueous phase, then, the nucleation is governed by the diffusion of these nuclei to the liquid interface in the solution monitoring the NCs properties.²²⁶ It is accordingly crucial to select an organic phase miscible to the aqueous solution, easily removable from the mixture and where the drug is highly soluble to ensure homogeneous NCs properties. In our study, MeOH was preferred as ETO was detected to be highly and freely soluble in it.

Additionally, from our understanding, the volume ratio of MeOH/H₂O used for the co-precipitation process is also essential for the preparation of the nanodispersion, indirectly it relies on the concentration of the drug in the organic phase when the mixing with the aqueous phase occurs. The drug nucleation to NCs depends on its initial concentration in the organic solvent as the diffusion of the molecule to the liquid interface (solvent- aqueous mixture) also change with the amount of drug. As shown in Figure 14, an increase of ETO NCs size is observed with a diminution of the MeOH: H₂O volume ratio. With a 1.5:2 ratio ETO NCs size were around 400 nm while a 1.5:10 ratio provided ETO NCs around 150 nm. Once again, this may be explained by the fact that the more the ETO is diluted in the mixture, the more its dispersion, changing the drug diffusion and therefore reducing the probability to form bigger nuclei and consequently large NCs. In consequence, for further experiments, MeOH:H₂O volume ratio of 1.5:10 was applied to produce the ETO NCs powder repeatably.

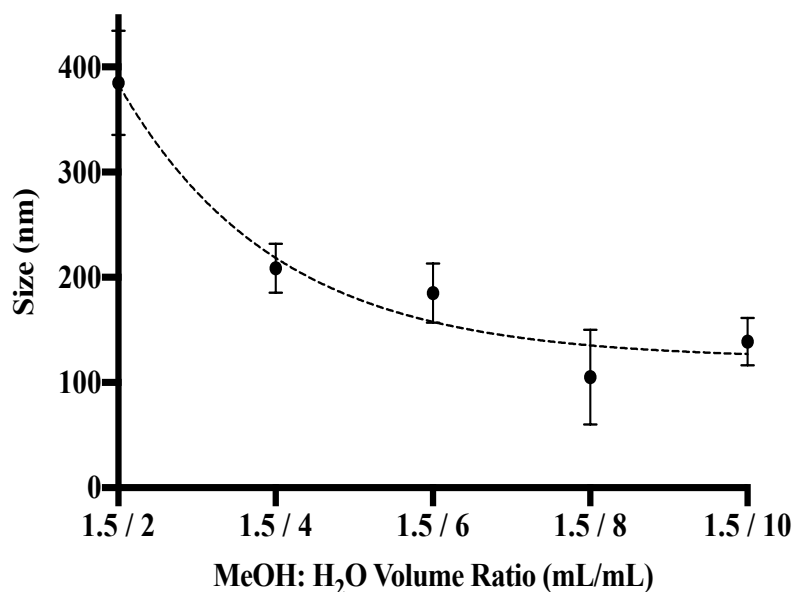


Figure 14 - Etoposide nanocrystals mean diameter size measured by dynamic light scattering versus MeOH/H₂O volume ratio after redispersion in water containing F-127 at 0.083% w/v.

Two striking parameters were identified for the preparation of ETO NCs using co-precipitation, the nature of the organic solvent and the solvent/antisolvent volume ratio. Furthermore, it will be discussed that the nature and the concentration of the stabilizing agent are important, as after ETO NCs formation, the nanoparticles immediately tend to agglomerate.

The NCs protection was done using poloxamer F-127 that is a non-ionic triblock copolymer comprising a middle hydrophobic block of polypropylene glycol (PPG) bordered by two hydrophilic blocks of PEG. Numerous parameters influence the NC stability, the polymer molecular mass, the hydrophobic/hydrophilic ratio of the chain, the nature of the chain functional groups and the polymer conformation.⁴⁷ Sharma *et al.* examined the size of indomethacin NCs produced by wet milling and high pressure homogenizer (HPH) using two dissimilar surfactants, Polyvinylpyrrolidone-K25 (PVP) and F-127, the results indicated a surface modification and a size difference between NC according to the nature of the polymer.⁴⁸ As previously mentioned, Lee *et al.* also evidenced the impact of the hydrophobic/hydrophilic polymer ratio on the NC steadiness by producing a polymer with the same hydrophobic part but diverse hydrophilic groups. The study concluded that the polymer hydrophobicity is a striking parameter to the particle stabilization. Indeed, the polymer should contain a minimum of 15% hydrophobicity moieties to present efficient stabilization, as the adsorption is better on the NC surface in such a case.⁴⁹ Hence, Pluronic F-68 and F-127 can be considered as stabilizing

agents for ETO NCs since their hydrophobicity moieties represent ~16% and ~25%, respectively.^{227,228}

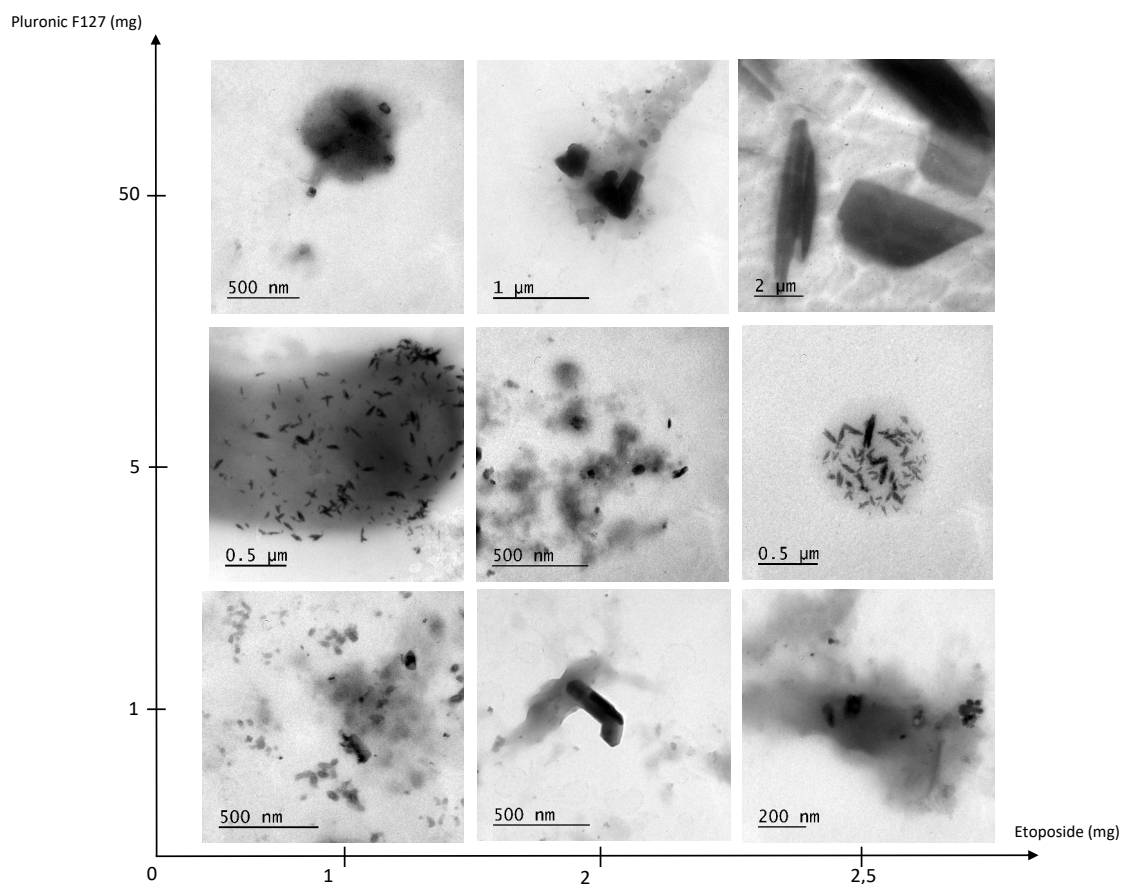


Figure 15 - Etoposide nanocrystals observed by TEM with different size and shape according to the API/Surfactant weight ratio.

Figure 15 gives an overview of the NCs that were synthesized according to the API/surfactant (P1) ratio. The NC physical state, size, shape and morphology, should be chosen in accordance to the application, the target and the route of administration of the drug NC (oral, ocular, parenteral administration). A fast dissolution of the drug and high saturation solubility are not always needed. These first experiments led to select a range of API/surfactant (P1) ratio and the mass of ETO necessary to elaborate the final NC formulation repeatably.

Hence, ETO has been solubilized in MeOH and then injected in water with different amount of F-127 (denoted as P1) comprised between 0 and 8 mg, followed by a complete evaporation and redispersion in water with 10 mg of F-127 (denoted as P2) to reinforce the stability in solution.

In that case, the ETO NCs size has been evaluated to explore the impact of the weight ratio API/P1 on the nanocrystal size (Fig. 16).

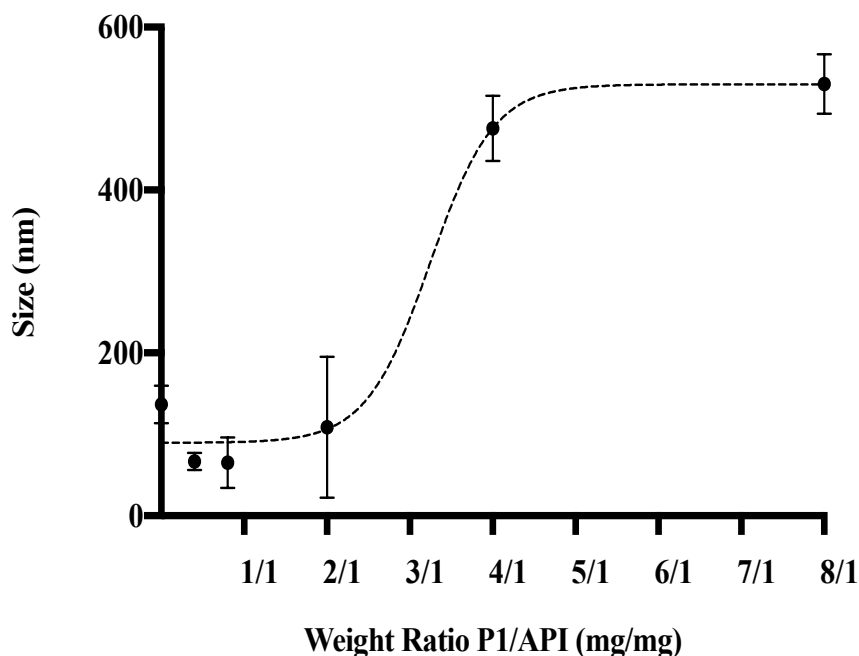


Figure 16 - Etoposide nanocrystals mean diameter size measured by dynamic light scattering versus P1/API weight ratio after redispersion in water.

As shown in Figure 16, the amount of stabilizing agent added before evaporation (P1) influences the size of ETO NCs in suspension. In particular, when 10 mg or less of F-127 for 2.5 mg total ETO is used, NCs size of approximately 100 nm are obtained, contrary to the nanodispersion prepared with more F-127, where NCs have a size ranging from 450 nm to 600 nm. The results obtained from these precipitation experiments showed that the stabilizing agent (stabilizing agent P1), was not needed in the aqueous solution for the evaporation step to have small NCs. These outcomes are counter-intuitive as literature concerning NC synthesis mainly used high stabilizer concentration to control drug nucleation and obtain small nanoparticle. Pouredetal worked on the preparation of azithromycin NCs using co-precipitation and studied the size effect of several stabilizers (HPMC, PVP, PVA, PEG) at a concentration range of 0.5 – 5.0% w/v. The obtained results revealed a drastic size diminution with the augmentation of the stabilizer concentration, and this whatever the type of the stabilizer. With Tween 80 at 1 mg/mL the size distribution was 4064 nm while at 4.5 mg/mL the size reached 504 nm.²²⁹

Similar conclusion was made by Mansouri *et al.* that prepared ibuprofen NCs with 5 different stabilizers (Triethanolamine, SDS, PVP, SLS, Tween 80), 3000 nm NCs were synthesized with SDS at 0.1 mg/mL whereas with 1 mg/mL SDS, ibuprofen nanoparticles had a size of around 900 nm.²³⁰ In our study, it has been demonstrated that the NCs size reduction can be done without stabilizer and be due to the solvent/antisolvent volume ratio and the nature of these solvent. The use of stabilizer is only necessary when redispersing the NCs in water after evaporation (stabilizing agent P2) to prevent NCs agglomeration in solution. Besides, adding the stabilizer only in the final step significantly impact the NC drug yielding as no stabilizer is present during the evaporation that usually creates foam potentially removing the drug.

In consequence, the ETO has been solubilized in methanol and then injected in water without F-127 (P1), followed by a complete evaporation and redispersion in water with different amount of F-127 or F-68 (P2). This experiment put in the spotlight the impact of the weight ratio of API/P2 on the nanocrystal size overtime and compare the impact of two different polymers (Table 7).

Table 7 – Diameter mean size in intensity and PDI (value \pm SD) of ETO NC in suspension measured by dynamic light scattering (Malvern). Comparison of F-127 or F-68 (stabilizing agent P2) at 0.033% and 0.083% w/v after redispersion in water

Formulation	Size (nm)		PDI		Size (nm)		PDI	
	t _{0h}		t _{5h}		t _{24h}			
ETO NC F-127 0.033% w/v	117 \pm 28	0.350 \pm 0.037	274 \pm 10	0.318 \pm 0.010	324 \pm 7		0.358 \pm 0.058	
ETO NC F-127 0.083% w/v	111 \pm 36	0.530 \pm 0.013	282 \pm 65	0.566 \pm 0.049	300 \pm 115		0.697 \pm 0.113	
ETO NC F-68 0.033% w/v	217 \pm 3	0.579 \pm 0.017	268 \pm 23	0.910 \pm 0.127	Precipitation		Precipitation	
ETO NC F-68 0.083% w/v	175 \pm 27	0.357 \pm 0.023	402 \pm 12	0.673 \pm 0.074	Precipitation		Precipitation	

We found that ETO NCs were better stabilized with 0.033% w/v of P2 stabilizing agent as regard to 0.083% w/v, for both F-127 and F-68. Moreover, the stability of NCs was found better with F-127 as its affinity (*via e.g.* hydrophobic/hydrophilic or van der Waals interactions) allow a better adsorption to the NC surface compared to the F-68. As can be seen on Table 7, the nanodispersion prepared with 0.033% w/v F-127 presents a size of approximately 250 nm after 5 h, and 300 nm at 24 h. The nanodispersion prepared with F-68 has a mean size of 268 nm

after 5 h, however the nanodispersion precipitated after 24 h revealing that nanocrystals were not fully stabilized with F-68. The results obtained led to a preferential use of F-127 as stabilizing agent P2, even though F-68 also led to nanoparticles in the nanosize range. The stabilizer concentration used in our study were optimized to be minimale in order to produce a safer formulation and prevent adverse effects. Commonly, in the literature, the stabilizer concentration is above 1% w/v and used a combination of stabilizer such as HPMC/PVP, F-68/PVP or PVP/ β -cyclodextrin.^{231,232}

The characterization by SEM and TEM of the size and morphology of ETO NCs were performed before and after redispersion in water. SEM images show raw ETO powder (Fig. 17 A, B) compared to ETO NCs powder before redispersion (Fig. 17 C, D). As expected, raw ETO presented particles in the micrometer range ($> 10 \mu\text{m}$) in comparison with the ETO NCs which presented agglomerates of $1 \mu\text{m}$ or lower justifying the size reduction of ETO after the co-precipitation process. The accurate size of ETO NCs cannot be observed with SEM because of the nanoparticles agglomeration, Merisko-Liversidge *et al.* acquired similar pictures of ETO NCs agglomerates after WBM process.¹³⁰ Agglomerates were also observed with fenofibrate NCs studied by Li *et al.*¹⁵⁶ Regarding the morphology of ETO, NCs agglomerates exhibited both rod and polyhedral shapes with a predominance for the polyhedral form. As to the raw ETO particles, most of them have a rod-like shape with a length up to $30 \mu\text{m}$ and width up to $10 \mu\text{m}$, that tag these particles as microcrystals. The production of the NCs without surfactant during the evaporation was preferentially used to open up possibilities concerning the NCs self-sheathing. Thus, the NCs coating was solely selected through the redispersion as it is mere to dissolve a great number of surfactants in water so as to prevent the NCs coalescence and perform as an active delivery nanosystem for *in vivo* experiments. ETO NCs suspensions with F-127 0.033% w/v (Fig. 18E) and ETO NCs suspensions with F-127 0.033% w/v + Alb 0.2% w/v (Fig. 18F) were then imaged by TEM to emphasize the difference between the ETO NCs powder and the ETO NCs organization in solution. In solution, the dispersed NCs powder is more uniformly reduced to nanosize particles in the range of 100 nm (Fig. 18E), rod and polyhedral morphologies can still be observed for both formulations. However, well-defined edge NCs are identified for the nanodispersion containing 0.033% w/v of F-127 (Fig. 18E) contrary to the nanodispersion with 0.2% w/v albumin (Alb) (Fig. 18F) where NCs seem spherical and embed in the polymeric matrix leading to NCs aggregation (Fig. 5F) as the combination of the poloxamer and albumin give to the nanosuspension a high surfactant

concentration. TEM pictures were obtained for indomethacin and IZN NCs stabilized by F-127 and F-68 with a stabilizer concentration superior at 2% w/v, NCs surface were also smoother and aggregated in the polymeric matrix as observed Fig. 18F.²³³

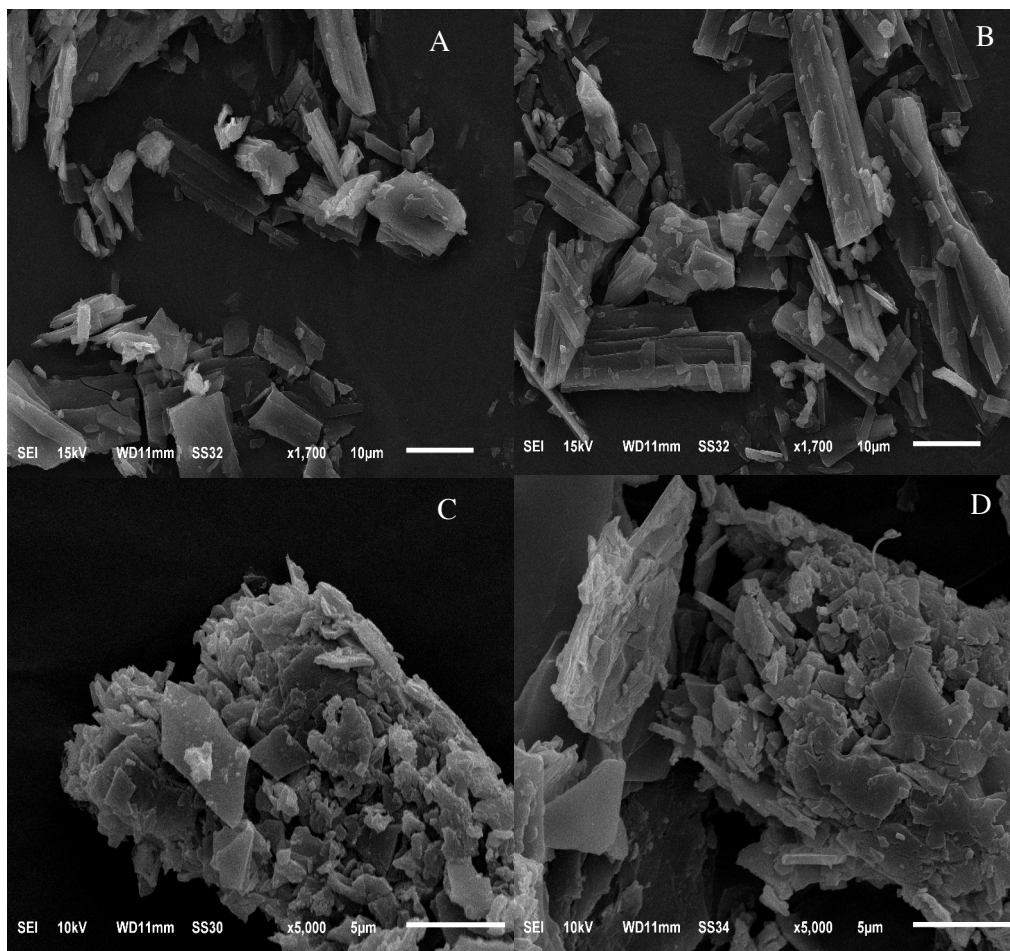


Figure 17 - SEM images of raw ETO powder (A and B, scale bar is 10µm, ETO NCs powder obtained after co-precipitation and evaporation of the solution (C and D), scale bar is 5µm.

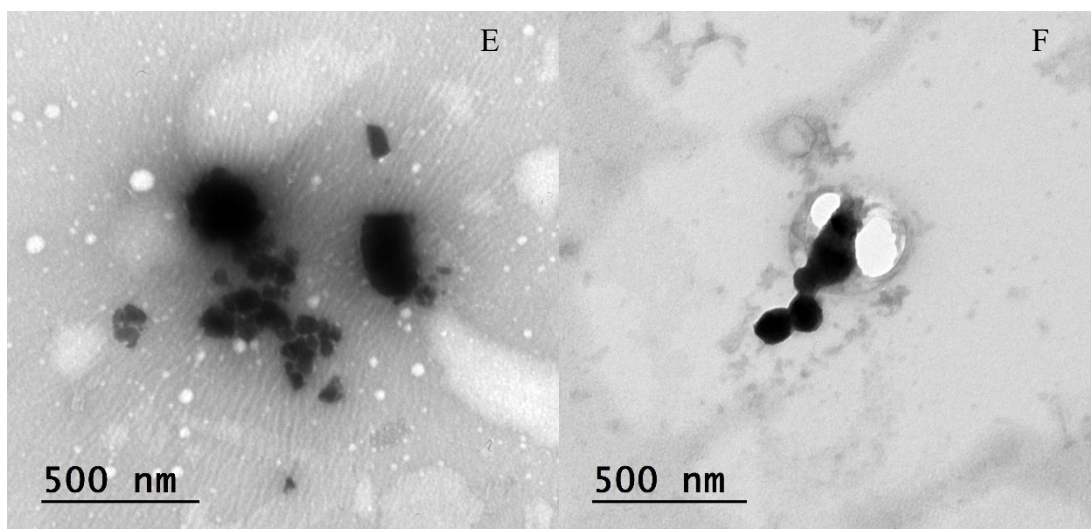


Figure 18 - TEM images of ETO NCs after redispersion in water with F-127 0.033% w/v (E) or with F-127 0.033% w/v + Albumin 0.2% w/v (F). Typical NCs dimensions, 100 nm

X Ray diffraction analysis

ETO crystalline structure were obtained by XRD analysis for the raw ETO powder (Fig 19), ETO NCs powder (Fig 19) and ETO NCs dispersion in solution with F-127 0.033 % w/v (Fig 20). The objective was to evidence the crystallinity of ETO NCs powder after the co-precipitation process and also to verify that NCs are still in the crystal form after redispersion in water. The XRD pattern obtained for ETO NCs powder confirms the total crystallinity of the ETO after process as sharp peaks can be detected.²³⁴ Even though, ETO NCs peak profiles can be assigned to the raw ETO powder, minor shifts are observed. This could be possibly explained by a partial formation of another crystalline form (polymorph) of ETO. Also, peaks intensity are affected by crystallinity, drug crystal size and also merely by the nanocrystals powder packing in the well sample holder, therefore it is not a reliable parameter to understand the crystallinity of the drug.²³⁵ The diffraction pattern obtained for the ETO were comparable to those reported in the literature.²³⁶

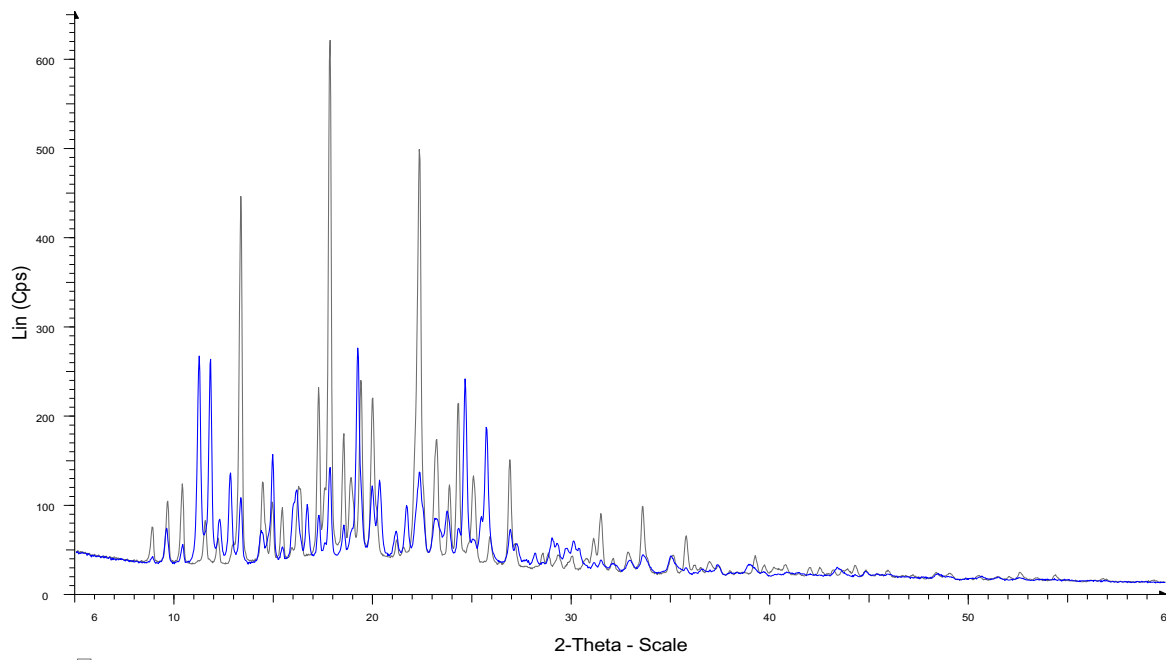


Figure 19 - XRD spectra of raw etoposide drug (blue) and etoposide nanocrystals (black).

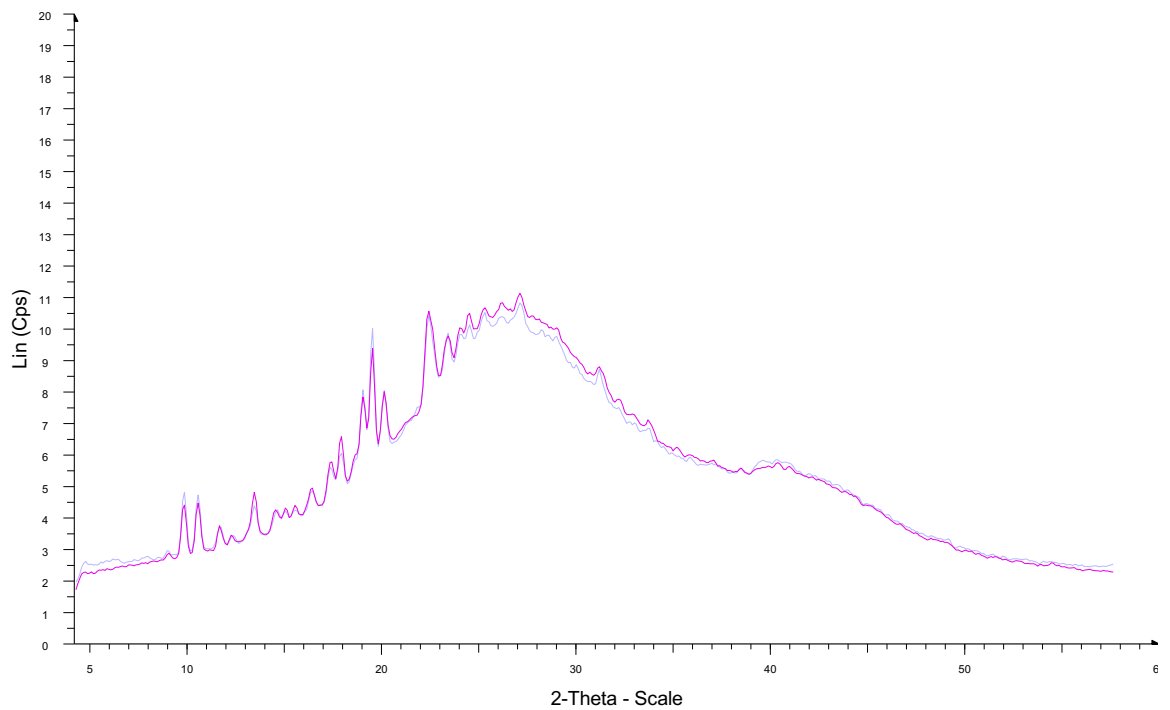


Figure 20 -XRD spectra in water of etoposide nanocrystals in still position (pink) or $\phi 360$ deg. (blue).

If the ETO nanoparticles are definitely crystalline in the solid state, the redispersion in solution ought to not affect their crystallinity. Indeed, XRD analysis of ETO NCs in solution was performed and clearly displayed sharp crystalline peak out of a broad peak corresponding to XRD glass holder and the water (Fig. 20). This result confirmed that ETO NCs kept their crystallinity after redispersion in solution. However, it is surprising that the ETO NCs displayed intense crystalline peak according to their 100 nm size, hence, the NCs coalescence in the glass capillary could have occurred until being sizeable to unveil crystalline peak on the diffraction pattern. This hypothesis cannot be verified by the literature as no publications have been interested in the crystallinity of drug NCs after redispersion in solution.

Dissolution study of etoposide nanocrystals

Conditions were chosen to avoid NCs precipitation in the dialysis bag and allow drug quantification with UV-VIS spectrometer. The objective was to compare ETO NCs F-127 0.03% w/v and ETO NCs F-127 0.17% w/v with ETO microcrystal (MCs) as control. The same experiment was done with ETO NCs F-127 0.03% w/v + Alb 0.2% w/v and ETO NCs F-127 0.17% w/v + Alb 0.2 % w/v in comparison with ETO MCs F-127 0.03% w/v + Alb 0.2% w/v.

Dissolution study of both ETO NCs with F-127 evidenced a significant ($p < 0.05$) sustained release of the ETO compared to the marketed product Toposar[®] (Fig. 21A) and also an increase of the dissolution rate with the size reduction of particles regarding ETO microcrystals ($p < 0.05$). The dissolution rate is correlated to the diffusion layer thickness that is thinner for small particles, enhancing the concentration gradient and therefore dissolution rate²³⁷. The ETO NCs dispersion (average size 100 nm) showed an increase of the dissolution velocity as the specific area is more consequent for this nanodispersion compared to the ETO MCs suspension where particles have a low specific area (larger particles size $> 3\mu\text{m}$) and hence a lower dissolution rate. Only 18 % of initial mass has been released after 6 hours for the MCs, whereas, for the both NCs formulation 35 % were released (Fig. 21A). The two ETO NCs formulation were not significantly different ($p > 0.05$), yet, it can be assumed that ETO release from the NCs form depends on the concentration of the F-127, higher the concentration, lower the release. F-127 acts as a shield to the nanocrystals protecting the drug from surface degradation by the surrounding medium, thus preventing drug dissolution.²³⁸ Obviously, for the conventional marketed product Toposar[®], 50 % of ETO were already released after 6 hours (Fig. 21A), as

the ETO is already solubilized in 33% of ethanol for this formulation, therefore rapidly released through the dialysis membrane.

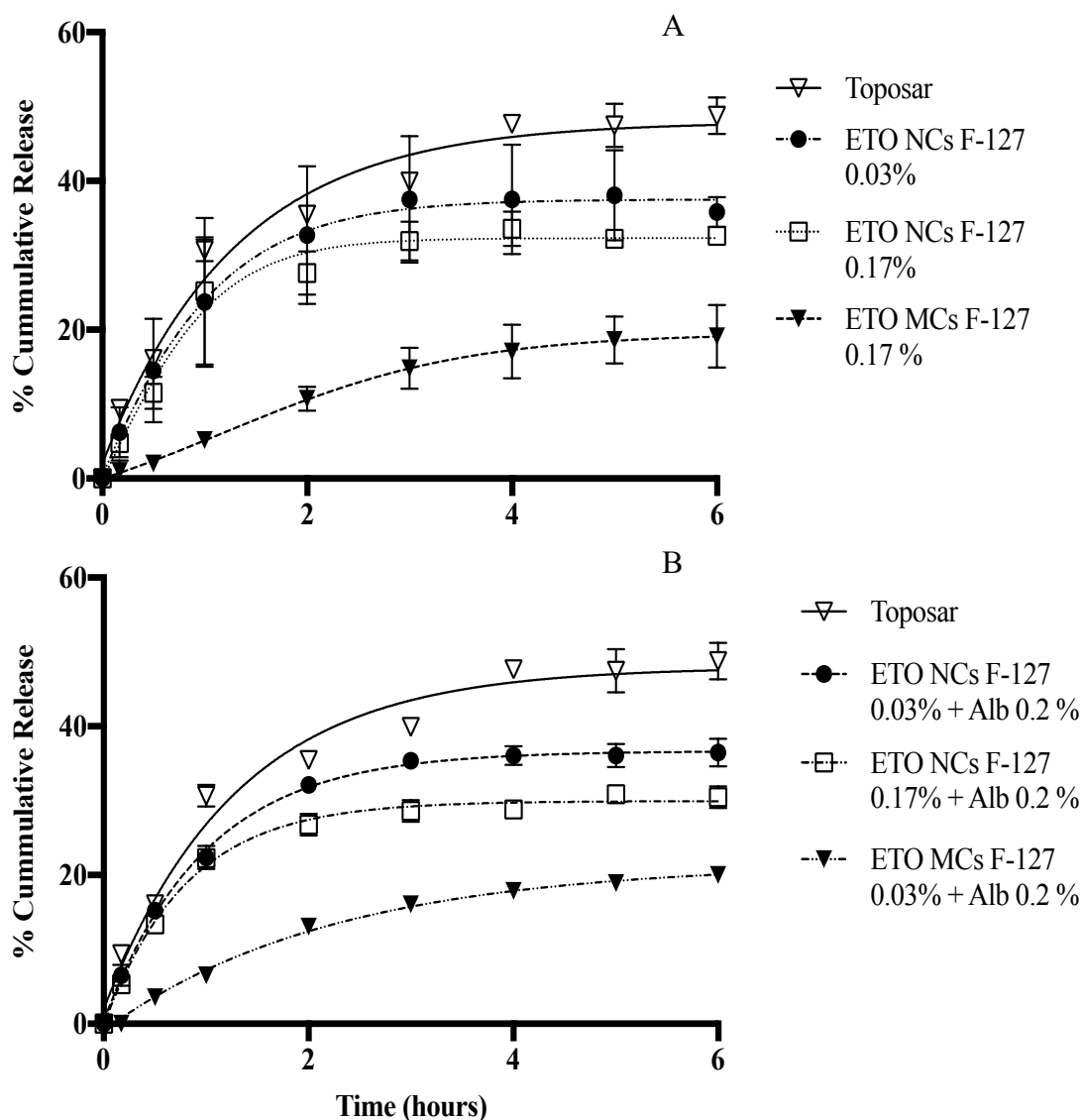


Figure 21 - Release kinetics of various etoposide nanocrystals and microcrystals formulation in HBS buffer incubating at 37 °C under constant agitation

The sustained release of the drug for both ETO NCs F-127 0.03% w/v + Alb 0.02% w/v is not reinforced (Fig. 21B), despite the addition of an extra coating layer surrounding ETO NCs. After 6 hours ETO NCs F-127 0.03% w/v + Alb 0.2% w/v released 37% of ETO while ETO NCs F-127 0.17% w/v + Alb 0.2% w/v released 30%. Both ETO NCs formulation showed significant ($p < 0.05$) enhanced released compared to the ETO MCs and sustained release compared to Toposar[®] (Fig. 21B). Moreover, the variability of the release seems to be better

controlled with formulations containing albumin. Han *et al.* witnessed comparable dialysis results with HCPT nanosuspension. After 1.5 hours, conventional product released 100% of HCPT, HCPT MCs released 20% and the HCPT NCs released only 40% at the same time, proving that these formulations would also display extended blood circulation lifetime and amplified the EPR effect.⁶⁶

Thermal analysis

The thermal behavior experiments were performed to compare ETO crystallinity before and the nanosizing process, to confirm the size reduction of ETO NCs and to understand the interactions of the drug with the polymer. The DSC curve of the raw ETO powder (Fig 22A) exhibits an endothermic peak with an onset temperature of 261 °C corresponding to the ETO melting, and a second endothermic peak at 272 °C due to the ETO degradation.

The DSC curve of ETO NCs powder without stabilizing agent F-127 exhibits two endothermic peaks with a precocious fusion peak at 261 °C (Fig. 22B). This can be explained by the size reduction of ETO NCs that shift the melting temperature to a lower temperature. Nevertheless, the degradation signal of ETO NCs takes place nearly at the same temperature as that of raw ETO (Fig. 22B). As far as the thermal behavior of ETO NCs/ F-127 solid dispersion is concerned, the corresponding DSC curve presents a melting peak at about 55 °C corresponding to the melting of F-127 and two other endothermic transformations (at about 97 °C and about 212 °C, *cf.* Fig. 22D). The depletion of 10 °C of the melting temperature of F-127 in the solid dispersion (Fig. 22D) compared to that of the raw polymer (Fig. 22C) evidences the API/excipient interactions. At this stage, the signal obtained for the solid dispersion around 97 °C cannot be explained (Fig. 22D). The signal around 212 °C obtained for the ETO NCs/ F-127 solid dispersion confirms the nanosized ETO distribution within the polymeric matrix since the temperature of the corresponding signal is lower than that of ETO NCs (Fig. 22D).

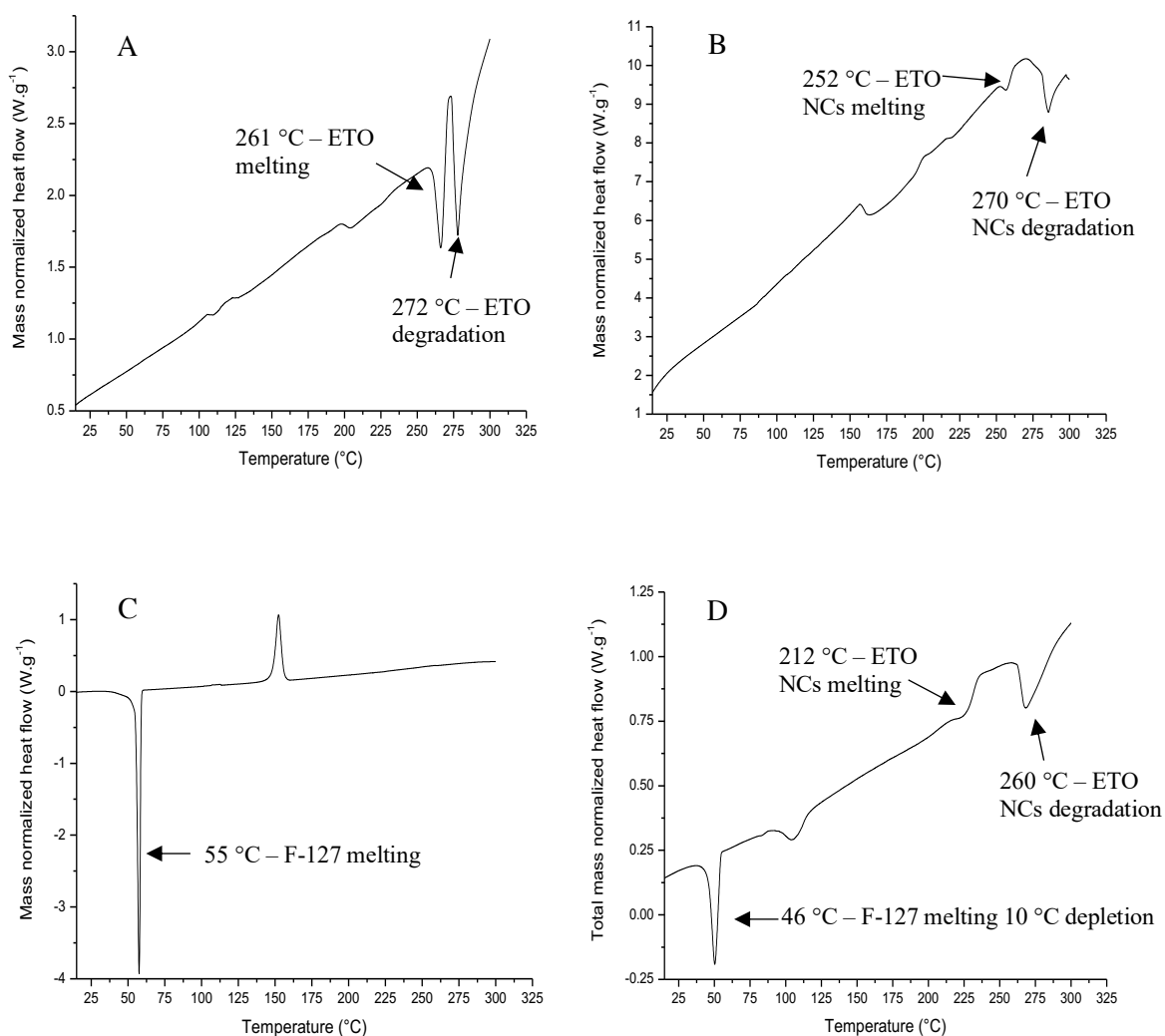


Figure 22 - DSC curves obtained for raw ETO (A), free F-127 ETO NCs (B), F-127 (C) and ETO NCs/F-127 (P2/API = 2/2.5) solid dispersion (D) samples. DSC thermograms are normalized to the total mass sample. Endothermic signals are pointing down.

Thermal microscopy characterization

Thermal microscopy was used as complementary examination to confirm the solid state of ETO NCs in the 0.03% w/v F-127 polymeric matrix. After redispersion of ETO NC in solution with F-127, the nanodispersion were evaporated to obtain a solid mixture of poloxamer and ETO NCs. At 21 °C, the initial solid gather the stabilizer and the ETO NCs that cannot be sighted (Fig. 23) up to 199 °C. The solid form of ETO NCs in the F-127 polymeric matrix is clearly evidenced once the latter has melted at 221 – 225 °C. ETO "fusion" in the F-127 molten system (*i.e.* ETO dissolution) is observed at ~ 220 °C which is good agreements with the above DSC results where the ETO melting was observed at 212 °C (Fig. 22D). Degradation of the ETO

dissolved in the molten ETO NCs/F-127 solid dispersions can be observed after the dissolution process at ~ 263 °C (brown coloration, Fig. 23), also confirming the DSC results described above.

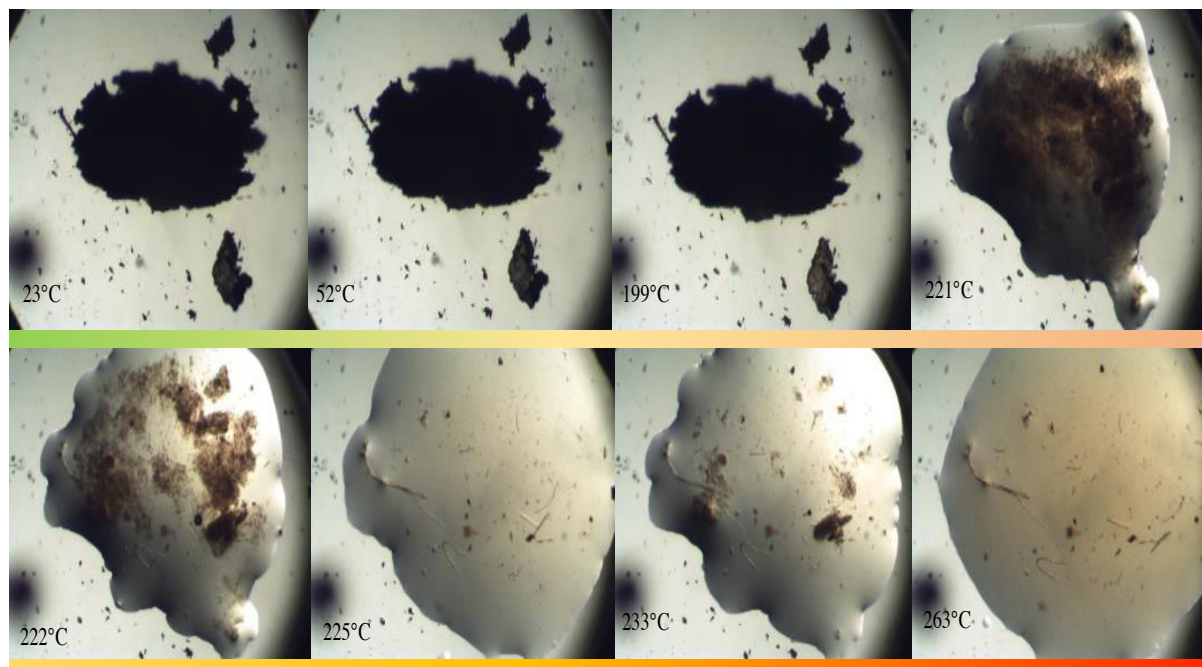


Figure 23 - Thermal microscopy images collected in a closed hot chamber from 20 to 300 °C, $\beta = 5$ °C/ min.

Conclusion and perspectives

The nanocrystal-based technology has been developed to offer a solution to poorly water-soluble drugs, specifically to exhibit better particle stability overtime, high drug loading and safeness compared to classic anticancer formulation. In this study, bottom up approach was apprehended to engineer ETO NCs, controlling the crystallization process to achieve nanoparticles with crucial features such as the size, for upcoming *in vitro* and *in vivo* studies. Indeed, NCs size impact their dissolution rate and therefore their *in vivo* performances, consequently smaller NCs give faster dissolution that is a required feature for oral administration; but not for i.v. injection for which larger NCs are preferred as they could lengthen the drug release resulting in better drug accumulation in the site of interest. The drug nanoparticle size has to be managed in consonance with the application. Surfactants plays an important role regarding the NCs drug release according to their interaction with the drug surface, also prevent the NCs coalescence and affect the drug recognition by the immune

system.²³⁹ Thus, for this study, Pluronic F-127 was found as the best stabilizing and protecting agent for keeping ETO NCs dispersions stable in a physico-chemical point of view, but also injectable in mice for therapeutic purpose. Furthermore, it has been proved that the thus-prepared ETO NCs powder could be stored for several days prior re-dispersion, *i.e.* before being administrated. For such case, long-term stability issues of the solid nanodispersions would be bypassed.

NCs has drawn a lot of academic attention for the last 20 years, yet few marketed formulations are commercially available. The results obtained in this study reinforce the legitimacy of drug NCs as potent forthcoming delivery systems for nanomedicines through several administration routes and slightly open up the way to potential marketability of NCs using co-precipitation.

**IV. Etoposide nanocrystals as
a new delivery system to
treat colon cancer in mice**

Abstract

The aim of this current study is to assess *in vitro* and *in vivo* cytotoxicity of selected ETO NC formulations prepared by co-precipitation in comparison with the conventional marketed product Toposar[®] and the free ETO. The MTT *in vitro* assay was performed on two cell lines (Carcinoma colon CT26 and 3LL Lewis lung cells), the drug uptake was also studied on these cell lines. *In vivo* studies were performed to see whether ETO NC formulations could outperform standard formulations. The plasma and tissues pharmacokinetics of ETO were realized to determine the fate of the drug after administration in mice. The anticancer efficacy was tested after ETO i.v. injection at 10 mg/kg in murine colon carcinoma model. Tumors volume were measured to determine the response to the anticancer treatment, blood samples were withdrawn for hematological analysis. The results obtained show that the delivery of ETO as a NC suspension is a novel promising technology for the therapy of cancer.

Introduction

ETO (synonym VP-16) is known as a semi-synthetic derivative of podophyllotoxin that is recovered from *Podophyllum peltatum* dried roots mainly found in the North of America.²⁰⁹ ETO inhibits the enzyme topoisomerase II that is crucial to control the DNA conformational arrangement by generating double-strand break in the DNA molecule.²¹¹ This compound is a well-known chemotherapy agent and often used as a synergic drug with cisplatin or bleomycin against small cells lung, breast or testicular cancer.²¹⁸ ETO cancer treatment is timetable dependent and prolonged ETO exposures of 2 up to 5 days was shown to be more efficient than a single administration.²²⁰ ETO is often administered as a one-hour administration intravenously. Its maximum dosage is about 500 mg/m² every 3 weeks. Repeated administration over 2 to 5 days increases antitumor activity significantly and the commonly dose is then 60 to 120 mg/m² per day. Toposar[®] is an approved clinical product for cancer treatment including ETO as active pharmaceutical ingredient (API). This therapeutic formulation and treatment are poorly tolerated by many patients resulting in unwell biological conditions such as nausea, hair loss, tiredness, giddiness. It could be mainly explained by the poor targeted delivery of the drug and the repeated administration of the concentrated excipients. Hence, the goal of scientific researches is the development of a new curative medicine with enhanced safety, targeting and efficiency compared to conventional marketed products. Nanocrystal technology offers numerous advantages such as long blood circulation

time, reduced side effects and low concentration excipients.²³⁹ In this study, synthesis of ETO as NC form is considered for i.v. injection against colon carcinoma cancer as this technology has a pharmaceutical potential and takes place among the current dynamic scientific works in nanomedicines.

Materials and Methods

Material

ETO (> 99% purity, CAS number: 33419-42-0) was purchased from Santa Cruz Biotechnology (United States of America), Pluronic F-127 was purchased from Sigma Aldrich (St. Louis, Missouri, United States). MeOH and dimethyl sulfoxide were purchased from Fisher Scientific (Waltham, Massachusetts, United States). All products and solvents were used without further purification. Toposar[®] was a gift from Hopital Gustave Roussy (Ivry Sur Seine, France). Human Serum Albumin (HSA) was purchased from Sigma-Aldrich. Deionized water used for the (by Milli-Q[®], filtered through 0.2 µm membrane) was used for the current study. 0.050 µm Whatman[®] Nuclepore polycarbonate membranes used for filtration were purchased from Fisher Scientific. Pluronic F-127 were purchased from Sigma Aldrich. CT26 and 3LL were purchased from American Type Culture Collection (ATCC, CRL-2638, LGC Standards, Molsheim, France) and cultured at 37 °C in a 5% CO₂-humidified atmosphere in Dulbecco's Modified Eagle Medium (DMEM, Gibco) containing 10% fetal bovine serum (FBS, Gibco Life technologies), 100 µM of streptomycin, and 100 U/mL of penicillin. Isoflurane for anesthesia were purchased from Centravet (France)

Animal

BALB/c female (6 weeks) were supplied by Janvier Laboratory (Le Genest Saint Isle, France). All of the animals were acclimatized at a temperature of 23 ± 2 ° C and under light/dark conditions for 4 week and provided food and water. The experiments were led in accordance with the European and national guidelines and were also validated by the ethics committee (APAFIS 18.118).

In vitro CT26 and 3LL

In vitro studies were performed to assess the potential of ETO nanocrystals on cancer cells and to lead future *in vivo* studies. Cytotoxicity studies of ETO NCs/ F-127 0.083% w/v, ETO NCs/ F-127 0.083 w/v + Alb 0.2% w/v, free ETO (Solubilized ETO in water with 10% DMSO), Toposar[®] (2 mg citric acid anhydrous, 650 mg polyethylene glycol 300, 80 mg polysorbate 80 and 33% v/v absolute ethanol) were tested on CT26 colon cancer and 3LL Lewis lung cancer cells. Protocol will be described for CT26, equivalent for 3LL. First, CT26 colon carcinoma cells were cultured in Dubelcco's modified Eagle's medium (DMEM) containing 10% foetal bovine serum and penicillin/streptomycin (50 mmol) at 37 °C. Cells were plated at the concentration of 200,000 cells/mL in 96 well plates for 24 h. Then, CT26 cells were incubated with both ETO NCs formulation, free ETO and Toposar[®]. After, 48 h and 72 h, the tested formulations were removed from wells and cells viability was performed using the colorimetric MTT test,²⁴⁰ absorbance was determined at 562 nm in a microplate reader (BioKinetics Reader, EL340). The results are displayed as percentage of viable cells.

Nanocrystal cellular uptake CT26 and 3LL

In vitro TEM imaging studies were performed to observe the internalization of the ETO NCs inside the cells. ETO NCs/ F-127 0.083% w/v, ETO NCs/F-127 0.083 w/v + Alb 0.2% w/v were tested on CT26 and 3LL cancer cells. Cells (2.10^5 cells/mL) were put in 25 cm³ culture flask for 24 h until confluence. Then, CT26 cells were incubated with each ETO NCs formulations for only 2 h. After this period, cells were trypsinized (Trypsin-EDTA 0.5%) and recovered in Falcon[®] tubes. Cells were water washed and fixed with paraformaldehyde 2% + glutaraldehyde 2.5% + Na cacodylate 0.1 M (pH 7.3) + CaCl₂ 5mM, samples were postfixed in 1% OsO₄ and stained with filtered (0.22 μm) uranyl acetate 1%. Then, specimens were rinsed in 0.1M phosphate buffer and dehydrated in an escalating streak of ethanol at 30, 50, 70, 95 and 100% (3 × 10 min. for each) and passed on with propylene oxide and ethanol (50/50 v/v mixture) for 10 min. Followed by polymerization in Epon at 60 °C for 72 h. Samples were sliced (80 nm) using a Leica ultracut S ultramicrotome fitted with a diamond knife.²⁴¹ The selected cell sheets were not additionally stained to avoid precipitates that could be confound with ETO NCs. Specimens were studied under a transmission electron microscope (JEM-100S, JEOL, Tokyo, Japan) at accelerating voltage of 80 kV.

Plasma and tissues pharmacokinetics of etoposide

Seventy-two BALB/c female (6 weeks) mice were used for the determination of the ETO NCs concentration overtime in the plasma and selected tissues (liver, rate, kidney, lungs). Four formulations were tested, ETO NCs/ F-127 0.2% w/v, ETO NCs/ F-127 0.2% w/v + Alb 0.48% w/v, free ETO and Toposar[®]. Each formulation was given intravenously at 10 mg/kg ETO. Then, retro-orbital blood sample were realized (200 µL) at different time, 1, 15, 30, 45, 60 and 120 min. and add in an Eppendorf tube containing 20 µL of EDTA. Plasma was collected by centrifugation at 2000 rpm for 15 min. and frozen at -20 °C for further high- performance liquid chromatography (HPLC) analysis. Tissues samples were taken after mice sacrifice at 45, 60 and 120 min. in order to have enough drug accumulation in the selected organs and frozen at -80 °C for further HPLC analysis. ETO contained in organs were recuperated by grinding organs in chloroform using Precellys[®] tubes. Liver and kidneys were crushed in 5 mL of chloroform in a 7 mL capacity Precellys[®] tubes, lungs and spleen in 1.2 mL of chloroform in a 2 mL capacity Precellys[®] tubes. Samples were centrifuged and chloroform was totally evaporated in glass vials, dry residues were redispersed in 130 µL of water: methanol mixture as a mobile phase (50/50 v/v) and ready for analysis. The HPLC was set as reversed phase (RP-HPLC, 1260 Infinity, Agilent[®]) with isocratic conditions. The analytical column was standard with a reversed phase C18 (250 mm × 4.6 mm, 5 µm, Waters). The injected volume was 50 µL for all samples.

Antitumoral efficacy

Sixty BALB/c female mice (Janvier, St Genest de Lisle, France) aged of 6 weeks were divided into 5 groups (5*n_{mice}=12), four groups received four different ETO formulations, ETO NCs /F-127 0.2% w/v, ETO NCs /F-127 0.2% w/v + Alb 0.48% w/v, free ETO, Toposar[®] and one group were used as control. The first 4 groups have received 4 injections of ETO at 10 mg/kg, an injection daily for two consecutive days, a day for rest, followed by an injection daily for two days in a row. The untreated control group was used as comparison for tumor volume. Murine carcinoma tumors CT26 were subcutaneous confined on day 1 using a 12-gauge trocar (38 mm) into the mouse flank previously disinfected with alcohol. After 8 days, mice were separated in groups in order to have homogeneous tumors volumes. The anticancer treatment started the same day as described above.

The anticancer treatment started on day 8 as described above to have homogeneous tumor growth in each group. Tumor size and body weight were evaluated using a digital caliper every two days until day 17. Tumors volume (V) were calculated as followed: $V = (\text{Length} \times \text{Width} \times 2)/2$.²⁴² For the survival study, weight loss superior to 10% or tumors size > 10% of the mice body weight were established as endpoints. All mice were anesthetized before ETO injection. in an induction chamber under a flow of oxygen/isoflurane (30/70) (Tec 7, Minerve, Carnaxide, USA).

Hematological Toxicity

Thirty BALB/c female mice (Janvier, St Genest de Lisle, France) aged of 6 weeks were divided into 5 groups ($5 \times n_{\text{mice}}=6$), four groups received four different ETO formulations, ETO NCs /F-127 0.2% w/v, ETO NCs /F-127 0.2% w/v + Alb 0.48% w/v, free ETO, Toposar[®] and one group were used as control. The drug schedule protocol was equivalent to the anticancer efficacy study. Blood samples were taken in the mice tail vein at 1, 12, 15, 17 and 22 days and transferred to Eppendorf tube containing 2 μL of EDTA for white blood cell (WBC) numbering using a MS9-5 (MS Pharmaceuticals, France). All mice were anesthetized before ETO injection in an induction chamber under a flow of oxygen/isoflurane (30/70) (Tec 7, Minerve, Carnaxide, USA).

Statistical analysis

The plasma and tissues pharmacokinetics, anticancer efficacy, hematological toxicity and *in vitro* data are shown as mean \pm standard deviation (SD). Statistical investigation was done by two-way ANOVA with Bonferroni correction with GraphPad Prism version 7. More precisely, plasma and tissues pharmacokinetics analysis were fit to a one phase decay and a gaussian model respectively. Anticancer efficacy, hematological toxicity analysis was fit to a baseline corrected model. *In vitro* studies were fit to a one phase decay model and submitted to a Student's *t* test examination.

Results and discussion

In vitro CT26 and 3LL

In vitro tests were performed to evaluate the efficiency of ETO NCs and the influence of the amount of surfactant on cytotoxicity. ETO NCs were compared to marketed product Toposar[®] and free ETO. The viability of CT26 cells has been evaluated after 48 and 72 h. The related results are presented in Figure 24 and the corresponding data are gathered in Table 8. The IC₅₀ after 48 h of ETO NCs on CT26 cells with and without albumin were 13.73 ± 5.52 and 20.06 ± 6.09 μM , respectively. At 72 h, these values are 4.66 ± 0.91 and 4.40 ± 1.20 μM , respectively (Fig. 24). The latter results clearly prove ETO NCs efficiency to inhibit cell growth. ETO NC formulations show similar results with and without albumin association after 48 h ($p > 0.05$) and 72 h ($p > 0.05$). Interestingly, the additional coating of albumin did not significantly improve the sustained release and cytotoxicity of ETO. However, the cytotoxicity of ETO NCs slightly outperformed the free ETO, for which the IC₅₀ at 72 h was 5.60 ± 0.10 μM . Essentially, the ETO NCs were not more efficient than Toposar[®] ($p > 0.05$), having an IC₅₀ at 48 and 72 h of 16.71 ± 9.95 and 4.55 ± 0.50 μM respectively.

Lia *et al.*⁵² also expected a better internalization of the drug formulated as NCs, but PTX NCs did not have better cytotoxicity than Taxol[®]. Regarding 3LL cells line (Fig. 25, Table 8), all formulations tested were notably more efficient ($p < 0.05$) in comparison with the IC₅₀ obtained for the CT26 cell lines. ETO is known to be very effective against lungs cancer cells as their genomic factors are limited (*e.g.* mutation or down regulation) decreasing drug resistance.^{243,244}

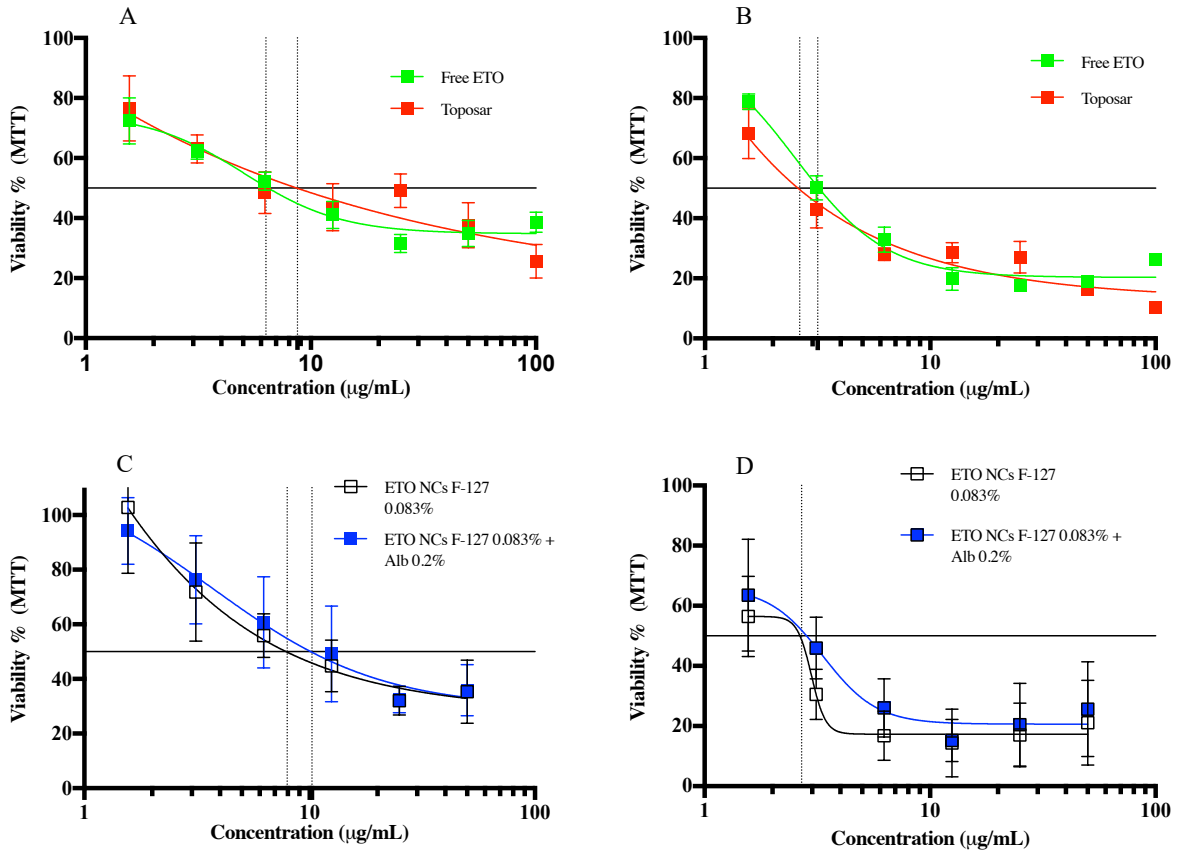


Figure 24 - CT26 cells viability after 48 h (A, C) and 72 h (B, D) for ETO NCs F-127 0.083 w/v, ETO NCs F-127 0.083 w/v + Alb 0.2 % w/v, Toposar® and free ETO.

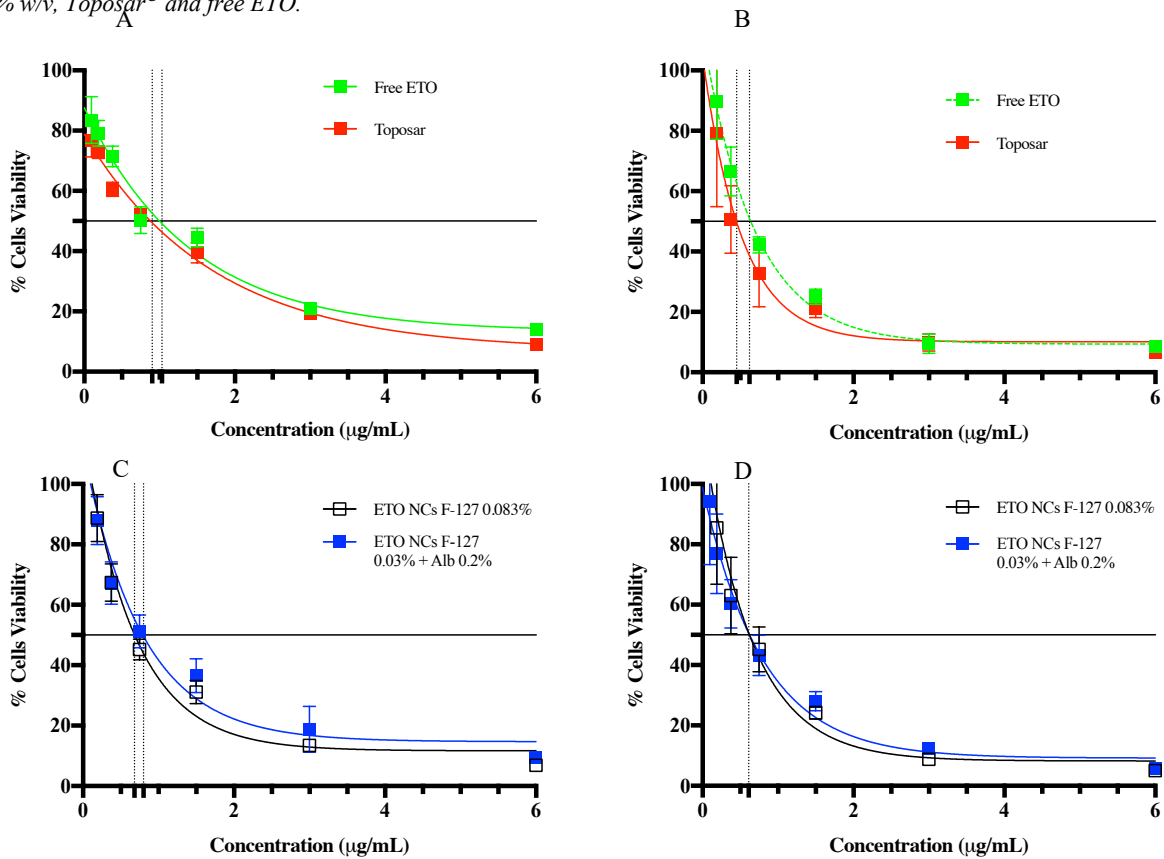


Figure 25 – 3LL cells viability after 48 h (A, C) and 72 h (B, D) for ETO NCs F-127 0.083 w/v, ETO NCs F-127 0.083 w/v + Alb 0.2 % w/v, Toposar® and free ETO

Table 8 - CT26 and 3LL viability (IC50) after 48 and 72 hours for ETO NCs F-127 0.083% w/v, ETO NCs F-127 0.083% w/v + Alb 0.2% w/v, Toposar® and free ETO. For each formulation, the related excipients were separately tested for the cell viability values normalization

Formulations	CT26 - IC50	CT26- IC50	3LL - IC 50	3LL - IC 50
	at 48 h (μM)	at 72 h (μM)	at 48 h (μM)	at 72 h (μM)
ETO NCs/F-127 0.083% w/v	13.73 ± 5.52	4.66 ± 0.91	1.17 ± 0.12	1.01 ± 0.24
ETO NCs/F-127 0.083% w/v + Alb 0.2% w/v	20.06 ± 6.09	4.40 ± 1.20	1.31 ± 0.26	1.00 ± 0.20
Free ETO	11.28 ± 1.40	5.60 ± 0.10	1.66 ± 0.13	1.05 ± 0.02
Toposar®	16.71 ± 9.95	4.55 ± 0.50	1.43 ± 0.13	0.75 ± 0.10

Nanocrystal cellular uptake on CT26 and 3LL

Cancer frequently acquires resistance to several drugs which is labelled as multidrug resistance (MDR) and represent a major drawbacks for cancer therapy, thus deliver a drug as nanoparticle to cancer cells could overcome MDR mechanisms.²⁴⁵ The mechanism of drug NC internalization has been evidenced to be among endocytosis pathways.^{246,247} *In vitro* cells imaging was performed with CT26 (Fig. 26A-C) and 3LL cells line (Fig. 26D-F) to evidence whether ETO NC could be internalized into the cells as NC or solubilized drug; since the phagocyte mechanism is completely different according to the size, shape, charge surface and nature of the drug, it could have been caveolae or clathrin mediated endocytosis, pinocytosis or phagocytosis pathway.²⁴⁸

After two hours, TEM pictures displayed that NCs can be internalized inside cells as single particle in the cell perinuclear area (Fig. 26B, C, E, F). Also, despite the NC shape diversity it seems that it does not influence the nanoparticle internalization as diverse shapes can be detected. For *in vivo* evaluation it reinforces the idea that ETO NC could be transported as nanoparticles to the cancer cells in the blood stream at 37 °C and will not be immediately solubilized after i.v. injection, hence changing the *in vivo* fate of NCs. In addition, the cell apoptosis beginning can also be evidenced by the damaged membrane and the small size of the cells that were incubated with ETO NCs formulations (Fig. 26B, C, E, F).

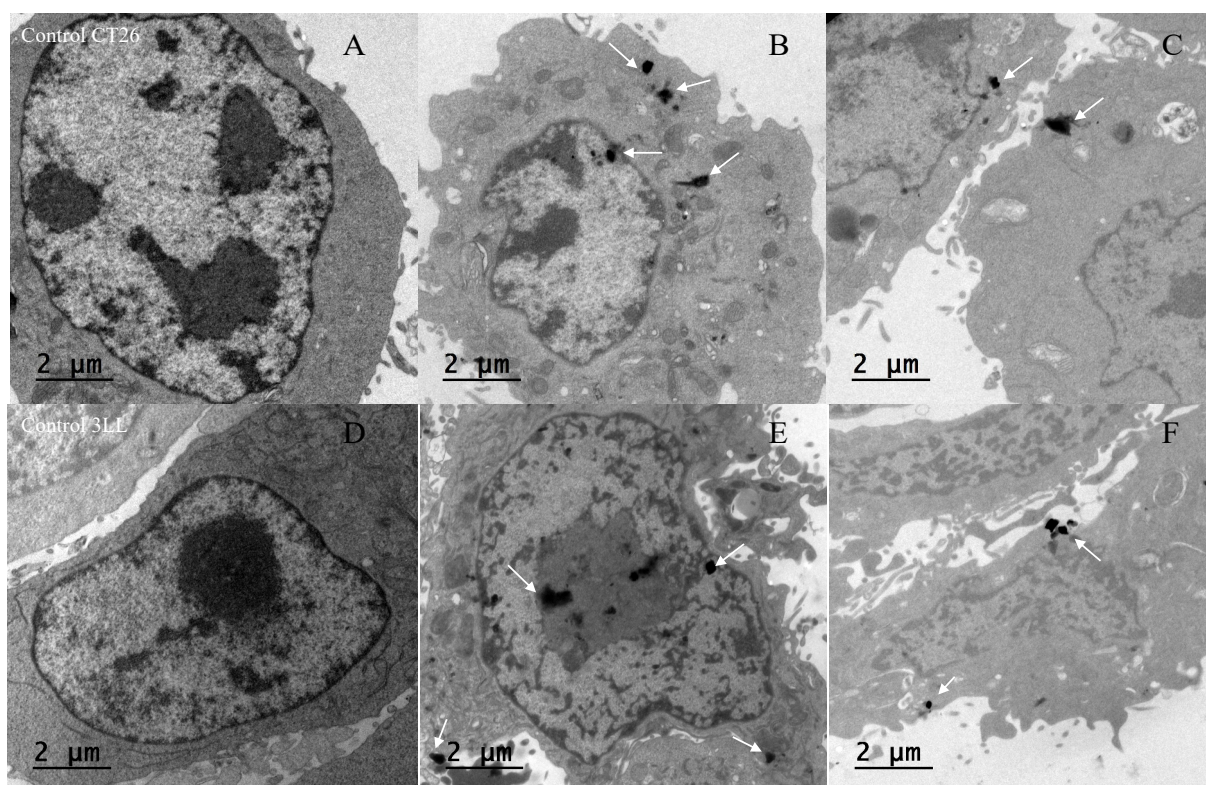


Figure 26 - TEM images for control CT26 (A), ETO NCs/F-127 0.083% w/v CT26 (B), ETO NCs/F-127 0.083 w/v + albumin 0.2% w/v CT26 (C), control 3LL (D), ETO NCs/F-127 0.083% w/v (E) 3LL, ETO NC/F-127 0.083 w/v+ albumin 0.2% w/v 3LL (F). White Arrows show ETO NCs.

Plasma and tissues pharmacokinetics of etoposide

The ETO plasma concentration profile in mice was assessed for the two ETO NCs formulation, the marketed product Toposar[®] and the free ETO. The pharmacokinetic results are presented in Figure 27 and Tables 9 - 10. They showed that both ETO NCs formulation have significantly higher ETO plasma concentration than the free ETO and the Toposar[®] with an $AUC_{0-120min}$ almost 2-fold greater and a higher mean residence time ($p < 0.05$). This is not the first time that NCs drug form were proved to have a better long-life time in C57BL/6 mice plasma than its solubilized analog.²⁴⁹ Ganta *et al.* intravenously injected asulacrine NCs and also perceived a 2.7-fold lifespan augmentation in the plasma compared to the asulacrine solution.¹¹⁷ Besides the solid form of NCs increasing the plasma life time,²⁵⁰ the use of stabilizer comprising PEG is known to reduce protein binding and therefore extend the particle's plasma concentration.^{251,252} Regarding specifically ETO NCs/F-127 0.2% w/v + Alb 0.48% w/v, it was expected to have a significant better blood stream lifespan in comparison with ETO NCs/F-127 0.2% w/v. Nanoparticles coated with albumin are well known to have an prolonged lifespan in blood as albumin has the ability to bind to the FcRn receptor protecting it from degradation, more specifically from endothelial catabolism.²⁵³ But in our study, ETO NCs with albumin had

equivalent $AUC_{0-120min}$ ($550 \pm 37.33 \mu\text{g}\cdot\text{min}/\text{mL}$) and MRT ($2.75 \pm 0.19 \text{ min}$) than ETO NCs ($p > 0.05$) stabilized with simply F-127. This result could be hypothetically justified by the poor albumin interaction with the F-127 hampering the NC stability and therefore its clearance from blood. It could be also explained by the fact that albumin does not prevent the interaction of circulating protein more than F-127 which has a long PEG moiety.

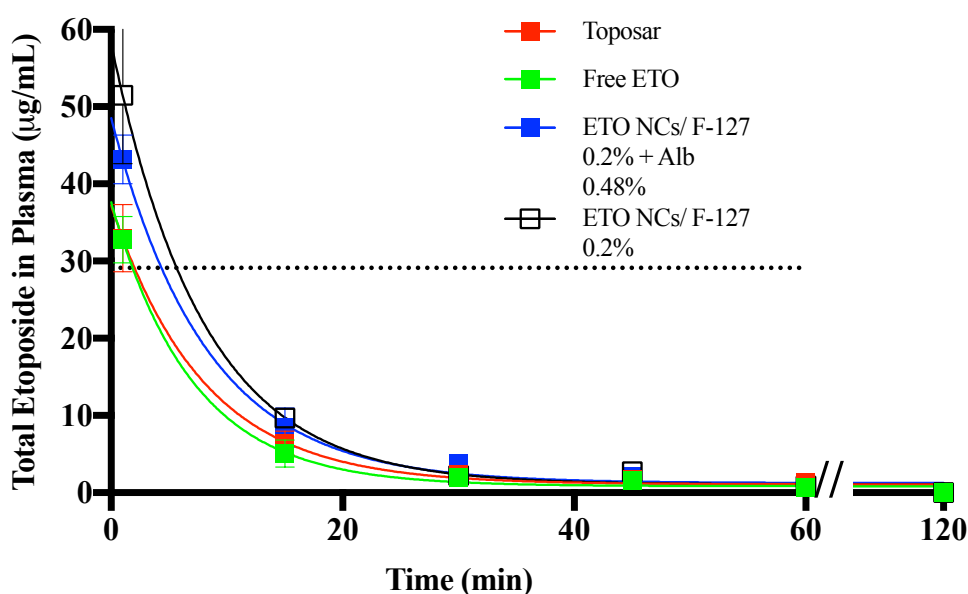


Figure 27- Amount of ETO (μg) in total mice plasma as a function of time after i.v. injection in the mice tail vein. Data shown are means \pm SD (Standard Deviation), $n_{mice} = 6$, injected dose = $10 \text{ mg}/\text{kg} = 200 \mu\text{g}$. Analysis was fit to a one phase decay model.

Table 9 – Pharmacokinetic parameters of etoposide for ETO NCs F-127 0.083% w/v, ETO NCs F-127 0.083% w/v + Alb 0.2% w/v, Toposar[®] and free ETO: maximum amount ($\mu\text{g}/\text{mL}$) in total mice plasma \pm SD ($n=6$), area under the curve ($AUC \pm$ SD ($n=6$)), half time ($t_{1/2}$), and mean residence time (MRT \pm SD ($n=6$)) based on $C_{theo=0}=200 \mu\text{g}$. *, $p_{ETO \text{ NC-Toposar}} < 0.05$, **, $p_{ETO \text{ NC-Free ETO}} < 0.05$

Formulations	Maximum amount in total mice plasma ($\mu\text{g}/\text{mL}$)	$AUC_{0-120min}$ ($\mu\text{g}\cdot\text{min}/\text{mL}$)	$t_{1/2}$ (min)	MRT (min)
ETO NCs/ F-127 0.2% w/v	58.22 ± 1.92	$608 \pm 66.84^{*, **}$	5.52	3.04 ± 0.33
ETO NCs/ F-127 0.2% w/v + Alb 0.48% w/v	48.22 ± 0.98	550 ± 37.33	5.70	2.75 ± 0.19
Free ETO	37.62 ± 0.85	378 ± 29.24	4.89	1.89 ± 0.15
Toposar [®]	37.22 ± 1.05	436 ± 42.59	5.51	2.18 ± 0.21

Table 10 - Drug distribution in liver and lungs for ETO NCs F-127 0.083% w/v, ETO NCs F-127 0.083% w/v + Alb 0.2% w/v, Toposar[®] and free ETO after an i.v. injection at 10 mg/kg in mice. Data were collected 45, 60 and 120 minutes after the

Formulations	Etoposide distribution (µg/g)					
	Liver			Lungs		
	45 min	60 min	120 min	45 min	60 min	120 min
ETO NCs/F-127 0.2% w/v	10.50 ± 9.2	4.33 ± 4.9	–	51.29 ± 19.9	21.80 ± 11.3	–
ETO NCs/F-127 0.2% w/v + Alb 0.48% w/v	13.59 ± 3.9	12.13 ± 7.3	9.41 ± 9.6	16.68 ± 9.1	–	–
Free ETO	7.46 ± 6.4	7.29 ± 6.5	0.46 ± 1.1	15.23 ± 1.2	–	–
Toposar [®]	5.86 ± 4.7	6.41 ± 2.3	–	86.92 ± 6.9	8.94 ± 5.4	–

injection and are presented as followed µg of ETO per g of organ ± SD (n=6). Analysis was fit to a gaussian model

Table 11 – AUC_{0-120min} comparison for ETO NCs F-127 0.083% w/v, ETO NCs F-127 0.083% w/v + Alb 0.2% w/v, Toposar[®] and free ETO in liver and lungs. Data are presented as followed AUC_{0-120min} (µg.min/g) ± SD (n=6). *, p_{ETO NC-Toposar} < 0.05, ** p_{ETO NC-Free ETO} < 0.05, *, p_{ETO NC-Toposar} < 0.05

Tissues	Etoposide AUC _{0-120min} (µg.min/g)			
	Toposar [®]	Free ETO	ETO NCs/F-127 0.2% w/v	ETO NCs/F-127 0.2% w/v + Alb 0.48% w/v
Liver	416.0 ± 131.1	497.0 ± 250.1	517.3 ± 283.3	1145 ± 376.8*,**
Lungs	2943 ± 2304	457 ± 28.62	2577 ± 671.3	500.4 ± 214.9*

Tissues biodistribution analysis was performed after mice sacrifice at 45 min. The main recovery of ETO was found in the lungs and liver for all formulations. ETO was not detected in the kidneys or spleen at any time whatever the ETO formulation, thus data for these organs are not shown. ETO NCs /F-127 0.2% w/v + Alb 0.48% w/v exhibits significantly higher AUC_{0-120min} (p < 0.05) and lower clearance rate for the liver compared to Toposar[®], free ETO and ETO NCs /F-127 0.2% w/v (Table 11). Commonly, albumin coated drug were found to have lower clearance rate, as mentioned above, the albumin interacts with the hepatic FcRn receptor accountable for upholding its lifespan.^{253,254} For the three previous formulation, the AUC_{0-120min} in the liver were not significantly different (p > 0.05), therefore the biodistribution can be considered equivalent after 120 min. The ETO accumulation in the liver is explained by the physical state (e.g. size) of the nanoparticles but additionally by its recognition by the cells of the mononuclear phagocyte system (MPS) that uptake and remove exogenous agents.²⁵⁵

Regarding the lungs, the $AUC_{0-120\text{min}}$ for Toposar[®] was notably greater ($p > 0.05$), 2943 $\mu\text{g}\cdot\text{min}/\text{g}$, in comparison with free ETO and ETO NCs /F-127 0.2% w/v + Alb 0.48% w/v having an $AUC_{0-120\text{min}}$ of 457 and 500 $\mu\text{g}\cdot\text{min}/\text{g}$, respectively (Table 11). Indeed, for IV, rod-shaped nanoparticles between 20 up to 150 nm, like ETO NCs, were proved to end up in organs as the lungs and the liver, in contrary bigger spherical-shaped particles, as Toposar[®] finish up essentially in the lungs.²⁵⁶ Hence, the drug accumulation in the lungs could be elucidated by the size of NCs comprised between 100 - 300 nm, undeniably particles size and shape change the nanoparticle biodistribution, the circulation lifespan related to the recognition by the MPS, and the particle extravasation in the blood stream.²⁵⁷ In addition, free ETO (10% v/v DMSO), despite its solubilized form were also detected in the lungs as much as ETO NCs/F-127 0.2% w/v + Alb 0.48% w/v with an $AUC_{0-120\text{min}}$ of 457 $\mu\text{g}\cdot\text{min}/\text{g}$, hypothetically, it could be elucidated by a partial precipitation of the ETO right after i.v. injection and accumulation in the lungs.²⁵⁸ In conclusion, it is interesting to notice that ETO NC formulations have similar elimination properties than Toposar[®].

Anticancer Efficacy and Hematological Toxicity

The therapeutic efficacy following 4 different ETO treatment was evaluated on BALB/c female mice (Fig. 28A). Mice received 4 injections of ETO at 10 mg/kg, an injection daily for two consecutive days, a day for rest, followed by an injection daily for two days in a row. The treatment started after 8 days. Tumor growth inhibition was compared for ETO NCs F-127 0.2 w/v, ETO NCs F-127 0.2 w/v + Alb 0.48 % w/v, Toposar[®] and free ETO. Figure 28B shows the tumor growth inhibition of the applying formulations. As can be seen in Figure 28B, for all the formulation tested, tumor inhibition was equivalent up to 12 days ($p > 0.05$). However, after 15 days, ETO NCs/F-127 0.2% w/v were significantly more profitable than the marketed product Toposar[®] ($p < 0.05$). The tumor volume was even more decreased after 17 days (3 days after the last ETO injection) in comparison with the Toposar[®] ($p < 0.05$). Similar results were obtained by Liu *et al.* with a taxane chemotherapy, tumor inhibition effect of PTX NCs was better than Taxol[®] injected intravenously at a concentration of 10 mg/kg.⁵² Hypothetically, this could be justified by the size and the solid form of NCs that are EPR-shaped and have a longer blood stream lifespan. It has also been proven that nanoparticles have a better penetration into the surrounding interstitium of the tumor leading to a better bioavailability and thus anticancer

efficacy.^{259,260} ETO NCs formulations were compared with different excipient composition to observe whether the effect on the tumor inhibition was major or not. At day 17, ETO NCs /F-127 0.2% w/v was significantly better than ETO NCs /F-127 0.2% w/v + Alb 0.48% w/v ($p < 0.05$), indicating that low concentration of surfactant is more favorable for cancer treatment, and assuming that the nature of interactions and the force of the adsorptive bindings to the ETO NCs are dissimilar with the excipient composition and its concentration.^{261,262} For ETO NCs/F-127 0.2% w/v, the time to reach the median tumor volume in comparison with Control was delayed of 5.31 days, slightly lower 3.27 days for ETO NCs/F-127 0.2% w/v + Alb 0.48% w/v respectively (Table 11). Toposar[®] and free ETO have barely postponed the median tumor volume of about half a day revealing a poor treatment response for these two formulations (Table 12). Regarding, the mice weight loss (Fig. 28C) throughout the investigation, ETO NCs /F-127 0.2% w/v had a slight weight loss of -0.83% proving that this treatment is well tolerated. Nevertheless, for the other two ETO NCs, for Toposar[®] and free ETO formulations a decrease is observed that can be primarily explained by a poor targeting of the ETO to the tumor and therefore to healthy organs. Also, a higher concentration of toxic excipients could foster unwanted side effect causing loss of appetite and thus the mice weight loss.²⁶³

Blood samples were taken at day 1 as control, then at 12, 15, 17 and 22 days (Fig. 28A). The leukocyte count and red blood cells (RBC) nadir were identified the last day of treatment for all groups (Tables 13 and 14). ETO NC formulations and Toposar[®] had a notable leukocyte and RBC decrease compared to the control ($p < 0.05$) after 12 days (Fig. 29). No hematological significant change was observed for both NC formulations in comparison with Toposar[®] ($p < 0.05$) the same day. The recovery of RBC and WBC from day 12 to day 22 was also equivalent for both ETO NC formulations in opposition with the Toposar[®] ($p > 0.05$). In contrast, Liu *et al* injected solubilized ETO at 5 mg/kg in Balb/c mice two days consecutively and observed a leucocyte decrease from 11 to $8 \times 10^9/L$ (18% loss) that is in accordance with our protocol where ETO NCs were injected at 10 mg/kg four times and a leucocyte decrease from 11 to $2 \times 10^9/L$ was observed (82% loss).²⁶⁴

Mice that did not receive treatment and Toposar[®] reached the final stage at day 17, expressing the virulence of the CT26 colon tumors (Fig. 28D). ETO NCs/F-127 0.2% w/v + Alb 0.48% w/v and ETO NCs/F-127 0.2% w/v prolonged the median survival time (MRT) in comparison to Toposar[®] to 9 and 7 days respectively ($p < 0.05$ vs. Toposar[®] by Log-rank test).²⁶⁵ This outcome strengthens that ETO NCs formulation had a better antitumor efficiency that perdured

longer than Toposar[®], probably enlightened by a extend blood life time and enhanced accumulation in CT26 tumor.

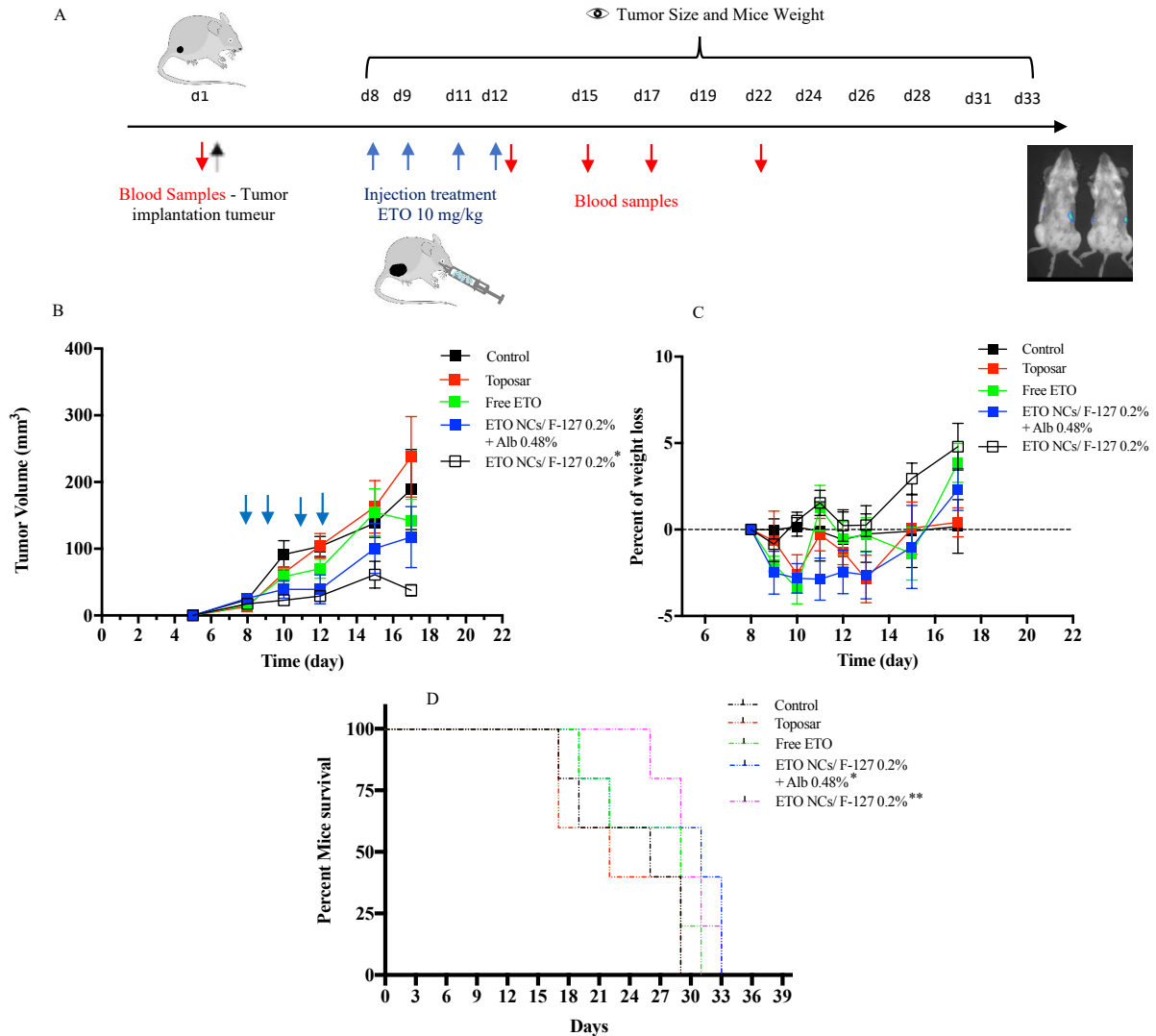


Figure 28 – (A) Schedule treatment for Balb/c female mice implanted with CT26 subcutaneous tumor. (B) Tumor growth inhibition for ETO NCs F-127 0.2% w/v, ETO NCs F-127 0.2% w/v + Alb 0.48 % w/v, Toposar[®], free ETO and control. Blue arrows show the days of i.v. administration. *, $p_{ETO\ NC-Toposar} < 0.05$. (C) Percent of weight loss of Balb/c mice induced by the ETO anticancer treatment. Weight was estimated every two days and expressed as a percentage of weight at day 8 of the experimentation. (D) Kaplan–Meier survival curve for Control, Toposar[®], ETO NCs F-127 0.2% w/v, ETO NCs F-127 0.2% w/v + Alb 0.48 % w/v. *, $p_{ETO\ NC-Toposar} < 0.05$, **, $p_{ETO\ NC-Toposar} < 0.05$.

Table 12 - Antitumoral effect of ETO NCs F-127 0.2% w/v, ETO NCs F-127 0.2% w/v + Alb 0.48% w/v, Toposar[®], free ETO and Control. ETO dosage: 10 mg/kg. Administration schedule: d8, d9, d11, and d12. Tumor growth inhibition ratio (T/C) = $((MTV_{control} - MTV_{treated\ groups}) * MTV_{control}) * 100$. Tumor growth inhibition delay in comparison to control (T-C)

Formulations	Body weight variation in % (day of nadir)	Median tumor volume (mm ³ on day 12)	T/C (%)	Time for median tumor to reach 50 mm ³ (day)	T-C (day)
Control	–	104	–	8.9	–
ETO NCs/ F-127 0.2% w/v	-0.83 (d9) +4.79 (d17)	30	71.2	14.21	5.31
ETO NCs/ F-127 0.2% + Alb 0.48%	-2.49 (d9) +2.31 (d17)	40	61.5	12.8	3.9
Free ETO	-3.40 (d10) +3.85 (d17)	69	33.7	9.5	0.6
Toposar [®]	-2.86 (d13) +0.41 (d17)	105	-1	9.5	0.6

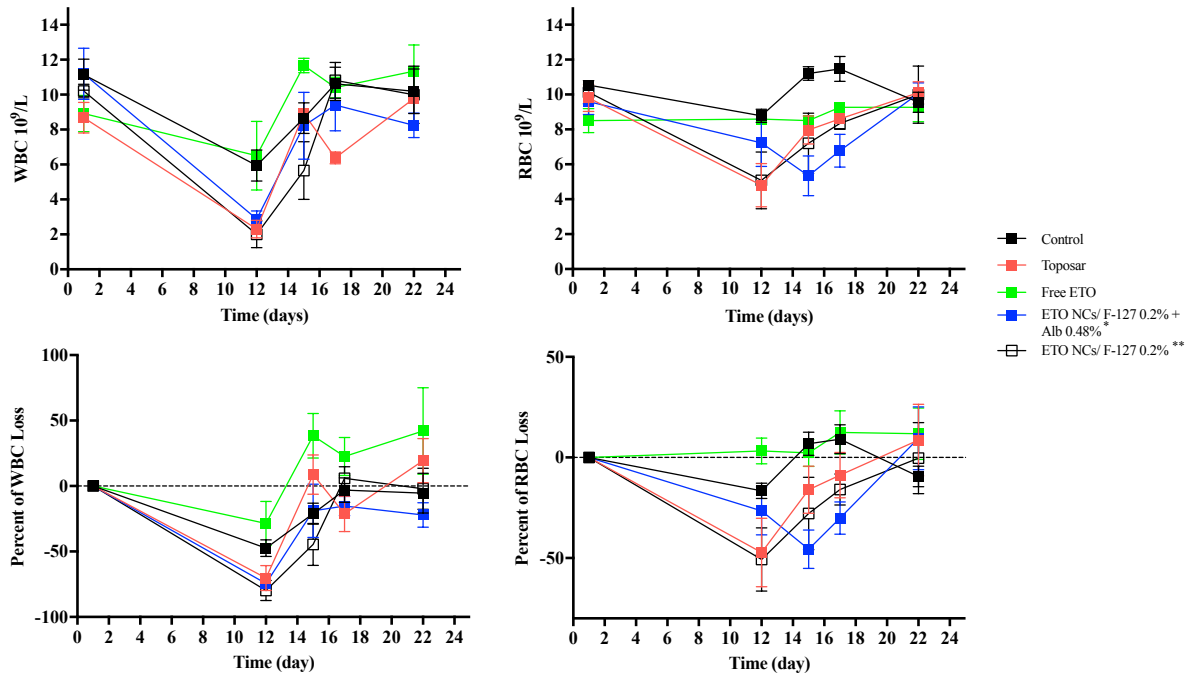


Figure 29 - White (left) and red (right) blood cell counts of BALB/c mice implanted with CT26 colorectal adenocarcinoma cancer. No hematological changes were observed for ETO NCs F-127 0.2% w/v and ETO NCs F-127 0.2% w/v + Alb 0.48% w/v in comparison with the Toposar[®]. *, $p_{ETO\ NC-Toposar} > 0.05$, **, $p_{ETO\ NC-Toposar} > 0.05$.

Table 13 – White Blood Cell (WBC) data recovered at days 1, 12, 15 17, and 22 from adult female BALB/c mice (n = 6). The i.v. injections (10 mg/kg) of ETO NCs F-127 0.2% w/v, ETO NCs F-127 0.2% w/v + Alb 0.48% w/v, Toposar[®], and free ETO were performed at days 8, 9, 11 and 12. WBCs normality range $4 - 15 \times 10^9$ per liter

Formulations	White blood cell count (10^9 cells/L)				
	Day 1	Day 12	Day 15	Day 17	Day 22
Control	11.1 ± 2.1	6.0 ± 2.2	8.7 ± 2.1	10.6 ± 2.3	10.2 ± 3.1
ETO NCs/ F-127 0.2% w/v	10.2 ± 0.9	2.0 ± 1.8	5.7 ± 3.7	10.8 ± 2.3	10.0 ± 3.6
ETO NCs/ F-127 0.2% w/v + Alb 0.48% w/v	11.1 ± 3.2	2.8 ± 1.0	8.2 ± 4.3	9.4 ± 3.3	8.3 ± 1.5
Free ETO	8.9 ± 2.3	6.5 ± 4.4	11.6 ± 0.9	10.4 ± 1.3	11.3 ± 3.4
Toposar [®]	8.7 ± 1.9	2.3 ± 1.1	8.9 ± 0.6	6.4 ± 0.8	9.8 ± 0.5

Table 14 - Red Blood Cell (RBC) data recovered at days 1, 12, 15 17, and 22 from adult female BALB/c mice (n = 6). The i.v. injections (10 mg/kg) of ETO NCs F-127 0.2% w/v, ETO NCs F-127 0.2% w/v + Alb 0.48% w/v, Toposar[®], and free ETO were performed at days 8, 9, 11 and 12. RBCs normality range $6 - 11 \times 10^9$ per liter

Formulations	Red blood cell count (10^9 cells/L)				
	Day 1	Day 12	Day 15	Day 17	Day 22
Control	10.5 ± 0.6	8.8 ± 0.9	11.2 ± 0.9	11.5 ± 1.8	9.6 ± 1.4
ETO NCs/ F-127 0.2% w/v	10.1 ± 1.5	5.1 ± 3.6	7.2 ± 3.9	8.3 ± 0.18	10.0 ± 3.7
ETO NCs/ F-127 0.2% w/v + Alb 0.48% w/v	9.6 ± 1.6	7.2 ± 3.0	5.3 ± 2.5	6.8 ± 2.1	10.0 ± 1.3
Free ETO	8.5 ± 1.5	8.6 ± 0.5	8.5 ± 0.6	9.3 ± 0.5	9.4 ± 1.8
Toposar [®]	9.8 ± 1.8	4.8 ± 2.8	5.3 ± 2.5	6.7 ± 2.1	10.1 ± 1.4

Conclusion

The ETO topoisomerase II inhibitor was formulated as aqueous solution dispersed nanocrystals which efficacy was tested *in vitro* on CT26 and 3LL cells. These nanoparticles with a size around 150 nm were adapted for *in vivo* studies and could be intravenously administered as healing agent to treat murine subcutaneous carcinoma model. It was established that ETO NCs could be more effective and safer than the conventional marketed product Toposar[®]. Polymer-coated and/or Polymer/protein-coated NCs delivery offered better blood stream life span, better targeted ability versus murine carcinoma cancer and better drug tolerance characterized by lower weight lost after treatment. All these conclusions highlight the benefit of NCs technology of poorly soluble compounds for i.v. dosage forms and should orientate laboratory towards further development and production of such pharmaceutical forms.

V. Conclusion and perspectives

Conclusion and perspectives

In medicine, it is common to think that this science alleviates the effect of discomfort, anxiety or pain. Nevertheless, it is true and admitted that medicine can be also accountable for a lot of violence throughout the entire patient treatment in and out of the hospital. The violence of treatment, such as chemotherapy, does not take into account the inconvenience for the patient and is mainly focuses on the biological answer of cancer, frequently low. In consequence, there is a strong need to improve the efficacy of treatment while using safer therapeutic formulations involving fewer toxic drug final product components, better bioavailability and targeted payload delivery. For public judgement, the nanotechnology can be seen as a thriving breakthrough technology for medicine, but also dreaded as its impact on human health is often misunderstood. The society demands to be informed regarding the potential risks of nanotechnology and want to instore legal measures and frameworks in order to control and understand the fate of nanotechnologies. So far nanomedicine technologies are poorly ruled, offering flexibility for researchers and companies, but it is crucial to guarantee that the potential hazards related to the commercial and research application of nanomedicines do not outshine its potential welfares of a brand-new therapeutic formulation. Thus, the nanomedicines are subject to intensive researches for their optimization and future marketing development. Often, in the applicable product specifications, complex or simple nanoparticles have to provide a targeted and/or controlled release of the pharmaceutical payload while offering a significative clinical benefit. Moreover, nanoparticles production also has to meet precise requirements for a safe production of the nanomedicines. These limitations shrink the scope of nanomedicines and compel to discover brand new technologies in accordance with the current necessities. Hence, a better monitoring, nanoparticle architecture and improvement of biological mechanisms from the nano-range level has to be performed to reach medical breakthroughs. Moreover, it is important to notice that pharmaceutic companies aim to acquire new knowledge and abilities in order to develop new products or services, or to bring about a major enhancement in existing products. The requirements to achieve these goals are often not take into account throughout an academic project, questioning the interest of the diverse routes taken during the thesis, therefore limiting the scope of the scientific discovery. Another crucial point when it comes down to nanomedicines development, is the correlation between *in vitro* and *in vivo* experiments that cannot be taken for granted, *in vitro* assays must be more reliable to improve further *in vivo* testing, reducing the drug development phase, saving resources and therefore a better final product quality.

The present thesis reflects the R&D preparation and application of ETO NCs as topoisomerase II inhibitor for the treatment of the colon carcinoma cancer. The co-precipitation was used over milling and high-pressure techniques to engineer the EPR-adapted NCs, as it is an applicable process to industrial scale at low cost, also a low temperature process with no external residual content and no drug degradation. Another striking point is the yielding, with this technique, it can be up to 100%, whereas with milling and HPH techniques NC yield is often below 80 % or worse.^{266,267}

It has been proved that ETO NCs offer numerous benefits including, high drug loading, sustained released, prolonged bloodstream lifespan and were specifically efficient against cancer cells both *in vitro* and *in vivo*. These features are mainly due to the physical state of the nanoparticle and their steadiness overtime thanks to the utilization of the surfactant F-127. In most of studies, unfortunately, the NC stability is often chosen over *in vitro* and *in vivo* NC performances, yet, it might have been more valuable to employ different surfactants to assess the influence on the cell internalization, on the nanoparticle biodistribution and on the cancer cell or tumor activity. As ETO NCs were redispersed extemporaneously, the overtime stability was not a striking parameter for *in vivo* studies, but the excipient nature and its concentration are crucial, as evidenced in this thesis and by Aroujo *et al.*²⁶¹

All the results achieved throughout the present thesis, emphasize the potentiality of the nano-size ETO drug crystal formulation, giving new possibilities to treat cancer while decreasing side-effects. All of these could boost the clinical activity of ETO that is mainly focused on the scheduling treatment of the marketed product Toposar[®]. It is noteworthy that ETO NCs outperformed or at least was as efficient as Toposar[®] with a cheaper, easy made, and above all, a safer formulation. Drug nanocrystals synthesized using the anti-solvent precipitation could be successfully applied to numerous API and be effective to many therapies such as cancer treatments. NC technology represent a pronounced interest for pharmaceutical laboratories, where 70% of poorly soluble drugs are in development. Only 11 products based on NC technology are on market and none of them are prescribed for cancer treatment assuming a huge potential that needs to be explore in the coming years.

For this project, NCs have been exclusively used via i.v. route since the latter is the most used for chemotherapy treatments. In that case, the drugs are injected straight into the patient's vein, maximizing the active ingredient bioavailability in the bloodstream. Likewise, injected

intravenously, the dosage is precisely adjusted to patient pathology and is faster delivered, for minutes up to hours. However, there is a growing attention on the intratumoral injection of drug to the tumor, as pretreatment to common i.v. chemotherapy to ensure better overall efficiency. Intratumoral chemotherapy (*i.e.* non-systemic delivery) has lower toxicity compared to systemic anticancer treatment and has better bioavailability to the site of interest. Indeed, i.v. administration provides full drug bioavailability in the bloodstream, not to the site of interest, the EPR effect has been proven to be highly variable, considerably reducing the amount of drug to the cancer. Dai *et al.* quantified the cancer cell targeting efficacies of folic acid coated gold and silica nanoparticles in mice tumor models. Only $1.4 \times 10^{-3}\%$ of the intravenously injected dose of both nanoparticles reached cancer cells, equivalent to only 2% of cancer cells interrelating with the nano-objects.²⁶⁸ The EPR effect is strongly fluctuating with the blood and interstitial fluid pressure in the tumor, their volume and the nature of vessels where the cancer is located.²⁶⁹ Wilhelm *et al.* also highlighted the poor delivery efficiency of nanomedicines that commonly achieve only 0.7% of the inoculated dose to the cancer.²⁷⁰ Consequently, developing intratumoral approaches to overcome the EPR variability is relevant as perspective of the present work. Incorporating NCs inside hydrogel for intratumoral application for curative treatment draw a lot of interest, as the sustained and stable release are better managed, it facilitates and enhances the antitumor treatment. A thermo-sensitive hydrogel with PTX NCs was made by Lin *et al.* to treat intratumorally 4T1 breast tumor murine model in comparison to Taxol[®], it was evidenced that the hydrogel embedded PTX NCs released the API more gradually and uphold more drug content after an intratumoral injection for a superior efficacy than Taxol[®].²⁷¹ Thus, hydrogel as delivery matrix for ETO NCs encapsulation has to be explored.

VI. References

References

1. Brittain, H. G. *Polymorphism in Pharmaceutical Solids*. **192**, (1999).
2. Aaltonen, J., Allesø, M., Mirza, S., Koradia, V., Gordon, K. C. & Rantanen, J. Solid form screening - A review. *Eur. J. Pharm. Biopharm.* **71**, 23–37 (2009).
3. Kawabata, Y., Wada, K., Nakatani, M., Yamada, S. & Onoue, S. Formulation design for poorly water-soluble drugs based on biopharmaceutics classification system: Basic approaches and practical applications. *Int. J. Pharm.* **420**, 1–10 (2011).
4. Chan, C. C., Chow, K., McKay, B. & Fung, M. Therapeutic Delivery Solutions. *Ther. Deliv. Solut.* 1–410 (2014).
5. L Hart, M., Duc P Do, Ansari, R. A. & Syed A A Rizv. Brief Overview of Various Approaches to Enhance Drug Solubility. *J Dev. Drugs* **02**, 1–7 (2013).
6. Khadka, P., Ro, J., Kim, H., Kim, I., Kim, J. T., Kim, H., Cho, J. M., Yun, G. & Lee, J. Pharmaceutical particle technologies: An approach to improve drug solubility, dissolution and bioavailability. *Asian J. Pharm. Sci.* **9**, 304–316 (2014).
7. Amidon, G. L., Lennernäs, H., Shah, V. P. & Crison, J. R. A Theoretical Basis for a Biopharmaceutic Drug Classification: The Correlation of in Vitro Drug Product Dissolution and in Vivo Bioavailability. *Pharmaceutical Research: An Official Journal of the American Association of Pharmaceutical Scientists* **12**, 413–420 (1995).
8. CDER/FDA. Guidance for Industry, Waiver of in vivo bioavailability and bioequivalence studies for immediate release solid oral dosage forms based on a biopharmaceutics classification system. *Cent. Drug Eval. Res.* 1–2 (2015).
9. Qi, S., Roser, S., Edler, K. J., Pigliacelli, C., Rogerson, M., Weuts, I., Van Dycke, F. & Stokbroekx, S. Insights into the role of polymer-surfactant complexes in drug solubilisation/stabilisation during drug release from solid dispersions. *Pharm. Res.* **30**, 290–302 (2013).
10. Rekdal, M., pai, A. & BS, M. Experimental data of co-crystals of Etravirine and L-tartaric acid. *Data Br.* **16**, 135–140 (2018).
11. Lindenberg, M., Kopp, S. & Dressman, J. B. Classification of orally administered drugs on the World Health Organization Model list of Essential Medicines according to the biopharmaceutics classification system. *Eur. J. Pharm. Biopharm.* **58**, 265–278 (2004).
12. Lee, H. L., Vasoya, J. M., De Lima Cirqueira, M., Yeh, K. L., Lee, T. & Serajuddin, A. T. M. Continuous preparation of 1:1 haloperidol-maleic acid salt by a novel solvent-free method using a twin screw melt extruder. *Mol. Pharm.* **14**, 1278–1291 (2017).

13. McCrone, W. *Polymorphism*. **2**, (Physics and Chemistry of the Organic Solid State, 1965).
14. S.Rosenstein, P. P. L. Some aspects of polymorphism. *J.Hosp.Pharm* **26**, 598–601 (1969).
15. Corvis, Y., Négrier, P., Massip, S., Leger, J. M. & Espeau, P. Insights into the crystal structure, polymorphism and thermal behavior of menthol optical isomers and racemates. *CrystEngComm* **14**, 7055–7064 (2012).
16. Corvis, Y., Wurm, A., Schick, C. & Espeau, P. New menthol polymorphs identified by flash scanning calorimetry. *CrystEngComm* **17**, 5357–5359 (2015).
17. Lee, E. H. A practical guide to pharmaceutical polymorph screening & selection. *Asian J. Pharm. Sci.* **9**, 163–175 (2014).
18. Singhal, D. & Curatolo, W. Drug polymorphism and dosage form design: A practical perspective. *Adv. Drug Deliv. Rev.* **56**, 335–347 (2004).
19. Moussaoui, N. El & Bendriss, A. The Influence of Storage Conditions on Melatonin Stability. *Int. J. Eng. Res. Technol.* **3**, 2243–2246 (2014).
20. Raza, K., Kumar, P., Ratan, S., Malik, R. & Arora, S. Polymorphism : The Phenomenon Affecting the Performance of Drugs. *SOJ Pharm. Pharm. Sci.* **1**, 1–10 (2014).
21. Bauer, J. F. & Development, P. Critical Consideration in. *J. Valid. Technol.* **19**, 15–23 (2013).
22. Savjani, K. T., Gajjar, A. K. & Savjani, J. K. Drug Solubility: Importance and Enhancement Techniques. *ISRIN Pharm.* **2012**, 1–10 (2012).
23. Healy, A. M., Worku, Z. A., Kumar, D. & Madi, A. M. Pharmaceutical solvates, hydrates and amorphous forms: A special emphasis on cocrystals. *Adv. Drug Deliv. Rev.* **117**, 25–46 (2017).
24. Karpinski, P. H. Polymorphism of Active Pharmaceutical Ingredients. *Chem. Eng. Technol.* **29**, 233–237 (2006).
25. Stahl, P. H. & Guillory, J. K. Handbook of Pharmaceutical Salts: Properties, Selection, and Use. *J. Med. Chem.* **46**, (2003).
26. Gandhi, R., Pillai, O., Thilagavathi, R., Gopalakrishnan, B., Kaul, C. L. & Panchagnula, R. Characterization of azithromycin hydrates. *Eur. J. Pharm. Sci.* **16**, 175–184 (2002).
27. Salameh, A. K. & Taylor, L. S. Physical stability of crystal hydrates and their anhydrides in the presence of excipients. *J. Pharm. Sci.* **95**, 446–461 (2006).
28. Jamaludin, A., Mohamad, M., Navaratnam, V., Selliah, K. & Yuen, K. H. Relative bioavailability. **25**, 261–263 (1988).

29. Jones, W., Motherwell, W. D. S. & Trask, A. V. Pharmaceutical Cocrystals: An Emerging Approach to Physical Property Enhancement. *MRS Bull. Former. Mater. Res. Soc. Newsl.* **31**, 875–879 (2006).
30. Corvis, Y., Négrier, P., Lazerges, M., Massip, S., Léger, J. M. & Espeau, P. Lidocaine/1-menthol binary system: Cocrystallization versus solid-state immiscibility. *J. Phys. Chem. B* **114**, 5420–5426 (2010).
31. Yeh, K. L. & Lee, T. Intensified Crystallization Processes for 1:1 Drug-Drug Cocrystals of Sulfathiazole-Theophylline, and Sulfathiazole-Sulfanilamide. *Cryst. Growth Des.* **18**, 1339–1349 (2018).
32. Drozd, K. V, Manin, A. N., Churakov, A. V & Perlovich, G. L. European Journal of Pharmaceutical Sciences Drug-drug cocrystals of antituberculous 4-aminosalicylic acid : Screening , crystal structures , thermochemical and solubility studies. *Eur. J. Pharm. Sci.* **99**, 228–239 (2017).
33. Grossjohann, C., Eccles, K. S., Maguire, A. R., Lawrence, S. E., Tajber, L., Corrigan, O. I. & Healy, A. M. Characterisation, solubility and intrinsic dissolution behaviour of benzamide: Dibenzyl sulfoxide cocrystal. *Int. J. Pharm.* **422**, 24–32 (2012).
34. Hancock, B. C. & Parks, M. What is the true solubility advantage for amorphous pharmaceuticals? *Pharm. Res.* **17**, 397–404 (2000).
35. Yang, W., Johnston, K. P. & Williams, R. O. Comparison of bioavailability of amorphous versus crystalline itraconazole nanoparticles via pulmonary administration in rats. *Eur. J. Pharm. Biopharm.* **75**, 33–41 (2010).
36. Vasanthavada, M., Tong, W. Q., Joshi, Y. & Kislalioglu, M. S. Phase behavior of amorphous molecular dispersions I: Determination of the degree and mechanism of solid solubility. *Pharm. Res.* **21**, 1598–1606 (2004).
37. Wyttenbach, N. & Kuentz, M. Glass-forming ability of compounds in marketed amorphous drug products. *Eur. J. Pharm. Biopharm.* **112**, 204–208 (2017).
38. Kalepu, S. & Nekkanti, V. Insoluble drug delivery strategies: Review of recent advances and business prospects. *Acta Pharm. Sin. B* **5**, 442–453 (2015).
39. Junyaprasert, V. B. & Morakul, B. Nanocrystals for enhancement of oral bioavailability of poorly water-soluble drugs. *Asian J. Pharm. Sci.* **10**, 13–23 (2015).
40. Niebergall, P. J., Milosovich, G. & Goyan, J. E. Dissolution Rate Studies II. *J. Pharm. Sci.* **52**, 236–241 (1963).
41. Bisrat, M. & Nyström, C. Physicochemical aspects of drug release. VIII. The relation between particle size and surface specific dissolution rate in agitated suspensions. *Int. J.*

- Pharm.* **47**, 223–231 (1988).
42. Liversidge, G. G. & Cundy, K. C. Particle size reduction for improvement of oral bioavailability of hydrophobic drugs: I. Absolute oral bioavailability of nanocrystalline danazol in beagle dogs. *Int. J. Pharm.* **125**, 91–97 (1995).
 43. Hecq, J., Deleers, M., Fanara, D., Vranckx, H., Boulanger, P., Le Lamer, S. & Amighi, K. Preparation and in vitro/in vivo evaluation of nano-sized crystals for dissolution rate enhancement of ucb-35440-3, a highly dosed poorly water-soluble weak base. *Eur. J. Pharm. Biopharm.* **64**, 360–368 (2006).
 44. Zuo, B., Sun, Y., Li, H., Liu, X., Zhai, Y., Sun, J. & He, Z. Preparation and in vitro/in vivo evaluation of fenofibrate nanocrystals. *Int. J. Pharm.* **455**, 267–275 (2013).
 45. Lindfors, L., Skantze, P., Skantze, U., Rasmusson, M., Zackrisson, A. & Olsson, U. Amorphous drug nanosuspensions. 1. Inhibition of ostwald ripening. *Langmuir* **22**, 906–910 (2006).
 46. W. Briscoe. *Colloid Science: Principles, Methods and Applications*. (John Wiley & Sons Ltd, 2010).
 47. Demetzos, C. *Pharmaceutical Nanotechnology Fundamentals and Practical Applications*. (Adis, 2016).
 48. Sharma, P., Denny, W. A. & Garg, S. Effect of wet milling process on the solid state of indomethacin and simvastatin. *Int. J. Pharm.* **380**, 40–48 (2009).
 49. Lee, J., Lee, S., Choi, J., Youn, J. & Ahn, C. Amphiphilic amino acid copolymers as stabilizers for the preparation of nanocrystal dispersion. **24**, 441–449 (2005).
 50. Kurakula, M. ., El-Helw, A. M. ., Sobahi, T. R. . & Abdelaal, M. . Chitosan based atorvastatin nanocrystals : effect of cationic charge on particle size , formulation stability , and in-vivo efficacy. *Int. J. Nanomed.* **10**, 321–334 (2015).
 51. Sun, W., Tian, W., Zhang, Y. & He, J. Effect of novel stabilizers — cationic polymers on the particle size and physical stability of poorly soluble drug nanocrystals. *Nanomedicine Nanotechnology, Biol. Med.* **8**, 460–467 (2012).
 52. Liu, Y., Huang, L. & Liu, F. Paclitaxel nanocrystals for overcoming multidrug resistance in cancer. *Mol. Pharm.* **7**, 863–869 (2010).
 53. Sharma, S., Verma, A., Teja, B. V., Shukla, P. & Mishra, P. R. Development of stabilized Paclitaxel nanocrystals: In-vitro and in-vivo efficacy studies. *Eur. J. Pharm. Sci.* **69**, 51–60 (2015).
 54. Sinico, C., Pireddu, R., Pini, E., Valenti, D., Caddeo, C., Fadda, A. M. & Lai, F. Enhancing Topical Delivery of Resveratrol through a Nanosizing Approach. *Planta*

- Med.* **83**, 476–481 (2017).
55. Lu, Y., Wang, Z. H., Li, T., McNally, H., Park, K. & Sturek, M. Development and evaluation of transferrin-stabilized paclitaxel nanocrystal formulation. *J. Control. Release* **176**, 76–85 (2014).
 56. Wu, L., Zhang, J. & Watanabe, W. Physical and chemical stability of drug nanoparticles. *Adv. Drug Deliv. Rev.* **63**, 456–469 (2011).
 57. Liversidge, I. E., Chester, W., Harbour, W. & Street, K. Stabilization of chemical compounds using nanoparticulate formulations. **1**, (2003).
 58. Möschwitzer, J., Achleitner, G., Pomper, H. & Müller, R. H. Development of an intravenously injectable chemically stable aqueous omeprazole formulation using nanosuspension technology. *Eur. J. Pharm. Biopharm.* **58**, 615–619 (2004).
 59. Park, J., Yan, Y., Chi, S., Hwang, D. H., Shanmugam, S., Lyoo, W. S., Woo, J. S., Yong, C. S. & Choi, H. Preparation and evaluation of Cremophor-free paclitaxel solid dispersion by a supercritical antisolvent process. **63**, 491–499 (2011).
 60. Gao, L., Liu, G., Wang, X., Liu, F., Xu, Y. & Ma, J. Preparation of a chemically stable quercetin formulation using nanosuspension technology. *Int. J. Pharm.* **404**, 231–237 (2011).
 61. Pu, X., Sun, J., Wang, Y., Wang, Y., Liu, X., Zhang, P., Tang, X., Pan, W., Han, J. & He, Z. Development of a chemically stable 10-hydroxycamptothecin nanosuspensions. **379**, 167–173 (2009).
 62. Singh, S. K., Srinivasan, K. K., Gowthamarajan, K., Singare, D. S., Prakash, D. & Gaikwad, N. B. Investigation of preparation parameters of nanosuspension by top-down media milling to improve the dissolution of poorly water-soluble glyburide. *Eur. J. Pharm. Biopharm.* **78**, 441–446 (2011).
 63. Liu, T., Yao, G., Zhang, X., Zuo, X., Wang, L., Yin, H. & Möschwitzer, J. P. Systematical Investigation of Different Drug Nanocrystal Technologies to Produce Fast Dissolving Meloxicam Tablets. *AAPS PharmSciTech* (2017).
 64. Guo, M., Dong, Y., Wang, Y., Ma, M., He, Z. & Fu, Q. Fabrication, characterization, stability and in vitro evaluation of nitrendipine nanocrystals by media milling. *Powder Technol.* (2018).
 65. Müller, R. H., Gohla, S. & Keck, C. M. State of the art of nanocrystals - Special features, production, nanotoxicology aspects and intracellular delivery. *Eur. J. Pharm. Biopharm.* **78**, 1–9 (2011).
 66. Han, M., Liu, X., Guo, Y., Wang, Y. & Wang, X. Preparation, characterization,

- biodistribution and antitumor efficacy of hydroxycamptothecin nanosuspensions. *Int. J. Pharm.* **455**, 85–92 (2013).
67. Zhao, Y. X., Hua, H. Y., Chang, M., Liu, W. J., Zhao, Y. & Liu, H. M. Preparation and cytotoxic activity of hydroxycamptothecin nanosuspensions. *Int. J. Pharm.* **392**, 64–71 (2010).
 68. Junghanns, J. U. A. H. & Müller, R. H. Nanocrystal technology, drug delivery and clinical applications. *Int. J. Nanomedicine* **3**, 295–309 (2008).
 69. Grau, M. J., Kayser, O. & Müller, R. H. Nanosuspensions of poorly soluble drugs reproducibility of small scale production. *Int. J. Pharm.* **196**, 155–159 (2000).
 70. Agrawal, Y. & Patel, V. Nanosuspension: An approach to enhance solubility of drugs. *J. Adv. Pharm. Technol. Res.* **2**, 81 (2011).
 71. Möschwitzer, J. P. & Müller, R. H. Factors influencing the release kinetics of drug nanocrystal-loaded pellet formulations. *Drug Dev. Ind. Pharm.* **39**, 762–9 (2013).
 72. Keck, C. U.S. Pat. Appl. Publ. **1**, (2013).
 73. Lu, Y., Li, Y. & Wu, W. Injected nanocrystals for targeted drug delivery. *Acta Pharm. Sin. B* **6**, 106–113 (2016).
 74. Kumar, D., Worku, Z. A., Gao, Y., Kamaraju, V. K., Glennon, B., Babu, R. P. & Healy, A. M. Comparison of wet milling and dry milling routes for ibuprofen pharmaceutical crystals and their impact on pharmaceutical and biopharmaceutical properties. *Powder Technol.* **330**, 228–238 (2018).
 75. Tanaka, Y., Inkyo, M., Yumoto, R., Nagai, J., Takano, M. & Nagata, S. Nanoparticulation of probucol, a poorly water-soluble drug, using a novel wet-milling process to improve in vitro dissolution and in vivo oral absorption. *Drug Dev. Ind. Pharm.* **38**, 1015–23 (2012).
 76. Dai, L., Li, C., Zhang, J. & Cheng, F. Preparation and characterization of starch nanocrystals combining ball milling with acid hydrolysis. *Carbohydr. Polym.* **180**, 122–127 (2018).
 77. Gao, L., Liu, G., Ma, J., Wang, X., Zhou, L. & Li, X. Drug nanocrystals: In vivo performances. *J. Control. Release* **160**, 418–430 (2012).
 78. Chen, T., Li, C., Li, Y., Yi, X., Lee, S. M.-Y. & Zheng, Y. Oral Delivery of a Nanocrystal Formulation of Schisantherin A with Improved Bioavailability and Brain Delivery for the Treatment of Parkinson's Disease. *Mol. Pharm.* **13**, 3864–3875 (2016).
 79. Hanafy, A., Spahn-Langguth, H., Vergnault, G., Grenier, P., Tubic Grozdanis, M., Lenhardt, T. & Langguth, P. Pharmacokinetic evaluation of oral fenofibrate

- nanosuspensions and SLN in comparison to conventional suspensions of micronized drug. *Adv. Drug Deliv. Rev.* **59**, 419–426 (2007).
80. Nassar, T., Rom, A., Nyska, A. & Benita, S. Novel double coated nanocapsules for intestinal delivery and enhanced oral bioavailability of tacrolimus, a P-gp substrate drug. *J. Control. Release* **133**, 77–84 (2009).
 81. Knight, B., Troutman, M. & Thakker, D. R. Deconvoluting the effects of P-glycoprotein on intestinal CYP3A: a major challenge. *Curr. Opin. Pharmacol.* **6**, 528–532 (2006).
 82. Apte Prakash, S. Selecting surfactants for the maximum inhibition of the activity of the multidrug resistance efflux pump transporter , P-glycoprotein : conceptual development . *J. Excipients Food Chem.* **1**, 51–59 (2010).
 83. Jani, P., Halbert, G. W., Langridge, J. & Florence, A. T. Nanoparticle Uptake by the Rat Gastrointestinal Mucosa: Quantitation and Particle Size Dependency. *J. Pharm. Pharmacol.* **42**, 821–826 (1990).
 84. Arbor, A. & Witzmann, F. A. Knowledge Gaps. *Int. J. Biomed.* (2013).
 85. Fowler, R., Vllasaliu, D., Trillo, F. F., Garnett, M., Alexander, C., Horsley, H., Smith, B., Whitcombe, I., Eaton, M. & Stolnik, S. Nanoparticle transport in epithelial cells: Pathway switching through bioconjugation. *Small* **9**, 3282–3294 (2013).
 86. Prausnitz, M. R., Elias, P. M., Franz, T. J., Schmuth, M., Tsai, J.-C., Menon, G. K., Holleran, W. M. & Feingold, K. R. Skin Barrier and Transdermal Drug Delivery. *Med. Ther.* **124**, 2065–2073 (2012).
 87. Prow, T. W., Grice, J. E., Lin, L. L., Faye, R., Butler, M., Becker, W., Wurm, E. M. T., Yoong, C., Robertson, T. A., Soyer, H. P. & Roberts, M. S. Nanoparticles and microparticles for skin drug delivery. *Adv. Drug Deliv. Rev.* **63**, 470–491 (2011).
 88. Pelikh, O., Stahr, P. L., Huang, J., Gerst, M., Scholz, P., Dietrich, H., Geisel, N. & Keck, C. M. Nanocrystals for improved dermal drug delivery. *Eur. J. Pharm. Biopharm.* **128**, 170–178 (2018).
 89. Vidlářová, L., Romero, G. B., Hanuš, J., Štěpánek, F. & Müller, R. H. Nanocrystals for dermal penetration enhancement - Effect of concentration and underlying mechanisms using curcumin as model. *Eur. J. Pharm. Biopharm.* **104**, 216–225 (2016).
 90. Araújo, J., Gonzalez, E., Egea, M. A., Garcia, M. L. & Souto, E. B. Nanomedicines for ocular NSAIDs: safety on drug delivery. *Nanomedicine Nanotechnology, Biol. Med.* **5**, 394–401 (2009).
 91. Sharma, O. P., Patel, V. & Mehta, T. Nanocrystal for ocular drug delivery: hope or hype. *Drug Deliv. Transl. Res.* **6**, 399–413 (2016).

92. Ahuja, M., Verma, P. & Bhatia, M. Preparation and evaluation of chitosan–itraconazole co-precipitated nanosuspension for ocular delivery. *J. Exp. Nanosci.* **10**, 209–221 (2015).
93. Tuomela, A., Liu, P., Puranen, J., Rönkkö, S., Laaksonen, T., Kalesnykas, G., Oksala, O., Ilkka, J., Laru, J., Järvinen, K., Hirvonen, J. & Peltonen, L. Brinzolamide nanocrystal formulations for ophthalmic delivery: Reduction of elevated intraocular pressure in vivo. *Int. J. Pharm.* **467**, 34–41 (2014).
94. Pignatello, R., Bucolob, C., Ferrara, P., Maltese, A., Puleo, A. & Puglisi, G. Eudragit RS100 nanosuspensions for the ophthalmic controlled delivery of ibuprofen. *J. Pharm. Biomed. Sci.* **16**, 53–61 (2002).
95. Colomer, R., Alba, E., González-Martin, A., Paz-Ares, L., Martín, M., Llombart, A., Rodríguez Lescure, Á., Salvador, J., Albanell, J., Isla, D., Lomas, M., Rodríguez, C. A., Trigo, J. M., Germà, J. R., Bellmunt, J., Tabernero, J., Rosell, R., Aranda, E., *et al.* Treatment of cancer with oral drugs: A position statement by the Spanish Society of Medical Oncology (SEOM). *Ann. Oncol.* **21**, 195–198 (2010).
96. Behrends, A., Dafinger, A. & Eckert, J. Governance – and the State: An Anthropological Approach. *Ethnoscripts* **14**, 14–34 (2012).
97. Ye, Y., Zhang, X., Zhang, T., Wang, H. & Wu, B. Design and evaluation of injectable niclosamide nanocrystals prepared by wet media milling technique. *Drug Dev Ind Pharm* **41**, 1416–1424 (2015).
98. Hao, L., Luan, J., Zhang, D., Li, C., Guo, H., Qi, L., Liu, X., Li, T. & Zhang, Q. Research on the in vitro anticancer activity and in vivo tissue distribution of Amoitone B nanocrystals. *Colloids Surf. B* **117**, 258–266 (2014).
99. Maeda, H., Wu, J., Sawa, T., Matsumura, Y. & Hori, K. Tumor vascular permeability and the EPR effect in macromolecular therapeutics: A review. *J. Control. Release* **65**, 271–284 (2000).
100. Hollis, C. P., Weiss, H. L., Leggas, M., Evers, B. M., Gemeinhart, R. A. & Li, T. Biodistribution and bioimaging studies of hybrid paclitaxel nanocrystals: Lessons learned of the EPR effect and image-guided drug delivery. *J. Control. Release* **172**, 12–21 (2013).
101. Nel, A. E., Mädler, L., Velegol, D., Xia, T., Hoek, E. M. V., Somasundaran, P., Klaessig, F., Castranova, V. & Thompson, M. Understanding biophysicochemical interactions at the nano-bio interface. *Nat. Mater.* **8**, 543–557 (2009).
102. Iversen, T. G., Skotland, T. & Sandvig, K. Endocytosis and intracellular transport of nanoparticles: Present knowledge and need for future studies. *Nano Today* **6**, 176–185 (2011).

- (2011).
103. Park, J., Sun, B. & Yeo, Y. Albumin-coated nanocrystals for carrier-free delivery of paclitaxel. *J. Control. Release* **263**, 90–101 (2016).
 104. Kratz, F. & Elsadek, B. Clinical impact of serum proteins on drug delivery. *J. Control. Release* **161**, 429–445 (2012).
 105. Luo, C., Li, Y., Sun, J., Zhang, Y., Chen, Q., Liu, X. & He, Z. Felodipine nanosuspension: A faster in vitro dissolution rate and higher oral absorption efficiency. *J. Drug Deliv. Sci. Technol.* **24**, 173–177 (2014).
 106. Shubar, H. M., Lachenmaier, S., Heimesaat, M. M., Lohman, U., Mauludin, R., Mueller, R. H., Fitzner, R., Borner, K. & Liesenfeld, O. SDS-coated atovaquone nanosuspensions show improved therapeutic efficacy against experimental acquired and reactivated toxoplasmosis by improving passage of gastrointestinal and blood-brain barriers. *J. Drug Target.* **19**, 114–24 (2011).
 107. Kim, S. & Lee, J. Folate-targeted drug-delivery systems prepared by nano-comminution. *Drug Dev. Ind. Pharm.* **37**, 131–138 (2011).
 108. Tuomela, A., Hirvonen, J. & Peltonen, L. Stabilizing agents for drug nanocrystals: Effect on bioavailability. *Pharmaceutics* **8**, 16 (2016).
 109. Chiang, P.-C., Ran, Y., Chou, K.-J., Cui, Y. & Wong, H. Investigation of utilization of nanosuspension formulation to enhance exposure of 1,3-dicyclohexylurea in rats: Preparation for PK/PD study via subcutaneous route of nanosuspension drug delivery. *Nanoscale Res. Lett.* **6**, 413 (2011).
 110. Rahim, H., Sadiq, A., Khan, S., Khan, M. A., Shah, S. M. H., Hussain, Z., Ullah, R., Shahat, A. A. & Ibrahim, K. Aceclofenac nanocrystals with enhanced in vitro, in vivo performance: Formulation optimization, characterization, analgesic and acute toxicity studies. *Drug Des. Devel. Ther.* **11**, 2443–2452 (2017).
 111. Paredes, A. J., Litterio, N., Dib, A., Allemandi, D. A., Lanusse, C., Bruni, S. S. & Palma, S. D. A nanocrystal-based formulation improves the pharmacokinetic performance and therapeutic response of albendazole in dogs. *J. Pharm. Pharmacol.* **70**, 51–58 (2018).
 112. Hou, Y., Shao, J., Fu, Q., Li, J., Sun, J. & He, Z. Spray-dried nanocrystals for a highly hydrophobic drug: Increased drug loading, enhanced redispersity, and improved oral bioavailability. *Int. J. Pharm.* **516**, 372–379 (2017).
 113. Kayser, O., Olbrich, C., Yardley, V., Kiderlen, A. F. & Croft, S. L. Formulation of amphotericin B as nanosuspension for oral administration. *Int. J. Pharm.* **254**, 73–75 (2003).

114. Wu, Y., Loper, A., Landis, E., Hettrick, L., Novak, L., Lynn, K., Chen, C., Thompson, K., Higgins, R., Batra, U., Shelukar, S., Kwei, G. & Storey, D. The role of biopharmaceutics in the development of a clinical nanoparticle formulation of MK-0869: A Beagle dog model predicts improved bioavailability and diminished food effect on absorption in human. *Int. J. Pharm.* **285**, 135–146 (2004).
115. Al-Dhubiab, B. E. Aripiprazole Nanocrystal Impregnated Buccoadhesive Films for Schizophrenia. *J. Nanosci. Nanotechnol.* **17**, 2345–2352 (2017).
116. Teeranachaideekul, V., Junyaprasert, V. B., Souto, E. B. & Müller, R. H. Development of ascorbyl palmitate nanocrystals applying the nanosuspension technology. *Int. J. Pharm.* **354**, 227–234 (2008).
117. Ganta, S., Paxton, J. W., Baguley, B. C. & Garg, S. Formulation and pharmacokinetic evaluation of an asulacrine nanocrystalline suspension for intravenous delivery. *Int. J. Pharm.* **367**, 179–186 (2009).
118. Soliman, K. A. B., Ibrahim, H. K. & Ghorab, M. M. Effects of different combinations of nanocrystallization technologies on avanafil nanoparticles: in vitro, in vivo and stability evaluation. *Int. J. Pharm.* **517**, 148–156 (2017).
119. Sigfridsson, K., Forssén, S., Holländer, P., Skantze, U. & de Verdier, J. A formulation comparison, using a solution and different nanosuspensions of a poorly soluble compound. *Eur. J. Pharm. Biopharm.* **67**, 540–547 (2007).
120. Zhang, D., Tan, T., Gao, L., Zhao, W. & Wang, P. Preparation of azithromycin nanosuspensions by high pressure homogenization and its physicochemical characteristics studies. *Drug Dev. Ind. Pharm.* **33**, 569–575 (2007).
121. Liu, Y., Ma, Y., Xu, J., Chen, Y., Xie, J., Yue, P., Zheng, Q. & Yang, M. Apolipoproteins adsorption and brain-targeting evaluation of baicalin nanocrystals modified by combination of Tween80 and TPGS. *Colloids Surf. B* **160**, 619–627 (2017).
122. Wang, Y., Rong, J., Zhang, J., Liu, Y., Meng, X., Guo, H., Liu, H. & Chen, L. Morphology, in vivo distribution and antitumor activity of bexarotene nanocrystals in lung cancer. *Drug Dev. Ind. Pharm.* **43**, 132–141 (2017).
123. Wang, H., Zhang, G., Ma, X., Liu, Y., Feng, J., Park, K. & Wang, W. Enhanced encapsulation and bioavailability of breviscapine in PLGA microparticles by nanocrystal and water-soluble polymer template techniques. *Eur. J. Pharm. Biopharm.* **115**, 177–185 (2017).
124. Hu, J., Dong, Y., Ng, W. K. & Pastorin, G. Preparation of drug nanocrystals embedded in mannitol microcrystals via liquid antisolvent precipitation followed by immediate (on-

- line) spray drying. *Adv. Powder Technol.* **29**, 957–963 (2018).
125. Liu, T., Han, M., Tian, F., Cun, D., Rantanen, J. & Yang, M. Budesonide nanocrystal-loaded hyaluronic acid microparticles for inhalation: In vitro and in vivo evaluation. *Carbohydr. Polym.* **181**, 1143–1152 (2018).
 126. Jacobs, C. & Müller, R. H. Production and characterization of a budesonide nanosuspension for pulmonary administration. *Pharm. Res.* **19**, 189–194 (2002).
 127. Kraft, W. K., Steiger, B., Beussink, D., Quiring, J. N., Fitzgerald, N., Greenberg, H. E. & Waldman, S. a. The pharmacokinetics of nebulized nanocrystal budesonide suspension in healthy volunteers. *J. Clin. Pharmacol.* **44**, 67–72 (2004).
 128. Shrewsbury, S. B., Bosco, A. P. & Uster, P. S. Pharmacokinetics of a novel submicron budesonide dispersion for nebulized delivery in asthma. *Int. J. Pharm.* **365**, 12–17 (2009).
 129. Jacobs, C., Kayser, O. & Müller, R. H. Production and characterisation of mucoadhesive nanosuspensions for the formulation of bupravaquone. *Int. J. Pharm.* **214**, 3–7 (2001).
 130. Merisko-Liversidge, E., Sarpotdar, P., Bruno, J., Hajj, S., Wei, L., Peltier, N., Rake, J., Shaw, J. M., Pugh, S., Polin, L., Jones, J., Corbett, T., Cooper, E. & Liversidge, G. G. Formulation and antitumor activity evaluation of nanocrystalline suspensions of poorly soluble anticancer drugs. *Pharmaceutical Research* **13**, 272–278 (1996).
 131. Zhang, H., Wang, X., Dai, W., Gemeinhart, R. A., Zhang, Q. & Li, T. Pharmacokinetics and treatment efficacy of camptothecin nanocrystals on lung metastasis. *Mol. Pharm.* **11**, 226–233 (2014).
 132. Zhan, H., Jagtiani, T. & Liang, J. F. A new targeted delivery approach by functionalizing drug nanocrystals through polydopamine coating. *Eur. J. Pharm. Biopharm.* **114**, 221–229 (2017).
 133. Beirowski, J., Inghelbrecht, S., Arien, A. & Gieseler, H. Freeze-drying of nanosuspensions, 1: Freezing rate versus formulation design as critical factors to preserve the original particle size distribution. *J. Pharm. Sci.* **100**, 1958–1968 (2011).
 134. Dolenc, A., Kristl, J., Baumgartner, S. & Planinšek, O. Advantages of celecoxib nanosuspension formulation and transformation into tablets. *Int. J. Pharm.* **376**, 204–212 (2009).
 135. Jinno, J. ichi, Kamada, N., Miyake, M., Yamada, K., Mukai, T., Odomi, M., Toguchi, H., Liversidge, G. G., Higaki, K. & Kimura, T. In vitro-in vivo correlation for wet-milled tablet of poorly water-soluble cilostazol. *J. Control. Release* **130**, 29–37 (2008).
 136. Miao, X., Sun, C., Jiang, T., Zheng, L., Wang, T. & Wang, S. Investigation of nanosized

- crystalline form to improve the oral bioavailability of poorly water soluble cilostazol. *J. Pharm. Pharm. Sci.* **14**, 196–214 (2011).
137. Jinno, J. I., Kamada, N., Miyake, M., Yamada, K., Mukai, T., Odomi, M., Toguchi, H., Liversidge, G. G., Higaki, K. & Kimura, T. Effect of particle size reduction on dissolution and oral absorption of a poorly water-soluble drug, cilostazol, in beagle dogs. *J. Control. Release* **111**, 56–64 (2006).
 138. Kayaert, P., Anné, M. & Van Den Mooter, G. Bead layering as a process to stabilize nanosuspensions: Influence of drug hydrophobicity on nanocrystal reagglomeration following in-vitro release from sugar beads. *J. Pharm. Pharmacol.* **63**, 1446–1453 (2011).
 139. Peters, K., Leitzke, S., Diederichs, J. E., Borner, K., Hahn, H., Müller, R. H. & Ehlers, S. Preparation of a clofazimine nanosuspension for intravenous use and evaluation of its therapeutic efficacy in murine *Mycobacterium avium* infection. *J. Antimicrob. Chemother.* **45**, 77–83 (2000).
 140. Borner, K., Hartwig, H., Leitzke, S., Hahn, H., Müller, R. H. & Ehlers, S. HPLC determination of clofazimine in tissues and serum of mice after intravenous administration of nanocrystalline or liposomal formulations. *Int. J. Antimicrob. Agents* **11**, 75–79 (1999).
 141. Hu, L., Kong, D., Hu, Q., Gao, N. & Pang, S. Evaluation of High-Performance Curcumin Nanocrystals for Pulmonary Drug Delivery Both In Vitro and In Vivo. *Nanoscale Res. Lett.* **10**, 1–9 (2015).
 142. Rajasekar, A. & Devasena, T. Facile Synthesis of Curcumin Nanocrystals and Validation of Its Antioxidant Activity Against Circulatory Toxicity in Wistar Rats. *J. Nanosci. Nanotechnol.* **15**, 4119–25 (2015).
 143. Hu, X., Yang, F. F., Wei, X. L., Yao, G. Y., Liu, C. Y., Zheng, Y. & Liao, Y. H. Curcumin acetate nanocrystals for sustained pulmonary delivery: Preparation, characterization and in vivo evaluation. *J. Biomed. Nanotechnol.* **13**, 99–109 (2017).
 144. Nakarani, M., Patel, P., Patel, J., Patel, P., Murthy, R. S. R. & Vaghani, S. S. Cyclosporine A-Nanosuspension: Formulation, characterization and in vivo comparison with a marketed formulation. *Sci. Pharm.* **78**, 345–361 (2010).
 145. Müller, R. H., Runge, S., Ravelli, V., Mehnert, W., Thünemann, A. F. & Souto, E. B. Oral bioavailability of cyclosporine: Solid lipid nanoparticles (SLN) versus drug nanocrystals. *Int. J. Pharm.* **317**, 82–89 (2006).
 146. Crisp, M. T., Tucker, C. J., Rogers, T. L., Williams, R. O. & Johnston, K. P.

- Turbidimetric measurement and prediction of dissolution rates of poorly soluble drug nanocrystals. *J. Control. Release* **117**, 351–359 (2007).
147. Nguyen, D. N., Clasen, C. & Van den Mooter, G. Encapsulating darunavir nanocrystals within Eudragit L100 using coaxial electrospraying. *Eur. J. Pharm. Biopharm.* **113**, 50–59 (2017).
 148. Kassem, M. A., Abdel Rahman, A. A., Ghorab, M. M., Ahmed, M. B. & Khalil, R. M. Nanosuspension as an ophthalmic delivery system for certain glucocorticoid drugs. *Int. J. Pharm.* **340**, 126–133 (2007).
 149. Maudens, P., Seemayer, C. A., Pfefferlé, F., Jordan, O. & Allémann, E. Nanocrystals of a potent p38 MAPK inhibitor embedded in microparticles: Therapeutic effects in inflammatory and mechanistic murine models of osteoarthritis. *J. Control. Release* **276**, 102–112 (2018).
 150. Lai, F., Sinico, C., Ennas, G., Marongiu, F., Marongiu, G. & Fadda, A. M. Diclofenac nanosuspensions: Influence of preparation procedure and crystal form on drug dissolution behaviour. *Int. J. Pharm.* **373**, 124–132 (2009).
 151. Pireddu, R., Caddeo, C., Valenti, D., Marongiu, F., Scano, A., Ennas, G., Lai, F., Fadda, A. M. & Sinico, C. Diclofenac acid nanocrystals as an effective strategy to reduce in vivo skin inflammation by improving dermal drug bioavailability. *Colloids Surf. B* **143**, 64–70 (2016).
 152. Wang, L., Li, M. & Zhang, N. Folate-targeted docetaxel-lipid-based nanosuspensions for active-targeted cancer therapy. *Int. J. Nanomedicine* **7**, 3281–3294 (2012).
 153. Gad, S. F., Park, J., Park, J. E., Fetih, G. N., Tous, S. S., Lee, W. & Yeo, Y. Enhancing Docetaxel Delivery to Multidrug-Resistant Cancer Cells with Albumin-Coated Nanocrystals. *Mol. Pharm.* **15**, 871–881 (2018).
 154. Wang, X., Ma, Y., Chen, H., Wu, X., Qian, H., Yang, X. & Zha, Z. Novel doxorubicin loaded PEGylated cuprous telluride nanocrystals for combined photothermal-chemo cancer treatment. *Colloids Surf. B* **152**, 449–458 (2017).
 155. Sartori, G. J., Prado, L. D. & Rocha, H. V. A. Efavirenz Dissolution Enhancement IV—Antisolvent Nanocrystallization by Sonication, Physical Stability, and Dissolution. *AAPS PharmSciTech* **18**, 3011–3020 (2017).
 156. Li, X., Gu, L., Xu, Y. & Wang, Y. Preparation of fenofibrate nanosuspension and study of its pharmacokinetic behavior in rats. *Drug Dev. Ind. Pharm.* **35**, 827–833 (2009).
 157. Hua Zhang, Yuan Meng, Xueqing Wang, Wenbing Dai, Xinglin Wang, Q. Z. Pharmaceutical and pharmacokinetic characteristics of different types of fenofibrate

- nanocrystals prepared by different bottom-up approaches. *Drug Deliv.* **21**, 588–594 (2014).
158. Li, T., Lei, Y., Guo, M. & Yan, H. Crosslinked poly(vinyl alcohol) hydrogel microspheres containing dispersed fenofibrate nanocrystals as an oral sustained delivery system. *Eur. Polym. J.* **101**, 77–82 (2018).
 159. Ali, H. S. M. & Hanafy, A. F. Glibenclamide Nanocrystals in a Biodegradable Chitosan Patch for Transdermal Delivery: Engineering, Formulation, and Evaluation. *J. Pharm. Sci.* **106**, 402–410 (2017).
 160. Van Eerdenbrugh, B., Froyen, L., Van Humbeeck, J., Martens, J. A., Augustijns, P. & Van den Mooter, G. Drying of crystalline drug nanosuspensions-The importance of surface hydrophobicity on dissolution behavior upon redispersion. *Eur. J. Pharm. Sci.* **35**, 127–135 (2008).
 161. Mishra, P. R., Shaal, L. Al, Müller, R. H. & Keck, C. M. Production and characterization of Hesperetin nanosuspensions for dermal delivery. *Int. J. Pharm.* **371**, 182–189 (2009).
 162. Pelikh, O., Stahr, P., Huang, C., Gerst, M., Scholz, P., Dietrich, H., Geisel, N. & Keck, C. M. Nanocrystals for improved dermal drug delivery. *Eur. J. Pharm. Biopharm.* **128**, 170–178 (2018).
 163. Baba, K., Pudavar, H. E., Roy, I., Ohulchansky, T. Y., Chen, Y., Pandey, R. K. & Prasad, P. N. New method for delivering a hydrophobic drug for photodynamic therapy using pure nanocrystal form of the drug. *Mol. Pharm.* **4**, 289–297 (2007).
 164. Ali, H. S. M., York, P., Ali, A. M. A. & Blagden, N. Hydrocortisone nanosuspensions for ophthalmic delivery: A comparative study between microfluidic nanoprecipitation and wet milling. *J. Control. Release* **149**, 175–181 (2011).
 165. Van Eerdenbrugh, B., Stuyven, B., Froyen, L., Van Humbeeck, J., Martens, J. A., Augustijns, P. & Van den Mooter, G. Downscaling Drug Nanosuspension Production: Processing Aspects and Physicochemical Characterization. *Aaps Pharmscitech* **10**, 44–53 (2009).
 166. Fernandes, A. R., Dias-Ferreira, J., Cabral, C., Garcia, M. L. & Souto, E. B. Release kinetics and cell viability of ibuprofen nanocrystals produced by melt-emulsification. *Colloids Surf. B* **166**, 24–28 (2018).
 167. Tuomela, A., Laaksonen, T., Laru, J., Antikainen, O., Kiesvaara, J., Ilkka, J., Oksala, O., Rönkkö, S., Järvinen, K., Hirvonen, J. & Peltonen, L. Solid formulations by a nanocrystal approach: Critical process parameters regarding scale-ability of nanocrystals for tableting applications. *Int. J. Pharm.* **485**, 77–86 (2015).

168. Foglio Bonda, A., Rinaldi, M., Segale, L., Palugan, L., Cerea, M., Vecchio, C. & Pattarino, F. Nanonized itraconazole powders for extemporaneous oral suspensions: Role of formulation components studied by a mixture design. *Eur. J. Pharm. Sci.* **83**, 175–183 (2016).
169. Vaughn, J. M., Wiederhold, N. P., McConville, J. T., Coalson, J. J., Talbert, R. L., Burgess, D. S., Johnston, K. P., Williams, R. O. & Peters, J. I. Murine airway histology and intracellular uptake of inhaled amorphous itraconazole. *Int. J. Pharm.* **338**, 219–224 (2007).
170. Mou, D., Chen, H., Wan, J., Xu, H. & Yang, X. Potent dried drug nanosuspensions for oral bioavailability enhancement of poorly soluble drugs with pH-dependent solubility. *Int. J. Pharm.* **413**, 237–244 (2011).
171. Basa, S., Muniyappan, T., Karatgi, P., Prabhu, R. & Pillai, R. Production and in vitro characterization of solid dosage form incorporating drug nanoparticles. *Drug Dev. Ind. Pharm.* **34**, 1209–1218 (2008).
172. Touzet, A., Pfefferlé, F., der Wel, P. van, Lamprecht, A. & Pellequer, Y. Active freeze drying for production of nanocrystal-based powder: A pilot study. *Int. J. Pharm.* **536**, 222–230 (2018).
173. Vergote, G. J., Vervaet, C., Van Driessche, I., Hoste, S., De Smedt, S., Demeester, J., Jain, R. A., Ruddy, S. & Remon, J. P. In vivo evaluation of matrix pellets containing nanocrystalline ketoprofen. *Int. J. Pharm.* **240**, 79–84 (2002).
174. Van Eerdenbrugh, B., Froyen, L., Martens, J. A., Bleton, N., Augustijns, P., Brewster, M. & Van den Mooter, G. Characterization of physico-chemical properties and pharmaceutical performance of sucrose co-freeze-dried solid nanoparticulate powders of the anti-HIV agent loviride prepared by media milling. *Int. J. Pharm.* **338**, 198–206 (2007).
175. Liu, C., Chang, D., Zhang, X., Sui, H., Kong, Y., Zhu, R. & Wang, W. Oral fast-dissolving films containing lutein nanocrystals for improved bioavailability: formulation development, in vitro and in vivo evaluation. *AAPS PharmSciTech* **18**, 2957–2964 (2017).
176. Konnerth, C., Braig, V., Ito, A., Schmidt, J., Lee, G. & Peukert, W. Formation of Mefenamic Acid Nanocrystals with Improved Dissolution Characteristics. *Chemie-Ingenieur-Technik* **89**, 1060–1071 (2017).
177. Bodnar, K., Hudson, S. P. & Rasmuson, Å. C. Stepwise use of additives for improved control over formation & stability of mefenamic acid nanocrystals produced by

- antisolvent precipitation. *Cryst. Growth Des.* **17**, 454–466 (2017).
178. Song, Q., Shen, C., Shen, B., Lian, W., Liu, X., Dai, B. & Yuan, H. Development of a fast dissolving sublingual film containing meloxicam nanocrystals for enhanced dissolution and earlier absorption. *J. Drug Deliv. Sci. Technol.* **43**, 243–252 (2018).
179. Calleja, P., Irache, J. M., Zandueta, C., Martínez-Oharriz, C. & Espuelas, S. A combination of nanosystems for the delivery of cancer chemoimmunotherapeutic combinations: 1-Methyltryptophan nanocrystals and paclitaxel nanoparticles. *Pharmacol. Res.* **126**, 77–83 (2017).
180. Pyo, S. M., Hespeler, D., Keck, C. M. & Müller, R. H. Dermal miconazole nitrate nanocrystals – formulation development, increased antifungal efficacy & skin penetration. *Int. J. Pharm.* **531**, 350–359 (2017).
181. Chen, M., Li, Y., Zhou, J., Yang, Z., Li, Z., Mei, X. & Wang, Z. In vitro toxicity assessment of nanocrystals in tissue - type cells and macrophage cells. *J. Appl. Toxicol.* **38**, 656–664 (2018).
182. Danhier, F., Ucakar, B., Vanderhaegen, M. L., Brewster, M. E., Arien, T. & Préat, V. Nanosuspension for the delivery of a poorly soluble anti-cancer kinase inhibitor. *Eur. J. Pharm. Biopharm.* **88**, 252–260 (2014).
183. Liversidge, G. G. & Conzentino, P. Drug particle size reduction for decreasing gastric irritancy and enhancing absorption of naproxen in rats. *Int. J. Pharm.* **125**, 309–313 (1995).
184. Xiong, R., Lu, W., Li, J., Wang, P., Xu, R. & Chen, T. Preparation and characterization of intravenously injectable nimodipine nanosuspension. *Int. J. Pharm.* **350**, 338–343 (2008).
185. Fu, Q., Sun, J., Zhang, D., Li, M., Wang, Y., Ling, G., Liu, X., Sun, Y., Sui, X., Luo, C., Sun, L., Han, X., Lian, H., Zhu, M., Wang, S. & He, Z. Nimodipine nanocrystals for oral bioavailability improvement: Preparation, characterization and pharmacokinetic studies. *Colloids Surf. B* **109**, 161–166 (2013).
186. Fu, Q., Ma, M., Li, M., Wang, G., Guo, M., Li, J., Hou, Y. & Fang, M. Improvement of oral bioavailability for nisoldipine using nanocrystals. *Powder Technol.* **305**, 757–763 (2017).
187. Jain, S., Patel, K., Arora, S., Reddy, V. A. & Dora, C. P. Formulation, optimization, and in vitro–in vivo evaluation of olmesartan medoxomil nanocrystals. *Drug Deliv. Transl. Res.* **7**, 292–303 (2017).
188. Zhang, Z., Zhang, X., Xue, W., Yangyang, Y., Xu, D., Zhao, Y. & Lou, H. Effects of

- oridonin nanosuspension on cell proliferation and apoptosis of human prostatic carcinoma PC-3 cell line. *Int. J. Nanomedicine* **5**, 735–42 (2010).
189. Lou, H., Zhang, X., Gao, L., Feng, F., Wang, J., Wei, X., Yu, Z., Zhang, D. & Zhang, Q. In vitro and in vivo antitumor activity of oridonin nanosuspension. *Int. J. Pharm.* **379**, 181–186 (2009).
190. Gao, L., Zhang, D., Chen, M., Duan, C., Dai, W., Jia, L. & Zhao, W. Studies on pharmacokinetics and tissue distribution of oridonin nanosuspensions. *Int. J. Pharm.* **355**, 321–327 (2008).
191. Guo, F., Shang, J., Zhao, H., Lai, K., Li, Y., Fan, Z., Hou, Z. & Su, G. Cube-shaped theranostic paclitaxel prodrug nanocrystals with surface functionalization of SPC and MPEG-DSPE for imaging and chemotherapy. *Colloids Surf. B* **160**, 649–660 (2017).
192. Li, W., Li, Z., Wei, L. & Zheng, A. Evaluation of Paclitaxel Nanocrystals in Vitro and in Vivo. *Drug Res.* **68**, 205–212 (2018).
193. Deng, F., Zhang, H., Wang, X., Zhang, Y., Hu, H., Song, S., Dai, W., He, B., Zheng, Y., Wang, X. & Zhang, Q. Transmembrane Pathways and Mechanisms of Rod-like Paclitaxel Nanocrystals through MDCK Polarized Monolayer. *ACS Appl. Mater. Interfaces* **9**, 5803–5816 (2017).
194. Liu, F., Park, J.-Y., Zhang, Y., Conwell, C., Liu, Y., Bathula, S. R. & Huang, L. Targeted Cancer Therapy With Novel High Drug-Loading Nanocrystals. *J. Pharm. Sci.* **99**, 4215–4227 (2010).
195. Lee, S. E., Bairstow, S. F., Werling, J. O., Chaubal, M. V, Lin, L., Murphy, M. A., DiOrio, J. P., Gass, J., Rabinow, B., Wang, X., Zhang, Y., Yang, Z. & Hoffman, R. M. Paclitaxel nanosuspensions for targeted chemotherapy - nanosuspension preparation, characterization, and use. *Pharm. Dev. Technol.* **19**, 438–53 (2014).
196. Gao, L., Liu, G., Kang, J., Niu, M., Wang, Z., Wang, H., Ma, J. & Wang, X. Paclitaxel nanosuspensions coated with P-gp inhibitory surfactants: I. Acute toxicity and pharmacokinetics studies. *Colloids Surf. B* **111**, 277–281 (2013).
197. Talekar, M., Ganta, S., Amiji, M., Jamieson, S., Kendall, J., Denny, W. A. & Garg, S. Development of PIK-75 nanosuspension formulation with enhanced delivery efficiency and cytotoxicity for targeted anti-cancer therapy. *Int. J. Pharm.* **450**, 278–289 (2013).
198. Wang, Y., Ma, Y., Zheng, Y., Song, J., Yang, X., Bi, C., Zhang, D. & Zhang, Q. In vitro and in vivo anticancer activity of a novel puerarin nanosuspension against colon cancer, with high efficacy and low toxicity. *Int. J. Pharm.* **441**, 728–735 (2013).
199. Pardeike, J. & Müller, R. H. Nanosuspensions: A promising formulation for the new

- phospholipase A2 inhibitor PX-18. *Int. J. Pharm.* **391**, 322–329 (2010).
200. Kobierski, S. & Mu, R. H. Resveratrol nanosuspensions for dermal application – production , characterization , and physical stability. *Pharmazie* **64**, 741–747 (2009).
 201. Sinico, C., Pireddu, R., Pini, E., Valenti, D., Caddeo, C., Fadda, A. M. & Lai, F. Enhancing Topical Delivery of Resveratrol through a Nanosizing Approach. *Planta Med.* 476–481 (2016).
 202. Liu, G., Zhang, D., Jiao, Y., Guo, H., Zheng, D., Jia, L., Duan, C., Liu, Y., Tian, X., Shen, J., Li, C., Zhang, Q. & Lou, H. In vitro and in vivo evaluation of riccardin D nanosuspensions with different particle size. *Colloids Surf. B* **102**, 620–626 (2013).
 203. Krause, K. P., Kayser, O., Mäder, K., Gust, R. & Müller, R. H. Heavy metal contamination of nanosuspensions produced by high-pressure homogenisation. *Int. J. Pharm.* **196**, 169–172 (2000).
 204. Mauludin, R., Müller, R. H. & Keck, C. M. Kinetic solubility and dissolution velocity of rutin nanocrystals. *Eur. J. Pharm. Sci.* **36**, 502–510 (2009).
 205. Langguth, P., Hanafy, A., Frenzel, D., Grenier, P., Nhamias, A., Ohlig, T., Vergnault, G. & Spahn-Langguth, H. Nanosuspension Formulations for Low-Soluble Drugs: Pharmacokinetic Evaluation Using Spironolactone as Model Compound. *Drug Dev. Ind. Pharm.* **31**, 319–329 (2005).
 206. Jacobs, C., Kayser, O. & Müller, R. H. Nanosuspensions as a new approach for the formulation for the poorly soluble drug tarazepide. *Int. J. Pharm.* **196**, 161–164 (2000).
 207. Sigfridsson, K., Lundqvist, A. J. & Strimfors, M. Particle size reduction for improvement of oral absorption of the poorly soluble drug UG558 in rats during early development. *Drug Dev. Ind. Pharm.* **35**, 1479–1486 (2009).
 208. Koradia, K. D., Sheth, N. R., Koradia, H. D. & Dabhi, M. R. Ziprasidone nanocrystals by wet media milling followed by spray drying and lyophilization: Formulation and process parameter optimization. *J. Drug Deliv. Sci. Technol.* **43**, 73–84 (2018).
 209. Corral, J. M. M., Castro, M. A. & Go, M. A. Podophyllotoxin : distribution , sources , applications and new cytotoxic derivatives. **44**, 441–459 (2004).
 210. Ayres, D. D. C. & John D. Loike. Lignans: Chemical, Biological and Clinical Properties. *Biochem. Syst. Ecol.* **20**, 110–135 (1992).
 211. Nitiss, J. L. Targeting DNA topoisomerase II in cancer chemotherapy. *Nature* **9**, 338–350 (2009).
 212. Montecucco, A., Zanetta, F. & Biamonti, G. Molecular Mechanisms of Etoposide Etoposide Is a Topoisomerase II Poison. *Excli J.* **14**, 95–108 (2015).

213. Williams, S. D., Einhorn, L. H., Anthony Greco, F., Oldham, R. & Fletcher, R. VP-16–213 salvage therapy for refractory germinal neoplasms. *Cancer* **46**, 2154–2158 (1980).
214. Atienza, D. M., Vogel, C. L., Trock, B. & Swain, S. M. Phase II study of oral etoposide for patients with advanced breast cancer. *Cancer* **76**, 2485–2490 (1995).
215. Thatcher, N., Clark, P. I., Girling, D. J., Hopwood, P., Widdy, S. T., Stephens, R. J., Bailey, A. J. & Machin, D. Comparison of oral etoposide and standard intravenous multidrug chemotherapy for small-cell lung cancer: A stopped multicentre randomised trial. *Lancet* **348**, 563–566 (1996).
216. Leaf, A. N., Wolf, B. C., Kirkwood, J. M. & Haselow, R. E. Phase II study of etoposide (VP-16) in patients with thyroid cancer with no prior chemotherapy: An eastern cooperative oncology group study (E1385). *Med. Oncol.* **17**, 47–51 (2000).
217. Rezonja, R., Knez, L., Cufer, T. & Mrhar, A. Oral treatment with etoposide in small cell lung cancer-dilemmas and solutions. *Radiol. Oncol.* **47**, 1–13 (2013).
218. IARC Monographs on the Evaluation of Carcinogenic Risks to Humans. *Pharmaceuticals - A review of Human Carcinogens. Book 100*, (2012).
219. Loehrer, P. J. Etoposide therapy for testicular cancer. *Cancer* **67**, 220–224 (1991).
220. Slevin, M. L. *The clinical pharmacology of etoposide*. **16**, (Cancer, 1991).
221. Heck, M. M., Hittelman, W. N. & Earnshaw, W. C. Differential expression of DNA topoisomerases I and II during the eukaryotic cell cycle. *Proc. Natl. Acad. Sci. USA* **85**, 1086–1090 (1988).
222. Clark, P., Slevin, M., Joel, S., Osborne, R., Talbot, D., Johnson, P., Reznick, R., Masud, T., Grepory, W. & Wrigley, P. A randomized trial of two etoposide schedules in small-cell lung cancer: the influence of pharmacokinetics on efficacy and toxicity. *J. Clin. Oncol.* **12**, 1427–35 (1994).
223. Clark, P., Slevin, M., Joel, S., Osborne, R., Talbot, D., Johnson, P., Reznick, R., Masud, T., Grepory, W. & Wrigley, P. A randomized trial to evaluate the effect of schedule on the activity of etoposide in small cell lung cancer. *J. Clin. Oncol.* **7**, 1333–1340 (1989).
224. Zhang, X., Xing, H., Zhao, Y. & Ma, Z. Pharmaceutical dispersion techniques for dissolution and bioavailability enhancement of poorly water-soluble drugs. *Pharmaceutics* **10**, (2018).
225. Che, E., Zheng, X., Sun, C., Chang, D., Jiang, T. & Wang, S. Drug nanocrystals: A state of the art formulation strategy for preparing the poorly water-soluble drugs. *Asian J. Pharm. Sci.* **7**, 85–95 (2012).
226. Erdemir, D., Lee, A. Y. & Myerson, A. S. Nucleation of Crystals from Solution :

- Classical and Two-Step Models. *Acc. Chem. Res.* **42**, (2009).
227. Shubhra, Q. T. H., Oth, J. T. & Gyenis, J. A. Poloxamers for Surface Modification of Hydrophobic Drug Carriers and Their Effects. *Polym. Rev.* 112–138 (2014).
228. Kabanov, A. V., Batrakova, E. V. & Alakhov, V. Y. Pluronic® block copolymers as novel polymer therapeutics for drug and gene delivery. *J. Control. Release* **82**, 189–212 (2002).
229. Pouretedal, H. R. Preparation and characterization of azithromycin nanodrug using solvent / antisolvent method. *Int Nano Lett* **4**, (2014).
230. Mansouri, M., Pouretedal, H. R. & Vosoughi, V. Preparation and Characterization of Ibuprofen Nanoparticles by using Solvent / Antisolvent Precipitation. *Open Conf Proc J* **1050**, 88–94 (2011).
231. Khan, S., Matas, M. De, Zhang, J. & Anwar, J. Nanocrystal Preparation: Low-Energy Precipitation Method Revisited. *Cryst. Growth Des.* **13**, 2766–2777 (2013).
232. Yarraguntla, S. R., Enturi, V., Vyadana, R. & Bommala, S. Formulation and Evaluation of Lornoxicam Nanocrystals with Different Stabilizers at Different Concentrations. *Asian J. Pharm.* **10**, 198–207 (2016).
233. Liu, P., Rong, X., Laru, J., Veen, B. Van, Kiesvaara, J., Hirvonen, J., Laaksonen, T. & Peltonen, L. Nanosuspensions of poorly soluble drugs : Preparation and development by wet milling. *Int. J. Pharm.* **411**, 215–222 (2011).
234. Nanjwade, B. K., Derkar, G. K., Behra, H. M., Nanjwade, V. K. & Manvi, F. V. Design and Characterization of Nanocrystals of Lovastatin for Solubility and Dissolution Enhancement Nanomedicine & Nanotechnology. *J. Nanomedicine Nanotechnol.* **2**, (2011).
235. Gibson, M. *Pharmaceutical Preformulation and Formulation—A Practical Guide from Candidate Drug Selection to Commercial Dosage Form.* **199**,
236. Hücrelerini, K., Etopozit, H., Yeni, İ. & Thangarasu, V. Preparation and Biopharmaceutical Evaluation of Novel Polymeric Nanoparticles Containing Etoposide for Targeting Cancer Cells. **16**, 132–140 (2019).
237. Sun, J., Wang, F., Sui, Y., She, Z., Zhai, W., Wang, C. & Deng, Y. Effect of particle size on solubility, dissolution rate, and oral bioavailability: Evaluation using coenzyme Q10 as naked nanocrystals. *Int. J. Nanomedicine* **7**, 5733–5744 (2012).
238. Rao, P., Montenegro-nicolini, M., Morales, J. O. & Velaga, S. Effect of surfactants and drug load on physico-mechanical and dissolution properties of nanocrystalline tadalafil-loaded oral films. *Eur. J. Pharm. Sci.* **109**, 372–380 (2017).

239. Gigliobianco, M., Casadidio, C., Censi, R., Di Martino, P., Gigliobianco, M. R., Casadidio, C., Censi, R. & Di Martino, P. Nanocrystals of Poorly Soluble Drugs: Drug Bioavailability and Physicochemical Stability. *Pharmaceutics* **10**, 134 (2018).
240. Midoux, P., Scherman, D., Herscovici, J., Pichon, C. & Mignet, N. Comparative gene transfer between cationic and thiourea lipoplexes. *J. gene Med.* 45–54 (2010).
241. Taib, T., Leconte, C., Steenwinckel, J. Van, Cho, A. H., Palmier, B., Torsello, E., Kuen, R. L., Onyeomah, S., Ecomard, K., Novak, A., Deou, E., Plotkine, M., Gressens, P. & Marchand-leroux, C. Neuroinflammation , myelin and behavior : Temporal patterns following mild traumatic brain injury in mice. *PLoS One* **12**, (2017).
242. Euhus, D. M., Hudd, C., Laregina, M. C. & Johnson, F. E. Tumor Measurement in the Nude Mouse. *J. Surg. Oncol.* **31**, 229–234 (1986).
243. Gupta, S., Chaudhary, K., Kumar, R. & Gautam, A. Prioritization of anticancer drugs against a cancer using genomic features of cancer cells : A step towards personalized medicine. *Nat. Publ. Gr.* **6**, 1–11 (2016).
244. Longacre, M., Snyder, N. & Sarkar, S. Drug Resistance in Cancer : An Overview. *Cancer* **6**, 1769–1792 (2014).
245. Zhang, M., Liu, E., Cui, Y. & Huang, Y. Nanotechnology-based combination therapy for overcoming multidrug-resistant cancer. *Cancer Biol. Med.* **14**, 212 (2017).
246. Chen, Y. & Li, T. Cellular Uptake Mechanism of Paclitaxel Nanocrystals Determined by Confocal Imaging and Kinetic Measurement. *AAPS* **7**, 1126–1134 (2015).
247. Tian, B., Zhang, X., Yu, C., Zhou, M. & Zhang, X. Aspect ratio effect of drug nanocrystals on cellular internalization efficiencies, uptake mechanisms, in vitro and in vivo anticancer efficiencies. *Nanoscale Res. Lett.* **7**, 3588–3593 (2015).
248. N, O. & JH, P. Endocytosis and exocytosis of nanoparticles in mammalian cells. *Int. J. Nanomedicine* **1**, 51–63 (2014).
249. Pundlikrao, P., Baria, R. K. & Gattani, S. G. Colloids and Surfaces B : Biointerfaces Fabrication of fenofibrate nanocrystals by probe sonication method for enhancement of dissolution rate and oral bioavailability. *Colloids Surfaces B Biointerfaces* **108**, 366–373 (2013).
250. Güncüm E, Bakirel T, Anlaş C, Ekici H & Işıklan N. Novel amoxicillin nanoparticles formulated as sustained release delivery system for poultry use. *J. Vet. Pharmacol. Ther.* **41**, 588–598 (2018).
251. Peracchia, M. T., Harnisch, S., Gulik, A., Dedieu, J. C., Desmae, D., Angelo, J., Mu, R. H. & Couvreur, P. Visualization of in vitro protein-rejecting properties of PEGylated

- stealth polycyanoacrylate nanoparticles. *Biomaterials* **20**, 1269–1275 (1999).
252. Zahr, A. S., Davis, C. A., Pishko, M. V, Park, U. V, Pennsylv, V., April, R. V, Final, I. & June, F. Macrophage Uptake of Core - Shell Nanoparticles Surface Modified with Poly(ethylene glycol). *Langmuir* **22**, 8178–8185 (2006).
253. Chaudhury, C., Mehnaz, S., Robinson, J. M., Hayton, W. L., Pearl, D. K., Roopenian, D. C. & Anderson, C. L. The Major Histocompatibility Complex – related Fc Receptor for IgG (FcRn) Binds Albumin and Prolongs Its Lifespan. *J. Exp. Med.* **197**, (2003).
254. Pyzik, M., Rath, T., Kuo, T. T., Win, S., Baker, K., Hubbard, J. J., Grenha, R. & Cre, C. Hepatic FcRn regulates albumin homeostasis and susceptibility to liver injury. *Proc. Natl. Acad. Sci. U. S. A.* **114**, 1–10 (2017).
255. *Pharmaceutical Aspects of Oligonucleotides*. (Taylor & Francis Ltd, 1999).
256. Blanco, E., Shen, H. & Ferrari, M. Principles of nanoparticle design for overcoming biological barriers to drug delivery. *Nat. Biotechnol.* **33**, 941–951 (2015).
257. Lavoie, P. M. & Levy, O. *Mononuclear Phagocyte System. Fetal and Neonatal Physiology* (Elsevier Inc., 2016).
258. Yalkowsky, S. H. & Valvani, S. C. Precipitation of solubilized drugs due to injection or dilution. *Drug Intell. Clin. Pharm.* **11**, 417–419 (1977).
259. Matsumura, Y. & Maeda, H. A New Concept for Macromolecular Therapeutics in Cancer Chemotherapy: Mechanism of Tumor-tropic Accumulation of Proteins and the Antitumor Agent Smancs. *Cancer Res.* **46**, 6387–6392 (1986).
260. Run, Y. Z., Li, L. H., Du, W. H. J. & Wang, J. Strategies to improve tumor penetration of nanomedicines through nanoparticle design. **11**, 1–12 (2018).
261. Araujo, L., Lobenberg, R. & Kreuter, J. Influence of the Surfactant Concentration on the Body Distribution of Nanoparticles. **6**, 373–385 (1999).
262. Gao, W., Chen, Y., Thompson, D. H., Park, K. & Li, T. Impact of surfactant treatment of paclitaxel nanocrystals on biodistribution and tumor accumulation in tumor-bearing mice. *J. Control. Release* **237**, 168–176 (2016).
263. Golightly, L. & Rumack, B. H. Pharmaceutical Excipients Adverse Effects Associated with Inactive Ingredients in Drug Products. *Med. Toxicol.* **3**, 128–165 (1988).
264. Liu, C. Y., Liao, H. F., Wang, T. E., Lin, S. C., Shih, S. C., Chang, W. H., Yang, Y. C., Lin, C. C. & Chen, Y. J. Etoposide sensitizes CT26 colorectal adenocarcinoma to radiation therapy in BALB/c mice. *World J. Gastroenterol.* **11**, 4895–4898 (2005).
265. Park, J., Park, J. E., Hedrick, V. E., Wood, K. V., Bonham, C., Lee, W. & Yeo, Y. A Comparative In Vivo Study of Albumin-Coated Paclitaxel Nanocrystals and Abraxane.

- Small* **14**, 1–10 (2018).
266. Keck, C. M. & Müller, R. H. Drug nanocrystals of poorly soluble drugs produced by high pressure homogenisation. *Eur. J. Pharm. Biopharm.* **62**, 3–16 (2006).
267. Attaria, Z., Kalvakuntlaa, S., Reddya, M. S., Deshpandeb, M., Raoc, C. M. & Koteswararaa, K. B. Formulation and characterisation of nanosuspensions of BCS class II and IV drugs by combinative method. *J. Exp. Nanosci.* **11**, 276–288 (2015).
268. Dai, Q., Wilhelm, S., Ding, D., Syed, A. M., Sindhvani, S., Zhang, Y., Chen, Y. Y., Macmillan, P. & Chan, W. C. W. Quantifying the Ligand-Coated Nanoparticle Delivery to Cancer Cells in Solid Tumors. *ACS Nano* **12**, 8423–8435 (2018).
269. Harrington, K. J., Mohammadtaghi, S., Uster, P. S., Glass, D., Peters, A. M., Vile, R. G. & Stewart, J. S. W. Effective Targeting of Solid Tumors in Patients With Locally Advanced Cancers by Radiolabeled Pegylated Liposomes. **7**, 243–254 (2001).
270. Wilhelm, S., Tavares, A. J., Dai, Q., Ohta, S., Audet, J., Dvorak, H. F. & Chan, W. C. W. Analysis of nanoparticle delivery to tumours. *Nature* **1**, (2016).
271. Lin, Z., Gao, W., Hu, H., Ma, K., He, B., Dai, W., Wang, X., Wang, J., Zhang, X. & Zhang, Q. Novel thermo-sensitive hydrogel system with paclitaxel nanocrystals: High drug-loading, sustained drug release and extended local retention guaranteeing better efficacy and lower toxicity. *J. Control. Release* **174**, 161–170 (2014).

Annexes

Annexes

Annexe 1: B. M. Couillaud, P. Espeau, N. Mignet, and Y. Corvis, “State of the Art of Pharmaceutical Solid Forms : from Crystal Property Issues to Nanocrystals Formulation,” pp. 8–23, 2019.

Annexe 2: European Patent n° EP18306138.1 “Preparation of Nanosuspension Comprising Nanocrystals of Active Pharmaceutical Ingredients with Little or No Stabilizing Agents “. 2018.



State of the Art of Pharmaceutical Solid Forms: from Crystal Property Issues to Nanocrystals Formulation

Brice Martin Couillaud, Philippe Espeau, Nathalie Mignet, and Yohann Corvis*^[a]

The solid-form screening of active principal ingredients is a challenge for pharmaceutical drug development, as more than 80% of marketed drugs are formulated in the solid form. A broad and comprehensive study of the various solid forms of drugs is needed to enhance their translation into the clinic. Therefore, the most suitable solid form must be taken into consideration regarding *ex vivo* and *in vivo* stability, targeting, solubility, dissolution rate, and bioavailability. In this review,

techniques of solid-form screening are covered, including differences in solid forms such as polymorphs, solvates, salts, co-crystals, and amorphous particles. Moreover, solid drug size reduction is also discussed, with insight into the emergence of drug nanocrystal formulations. An overview of the smallest nanocrystals reported in the literature and on the market is also provided, along with their applications and routes of administration.

1. Introduction

More than 80 percent of formulated drugs are in the solid state, for reasons of stability from the handling and storage of unprocessed material to the drug-development process. In most cases, pharmaceutical solids have high melting points, i.e., low aqueous solubility. Therefore, the enhancement of drug solubility is a primary challenge in pharmaceutical research in order to ensure therapeutic efficiency, to minimize toxicity, and to optimize the cost of production. In the solid state, the various structural possibilities of a given active pharmaceutical ingredient (API) can significantly influence its chemical, physical, and biopharmaceutical properties.^[1] Salt formation, co-crystallization techniques, amorphization, polymorphic transition, and nanosizing can drastically modify the therapeutic impact of an API. Thereby, the physicochemical characterization of each possible form allows a better assessment of its pharmaceutical properties. Research into the most suitable pharmaceutical forms of a given drug, also defined as solid-form screening,^[2] helps to ensure the quality and effectiveness of the treatment, and in some cases, the comfort of patients. Solid-form screening allows determination of the best pharmaceutical form and excipient. Finding the most suitable solid form allows safer pharmacological and toxicological studies, thereby saving time and thus benefiting the drug-development process. The aim of this review is to provide a pharmaceutical outlook on various solid forms, namely, polymorphs,

co-crystals, salts, solvates, amorphous solids, and their eventual combinations with an emphasis on nanocrystal formulations. This is followed by a discussion on the advantages and disadvantages of each solid form from a pharmaceutical point of view.

2. The Biopharmaceuticals Classification System (BCS)

Solid-form screening for pharmaceutical development has helped increase the bioavailability of poorly soluble drug candidates.^[3–5] Currently, around 70% of drugs are classified as poorly soluble.^[6] The solubility of a drug affects its dissolution rate, which strongly governs its *in vivo* performance. It is therefore crucial to identify drug candidates with the best solubility properties suitable for pharmaceutical applications.


The Biopharmaceuticals Classification System (BCS), established by Amidon et al.,^[7] is a tool for decision making in drug development, based on two primary factors: solubility and permeability (Figure 1). These factors have proven themselves to be crucial from drug design to its bioequivalence, taking into account the dissolution rate.

The BCS classifies drugs into four classes:

- Class I: high solubility/high permeability profiles (e.g., metoprolol, diltiazem hydrochloride);
- Class II: low solubility/high permeability profiles (e.g., diclofenac sodium, griseofulvin);
- Class III: high solubility/low permeability profiles (e.g., atenolol, lisinopril);
- Class IV: low solubility/low permeability profiles (e.g., etravirine, hydrochlorothiazide).

The US Food and Drug Administration (FDA) defines a highly water-soluble drug as one that, at the drug product's

[a] B. M. Couillaud, Dr. P. Espeau, Dr. N. Mignet, Dr. Y. Corvis
Team Nanovectors for Targeted Therapy and Molecular Imaging (VICT),
Chemical and Biological Technologies for Health Unit (UTCBS), CNRS
UMR8258, INSERM U1022, Paris Descartes University, Sorbonne-Paris-Cité,
Chimie ParisTech, PSL Research University, School of Pharmacy, 4 avenue
de l'Observatoire 75006 Paris (France)
E-mail: yohann.corvis@parisdescartes.fr

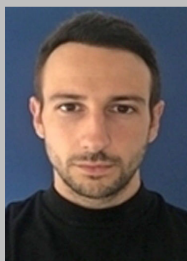
 The ORCID identification number(s) for the author(s) of this article can be found under:
<https://doi.org/10.1002/cmdc.201800612>.

highest strength, can be dissolved in 250 mL aqueous media at most, in a pH range of 1–6.8; it is considered highly permeable when the absorption in the human body is >90% relative to the intravenous (i.v.) administered dose.^[6] The expectations

from these four classes regarding in vivo and in vitro correlations are described below, according to Amidon et al.^[7]

BCS class I drugs dissolve and absorb quickly, and no rate-limiting step is expected for oral absorption. For a drug disso-

Brice Martin Couillaud has been a PhD student in the Faculty of Pharmacy (Paris Descartes University) since 2016 under the supervision of Dr. Yohann Corvis. He focuses on the preparation of antitumor nanocrystal suspensions by co-precipitation for enhanced targeting and sustained release for cancer therapy. His work consists of nanocrystal synthesis, structural characterization, dissolution studies, in vitro and in vivo studies, and to highlight the advantages of such innovative systems. Recently, his main concerns have been to assess the bloodstream lifespan of nanocrystals in mice relative to the marketed product.



Dr. Nathalie Mignet is director of research at the National Center for Scientific Research in France (Laboratory: CNRS UMR8258, INSERM U1022, Paris Descartes University, Chimie ParisTech, Paris). After completing her PhD in organic chemistry (Prof. Jean-Louis Imbach, Université de Montpellier II), she was hired by Lynx Therapeutics in San Francisco, CA, USA. She then joined the faculty at the University of Sheffield in the UK. In 1998, she was hired by the French biotech company Capsulis to work on onion-like nanoparticles called spherulites. She joined the CNRS as a research scientist in 2000 to work on non-viral gene delivery. Since then, she has expanded her domain of interest from drug delivery systems to nanomedicines designed for triggered delivery or imaging. In 2014, she became leader of the team "Nanovectors for Targeted Therapy and Molecular Imaging", which is pursuing nanomedicines for delivery or imaging, going from fundamental research to preclinical studies. She is the coauthor of 76 articles, 14 book chapters, and eight patents. She is also the founder and president of the French Society for Nanomedicine, SFNano.



Dr. Philippe Espeau is an associate professor in the Faculty of Pharmacy (Paris Descartes University). He joined the team "Nanovectors for Targeted Therapy and Molecular Imaging" of the UTCBS unit after his position as Head of the "Physical Chemistry of Drugs" research unit from 2010 to 2013. After defending his PhD thesis on the study of phase-change materials and phase diagrams in 1995 at the University of Bordeaux, he held a postdoctoral position in the Research School of Chemistry at the Australian National University (Canberra), where he carried out research on the thermodynamics of the confinement of alkanes in porous graphite. In 1998, he joined the Faculty of Pharmacy at Paris and started working on the solid state of drugs. His current research focuses on the stability of the ingredients used to manufacture drugs and on the interactions between active ingredients and excipients in the solid state. His studies are carried out by thermal analyses, powder X-ray diffraction, and thermodynamic assessments. He is the author of more than 60 international publications, and is vice president of Section 85 of the National Council of Universities.



Dr. Yohann Corvis holds an engineering doctorate in physical chemistry, material sciences and process (Lorraine University, 2005). His doctoral work dealt with the elaboration of biocatalytic surfaces by self-assembly of organic systems such as oxidoreductases, esterases, cyclodextrin, calixarene, and fullerene derivatives on protein-coated surfaces. After two years of postdoctoral studies at Warsaw University, Metz University, and IFPEN Rueil-Malmaison Institute, he was recruited to the Faculty of Pharmacy (Paris Descartes University) in 2008 as an associate professor in the physical chemistry of drugs; there, he obtained his habilitation to supervise research in 2013. He currently works in the team "Nanovectors for Targeted Therapy and Molecular Imaging" on state of matter of raw pharmaceutical materials, characterization of intermolecular interactions, and the formulation of final products for anesthetic, antitumor, and anti-inflammatory therapies, from preformulation to in vivo evaluation of the formulated systems. He has authored 40 publications, three patents, and one book chapter. He has supervised 30 internship students and one PhD student. His work has been presented at 51 international symposia, 29 national symposia, and 17 invited talks.



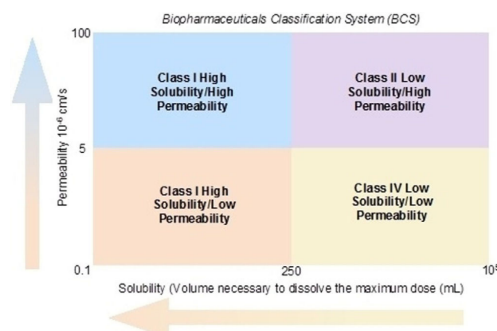


Figure 1. Biopharmaceuticals Classification System.

lution rate lower than that of gastric emptying, in vitro and in vivo studies are correlated. BCS class II drugs dissolve slowly and absorb rapidly, and thus dissolution is the rate-limiting step. Bioavailability is controlled by dosage form and drug dissolution. Consequently, both oral and i.v. administration routes are privileged. BCS class III drugs dissolve quickly, but their absorbance is limited, so no in vivo and in vitro correlation is expected with dissolution rate. In this case, both oral and i.v. routes can be considered. BCS class IV drugs have low dissolution rates and low permeability, implying that in vitro and in vivo correlation is not expected. This class of API is not preferred for oral administration, and i.v. administration is more convenient.^[7] However, in some cases, the oral administration route can still be chosen for such BCS class IV APIs as etravirine, by modifying their physicochemical properties.^[9,10] Indeed, a list of mainly orally administered drugs according to the BCS has been compiled by Lindenberg et al.^[11]

The solid state of a drug can be adapted to optimize its pharmaceutical properties. Selecting the suitable physical form of a drug provides a strategic alternative for optimizing physicochemical properties such as chemical and physical stability, solubility, dissolution rate, and bioavailability. Those strategies are mainly applied for drugs with low solubility such as BCS class II drugs. In the pharmaceutical research field, polymorphs, solvates, amorphous solids, salts, and co-crystals are good approaches toward increasing drug solubility, especially decreasing the required dosage of API in question. Moreover, nano-crystals may increase API loading in a given formulation with enhanced solubility properties. This review details the various solid forms encountered in the pharmaceutical sciences.

3. Solid Forms and Their Implications on Physical, Chemical, Pharmaceutical, and Biopharmaceutical Properties

When the external environment cannot provide sufficient energy to a given system, translational movements of the molecules in the system are limited. As a result, particles tend to organize themselves by forming a lattice in order to minimize the internal energy of the system. The compound is then in the crystalline state, which is the ordered form of matter,

whereas in the amorphous state, there is no explicit range order. Various crystalline structures can be used in the pharmaceutical sciences to improve drug properties.^[12]

Polymorphism, first introduced by McCrone in 1965,^[13] then by Lamy and Rosenstein in 1969,^[14] is the ability of a given compound to exist in several crystalline solid states.^[15,16] Therefore, **polymorphs** contain molecules of a single chemical nature. The term *packing polymorphism* is used when differences in crystal packing are observed: molecules are in the same molecular arrangement, but are grouped differently in three-dimensional space. *Conformational polymorphism* is used to describe crystal forms that consist of molecules with different conformations packed in several arrangements.^[17] In pharmaceutical sciences, most drugs exhibit polymorphism;^[18] however, the most stable form is recommended to ensure reproducibility of the product formulation and stability throughout its lifespan.^[19] Indeed, the polymorphism may have an influence on powder flow, compactibility, physicochemical stability, and the dissolution rate of raw material.^[20] A well-known example is ritonavir, an anti-retroviral drug used to treat HIV-1 infection. Approved in 1996, it was removed from the market in 1998 because of its tendency toward polymorphism. Indeed, crystals of a new polymorph were discovered in i.v. bags, and exhibited lower solubility than the initially prepared form.^[21] As a matter of fact, the lower the stability of a given polymorph, the higher its solubility.^[22] Therefore, to enhance drug bioavailability, one can increase its solubility by stabilizing the kinetically metastable polymorph of a given API. However, such systems are sensitive to external stimuli such as pH, temperature, radiation, and pressure variations.

Solvates are solid crystals with solvent molecules (e.g., ethanol, ethyl acetate) included in the lattice structure.^[23] It has been demonstrated that an organic compound with high polymorphism abilities also has a high propensity to form solvates.^[24] In the case of one or more water molecules as solvent, solvates are known as hydrates, whereas compounds with no water in crystallization are called anhydrides. Around 33% of APIs form hydrates,^[25] which can be mono- or poly-hydrated according to the number of water molecules embedded in the crystal lattice.^[26] Hydrates can be divided into three categories: crystalline hydrates based on their structure (Class I, when the water molecule interacts only with the main molecule; class II, when channels of water molecules are present throughout the crystal structure; and class III, when metal ions of the crystal structure are coordinated with water). Interestingly, a hydrate's solubility depends on its hydration state. With some drugs such as azithromycin, hydrates are more soluble than the corresponding anhydrate, and with other drugs it is the reverse.^[27] Consequently, it is important to evaluate the capacity of a pharmaceutical raw material to form hydrates during its manufacture or storage, and also to establish its relative stability against relative humidity.^[28]

Salt crystals are usually formed when drugs bear ionizable groups. Salts have been used to modify the physical and chemical properties of a drug. Formation of a salt improves drug solubility and therefore bioavailability. The nature of the host molecule (anions or cations) can alter salt solubility and

overall properties. A study carried out by Jamaludin et al. compared the solubility of various salts of quinine. Given its neutral taste, the authors recommended the quinine ethyl carbonate salt for treating children with malaria, as opposed to the bitter-tasting quinine hydrochloride and quinine sulfate.^[29]

Co-crystal formulation is a more recent approach to improve drug physicochemical properties. This results in the combination of two or more neutral substances tied together in a unique crystal lattice.^[30,31] Like the solid forms mentioned above, co-crystals may improve solubility and bioavailability according to the nature of their constituents.^[32] Drozd et al. studied the co-crystal structures of the anti-tuberculous drug 4-aminosalicylic acid (PASA), and observed that the solubility increased twofold with PASA-pyrazinamide (PYR), PASA-nicotinamide (NAM), PASA-isonicotinamide (iNAM), PASA-isoniazid (INH), and PASA-caffeine (CAF) co-crystal forms, in comparison with the intrinsic solubility of the pure form.^[33] Nevertheless, co-crystal forms may also decrease pure drug solubility, as PASA-theophylline (TPH) lowers PASA solubility by approximately twofold.^[33] This has been also evidenced by, for example, the work of Grossjohann et al. with the benzamide (BA)-dibenzyl sulfoxide (DBSO) 1:1 co-crystal, embedding the poorly water soluble DBSO with the more soluble BA. For both BA and DBSO components, the co-crystal solubility was lower than that of the pure components and to an equimolar physical mixture.^[34]

Polymorphs, solvates, salts, or co-crystals (Figure 2) can be the outcome of a design to enhance drug properties, but under no circumstances can the solubility, dissolution rate, and bioavailability be precisely predicted for drug combinations with host molecules, counter-molecules and so forth. As mentioned above with some examples, such solid forms can jeopardize drug quality owing to their relative stability in presence or absence of eventual host molecules. To avoid these issues, the approach of drug amorphization can be considered a better way to enhance API bioavailability.

The solid state of **amorphous** drugs is thermodynamically unstable, as amorphous compounds display a random organization of molecules. Due to the higher free energy of amorphous forms over crystalline forms, the former are more metastable, implying better solubility of amorphous pharmaceuticals.^[35] Indeed, an amorphous form dissolves more rapidly than the crystalline form because of stronger intermolecular forces

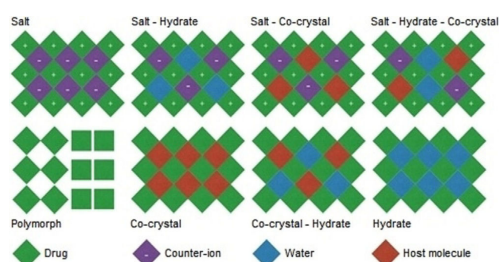


Figure 2. Various solid-state crystal forms for compounds of pharmaceutical interest.

and a higher degree of molecular organization in the latter.^[36] Despite their advantages in solubility and dissolution rate, amorphous forms have limited use in the pharmaceutical field as it is difficult to prevent their crystallization. Vasanthavada et al. studied the behavior in amorphous molecular dispersions of trehalose-dextran and trehalose-poly(vinylpyrrolidone) from returning to crystalline state in storage; the two dispersions were exposed to storage conditions of 23, 40, and 50 °C at 75% relative humidity and 23 °C at 69% relative humidity, respectively. It was found that neither of these two dispersions crystallized over the course of six months in storage.^[37] The advent of novel techniques to enhance the stability of amorphous forms has improved the odds of their use in pharmaceutical formulations. The two following tables list some examples of marketed products for which the API (Table 1) and the API/excipient mixture (Table 2) are in the amorphous state.^[38] Hence, other approaches are required to enhance drug properties for pharmaceutical purposes.

Table 1. Non-exhaustive list of amorphous active pharmaceutical ingredients on the market.

Trade name	Drug	FDA approval
Accolate®	Zafirlukast	1999
Accupril®	Quinapril hydrochloride	1991
Ceftin®	Cefuroxime acetyl	1994
Crestor®	Rosuvastatin calcium	2003
Viracept®	Nelfinavir mesylate	1996

Table 2. Non-exhaustive list of amorphous solid dispersions^[a] on the market.

Trade name	Drug	FDA approval
Intelence®	Etravirine	2008
Fenoglide®	Fenofibrate	1993
Gris-PEG®	Griseofulvin	1959
Sporanox®	Itraconazole	2001
Kalydeco®	Ivacaftor	2012
Kaletra®	Lopinavir/Ritonavir	2000
Cesamet®	Nabilone	1985
Prograf®	Tacrolimus	2000
Rezulin®	Troglitazone	1999
Isoptin®	Verapamil	1982
Zelboraf®	Verumafenib	2017

[a] Solid dispersion stands for solid mixtures of API/excipients (mostly polymers).

4. Decreasing Drug Size: an Approach to Improve Bioavailability, Dissolution, and Solubility

4.1. Large- and small-scale methods for decreasing solid dispersion size

4.1.1. Spray drying

Spray drying is a technology for developing solid drug dispersions from a liquid by atomization through an atomizer into a hot drying gas medium. This is followed by evaporation of the

mist and appearance of the solid phase, which is separated thanks to the moist air. The shape and size of the solid particles depend on the atomized product and the drying conditions, such as temperature, pressure, and humidity.^[39] Spray drying imparts precise control of the solid particle characteristics. Thanks to easy scale-up and an inexpensive process, this solvent-based technology is one of the most frequently used for amorphous solid dispersions.

4.1.2. Solvent evaporation vs. hot-melt extrusion

The solvent evaporation methods were developed for mixing drugs and surfactants that can endure heating. This technique consists of dissolving drug and surfactant in a solvent followed by evaporation under vacuum or at standard pressure and temperature, to recover a solid dispersion. The main drawback of the solvent evaporation method is the use of organic solvents, which can be found in the final solid dispersion. Therefore, if the drug can resist the heat process, a hot-melt extrusion would be preferred over solvent evaporation. The latter method is a likely source of cytotoxic residues in the final product, which could, incidentally, change the properties of the resulting solid dispersion. Indeed, for pharmaceutical applications, organic solvents should be nontoxic or avoided altogether. The hot-melt extrusion technique is therefore a 'green' technology that allows extrusion and melting of pharmaceutical materials under high temperature and pressure. This method enables mixing of the ingredients in a new solid dispersion amorphous matrix, after cooling the system.^[40]

4.1.3. Freeze drying

Freeze drying or lyophilization is another solvent-based method; the only difference from solvent evaporation is that the carrier/surfactant and the drug are dissolved in an organic solvent, then frozen under a cold atmosphere, generally liquid nitrogen. A major advantage of freeze drying is the minimal exposure time of drug/carrier to heat; this minimizes thermal stress and phase separation during the process. The main disadvantage is that volatile compounds can be removed under vacuum.^[41]

4.2. Micronization

Another way to improve drug properties without changing the chemical nature of the systems, such as salts and solvates, is to decrease the diameter of particles. The dissolution rate of a compound increases with surface area.^[42] Still, for drugs with very low solubility, the micronization approach can promote solubility and therefore drug bioavailability. Conventional mechanical technologies used to micronize particles are jet milling, ball milling, and high-pressure homogenization.

4.2.1. Jet milling

This principle is based on the fragmentation of particles by high-speed collision in a pressurized medium. A high-pressure

fluid (N_2 , CO_2 , air) is forced through dispersion holes where its expansion converts the pressure into kinetic energy, promoting collisions between particles at very high speed, which produces the fragmentation. Djokić et al. investigated the influence of the jet-milling approach on the physicochemical characteristics of carbamazepine III. This survey highlighted the impact of injector and ring nozzle diameters, as well as the applied pressure on particles size. Although jet milling is effective at improving dissolution rate, every parameter should be precisely monitored to ensure the appropriate drug properties.^[43]

4.2.2. Ball milling

Ball milling commonly consists of a cylindrical crushing system that is used for size reduction of powders in a wet or dry environment.^[44] The rotating crushing cylinder is filled with ceramic or stainless-steel balls falling on powders to produce a homogenous solid dispersion with enhanced bioavailability and dissolution rate. For powders, the minimum particle size that can be realized with conventional milling is ~2–3 μm , otherwise, wetting conditions are more suitable for scaling down particle size to below these values. Tanaka et al. were able to achieve a 17.1 μm particle size for probucol powder.^[45] Then, using wet-milling with zirconia beads at a rotation speed of 12 ms^{-1} combined with dispersing surfactants such as vitamin E-TPGS, Poloxamer 338, Gelucire®, the probucol particle sizes decreased to 77–176 nm to form a novel drug delivery system known as nanocrystals.

5. Nanocrystal Physical Properties

The micronization approach is not efficient enough for drugs that are highly hydrophobic, which represent 70% of new drug candidates.^[6] Therefore, a way to decrease particles further to the nanometer scale is required. Nanocrystals are an auspicious approach to enhance drug bioavailability by reducing particle size.^[46] Nanocrystal technology can therefore be considered either as an alternative to other solid-state preparation methods, or as a complementary approach for the solid forms presented in Section 3 above, depending on the choice of the nanocrystal production method.

5.1. Impact of particle size on solubility properties

The Kelvin equation [Eq. (1)] can be applied to the nanocrystal dissolution pressure taking into consideration its surface tension in solution. Decreasing the nanocrystal size increases the curvature, hence the dissolution pressure, P_r . As shown in the equation, P_r becomes substantial when the particle size is within the nanometer range:

$$\ln\left(\frac{P_r}{P_\infty}\right) = \left(\frac{4\gamma M}{d_{np}RT\rho}\right) \quad (1)$$

Here P_r and P_∞ are the dissolution pressures of the nanocrystal and an infinitely large nanocrystal, respectively; γ is the surface

tension in Nm^{-1} , M is the molecular weight of the nanoparticles in g mol^{-1} , d_{np} is the particle diameter in m , R is the gas constant in $\text{JK}^{-1}\text{mol}^{-1}$, T is the temperature in Kelvin, and ρ is the nanocrystal density in g m^{-3} .

The saturation solubility is also governed by Ostwald–Freundlich equation [Eq. (2)], which highlights the difference in solubility between different particle sizes. In particular, it implies a greater saturation solubility as the radius of the particle becomes smaller:

$$\log\left(\frac{C_s}{C_\infty}\right) = \frac{4\sigma V}{2.303 \times RT\rho d_{\text{np}}} \quad (2)$$

Here C_s is the saturation solubility, C_∞ is the solubility of a large particle, σ is the interfacial tension, V is the molar volume of the nanocrystal ($\text{m}^3\text{mol}^{-1}$), R is the gas constant ($\text{JK}^{-1}\text{mol}^{-1}$), T is the temperature (K), ρ is the particle density (g m^{-3}), and d_{np} is its diameter (m).

An enhancement in saturation solubility provides a high concentration gradient, fostering permeation and absorption through the gastrointestinal membrane and blood by passive diffusion.^[47]

5.2. Impact of particle size on dissolution rate

The dissolution rate can be determined by the Noyes–Whitney and Prandtl equations [Eqs. (3) and (4), respectively].

$$\frac{dm}{dt} = S\left(\frac{D}{d}\right)(C_s - C_p) \quad (3)$$

Here dm/dt is the dissolution rate ($\text{kg m}^2\text{s}^{-1}$), S defines the surface area of the particle (m^2), D is the coefficient of diffusion (m s^{-1}), d is the thickness of the hydrodynamic boundary layer (m), C_s is the saturation solubility (kg or mol L^{-1}), and C_p is the concentration surrounding the particle (kg or mol L^{-1}).

Notably, the intrinsic dissolution rate is the dissolution rate normalized to the specific surface of the system. Moreover, the size reduction of nanocrystals leads to a decrease in the diffusional distance d , as shown in Figure 3, and thus, according to Equation (3), to a better dissolution of particles.

The diffusional distance d , related to the hydrodynamic boundary layer h , is correlated to the nanoparticle size owing to the Prandtl equation [Eq. (4)].^[48] Bisrat and Nyström used the Prandtl boundary layer equation to clarify the effect of hy-

drodynamic boundary layer thickness h of flowing particles on their dissolution rate. Their research showed that size diminution of solid dispersions in solution under stirring decreases the particle surface in the flow direction, including a decrease in the liquid flow velocity near the nanoparticles.^[48,49]

$$h = c\left(\frac{L}{V}\right)^{1/2} \quad (4)$$

Here, h is the thickness of the hydrodynamic boundary layer, c is a constant parameter, L is the size of the particle surface in the flow direction, V is the velocity of the flowing liquid neighboring the particle.

Liversidge and Cundy revealed that nanocrystallization of danazol improves its saturation solubility and bioavailability properties.^[50] Three formulations—danazol nanocrystals (169 nm) produced by wet milling, a danazol–hydroxypropyl- β -cyclodextrin (HPB) complex, and a conventional microcrystal suspension of danazol (10 μm)—were orally administered at a dose of 3 mg kg^{-1} to fasted beagle dogs. The results showed the following bioavailability values: $82.3 \pm 10.1\%$ for danazol nanocrystals, $106 \pm 12.3\%$ for danazol nanocrystals–HPB complex, and only $5.1 \pm 1.9\%$ for danazol microcrystals, indicating an improvement in nanocrystal uptake relative to the microcrystal suspensions of danazol.^[50] Hecq and co-workers also investigated the dissolution rate of UCB-35440-3 nanocrystals (600 nm) produced by HPH and UCB-35440-3 microcrystals using dialysis bag methods. The results clearly showed an improvement in dissolution rate for the nanocrystal forms: more than 95% of the drug was solubilized after one hour compared with microcrystal forms, for which only 30% of the drug was dissolved over the same period and complete dissolution was not observed for the next 12 hours.^[51] The same results were obtained with fenofibrate nanocrystals relative to microcrystals.^[52]

6. Nanocrystals Production

The methods presented above in Section 4 can also be applied to produce nanocrystals; nevertheless, most of them are rarely used compared to precipitation, HPH, and milling processes.^[53–55] Moreover, each nanocrystal preparation technique is specific for a given active ingredient.

6.1. Precipitation

This process is established on the dropwise addition, under stirring, of a drug solubilized in a given solvent to another one in which the drug is unable to be dissolved. The main drawback of this method is the irreproducibility, as many parameters must be precisely supervised to obtain reproducible results, such as addition rate, temperature, solvent nature, and agitation speed. For this technique the drug must also have specific physicochemical features that fit the protocol to make it successful.^[56] However, an extended-parameter technique gives diverse combinations and makes it possible to study the

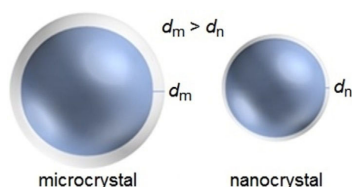


Figure 3. Comparison of the diffusional distance d for micro- (d_m) and nanocrystals (d_n).

impact on the final material in terms of size and morphology. With this bottom-up method, the particles obtained are often smaller than those generated from the top-down approach, in which a drug must be broken into smaller particles using mechanical energy.

6.2. High-pressure homogenization

The three most important technologies for HPH include the microfluidizer method (DD-PTM technology), the piston-gap homogenization method in water (Dissocubes®), and in-water mixture (Nanopure®).^[57] The Dissocubes® tool, engineered by Müller and co-workers at the end of the twentieth century, was a breakthrough technology.^[58] It involves the application of high pressure (up to 400 MPa) to an aqueous solution in which the drug is dispersed, creating a significant shear stress force when the solution passes through a tight gap by means of a homogenizer piston. The range of the gap homogenization covers 5–20 µm and must be chosen according to the viscosity of the solution, and obviously, the process pressure. The decrease in the section from centimeter to micrometer increases the dynamic pressure and decreases the static pressure under the boiling point of the continuous medium at ambient temperature. Gas bubbles are thus formed under pressure, which then burst, generating a high shear force that allows the decrease of particle size in solution.

The use of water as a dispersant solution may hydrolyze water-sensitive drugs and create abundant foam.^[57] Another method that uses the piston-gap homogenizer is Nanopure® technology. This consists of homogenization of the drug dispersed in non-aqueous medium at low temperature (close to 0 °C) and even below its freezing point. The applied pressure is low, preventing cavitation phenomena. The particle size diminution is still acceptable, below 1 µm.^[59,60] Only few studies in synthesizing nanocrystals have been reported using piston-gap homogenization technologies; generally microfluidizer technology is preferred.^[61,62] Microfluidizer technology uses a high-pressure pump that generates pressures up to 250 MPa to narrow the particles in suspension by frontal collision in an interaction chamber, then the final solution is recovered in an outlet reservoir. A high number of cycles (50–100) is recommended in order to effect a sufficient decrease in particle size; this also depends on the hardness of the particle. Indeed, the disadvantage of this method is the high amount of heat released, that may chemically denature the formulation.^[63]

6.3. Ball milling

As introduced in Section 4.2.2 above, ball-milling tools allow one to decrease particle sizes to the micro- and nanometer scales. For nanocrystal formulations, milling times longer than the grinding time necessary for microcrystal preparation may decrease the drug crystallinity due to partial or total amorphization. The latter phenomenon has been reported by Dai et al. for meloxicam nanocrystals.^[64]

7. Nanocrystal Overview

There are many published examples in which precipitation, HPH, and ball-milling methods were used. Even if the definition of a nanocrystal is not well harmonized in the literature, Table 3 shows an overview of the smallest drug nanocrystals manufactured with these technologies using stabilizers. The choice of stabilizer is essential, as it influences nanocrystal size and shape. Once nanocrystal growth is stopped, the stabilizer is strongly bound to the nanocrystal surface, giving it its solubility in a wide range of solvents. Surfactants must be used for both the synthesis of nanocrystals and long-term stability during storage.

7.1. Drug nanocrystals on the market

Drug nanocrystals have been investigated since the 1990s. Currently, there are more nanocrystal formulations on the market than in clinical trials (Tables 4 and 5). In October 2017, Endo Pharmaceuticals achieved a phase 2 clinical trial of Megace ES®, investigating weight gain in HIV-positive patients. Currently, one phase 2 clinical trial is studying the pharmacokinetics of various particle sizes of rilpivirine in healthy adults, despite the fact that no studies have given clear evidence of the crystal nature of rilpivirine in solution.

8. Administration Routes of Primary Nanocrystals

8.1. Oral delivery

As mentioned above, a poorly water-soluble and highly permeable drug can be classified as a BCS class II drug. The low oral bioavailability results in low concentrations of the drug in blood, thus minimizing the odds of addressing the target tissue or organ. Drug absorption in the gastrointestinal tract (GIT), more precisely through the gastrointestinal epithelium, is a challenge if the drug is not dissolved. To address this issue, nanocrystal formulation has beneficial effects on oral drug delivery, such as imparting the same bioequivalence regarding the fed or fasted state.^[175] Moreover, Chen et al. showed that the formulation of schisantherin A (SA) nanocrystals (160 nm), orally administered to rats at 4 mg kg⁻¹, improved its solubility and pharmacokinetic profile. In that case, the concentration of SA nanocrystals accumulated in the plasma was 6.7-fold higher than the SA suspension alone after oral administration.^[176] Another study conducted by Hanafy et al. arrived at a similar conclusion with a formulation of fenofibrate nanocrystals compared with a fenofibrate microsuspension orally administered at 100 mg kg⁻¹ to rats. The fenofibrate nanocrystals showed bioavailability enhancements ($C_{\max} = 222.7 \pm 21.9 \mu\text{g mL}^{-1}$) two-fold than those of the microcrystals suspension ($C_{\max} = 96.9 \pm 62.4 \mu\text{g mL}^{-1}$).^[114] The efficacy of nanocrystal formulations can be explained by better saturation solubility and dissolution rate properties. When drugs are delivered in the nanocrystal form, a significant drug concentration gradient between the GIT and systemic circulation is present, enhancing drug bio-

Table 3. Examples of pharmaceutical drug nanocrystals prepared by common wet ball milling (WBM), anti-solvent precipitation (ASP), high-pressure homogenization (HPH), and spray drying (SD).

Drug	Type	Technology	Stabilizer	Particle size [nm]	Ref.
1,3-Dicyclohexylurea	Anti-ischemic	WBM	Polysorbate 80	800	[65]
Aceclofenac	Anti-inflammatory	ASP	PVP-K30/HPMC-E5/SLS	112–930	[66]
Albendazole	Anthelmintic	HPH	Poloxamer 188	415	[67]
ALS-3	Treatment for amyotrophic lateral sclerosis	WBM/SD	Poloxamer 188/PVPK30/HPMC	300	[68]
Amoitone B	Antitumor	HPH	Mannitol	275 ± 8	[69]
Amphotericin B	Antibiotic	HPH	None	528	[70]
Aprepitant (MK-069)	Anti-nausea/Anti-vomiting	WBM	With surfactant	120	[71]
Aripiprazole	Antipsychotic	ASP	HPMC-E5/Poloxamer 188	450–500	[72]
Ascorbyl palmitate	Antioxidant/Vitamin C derivative	HPH	Sodium dodecyl sulfate (SDS) Polysorbate 80	365 348	[73]
Asulacrine	Antitumor	HPH	Poloxamer 188	133 ± 20	[74]
Avanafil	Erectile dysfunction	ASP	Poloxamer 188/Polysorbate 80	128–4868	[75]
AZ68	Anti-schizophrenia	WBM	PVD/Disodium salt	125 ± 30	[76]
Azithromycin	Antibiotic	HPH	Poloxamer 188/Polysorbate 80/Lecithin	400	[77]
Baicalin	Anxiolytic	HPH	Polysorbate 80/Poloxamer 188/Poloxamer 407/ TPGS	200–500	[78]
Bexarotene	Antineoplastic	ASP/HPH	Poloxamer 188/Lecithin	200	[79]
Breviscapine	Anti-inflammatory	ASP/FD ^(a)	Poly(lactic-co-glycolic acid)	239	[80]
Budesonide	Anti-inflammatory	ASP	Mannitol Poloxamer 188	440 259	[81] [82]
		HPH	Lecithin/Polysorbate 85/Tyloxapol/Cetyl alcohol	599	[83]
			/	75 up to 300	[84]
			/	< 1 μm	[85]
Bupravaquone	Antibiotic	HPH	Poloxamer 188/Lecithin	601	[86]
Camptothecin	Antitumor	WBM	Poloxamer 338	202 ± 30	[87]
		ASP	/	250	[88]
			Polydopamine	80–150	[89]
Candesartan cilexetil	Anti-ischemic	WBM	Poloxamer 338	128	[90]
Celecoxib	Anti-inflammatory	HPH	Polysorbate 80 PVP/SDS	320 360	[91]
Cilostazol	Anti-platelet	WBM	Hydropropyl cellulose/Docusate sodium	260	[92]
		HPH	HPMC (Methocel E15)	500 up to > 1000	[93]
		WBM	Hydropropyl cellulose/Docusate sodium	220	[94]
Cinnarizine	Antiallergic/Antihistaminic	WBM	TPGS TPGS/HPMC	366 ± 12 430 up to < 1000	[95]
Clofazimine	Antibacterial	HPH	Poloxamer 188/Phospholipon/Sodium cholic acid/ Mannitol	650	[96]
			/	420	[97]
Curcumin	Antitumor/Antioxidant	WBM	Polysorbate 80	924	[98]
		ASP/HPH	/	199	[99]
		WBM	Leucine	125	[100]
Cyclosporin	Anti-inflammatory/Immunosuppressant	WBM	Poloxamer 188	213	[101]
		WBM/HPH	Sodium cholate	962	[102]
Danazol	Anti-endometriosis	HPH	Poloxamer 407	300	[103]
		WBM	Polyvinyl pyrrolidone-K25	169	[50]
Darunavir	Anti-HIV	WBM/ES ^(b)	Polysorbate 80/Poloxamer 188/Poloxamer 407/ TPGS	295–1327	[104]

Table 3. (Continued)

Drug	Type	Technology	Stabilizer	Particle size [nm]	Ref.
Dexamethanose	Anti-inflammatory	HPH	Poloxamer F188	930	[105]
		WBM		370	[106]
Diclofenac	Anti-inflammatory	HPH	Poloxamer 188	< 800	[107]
		WBM		279 ± 8	[108]
Docetaxel	Antitumor	HPH	Lecithin/DSPE-PEG2000	204	[109]
			Lecithin/DSPE-PEG2000/DSPE2000-FA	221	
		ASP	Poloxamer 407	383	[110]
Doxorubicin	Anticancer	ASP	DSPE-PEG200	5	[111]
		ASP	PVP K30/Lutrol F127 F128	161–5267	[112]
Fenofibrate	Lowering triglycerides	HPH	Poloxamer 188/PVP K30	356 and 194	[113]
			Vitamin E/TPGS	340	[114]
		ASP	Polysorbate 80/Polyethylene glycol/PVP K30/Tragacanth	> 1000	[115]
			Hydrogel	200–400	[116]
Glibenclamide	Antidiabetic	ASP	Poloxamer 188	429	[117]
		WBM	Tocopherol polyethylene glycol 1000 succinate	256 ± 1	[118]
Hesperetin	Antitumor	HPH	Polysorbate 80	346 ± 30	[119]
			Poloxamer 188	301 ± 17	
			Plantacare 2000	304 ± 30	
			Inutec SP1	304 ± 40	
		WBM/HPH	Polyethylene glycol 30	200	[120]
HPPH	Antitumor	ASP	/	100 ± 20	[121]
Hydrocamptothecin	Antitumor	PJ ^(d)	Fetal calf serum	168 ± 3	[122]
		HPH	Lipoid S75/Poloxamer 188	283 ± 5	[123]
			Lipoid S75 + Soluto [®]	316 ± 13	
			Poloxamer 188	345 ± 17	
			Lipoid S75	365 ± 3	
Hydrocortisone	Anti-inflammatory	WBM	PVP/HMPC/Polysorbate 80	295 ± 32	[124]
		HPH	Poloxamer 338	539	[125]
Ibuprofen	Anti-inflammatory	ME ^(d)	Polysorbate 80	175	[126]
Indomethacin	Anti-inflammatory	HPH	Polyvinyl pyrrolidone-K25	80 ± 10	[127]
			Poloxamer 407	170 ± 30	
		WBM	Poloxamer 188	970 ± 30	[128]
Itraconazole	Antifungal	WBM	Poloxamer 407	550 ± 20	[128]
			Poloxamer 338	128	[90]
		HPH	Polysorbate 20	677 ± 53	[129]
		SP ^(d)	Polysorbate 80/Poloxamer 407	200 up to 1000	[130]
		ASP	Poloxamer 407	267	[131]
Ketoconazole	Antifungal	WBM	Poloxamer 188/PVP K-30/Hydroxypropyl methylcellulose	164	[132]
			Hydroxypropylcellulose/TPGS	147	[133]
Ketoprofen	Anti-inflammatory	WBM	SDS	265	[134]
Loviride	Antiviral	WBM	Polysorbate 80/Poloxamer 188	156	[135]
			Tocopherol polyethylene glycol 1000 succinate	156 ± 2	[118]
Lutein	Prevention of age-related macular degeneration	ASP	SDS/Soy phosphatidylcholine	377	[136]
Mebendazole	Anthelmintic	WBM	Tocopherol polyethylene glycol 1000 succinate	190 ± 2	[118]

Table 3. (Continued)

Drug	Type	Technology	Stabilizer	Particle size [nm]	Ref.	
Mefenamic	Anti-inflammatory	ASP	Hydroxypropylcellulose DOSS	106	[137]	
				312	[138]	
Meloxicam	Anti-inflammatory	ASP	Polysorbate 80/Poloxamer 188/Poloxamer 407	180	[139]	
Methyltryptophan	Tryptophan-catabolizing enzyme inhibitor	ASP	Poloxamer 188/TGPS	150 up to 1400	[140]	
Miconazole	Antifungal	WBM	Poloxamer 188/Poloxamer 407	355	[141]	
Monosodium urate	Immune regulator	ASP	DMEM 10%	26–137	[142]	
MTKi-327	Antitumor	WBM	Poloxamer 338/Lipoid S75/Glucose	195 ± 6	[143]	
Naproxen	Anti-inflammatory	WBM	Chitosan	250 ± 60	[144]	
			Poloxamer 188	270	[145]	
			TPGS/HPMC	370 ± 60	[95]	
Nimodipine	Anti-inflammatory/Anti-ischemic	HPH	Poloxamer 188/Sodium cholic acid/Mannitol	650	[146]	
			Mannitol/Maltose	159/503/833	[147]	
Nisoldipine	Calcium channel blocker	WBM/JM ^(f)	PVP-K30/HPMC-E5/SDS	240–1227	[148]	
Olmesartan medoxomil	Angiotensin II receptor antagonist	ASP/HPH	TPGS/Polysorbate 80	140	[149]	
Omeprazole	Anti-inflammatory	HPH	Poloxamer 188	500	[150]	
Oridonin	Antitumor	HPH	Polyvinyl pyrrolidone-K25/Lecithin	913	[151]	
			Poloxamer 188	897 ± 14	[152]	
			Poloxamer 188/Lecithin	103 ± 2	[153]	
Paclitaxel	Antitumor	ASP	Transferrin	303	[154]	
			Polysorbate 80	5	[155]	
			Poloxamer 407/DOSS	194	[156]	
			Poloxamer 407	150 up to 200	[157]	
			Cyclodextrin	263	[140]	
			Poloxamer 127	200	[158]	
			3PNET ^(g)	TPGS	150	[159]
			Poloxamer 407	122	[160]	
			HPH	DOTAP	160 ± 10	[161]
			EPAS ^(h)	TPGS	135	[162]
			WBM	Chitosan	330 ± 90	[144]
Poloxamer 407	279	[87]				
PIK-75	Antitumor	HPH	Poloxamer 188 (nontargeted)	182	[163]	
			Poloxamer 188-folic acid (targeted)	161		
Piposulfan	Antineoplastic	WBM	Polysorbate 80	210 ± 38	[105]	
Prednisolone	Anti-inflammatory	HPH	Poloxamer 188	211	[105]	
Pueranin	Antitumor	HPH	Lecithin/HPMC	481 ± 23	[164]	
PX-18	Neuroprotectant	HPH	Polysorbate 80	40–980	[165]	
Resveratrol	Antioxidant	HPH	Polysorbate 80	203 ± 20	[166]	
			Poloxamer 188	153 ± 40		
			Plantacare 2000	169 ± 20		
			Inutec SP1	216 ± 30		
			WBM	Poloxamer 188	304 ± 3	[167]
			Polysorbate 80	225 ± 35		
Riccardin	Antitumor	EPAS ^(h)	Poloxamer 188/PVPK30/HPMC	184	[168]	
			Poloxamer 188/PVPK30/HPMC	815		
RMKK98	Anti-inflammatory	HPH	Poloxamer 188/Polysorbate 80/Sodium cholate	913	[169]	
RMKP22	Antitumor	HPH	Polysorbate 80/Glycerol	502	[58]	
Rutin	Antioxidant/Anti-inflammatory	HPH	Polysorbate 80/Poloxamer 188	721	[170]	
Silybin	Antitumor	HPH	Lecithin/Poloxamer 188	127 up to 642	[164]	
Simvastatin	Lowering cholesterol	HPH	Polyvinyl pyrrolidone-K25	360 ± 30	[127]	
			Poloxamer 407	1140 ± 6		

Table 3. (Continued)

Drug	Type	Technology	Stabilizer	Particle size [nm]	Ref.
Spironolactone	Treatment of fluid retention	HPH	Polysorbate 80/Water	400	[171]
Tarazepide	Antiplasmodial	HPH	Poloxamer 188/Polysorbate 80	400	[172]
UCB-35440-3	Antiallergenic/Anti-asthma	HPH	HPMC (Methocel E15) Polyvinyl alcohol Acacia gum Poloxamer 407	182 ± 7 262 ± 54 407 ± 6 183 ± 3	[51]
UG558	/	WBM	HPMC (Methocel E15)	190	[173]
Ziprasidone	Antipsychotic	WBM	Poloxamer 407	200–1000	[174]

[a] Freeze-drying. [b] Electrospraying. [c] Precipitation ultrasonication. [d] Melt-emulsification. [e] Spray freezing. [f] Jet milling. [g] Three-phase nanoparticle engineering technology. [h] Evaporative precipitation into aqueous solution.

Table 4. List of marketed nanocrystals.

Trade name	Drug	Indication	Form	Route	Company	FDA approval
Emend®	Aprepitant	Anti-emetic	Pellets	Oral	Merck	2003
Invega Sustenna®	Paliperidone palmitate	Antipsychotic	Suspension	i.v.	Janssen	2009
Megace ES®	Megestrol	Anti-anorexic	Suspension	Oral	Par Pharmaceutical Companies	2005
Tricor®	Fenofibrate	Hypercholesterolemia	Pellets	Oral	Abbott	2004
Triglide®	Fenofibrate	Hypercholesterolemia	Pellets	Oral	Sciele Pharma Inc.	2005
Rapamune®	Rapamycin	Immunosuppressant	Pellets	Oral	Wyeth	2000

Table 5. List of nanocrystal formulations in clinical trials.

Drug	Studies / [Status]	Company	Route	Phase
Rilpivirine	Pharmacokinetics of various particle diameters after administration of long-acting parenteral formulation / [Ongoing]	Janssen R&D	Intramuscular	1
Megestrol/Megace ES®	Weight gain in HIV-positive patients with weight loss associated with AIDS-related wasting (anorexia/cachexia) / [Completed 2017]	Endo Pharmaceuticals	Oral	2

availability in the bloodstream (Figure 4). This explains, for instance, why the dose of fenofibrate can be decreased by 18% in marketed tablets of nanocrystals for the same bioequivalence of micronized fenofibrate.^[57,177]

In addition to the capacity of nanocrystals to cross the gastrointestinal epithelium, other research has shown that the enhanced bioavailability of nanocrystals comes from inhibition of P-glycoprotein (P-gp) in the apical membrane.^[178,179] More precisely, P-gp-mediated efflux is decreased by surfactants in the nanocrystal formulations. P-gp-driven efflux across the apical membrane can disrupt the rate and amount of drug traversing the basolateral membrane and into the bloodstream. Apte highlighted some common surfactants that impact P-gp-mediated efflux and thus drug uptake; surfactants with an optimal hydrophilic/lipophilic balance give better P-gp inhibition than surfactants that are hydrophobic.^[180] For drug nanocrystals, studies are still required to determine the uptake pathway and the main properties that affect it. However, many studies have been carried out on metallic nanoparticles to understand the

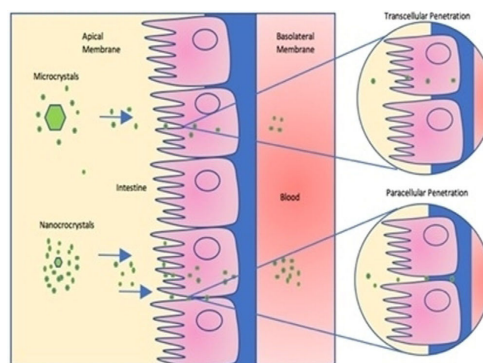


Figure 4. Nanocrystals induce a higher drug concentration gradient in blood vessels than microcrystals, leading better absorption of the active pharmaceutical ingredient.

impact of particle size on intestinal epithelial cell internalization.^[181–183]

8.2. Parenteral delivery

Intravenous injection is recommended when a drug is not absorbed by the digestive tract or when disease treatments require i.v. delivery, such as chemotherapy. In oncology, i.v. administration is preferred when oral forms present unpredictable bioavailability or side effects, and also in the case of targeted therapies.^[184] Additionally, the effectiveness of self-administered chemotherapy drugs depends highly on patient compliance.^[185] Given their nanoscale properties, crystal nanoparticles are suitable for parenteral (e.g., intramuscular, transdermal, intravenous), enteral, pulmonary, ocular, and transdermal administration with faster pharmaceutical effect. Indeed, one of the other advantages of nanocrystal-based drug formulations is that they can be delivered regardless of administration route, as they are much smaller than the smallest blood vessel diameter in humans.

Regarding the i.v. route, the carrier system will not have to pass through the gastrointestinal barrier resulting in higher bioavailability and reduced dosing. Moreover, i.v. nanocrystal delivery does not require excess excipient, which can be harmful to the patient. For cases in which drug nanocrystals are highly soluble in plasma, they can disband before hitting the target; thus the nanosuspension will mainly show a solution-like behavior.^[186] Otherwise, whether the nanocrystalline suspension remains poorly soluble, biodistribution following i.v. injection will be mainly governed by particle shape, size, and surface properties.

9. Targeted Delivery for Cancer Therapy

A principal issue associated with nanocrystal drug delivery is difficulty in reaching the target site without increasing nonspecific toxicity. Because the body is composed of sequential barriers, it is easy to understand how drug accumulation is not optimal to the target site, causing unwanted biodistribution to healthy tissues. To address this issue, parameters such as size, shape, and surface functionalization must be accurately managed.

9.1. Passive delivery

It has been observed that non-functionalized nanoparticles in the bloodstream cleared rapidly, as they are taken up by the liver, lungs, spleen, and kidneys. For healthy tissues, the intercellular junctions of the vascular endothelium are tight, which prevents nanoparticles from entering. In contrast, when tumor tissues develop, an inflammatory reaction occurs which is characterized by an increase in vascular permeability. This dilation of the endothelium allows nanoparticles to pass through and reach cancer tissues by diffusion (Figure 5). This passive targeting effect, otherwise known as the enhanced permeability and retention (EPR) effect, was initially proposed by Maeda and et al. in 2000.^[187]

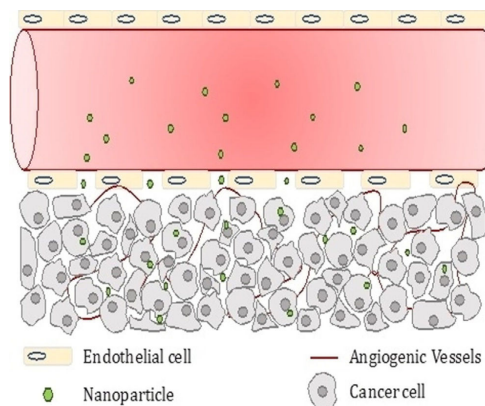


Figure 5. Illustration of the EPR effect: nanoparticles can shed out into tumor tissue via endothelial cell junctions.

Studies by Hollis et al. compared the EPR effect between solubilized and nanocrystal formulations of paclitaxel (PTX) using human HT-29 colon cancer xenografts in mice, and found that PTX nanocrystals were as effective as the conventional solubilized formulation, but with decreased toxic effects.^[188] This result supports nanocrystal formulation as a promising approach for cancer therapies.

However, it has been observed that once administered intravenously, nanoparticles gather essentially in the tissues of the reticuloendothelial system (liver and spleen). This observation can be explained by the large specific surface area of nanoparticles on which many plasma proteins, especially opsonins, can adhere. The formation of the protein corona surrounding nanoparticles relies on size, shape, crystallinity, surface instability, hydrophobicity, and electronic states.^[189] Following protein adsorption, nanoparticles are selectively recognized by macrophages, then internalized and carried to phagosomes and fused with lysosomes.^[190] Therefore, a balance between all these parameters is crucial to increase nanoparticle lifespan in the bloodstream to foster the EPR effect.

Another way to overcome recognition by the mononuclear phagocyte system is to functionalize the nanoparticle surface to repel these opsonins. Hence, there will be both a selective targeting effect as well as an accumulation in the tumor tissues due to the EPR effect.

9.2. Active delivery

Today, new nanoparticle formulations incorporate the approach of active targeting, which increases the specificity for a given site. This strategy involves functionalizing the nanoparticle surface with polymers, proteins, peptides, etc., which can be specifically recognized by receptors present on cancer cells.

To understand the impact of such functionalized nanocrystals, Park et al. compared the ability of PTX-coated nanocrystals with a conventional albumin-based PTX formulation (known as

Abraxane®) to treat B16F10 melanoma in mice. They showed that PTX nanocrystals with and without albumin have higher antitumor efficacy than Abraxane® at the same dose.^[157] The use of proteins as stabilizers is an encouraging approach, given their added capacity to attach to membrane proteins on tumor cells.^[191]

Likewise, nanocrystals coated with selective surfactants or polymers, such as sodium dodecyl sulfate, hydroxypropylmethyl cellulose, or polyvidone are valuable for improving oral bioavailability, and such surfactants offer steric hindrance, preventing nanocrystal aggregation and growth.^[192,193] In another study, the surfaces of docetaxel (DTX) nanocrystals were modified with poly(ethylene glycol) (PEG) (pLNS-DTX) and folic acid (tLNS-DTX). Wang and co-workers demonstrated that the cytotoxicity of tLNS-DTX against B16 cells (folate receptor positive) was more efficient than pLNS-DTX, inferring that nanocrystal surface modification is essential to specifically deliver a drug.^[109] Tuomela and co-workers investigated the selection of suitable stabilizers, their stabilizing effect, their role in final formulations, and difficulties in achieving *in vitro* and *in vivo* delivery. Their study presented some nanocrystal-API/stabilizer association cases, and also looked into the stabilizer outcomes for higher drug bioavailability.^[194]

10. Conclusions

Solubility enhancement of poorly water-soluble drugs is a major challenge in the pharmaceutical field, as 70% of drugs exhibit low solubility. Modulation of the solid state of pharmaceutical ingredients as function of intermolecular interactions (e.g., co-crystallization, polymorphism), chemical modification (e.g., solvatomorphism, salt formation), or physical modification (e.g., amorphization, particle size reduction) has afforded many opportunities to enhance the bioavailability of some APIs. For a decade, research into nanocrystal preparations for drug delivery has driven significant growth in the pharmaceutical field, as it offers several advantages and value. Nanocrystal formulation is one of the recent techniques developed to improve dissolution rate, solubility, and therefore the bioavailability of active ingredients, while increasing drug-loading capacity. Moreover, nanocrystal formulations can be administered through all routes—pulmonary, ocular, transdermal, enteral and parenteral—and provide better performance in terms of safety, targeting efficiency, pharmacodynamics, and pharmacokinetics than any other drug formulations. One of the main drawbacks of nanomedicines is their persistence in the human body, fostering the risk of toxicity. The outlook regarding the development of nanocrystals should focus on such undesirable toxicity, which could be avoided by improvements in targeted delivery and clearance from the body. To do so, functionalized nanocarriers may be conceptualized for nanocrystal encapsulation. This would allow prevention of systemic administration of the API by targeting the diseased tissues. Thus, the drug would be released with a faster dissolution profile only after opening of the nanocarrier is triggered. Furthermore, by combining crystallization techniques at the nanoscale level to different solid-state organizations described in this review, we

may drastically improve the bioavailability of APIs for optimized targeted delivery.

Conflict of interest

The authors declare no conflict of interest.

Keywords: dissolution · drug solid state · nanosizing · pharmacokinetics · solubility

- [1] *Polymorphism in Pharmaceutical Solids* (Ed.: H. G. Brittain), Informa Healthcare USA, 1999.
- [2] J. Aaltonen, M. Allesø, S. Mirza, V. Koradia, K. C. Gordon, J. Rantanen, *Eur. J. Pharm. Biopharm.* **2009**, *71*, 23–37.
- [3] Y. Kawabata, K. Wada, M. Nakatani, S. Yamada, S. Onoue, *Int. J. Pharm.* **2011**, *420*, 1–10.
- [4] C. C. Chan, K. Chow, B. McKay, M. Fung, *Ther. Deliv. Solut.* **2014**, 1–410.
- [5] M. L. Hart, D. P. Do, R. A. Ansari, S. A. A. Rizvi, *J. Develop. Drugs* **2013**, *2*, 1000115/1–1000115/7.
- [6] P. Khadka, J. Ro, H. Kim, I. Kim, J. T. Kim, H. Kim, J. M. Cho, G. Yun, J. Lee, *Asian J. Pharm. Sci.* **2014**, *9*, 304–316.
- [7] G. L. Amidon, H. Lennernäs, V. P. Shah, J. R. Crison, *Pharm. Res.* **1995**, *12*, 413–420.
- [8] *Dissolution Testing and Acceptance Criteria for Immediate-Release Solid Oral Dosage Form Drug Products Containing High Solubility Drug Substances: Guidance for Industry*, US Department of Health and Human Services, Food and Drug Administration, Center for Drug Evaluation and Research (CDER), August 2018, Part III.B, p. 3; <https://www.fda.gov/downloads/Drugs/Guidances/UCM456594.pdf>.
- [9] S. Qi, S. Roser, K. J. Edler, C. Pigliacelli, M. Rogerson, I. Weuts, F. Van Dyck, S. Stokbroek, *Pharm. Res.* **2013**, *30*, 290–302.
- [10] M. Rekdal, A. Pai, B. S. Muddukrishna, *Data Brief* **2018**, *16*, 135–140.
- [11] M. Lindenberg, S. Kopp, J. B. Dressman, *Eur. J. Pharm. Biopharm.* **2004**, *58*, 265–278.
- [12] H. L. Lee, J. M. Vasoya, M. De Lima Cirqueira, K. L. Yeh, T. Lee, A. T. M. Serajuddin, *Mol. Pharm.* **2017**, *14*, 1278–1291.
- [13] "Polymorphism", W. McCrone in *Physics and Chemistry of the Organic Solid State*, John Wiley & Sons, New York, 1965.
- [14] P. P. Lamy, S. Rosenstein, *J. Hosp. Pharm.* **1969**, *26*, 598–601.
- [15] Y. Corvis, P. Négrier, S. Massip, J. M. Leger, P. Espeau, *CrystEngComm* **2012**, *14*, 7055–7064.
- [16] Y. Corvis, A. Wurm, C. Schick, P. Espeau, *CrystEngComm* **2015**, *17*, 5357–5359.
- [17] E. H. Lee, *Asian J. Pharm. Sci.* **2014**, *9*, 163–175.
- [18] D. Singhal, W. Curatolo, *Adv. Drug Delivery Rev.* **2004**, *56*, 335–347.
- [19] N. El Moussaoui, A. Bendriss, *Int. J. Eng. Res. Technol.* **2014**, *3*, 2243–2246.
- [20] K. Raza, P. Kumar, S. Ratan, R. Malik, S. Arora, *SOJ Pharm. Pharm. Sci.* **2014**, DOI: <https://doi.org/10.15226/2374-6866/1/2/00111>.
- [21] "Polymorphism—A Critical Consideration in Pharmaceutical Development, Manufacturing, and Stability", J. F. Bauer, *Pharmaceutical Solids, Journal of Validation Technology*, **2008**, pp. 15–23; <http://cmbe.engr.uga.edu/bche4520/Other/Ch9/Bauer%202008.pdf>.
- [22] K. T. Savjani, A. K. Gajjar, J. K. Savjani, *ISRN Pharm.* **2012**, *2012*, 195727.
- [23] A. M. Healy, Z. A. Worku, D. Kumar, A. M. Madi, *Adv. Drug Delivery Rev.* **2017**, *117*, 25–46.
- [24] P. H. Karpinski, *Chem. Eng. Technol.* **2006**, *29*, 233–237.
- [25] "Crystallization", A. J. Hickey, S. Giovagnoli in *Pharmaceutical Powder and Particles*, Springer, Berlin, **2018**.
- [26] R. Rotival, P. Espeau, Y. Corvis, F. Guyon, B. Do, *J. Pharm. Sci.* **2011**, *100*, 3223–3232.
- [27] R. Gandhi, O. Pillai, R. Thilagavathi, B. Gopalakrishnan, C. L. Kaul, R. Panchagnula, *Eur. J. Pharm. Sci.* **2002**, *16*, 175–184.
- [28] A. K. Salameh, L. S. Taylor, *J. Pharm. Sci.* **2006**, *95*, 446–461.
- [29] A. Jamaludin, M. Mohamad, V. Navaratnam, K. Selliah, S. C. Tan, W. H. Wernsdorfer, K. H. Yuen, *Br. J. Clin. Pharmacol.* **1988**, *261*–263.
- [30] W. Jones, W. D. S. Motherwell, A. V. Trask, *MRS Bull.* **2006**, *31*, 875–879.

- [31] Y. Corvis, P. Négrier, M. Lazerges, S. Massip, J. M. Léger, P. Espeau, *J. Phys. Chem. B* **2010**, *114*, 5420–5426.
- [32] K. L. Yeh, T. Lee, *Cryst. Growth Des.* **2018**, *18*, 1339–1349.
- [33] K. V. Drozd, A. N. Manin, A. V. Churakov, G. L. Perlovich, *Eur. J. Pharm. Sci.* **2017**, *99*, 228–239.
- [34] C. Grossjohann, K. S. Eccles, A. R. Maguire, S. E. Lawrence, L. Tajber, O. I. Corrigan, A. M. Healy, *Int. J. Pharm.* **2012**, *422*, 24–32.
- [35] B. C. Hancock, M. Parks, *Pharm. Res.* **2000**, *17*, 397–404.
- [36] W. Yang, K. P. Johnston, R. O. Williams, *Eur. J. Pharm. Biopharm.* **2010**, *75*, 33–41.
- [37] M. Vasanthavada, W. Q. Tong, Y. Joshi, M. S. Kislalioglu, *Pharm. Res.* **2004**, *21*, 1598–1606.
- [38] N. Wyttenbach, M. Kuentz, *Eur. J. Pharm. Biopharm.* **2017**, *112*, 204–208.
- [39] R. Vehrings, *Pharm. Res.* **2008**, *25*, 999–1022.
- [40] M. A. Repka, S. Bandari, V. R. Kallakunta, A. Q. Vo, H. McFall, M. B. Pimparade, A. M. Bhagurkar, *Int. J. Pharm.* **2018**, *535*, 68–85.
- [41] G. Nireesha, L. Divya, C. Sowmya, N. Venkateshan, M. Niranjana Babu, V. Lavakumar, *Intl. J. Novel Trends Pharm. Sci. (JNTPS)* **2013**, *3*, 87–98.
- [42] J. Sun, F. Wang, Y. Sui, Z. She, W. Zhai, C. Wang, Y. Deng, *Int. J. Nanomed.* **2012**, *7*, 5733–5744.
- [43] M. Djokić, J. Djurić, L. Solomon, K. Kachrimanis, Z. Djurić, S. Ibrić, *Chem. Eng. Res. Des.* **2014**, *92*, 500–508.
- [44] D. Kumar, Z. A. Worku, Y. Gao, V. K. Kamaraju, B. Glennon, R. P. Babu, A. M. Healy, *Powder Technol.* **2018**, *330*, 228–238.
- [45] Y. Tanaka, M. Inkyo, R. Yumoto, J. Nagai, M. Takano, S. Nagata, *Drug Dev. Ind. Pharm.* **2012**, *38*, 1015–1023.
- [46] S. Kalepu, V. Nekkanti, *Acta Pharm. Sin. B* **2015**, *5*, 442–453.
- [47] V. B. Junyaprasert, B. Morakul, *Asian J. Pharm. Sci.* **2015**, *10*, 13–23.
- [48] P. J. Niebergall, G. Milosovich, J. E. Goyan, *J. Pharm. Sci.* **1963**, *52*, 236–241.
- [49] M. Bisrat, C. Nyström, *Int. J. Pharm.* **1988**, *47*, 223–231.
- [50] G. G. Liversidge, K. C. Cundy, *Int. J. Pharm.* **1995**, *125*, 91–97.
- [51] J. Hecca, M. Deleers, D. Fanara, H. Vranckx, P. Boulanger, S. Le Lamer, K. Amighi, *Eur. J. Pharm. Biopharm.* **2006**, *64*, 360–368.
- [52] B. Zuo, Y. Sun, H. Li, X. Liu, Y. Zhai, J. Sun, Z. He, *Int. J. Pharm.* **2013**, *455*, 267–275.
- [53] S. K. Singh, K. K. Srinivasan, K. Gowthamarajan, D. S. Singare, D. Prakash, N. B. Gaikwad, *Eur. J. Pharm. Biopharm.* **2011**, *78*, 441–446.
- [54] T. Liu, G. Yao, X. Zhang, X. Zuo, L. Wang, H. Yin, J. P. Möschwitzer, *AAPS PharmSciTech* **2018**, *19*, 783–791.
- [55] M. Guo, Y. Dong, Y. Wang, M. Ma, Z. He, Q. Fu, *Powder Technol.* **2018**, DOI: <https://doi.org/10.1016/j.powtec.2018.08.018>.
- [56] R. H. Müller, S. Gohla, C. M. Keck, *Eur. J. Pharm. Biopharm.* **2011**, *78*, 1–9.
- [57] J. U. Junghanns, R. H. Müller, *Int. J. Nanomed.* **2008**, *3*, 295–309.
- [58] M. J. Grau, O. Kayser, R. H. Müller, *Int. J. Pharm.* **2000**, *196*, 155–159.
- [59] N. Bushrab, R. Müller, *New Drugs* **2003**, *5*, 20–22.
- [60] Y. Agrawal, V. Patel, *J. Adv. Pharm. Technol. Res.* **2011**, *2*, 81.
- [61] J. P. Möschwitzer, R. H. Müller, *Drug Dev. Ind. Pharm.* **2013**, *39*, 762–769.
- [62] C. Keck (PharmaSol GmbH), US Pat. No. US20130095198 A1, **2013**.
- [63] Y. Lu, Y. Li, W. Wu, *Acta Pharm. Sin. B* **2016**, *6*, 106–113.
- [64] L. Dai, C. Li, J. Zhang, F. Cheng, *Carbohydr. Polym.* **2018**, *180*, 122–127.
- [65] P.-C. Chiang, Y. Ran, K.-J. Chou, Y. Cui, H. Wong, *Nanoscale Res. Lett.* **2011**, *6*, 413.
- [66] H. Rahim, A. Sadiq, S. Khan, M. A. Khan, S. M. H. Shah, Z. Hussain, R. Ullah, A. A. Shahat, K. Ibrahim, *Drug Des. Dev. Ther.* **2017**, *11*, 2443–2452.
- [67] A. J. Paredes, N. Litterio, A. Dib, D. A. Allemanni, C. Lanusse, S. S. Bruni, S. D. Palma, *J. Pharm. Pharmacol.* **2018**, *70*, 51–58.
- [68] Y. Hou, J. Shao, Q. Fu, J. Li, J. Sun, Z. He, *Int. J. Pharm.* **2017**, *516*, 372–379.
- [69] L. Hao, J. Luan, D. Zhang, C. Li, H. Guo, L. Qi, X. Liu, T. Li, Q. Zhang, *Colloids Surf. B* **2014**, *117*, 258–266.
- [70] O. Kayser, C. Olbrich, V. Yardley, A. F. Kiderlen, S. L. Croft, *Int. J. Pharm.* **2003**, *254*, 73–75.
- [71] Y. Wu, A. Loper, E. Landis, L. Hettrick, L. Novak, K. Lynn, C. Chen, K. Thompson, R. Higgins, U. Batra, et al., *Int. J. Pharm.* **2004**, *285*, 135–146.
- [72] B. E. Al-Dhubiab, *J. Nanosci. Nanotechnol.* **2017**, *17*, 2345–2352.
- [73] V. Teeranachaideekul, V. B. Junyaprasert, E. B. Souto, R. H. Müller, *Int. J. Pharm.* **2008**, *354*, 227–234.
- [74] S. Ganta, J. W. Paxton, B. C. Baguley, S. Garg, *Int. J. Pharm.* **2009**, *367*, 179–186.
- [75] K. A. B. Soliman, H. K. Ibrahim, M. M. Ghorab, *Int. J. Pharm.* **2017**, *517*, 148–156.
- [76] K. Sigfridsson, S. Forsén, P. Hölländer, U. Skantzé, J. de Verdier, *Eur. J. Pharm. Biopharm.* **2007**, *67*, 540–547.
- [77] D. Zhang, T. Tan, L. Gao, W. Zhao, P. Wang, *Drug Dev. Ind. Pharm.* **2007**, *33*, 569–575.
- [78] Y. Liu, Y. Ma, J. Xu, Y. Chen, J. Xie, P. Yue, Q. Zheng, M. Yang, *Colloids Surf. B* **2017**, *160*, 619–627.
- [79] Y. Wang, J. Rong, J. Zhang, Y. Liu, X. Meng, H. Guo, H. Liu, L. Chen, *Drug Dev. Ind. Pharm.* **2017**, *43*, 132–141.
- [80] H. Wang, G. Zhang, X. Ma, Y. Liu, J. Feng, K. Park, W. Wang, *Eur. J. Pharm. Biopharm.* **2017**, *115*, 177–185.
- [81] J. Hu, Y. Dong, W. K. Ng, G. Pastorin, *Adv. Powder Technol.* **2018**, *29*, 957–963.
- [82] T. Liu, M. Han, F. Tian, D. Cun, J. Rantanen, M. Yang, *Carbohydr. Polym.* **2018**, *181*, 1143–1152.
- [83] C. Jacobs, R. H. Müller, *Pharm. Res.* **2002**, *19*, 189–194.
- [84] W. K. Kraft, B. Steiger, D. Beussink, J. N. Quiring, N. Fitzgerald, H. E. Greenberg, S. A. Waldman, *J. Clin. Pharmacol.* **2004**, *44*, 67–72.
- [85] S. B. Shrewsbury, A. P. Bosco, P. S. Uster, *Int. J. Pharm.* **2009**, *365*, 12–17.
- [86] C. Jacobs, O. Kayser, R. H. Müller, *Int. J. Pharm.* **2001**, *214*, 3–7.
- [87] E. Merisko-Liversidge, P. Sarpotdar, J. Bruno, S. Hajj, L. Wei, N. Peltier, J. Rake, J. M. Shaw, S. Pugh, L. Polin, et al., *Pharm. Res.* **1996**, *13*, 272–278.
- [88] H. Zhang, X. Wang, W. Dai, R. A. Gemeinhart, Q. Zhang, T. Li, *Mol. Pharm.* **2014**, *11*, 226–233.
- [89] H. Zhan, T. Jagtiani, J. F. Liang, *Eur. J. Pharm. Biopharm.* **2017**, *114*, 221–229.
- [90] J. Beirowski, S. Inghelbrecht, A. Arien, H. Gieseler, *J. Pharm. Sci.* **2011**, *100*, 1958–1968.
- [91] A. Dolenc, J. Kristl, S. Baumgartner, O. Planinšek, *Int. J. Pharm.* **2009**, *376*, 204–212.
- [92] J. I. Jinno, N. Kamada, M. Miyake, K. Yamada, T. Mukai, M. Odomi, H. Toghuchi, G. G. Liversidge, K. Higaki, T. Kimura, *J. Controlled Release* **2008**, *130*, 29–37.
- [93] X. Miao, C. Sun, T. Jiang, L. Zheng, T. Wang, S. Wang, *J. Pharm. Pharm. Sci.* **2011**, *14*, 196–214.
- [94] J. I. Jinno, N. Kamada, M. Miyake, K. Yamada, T. Mukai, M. Odomi, H. Toghuchi, G. G. Liversidge, K. Higaki, T. Kimura, *J. Controlled Release* **2006**, *111*, 56–64.
- [95] P. Kayaert, M. Anné, G. Van Den Mooter, *J. Pharm. Pharmacol.* **2011**, *63*, 1446–1453.
- [96] K. Peters, S. Leitzke, J. E. Diederichs, K. Borner, H. Hahn, R. H. Müller, S. Ehlers, *J. Antimicrob. Chemother.* **2000**, *45*, 77–83.
- [97] K. Borner, H. Hartwig, S. Leitzke, H. Hahn, R. H. Müller, S. Ehlers, *Int. J. Antimicrob. Agents* **1999**, *11*, 75–79.
- [98] L. Hu, D. Kong, Q. Hu, N. Gao, S. Pang, *Nanoscale Res. Lett.* **2015**, *10*, 381.
- [99] A. Rajasekar, T. Devasena, *J. Nanosci. Nanotechnol.* **2015**, *15*, 4119–4125.
- [100] X. Hu, F. F. Yang, X. L. Wei, G. Y. Yao, C. Y. Liu, Y. Zheng, Y. H. Liao, *J. Biomed. Nanotechnol.* **2017**, *13*, 99–109.
- [101] M. Nakarani, P. Patel, J. Patel, P. Patel, R. S. R. Murthy, S. S. Vaghani, *Sci. Pharm.* **2010**, *78*, 345–361.
- [102] R. H. Müller, S. Runge, V. Ravelli, W. Mehnert, A. F. Thünemann, E. B. Souto, *Int. J. Pharm.* **2006**, *317*, 82–89.
- [103] M. T. Crisp, C. J. Tucker, T. L. Rogers, R. O. Williams, K. P. Johnston, *J. Controlled Release* **2007**, *117*, 351–359.
- [104] D. N. Nguyen, C. Clasen, G. Van den Mooter, *Eur. J. Pharm. Biopharm.* **2017**, *113*, 50–59.
- [105] M. A. Kassem, A. A. Abdel Rahman, M. M. Ghorab, M. B. Ahmed, R. M. Khalil, *Int. J. Pharm.* **2007**, *340*, 126–133.
- [106] P. Maudens, C. A. Seemayer, F. Pfefferlé, O. Jordan, E. Allémann, *J. Controlled Release* **2018**, *276*, 102–112.
- [107] F. Lai, C. Sinico, G. Ennas, F. Marongiu, G. Marongiu, A. M. Fadda, *Int. J. Pharm.* **2009**, *373*, 124–132.

- [108] R. Pireddu, C. Caddeo, D. Valenti, F. Marongiu, A. Scano, G. Ennas, F. Lai, A. M. Fadda, C. Sinico, *Colloids Surf. B* **2016**, *143*, 64–70.
- [109] L. Wang, M. Li, N. Zhang, *Int. J. Nanomed.* **2012**, *7*, 3281–3294.
- [110] S. F. Gad, J. Park, J. E. Park, G. N. Fetih, S. S. Tous, W. Lee, Y. Yeo, *Mol. Pharm.* **2018**, *15*, 871–881.
- [111] X. Wang, Y. Ma, H. Chen, X. Wu, H. Qian, X. Yang, Z. Zha, *Colloids Surf. B* **2017**, *152*, 449–458.
- [112] G. J. Sartori, L. D. Prado, H. V. A. Rocha, *AAPS PharmSciTech* **2017**, *18*, 3011–3020.
- [113] X. Li, L. Gu, Y. Xu, Y. Wang, *Drug Dev. Ind. Pharm.* **2009**, *35*, 827–833.
- [114] A. Hanafy, H. Spahn-Langguth, G. Vergnault, P. Grenier, M. Tubi Grozdanis, T. Lenhardt, P. Langguth, *Adv. Drug Delivery Rev.* **2007**, *59*, 419–426.
- [115] Q. Z. Hua Zhang, Y. Meng, X. Wang, W. Dai, X. Wang, *Drug Delivery* **2014**, *21*, 588–594.
- [116] T. Li, Y. Lei, M. Guo, H. Yan, *Eur. Polym. J.* **2018**, *101*, 77–82.
- [117] H. S. M. Ali, A. F. Hanafy, *J. Pharm. Sci.* **2017**, *106*, 402–410.
- [118] B. Van Eerdenbrugh, L. Froyen, J. Van Humbeeck, J. A. Martens, P. Augustijns, G. Van den Mooter, *Eur. J. Pharm. Sci.* **2008**, *35*, 127–135.
- [119] P. R. Mishra, L. Al Shaal, R. H. Müller, C. M. Keck, *Int. J. Pharm.* **2009**, *371*, 182–189.
- [120] O. Pelikh, P. Stahr, C. Huang, M. Gerst, P. Scholz, H. Dietrich, N. Geisel, C. M. Keck, *Eur. J. Pharm. Biopharm.* **2018**, *128*, 170–178.
- [121] K. Baba, H. E. Pudavar, I. Roy, T. Y. Ohulchanskyy, Y. Chen, R. K. Pandey, P. N. Prasad, *Mol. Pharm.* **2007**, *4*, 289–297.
- [122] M. Han, X. Liu, Y. Guo, Y. Wang, X. Wang, *Int. J. Pharm.* **2013**, *455*, 85–92.
- [123] Y. X. Zhao, H. Y. Hua, M. Chang, W. J. Liu, Y. Zhao, H. M. Liu, *Int. J. Pharm.* **2010**, *392*, 64–71.
- [124] H. S. M. Ali, P. York, A. M. A. Ali, N. Blagden, *J. Controlled Release* **2011**, *149*, 175–181.
- [125] B. Van Eerdenbrugh, B. Stuyven, L. Froyen, J. Van Humbeeck, J. A. Martens, P. Augustijns, G. Van den Mooter, *AAPS PharmSciTech* **2009**, *10*, 44–53.
- [126] A. R. Fernandes, J. Dias-Ferreira, C. Cabral, M. L. Garcia, E. B. Souto, *Colloids Surf. B* **2018**, *166*, 24–28.
- [127] P. Sharma, W. A. Denny, S. Garg, *Int. J. Pharm.* **2009**, *380*, 40–48.
- [128] A. Tuomela, T. Laaksonen, J. Laru, O. Antikainen, J. Kiesvaara, J. Ilkka, O. Oksala, S. Rönkkö, K. Järvinen, J. Hirvonen, et al., *Int. J. Pharm.* **2015**, *485*, 77–86.
- [129] A. Foglio Bonda, M. Rinaldi, L. Segale, L. Palugan, M. Cerea, C. Vecchio, F. Pattarino, *Eur. J. Pharm. Sci.* **2016**, *83*, 175–183.
- [130] J. M. Vaughn, N. P. Wiederhold, J. T. McConville, J. J. Coalson, R. L. Talbert, D. S. Burgess, K. P. Johnston, R. O. Williams, J. I. Peters, *Int. J. Pharm.* **2007**, *338*, 219–224.
- [131] D. Mou, H. Chen, J. Wan, H. Xu, X. Yang, *Int. J. Pharm.* **2011**, *413*, 237–244.
- [132] S. Basa, T. Muniyappan, P. Karatgi, R. Prabhu, R. Pillai, *Drug Dev. Ind. Pharm.* **2008**, *34*, 1209–1218.
- [133] A. Touzet, F. Pfefferlé, P. van der Wel, A. Lamprecht, Y. Pellequer, *Int. J. Pharm.* **2018**, *536*, 222–230.
- [134] G. J. Vergote, C. Vervaet, I. Van Driessche, S. Hoste, S. De Smedt, J. De-meester, R. A. Jain, S. Ruddy, J. P. Remon, *Int. J. Pharm.* **2002**, *240*, 79–84.
- [135] B. Van Eerdenbrugh, L. Froyen, J. A. Martens, N. Bleton, P. Augustijns, M. Brewster, G. Van den Mooter, *Int. J. Pharm.* **2007**, *338*, 198–206.
- [136] C. Liu, D. Chang, X. Zhang, H. Sui, Y. Kong, R. Zhu, W. Wang, *AAPS PharmSciTech* **2017**, *18*, 2957–2964.
- [137] C. Konnerth, V. Braig, A. Ito, J. Schmidt, G. Lee, W. Peukert, *Chem. Ing. Tech.* **2017**, *89*, 1060–1071.
- [138] K. Bodnár, S. P. Hudson, Å. C. Rasmuson, *Cryst. Growth Des.* **2017**, *17*, 454–466.
- [139] Q. Song, C. Shen, B. Shen, W. Lian, X. Liu, B. Dai, H. Yuan, *J. Drug Delivery Sci. Technol.* **2018**, *43*, 243–252.
- [140] P. Calleja, J. M. Iраche, C. Zanduetta, C. Martinez-Oharriz, S. Espuelas, *Pharmacol. Res.* **2017**, *126*, 77–83.
- [141] S. M. Pyo, D. Hespeler, C. M. Keck, R. H. Müller, *Int. J. Pharm.* **2017**, *531*, 350–359.
- [142] M. Chen, Y. Li, J. Zhou, Z. Yang, Z. Li, X. Mei, Z. Wang, *J. Appl. Toxicol.* **2018**, *38*, 656–664.
- [143] F. Danhier, B. Ucakar, M. L. Vanderhaegen, M. E. Brewster, T. Arien, V. Préat, *Eur. J. Pharm. Biopharm.* **2014**, *88*, 252–260.
- [144] S. Kim, J. Lee, *Drug Dev. Ind. Pharm.* **2011**, *37*, 131–138.
- [145] G. G. Liversidge, P. Conzentino, *Int. J. Pharm.* **1995**, *125*, 309–313.
- [146] R. Xiong, W. Lu, J. Li, P. Wang, R. Xu, T. Chen, *Int. J. Pharm.* **2008**, *350*, 338–343.
- [147] Q. Fu, J. Sun, D. Zhang, M. Li, Y. Wang, G. Ling, X. Liu, Y. Sun, X. Sui, C. Luo, et al., *Colloids Surfaces B Biointerfaces* **2013**, *109*, 161–166.
- [148] Q. Fu, M. Ma, M. Li, G. Wang, M. Guo, J. Li, Y. Hou, M. Fang, *Powder Technol.* **2017**, *305*, 757–763.
- [149] S. Jain, K. Patel, S. Arora, V. A. Reddy, C. P. Dora, *Drug Deliv. Transl. Res.* **2017**, *7*, 292–303.
- [150] J. Möschwitzer, G. Achleitner, H. Pomper, R. H. Müller, *Eur. J. Pharm. Biopharm.* **2004**, *58*, 615–619.
- [151] Z. Zhang, X. Zhang, W. Xue, Y. Yangyang, D. Xu, Y. Zhao, H. Lou, *Int. J. Nanomed.* **2010**, *5*, 735–742.
- [152] H. Lou, X. Zhang, L. Gao, F. Feng, J. Wang, X. Wei, Z. Yu, D. Zhang, Q. Zhang, *Int. J. Pharm.* **2009**, *379*, 181–186.
- [153] L. Gao, D. Zhang, M. Chen, C. Duan, W. Dai, L. Jia, W. Zhao, *Int. J. Pharm.* **2008**, *355*, 321–327.
- [154] Y. Lu, Z. H. Wang, T. Li, H. McNally, K. Park, M. Sturek, *J. Controlled Release* **2014**, *176*, 76–85.
- [155] F. Guo, J. Shang, H. Zhao, K. Lai, Y. Li, Z. Fan, Z. Hou, G. Su, *Colloids Surf. B* **2017**, *160*, 649–660.
- [156] W. Li, Z. Li, L. Wei, A. Zheng, *Drug Res.* **2018**, *68*, 205–212.
- [157] J. Park, B. Sun, Y. Yeo, *J. Controlled Release* **2017**, *263*, 90–101.
- [158] F. Deng, H. Zhang, X. Wang, Y. Zhang, H. Hu, S. Song, W. Dai, B. He, Y. Zheng, X. Wang, et al., *ACS Appl. Mater. Interfaces* **2017**, *9*, 5803–5816.
- [159] Y. Liu, L. Huang, F. Liu, *Mol. Pharm.* **2010**, *7*, 863–869.
- [160] F. Liu, J.-Y. Park, Y. Zhang, C. Conwell, Y. Liu, S. R. Bathula, L. Huang, *J. Pharm. Sci.* **2010**, *99*, 4215–4227.
- [161] S. E. Lee, S. F. Bairstow, J. O. Werling, M. V. Chaulal, L. Lin, M. A. Murphy, J. P. DiOrio, J. Gass, B. Rabinow, X. Wang, et al., *Pharm. Dev. Technol.* **2014**, *19*, 438–453.
- [162] L. Gao, G. Liu, J. Kang, M. Niu, Z. Wang, H. Wang, J. Ma, X. Wang, *Colloids Surf. B* **2013**, *111*, 277–281.
- [163] M. Talekar, S. Ganta, M. Amiji, S. Jamieson, J. Kendall, W. A. Denny, S. Garg, *Int. J. Pharm.* **2013**, *450*, 278–289.
- [164] Y. Wang, Y. Ma, Y. Zheng, J. Song, X. Yang, C. Bi, D. Zhang, Q. Zhang, *Int. J. Pharm.* **2013**, *441*, 728–735.
- [165] J. Pardeike, R. H. Müller, *Int. J. Pharm.* **2010**, *391*, 322–329.
- [166] S. Kobierski, K. Ofori-Kwakye, R. H. Müller, C. M. Keck, *Pharmazie* **2009**, *64*, 741–747.
- [167] C. Sinico, R. Pireddu, E. Pini, D. Valenti, C. Caddeo, A. M. Fadda, F. Lai, *Planta Med.* **2016**, *476*–481.
- [168] G. Liu, D. Zhang, Y. Jiao, H. Guo, D. Zheng, L. Jia, C. Duan, Y. Liu, X. Tian, J. Shen, et al., *Colloids Surfaces B Biointerfaces* **2013**, *102*, 620–626.
- [169] K. P. Krause, O. Kayser, K. Mäder, R. Gust, R. H. Müller, *Int. J. Pharm.* **2000**, *196*, 169–172.
- [170] R. Mauludin, R. H. Müller, C. M. Keck, *Eur. J. Pharm. Sci.* **2009**, *36*, 502–510.
- [171] P. Langguth, A. Hanafy, D. Frenzel, P. Grenier, A. Nhamias, T. Ohlig, G. Vergnault, H. Spahn-Langguth, *Drug Dev. Ind. Pharm.* **2005**, *31*, 319–329.
- [172] C. Jacobs, O. Kayser, R. H. Müller, *Int. J. Pharm.* **2000**, *196*, 161–164.
- [173] K. Sigfridsson, A. J. Lundqvist, M. Strimfors, *Drug Dev. Ind. Pharm.* **2009**, *35*, 1479–1486.
- [174] K. D. Koradia, N. R. Sheth, H. D. Koradia, M. R. Dabhi, *J. Drug Delivery Sci. Technol.* **2018**, *43*, 73–84.
- [175] L. Gao, G. Liu, J. Ma, X. Wang, L. Zhou, X. Li, *J. Controlled Release* **2012**, *160*, 418–430.
- [176] T. Chen, C. Li, Y. Li, X. Yi, S. M.-Y. Lee, Y. Zheng, *Mol. Pharm.* **2016**, *13*, 3864–3875.
- [177] H. Ling, J. T. Luoma, D. Hilleman, *Cardiol. Res.* **2013**, *4*, 47–55.
- [178] T. Nassar, A. Rom, A. Nyska, S. Benita, *J. Controlled Release* **2009**, *133*, 77–84.
- [179] B. Knight, M. Troutman, D. R. Thakker, *Curr. Opin. Pharmacol.* **2006**, *6*, 528–532.
- [180] S. P. Apte, *J. Excip. Food Chem.* **2010**, *1*, 51–59.

Annexe 2:



Europäisches
Patentamt

European
Patent Office

Office européen
des brevets

Acknowledgement of receipt

We hereby acknowledge receipt of your request for grant of a European patent as follows:

Submission number	1000477171	
Application number	EP18306138.1	
File No. to be used for priority declarations	EP18306138	
Date of receipt	27 August 2018	
Your reference	B74703EPD38703	
Applicant	CENTRE NATIONAL DE LA RECHERCHE SCIENTIFIQUE (CNRS)	
Country	FR	
Title	PREPARATION OF NANOSUSPENSION COMPRISING NANOCRYSTALS OF ACTIVE PHARMACEUTICAL INGREDIENTS WITH LITTLE OR NO STABILIZING AGENTS	
Documents submitted	package-data.xml application-body.xml SPECEPO-1.pdf/figures dépôt.pdf (14 p.) f1002-1.pdf (1 p.)	ep-request.xml ep-request.pdf (5 p.) SPECEPO-2.pdf/texte depot_amy2.pdf (34 p.)
Submitted by	EMAIL=audren@regimbeau.eu,CN=Marie AUDREN,O=CABINET REGIMBEAU,C=FR	
Method of submission	Online	
Date and time receipt generated	27 August 2018, 17:45:08 (CEST)	
Official Digest of Submission	15:EE:EC:74:47:69:41:6A:A9:5E:D9:1D:6A:69:4E:19:83:29:78:DE	

/INPI, section dépôt/